THE SIBLEY GROUP:

a lithostratigraphic, geochemical, and paleomagnetic study

By
Becky Rogala ©

Submitted in partial fulfillment of
the requirements for the degree of

Masters of Science

Supervisor: Dr. P. Fralick

Geology Department
Lakehead University
Thunder Bay, ON
June 2003

Your file Votre référence
ISBN: 0-612-92258-8
Our file Notre référence
ISBN: 0-612-92258-8

ABSTRACT

The Sibley Group is an unmetamorphosed Mesoproterozoic red bed sequence, commonly flat-lying, that formed in an intracratonic basin between 1450 Ma and 1500 Ma. It covers an area of 15,000 km^2, and reaches a total thickness of 950 m. Recent drilling projects in the Nipigon Plate have provided a unique opportunity to study the basin using data obtained from a combination of 25 drill holes and surface outcrops. This has allowed a re-examination of the lithostratigraphy, as well as providing insight into the basin architecture. Previously, the Sibley Group consisted of only three formations: the Pass Lake Formation, the Rossport Formation, and the Kama Hill Formation (Cheadle, 1986a). Two additional formations have been introduced here: the Outan Island Formation and the Nipigon Bay Formation. The Pass Lake Formation, interpreted as a fluvial-lacustrine system, is divided into the Loon Lake Member and the Fork Bay Member (Cheadle, 1986a). The Rossport Formation is separated into the Channel Island Member, the Middlebrun Bay Member, and the Fire Hill Member (Cheadle, 1986a). These consist of cyclic dolomite-siltstone layers, stromatolites and red mudstone, which represent a playa lake, sabkha, and mudflat environments. The Kama Hill Formation is not subdivided, and is composed of purple shales and siltstones interpreted as subaerial mudflat deposits. The Outan Island Formation has been divided into the deltaic Lyon Member and the fluvial Hele Member. The Nipigon Bay Formation consists of cross-stratified sandstone beds, and is thought to denote an aeolian environment.

Geochemistry has been used to examine formation-scale trends in weathering characteristics and provenance. Samples were collected from drill holes spanning the entire thickness of the Sibley Group, and the concentrations of various elements were plotted against depth to appraise variations between Formations.

A paleomagnetic study was also conducted on the Sibley Group. The first part involved comparing paleopoles from samples of the Pass Lake, Kama Hill, and Nipigon Bay Formations. This revealed a probable depositional paleopole age between 1450 Ma and 1500 Ma, with remagnetization events at approximately 1350 Ma and 1100 Ma. The second part involved a study of paleo-secular variation in the Rossport Formation, which resulted in the documentation of one of the oldest known examples of paleo-secular variation yet discovered.

ACKNOWLEDGEMENTS

This thesis would not have been possible without the assistance of a number of people. I would like to thank Dr. Fralick and Dr. Borradaile for their suggestions and guidance throughout the study, and my anonymous external examiner for the helpful comments. A huge thank you to Anne Hammond, Allen Mackenzie, Ain Raitsakas, Keith Pringnitz, and Eleanor Jensen for their assistance with sample preparation, instrumentation, and sample analyses.

I would also like to thank Mark Smyk, Bernie Schnieders, and John Scott for pointing out field locations and the guided tour around the islands in Lake Superior. They were also instrumental in accessing some of the core. Access to core was also provided by Bob Middleton of East West Resources, Tech-Cominco, and Michael Carr of Bitter-root Resources.

A special thank you to Tom Hamilton for his assistance with the equipment in the paleomagnetics lab, proof-reading, and support throughout the entire project.

TABLE OF CONTENTS

LIST OF FIGURES

LIST OF TABLES

Chapter 1:

INTRODUCTION

1.1 Purpose

The present study of the Sibley Basin was initiated to increase the understanding of the stratigraphy, climatic history, and tectonic setting, and to put it into continental context. Previous studies have provided analyses of sedimentology, stratigraphy, and depositional environments (Franklin, 1970; Cheadle, 1986a,b). However, due to recent drilling projects in the Nipigon Plate, the opportunity to investigate the basin with data obtained from a combination of 25 drill holes and surface outcrops is available for the first time. This expanded database is certain to give new insights.

There are several aspects to this study of the Sibley Basin. The most fundamental part is the definition and interpretation of lithofacies associations. Two new formations have been added to the stratigraphy, and they must be adequately described. The first has only been seen in drill core and will consist of two members. The second new formation can be found in drill core and on Simpson Island in Lake Superior. Previously existing Formations and Members are also described and refined. Interpretations of depositional environments for all Formations and Members have also been made. Once the sedimentology and stratigraphy are defined, it is possible to begin modelling the basin. Information from the 25 drill holes available, as well as information from outcrops, has been compiled, allowing detailed three-dimensional basin-wide analysis of facies trends and distributions.

Formation-scale trends in provenance have been investigated with the use of geochemistry. Samples were collected from drill holes spanning the entire thickness of the Sibley Group. This data was then plotted against depth to appraise variations between Formations, possibly related to source changes.

The section on paleomagnetism began as the continuation of a pilot study on a section of core from the Rossport Formation. The data from this pilot study seems to indicate the presence of secular variation. The periodicity of this curve can give insight into the length of time it took for the Sibley Group to be deposited. The discovery of a secular variation curve lead to the idea that paleomagnetism could be used on a larger scale. Samples were then taken from each of the Formations in order to see if the paleopole position of the Sibley Group has changed over time. This could have potential implications for the age of the Sibley and the length of time for deposition based on the position and degree of movement of the paleopole.

1.2 Location and Access

The Sibley Basin is an ovoid depression approximately 175 km wide and 400 km long. Rocks filling the basin crop out discontinuously over a 15,000 km^2 area from the northern shore of Lake Superior to the western shore of Lake Nipigon and to Armstrong in the north, as shown in Figure 1.1. Outcrops are accessible along highway 11/17 and highway 587, as well as along a variety of gravel roads branching off the Black Sturgeon Road and Mawn Lake Road. Outcrops are also accessible by boat along the shore of Lake Nipigon and on several islands in Lake Superior.

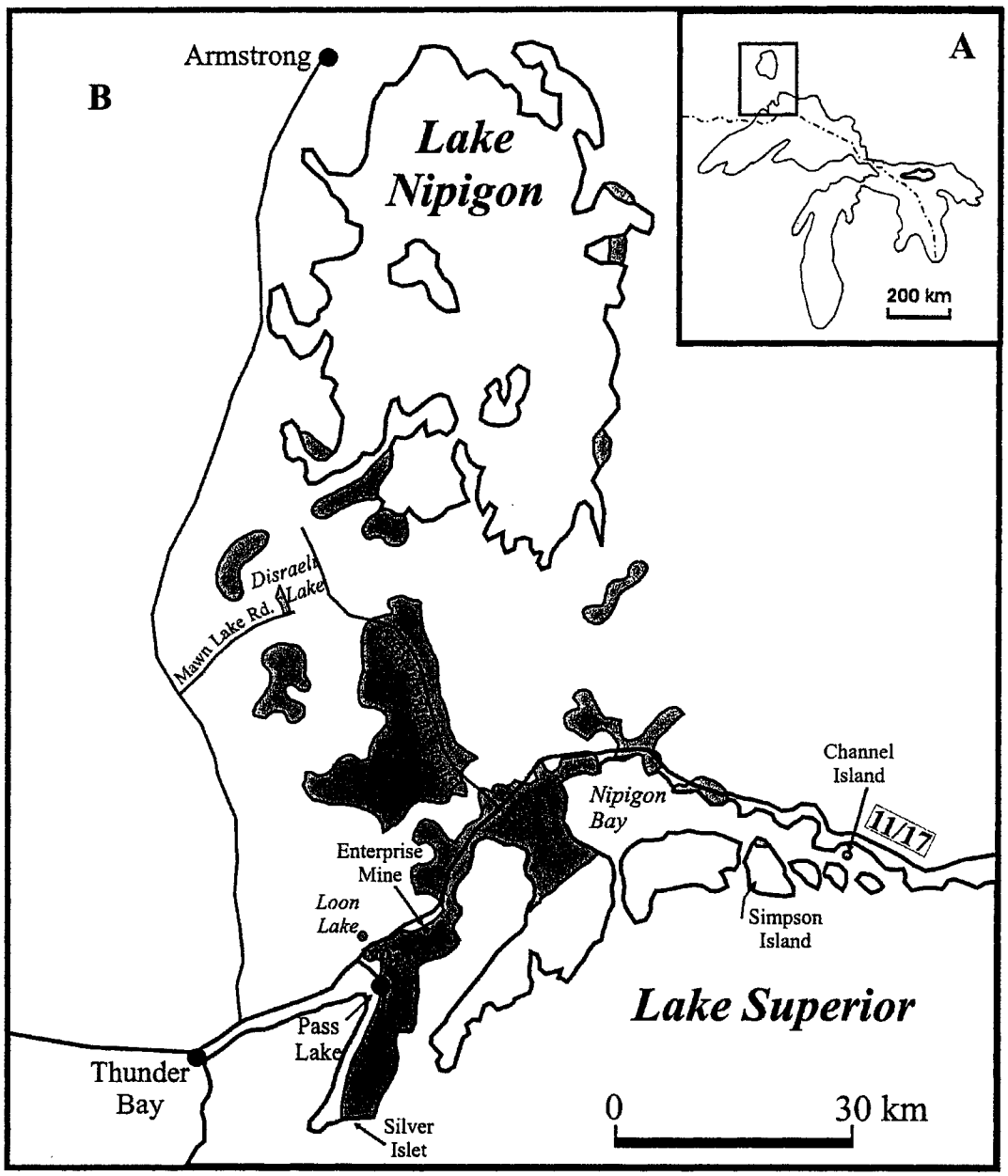

Figure 1.1. Location Map. (A) The outlined area on the inset map shows the location of the Sibley Basin. (B) The shaded area shows the distribution of the Sibley Group.

1.3 Regional Geology

The Sibley Group is underlain by the Archean metavolcanic, metasedimentary and granitic rocks, Animikie Group rocks, and Mesoproterozoic granites and rhyolites. Diabase sills intrude the Sibley Group and the Osler Group overlies it. This succession of stratigraphic units is summarized in Table 1.1 and the Sibley Group is shown in relation to the regional geology in Figure 1.2.

Table 1.1 Stratigraphic Summary of Units.

<table>
<tr><td>Osler Group Volcanics</td><td colspan="2"></td><td>1097 Ma</td></tr>
<tr><td>Diabase Sills</td><td colspan="2"></td><td>1110 Ma</td></tr>
<tr><td rowspan="9">Sibley Group</td><td>Nipigon Bay Formation</td><td></td><td rowspan="9">1339 Ma - 1537 Ma</td></tr>
<tr><td rowspan="2">Outan Island Formation</td><td>Hele Member</td></tr>
<tr><td>Lyon Member</td></tr>
<tr><td>Kama Hill Formation</td><td></td></tr>
<tr><td rowspan="3">Rossport Formation</td><td>Fire Hill Member</td></tr>
<tr><td>Middlebrun Bay Member</td></tr>
<tr><td>Channel Island Member</td></tr>
<tr><td rowspan="2">Pass Lake Formation</td><td>Fork Bay Member</td></tr>
<tr><td>Loon Lake Member</td></tr>
<tr><td>English Bay Intrusion</td><td colspan="2"></td><td>1537 Ma</td></tr>
<tr><td rowspan="2">Animikie Group</td><td>Rove Formation</td><td rowspan="2"></td><td rowspan="2">1878 Ma</td></tr>
<tr><td>Gunflint Formation</td></tr>
<tr><td>Quetico Subprovince</td><td colspan="2"></td><td>2700 Ma – 3000 Ma</td></tr>
<tr><td>Wabigoon Subprovince</td><td colspan="2"></td><td>2722 Ma - 2769 Ma</td></tr>
</table>

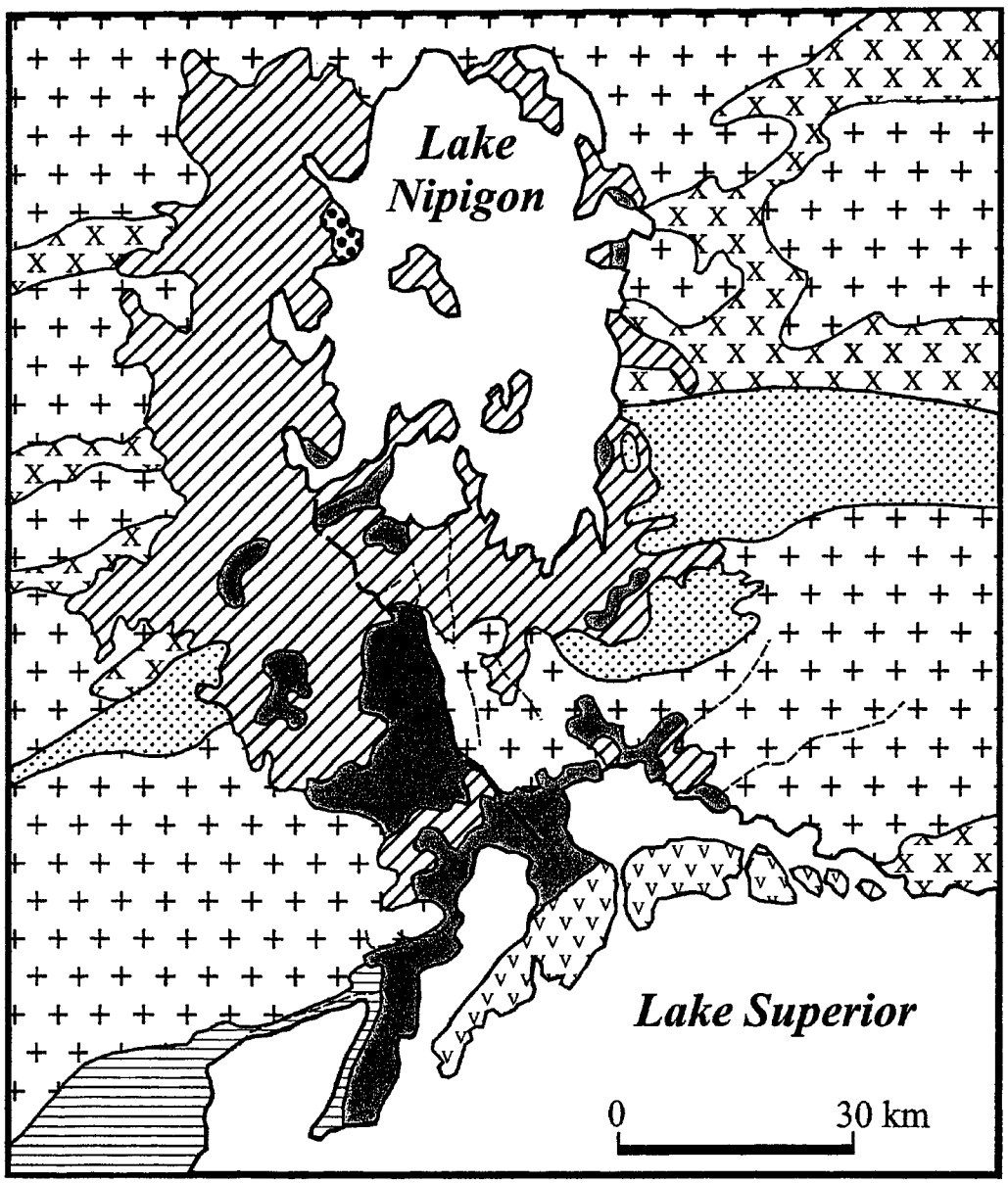

LEGEND

Proterozoic

- 1097 Ma Osler Group
- 1110 Ma Diabase
- > 1339 Ma Sibley Group
- 1537 Ma Granite and Rhyolite
- 1900 Ma Animikie Group

Archean

- Granitic Rocks
- Metasedimentary Rocks
- Metavolcanic Rocks

Figure 1.2. Regional Geology. Some minor faults are shown as thin red lines. The thick red line is the Black Sturgeon Fault.

Geophysical maps have shown that the greenstone belts of the Mesoarchean to Neoarchean Eastern Wabigoon Subprovince extend beneath the Proterozoic units of the Sibley Group in the northern and central areas of Lake Nipigon (Blackburn *et al.*, 1991). Supracrustal rocks and synvolcanic granitoid batholiths dominate the Eastern Wabigoon Subprovince (Blackburn *et al.*, 1991). The volcanism, consisting of metamorphosed mafic, felsic and ultramafic rocks, ranges from 2769+6/-5 Ma (Anglin *et al.*, 1988) to 2722±1 Ma (Davis *et al.*, 1989). Clastic sediments represent alluvial fan, fluvial, and turbiditic sequences (Barrett and Fralick, 1985, 1989; Devaney and Williams, 1989; Fralick and Barrett, 1995; Eriksson *et al.*, 1994, 1997). The Wabigoon Subprovince has been subjected to three phases of folding and shearing. The earlier phase includes imbrication and shallow-plunging folds, followed by belt-parallel, upright to steeply dipping folds. The final structures are due to brittle-ductile shearing, and are related to post-accretion convergence (Blackburn *et al.*, 1991).

The southern portion of the Sibley Group is predominantly underlain by rocks of the Quetico Subprovince. The Quetico Subprovince is principally composed of metamorphosed turbiditic sediment, derived from neighbouring subprovinces such as the Wabigoon (Williams, 1991; Fralick *et al.*, 1992; Fralick and Kronberg, 1997). Igneous rocks are typically felsic to intermediate intrusives, with rare mafic and felsic extrusives, and an even rarer suite of gabbroic and ultramafic rocks (Williams, 1991). Detrital zircon ages range from 3.0 Ga to 2.7 Ga (Williams, 1991). There are four major faults within the Quetico, although the only one affecting the Sibley Basin is the Quetico Fault, which partially defines the boundary between the Wabigoon and Quetico Subprovinces (Williams, 1991). The Sibley Group overlies the Quetico Fault to the southwest of Lake Nipigon.

There are also four deformational events, involving shearing and folding, that affect the Quetico (Williams, 1991). The first event is in the form of soft-sediment deformation and slumps, followed by bedding-parallel shearing that produced steep to variable-plunging folds. The third deformational event created upright to inclined shallow-plunging folds. The final deformation event is in the form of small-scale shear zones, representing compression from the south to southeast. The Quetico underwent two stages of metamorphism. The early stage is a high-pressure metamorphic event that is rarely preserved. This was followed by regional high-temperature metamorphism (Williams, 1991).

The Gunflint and Rove Formations of the Animikie Group can be found sporadically underlying the Sibley Group between Thunder Bay and Loon Lake (Figure 1.1). The Animikie Basin was formed on the southern margin of the Superior Province (Pufahl and Fralick, 2000), forming a southward thickening wedge deposited on a shelf during transgressive-regressive-transgressive cycles (Fralick and Barrett, 1995; Fralick *et al*, 2002). The sediments consist of basal conglomerate, black shales to slates, ferruginous carbonate, chert, jasper, and hematite/magnetite grainstones of the Gunflint Formation (Sutcliffe, 1991). The Rove Froamtion, a thick turbiditic shale-sandstone sequence, overlies the Gunflint Formation.

There is some debate as to the formation of the basin. Some researchers suggest that the Animikie Basin developed as a foreland basin (Ojakangas, Morey, and Southwick, 2001; Schneider *et al.*, 2002), while others suggest a back-arc basin setting (Fralick *et al.*, 2002). A euhedral zircon population from the Gunflint Formation, believed by Fralick *et al.* (2002) to be nearly synchronous with the time of deposition, gave a U-Pb age of

1878.3±1.3 Ma. The Animikie Basin was deformed and truncated to the south by the Paleoproterozoic Penokean Orogeny. A series of intrusive igneous phases were emplaced with the termination of the orogenic event.

The English Bay intrusion is located on the eastern shore of Lake Nipigon (Figure 1.1), directly underlying the Sibley Group. A lower age bracket of 1537+10/-2 Ma (Davis and Sutcliffe, 1985) is defined by U-Pb zircon age determinations obtained from the Redstone Point granite of the English Bay intrusion. A caldera structure found on the northern part of Lake Nipigon may be associated with its emplacement (Sutcliffe, 1991).

The Sibley Group is underlain by Archean metasediments, metavolcanics and granitic intrusions, Animikie sediments, and a Mesoproterozoic granite-rhyolite complex. A minimum depositional age for the Sibley is provided by a Rb-Sr whole rock age of 1339 ±33 Ma (Franklin, 1978) that was obtained from the siltstones of the Rossport and Kama Hill Formations. The English Bay Granite has been used to define an upper age limit.

The Keweenawan Supergroup typically refers to a group of mafic volcanics and sedimentary rocks deposited during a period of active magmatism and rifting, known as the Midcontinent Rift event. Eruptions occured between 1109 Ma and 1087 Ma (Ojakangas, Morey and Green, 2001). Gravity maps have recently been used to infer the presence of felsic intrusives within the mafic volcanics along the northern margin of the Midcontinent Rift (Thomas and Teskey, 1994). Keweenawan rocks can be found in an arcuate band from Kansas up to Lake Superior, and down to Lake Erie (Ojakangas, Morey, and Green, 2001). The rift encompasses a series of axial blocks, bounded by high-angle listric faults, with sedimentary basins forming in the half-grabens flanking them (Ojakangas, Morey, and

Green, 2001). The southernmost portion of the Sibley Basin was dissected by this rifting event (Figure 1.2).

A series of intrusions were emplaced shortly before or contemporaneously with Keweenawan volcanism and sedimentation. Several gabbroic intrusions have been emplaced into the Animikie and Keweenawan rocks (Sutcliffe, 1991). Two main series of sills have also been reported, the Logan sills and the sills around Lake Nipigon. The latter intrudes the Sibley Group. The Nipigon intrusions consist of an earlier phase of minor picrite intrusions and a later phase of olivine tholeiite diabase sills and dikes (Sutcliffe, 1991). The sills were determined to be 1108.8+4-2 Ma from U-Pb geochronology on zircons (Davis and Sutcliffe, 1985).

In the area of the Sibley Group, the Keweenawan Supergroup is represented by the Osler Group, which correlates with the Lower Keweenawan. The Osler Group is a 2.75 km thick sequence (Ojakangas, Morey and Green, 2001), comprised predominantly of subaerial tholeiitic basalts, with some andesite, rhyolite, and interflow sediments (Sutcliffe, 1991). Directly above the Sibley Group, the Osler occurs as a series of rhyolite flows. Above this, there are sporadic occurrences of conglomerate, rich in porphyritic clasts, as well as lenses of cross-bedded sandstone and siltstone. Interflow sediments are most common in the lower part of the Osler Group; while the top of the sequence is dominated by basalt flows (Sutcliffe, 1991). Davis and Sutcliffe (1985) gave age determinations for rhyolites above and below the magnetic reversal, bracketing it between 1107.5+4-2 Ma and 1097.6±3.7 Ma.

The bedrock in the region is sporadically covered by tills, glaciofluvial sands, and glaciolacustrine laminated mudstone deposited during the Pleistocene glaciation. Ice

receded from the tip of the Keweenaw Peninsula by 9500 years ago. As deglaciation proceeded, catastrophic floods drained through the Nipigon Basin into the Lake Superior Basin (Barnett, 1991). Over the next 500 years, water levels in Lake Superior stabilized (Barnett, 1991).

1.4 Previous Work

Logan (1863) was the first to discuss the Sibley sediments. He included them with the Upper Copper-Bearing Series of the Lake Superior region, tentatively calling them Lower Silurian based on a possible stratigraphic correlation with the Potsdam sandstone in Michigan. Hunt (1873) later divided the Upper Copper-Bearing Series into the Animikie and Keweenaw Groups, with the Sibley sediments being placed in the latter. Disagreements still arose as to the age of the Sibley. Van Hise and Leith (1909) supported a Precambrian age, while Wilson (1910) argued for a Paleozoic age. Tanton (1931) incorporated the Animikie and Keweenaw Groups into the Kaministikwa Group, which was subdivided into the lower Animikie Series, central Sibley Series, and an upper Osler Series. Comprehensive mapping by McIlwaine (1971a, 1971b, 1975) and Coates (1972) led to the investigations of the Sibley Group by Franklin (1970, 1978) and Franklin *et al.* (1980).

Franklin (1970) originally divided the Sibley Group into seven lithological units. These were (from bottom to top) conglomeratic lenses, sandstone, lower red sandy mudstone, stromatolite-chert, upper red limey mudstone, purple mudstone, and limestone. They were described based on their mineralogy and sedimentology. In 1980, Franklin *et al.* allocated the present names to the units in the Sibley Group: the Pass Lake, Rossport, and Kama Hill Formations. Franklin's (1980) Pass Lake Formation consisted of conglomeratic

lenses overlain by sandstones. He divided the Rossport Formation into Lower, Central, and Upper Members. The Lower Member was described as sandstone beds interlayered with hematitic dolomite beds. The Central and Upper Members are, respectively, correlated with the stromatolite chert and upper red limey mudstone units of his previous division.

Cheadle (1986a,b) described the Formations in great detail and refined the depositional environments attributed to each. He subdivided the Pass Lake Formation into the Loon Lake and Fork Bay Members, and the Rossport Formation into the Channel Island, Middlebrun Bay, and Fire Hill Members (Cheadle, 1986b). The Loon Lake Member replaced the conglomeratic facies from the Pass Lake Formation, as defined by Franklin (1980). The sandstone unit of the Pass Lake Formation was renamed the Fork Bay Member (Cheadle, 1986b). The Channel Island, Middlebrun Bay, and Fire Hill Members supplant the Lower, Middle, and Upper Members of the Rossport Formation.

There is some ongoing debate as to the origin of the Sibley Basin. Franklin *et al.* (1980) suggested that the basin was created as a failed arm of the Mid-continental Rift System. Cheadle (1986a) disagreed with this theory and suggested two possibilities to replace it. Although he pointed out inconsistencies between the Sibley Group and rift related basins, he tentatively suggested that the Sibley Basin might have developed due to extension associated with an earlier Elsonian rifting event. However, Cheadle's (1986a,b) preferred theory was that the Sibley Basin was a result of lithospheric stretching related to the very earliest extensional phases of the Midcontinent Rift. Fralick and Kissin (1996) proposed that the Sibley Basin was created during broad subsidence following thermal doming related to plume activity, which had resulted in the formation of the Redstone Point Granite (within the English Bay Intrusion) at 1537 Ma.

Chapter 2:

LITHOSTRATIGRAPHY & DEPOSITIONAL ENVIRONMENT

Recent drilling within the area of the Nipigon Plate has been undertaken by various companies in the process of mineral exploration. The drill core from these projects are located in the MNDM Conmee and James Street core libraries in Thunder Bay. Core from 25 drill holes were logged and are summarized in Table 2.1 and their positions are shown in Figure 2.1. Logs of all of the drill holes are included in Appendix A.

Table 2.1 Summary of Drill Core

Drill Hole	E (UTM)	N (UTM)	Length (m)	Elevation (m)
SB-101	377950	5383500	177.31	297
SB-102	377900	5383300	163.80	293
SO-1	384150	5433950	53.26	343
SO-2	384150	5433950	109.08	343
DO-82-1	377500	5410100	16.97	369.8
DO-82-2	377500	5410070	22.91	360.7
DO-82-3	377410	5410900	21.03	352.1
DO-82-4	377300	5410100	20.72	339.4
DO-82-5	377410	5409890	29.25	333.6
DO-82-6	377660	5410100	15.21	359.8
DO-82-7	378850	5410870	48.12	316.4
DO-82-8	377670	5410030	22.01	356.8
NI-92-5	356750	5468310	42.38	381
NI-92-7	353850	5443000	151.15	404
CYP-96-1	432500	5419940	464.5	183
NB-97-2	426990	5416241	677.8	183
NB-97-4	425430	5410540	1015.6	183
NB-97-5	427140	5411800	744.2	183
HE-02-01	391250	5423148	253.62	403
HE-02-02	393007	5449701	245.00	402
SR-02-01	363501	5439302	287.00	316
DDH-1	376365	5437493	120.81	290
DDH-2	376371	5446449	86.63	297
DDH-3	346299	5446449	53.75	297
DDH-5	373679	5444646	39.30	290

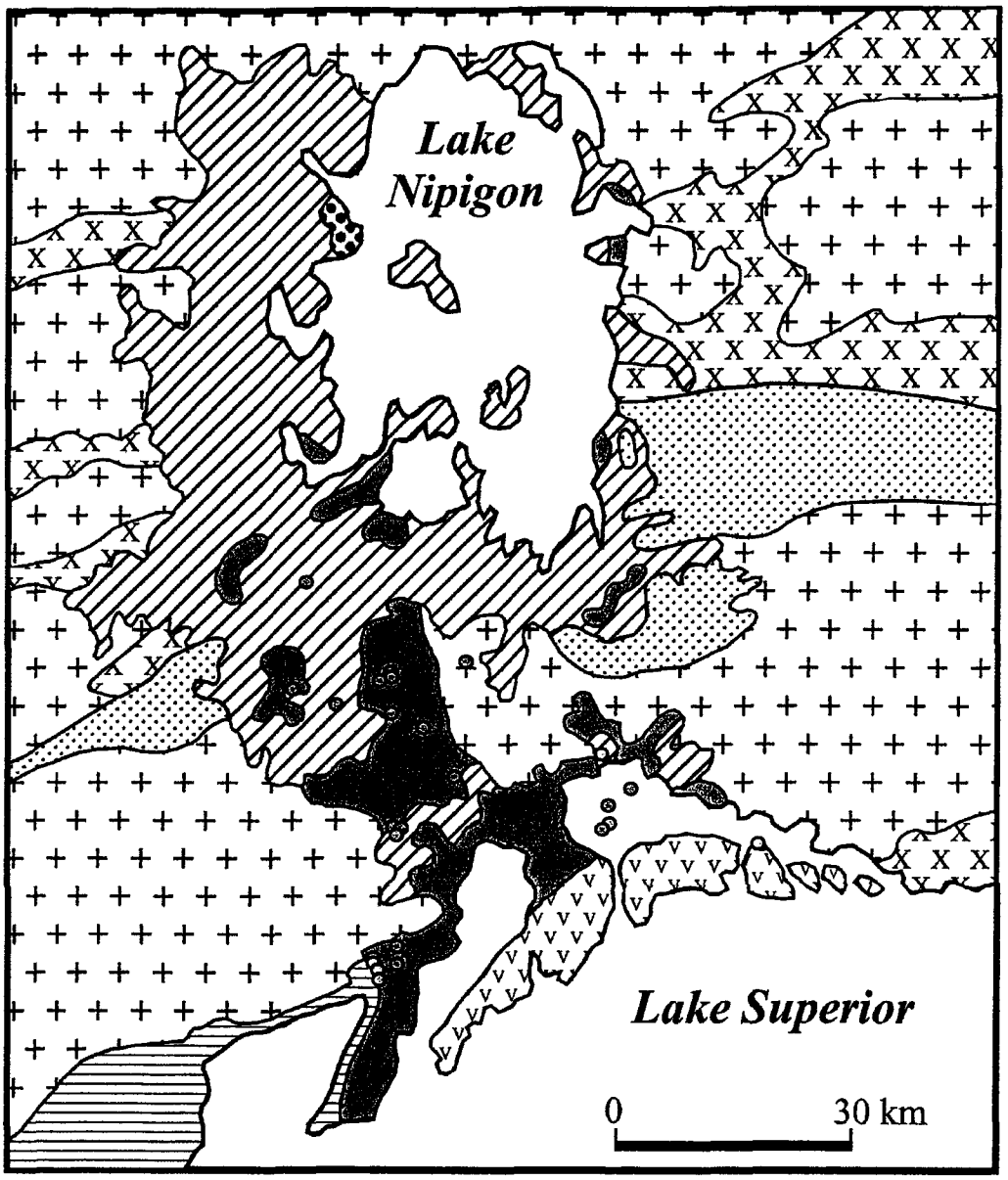

LEGEND

Proterozoic

- 1097 Ma Osler Group
- 1110 Ma Diabase
- > 1339 Ma Sibley Group
- 1537 Ma Granite and Rhyolite
- 1900 Ma Animikie Group

Archean

- Granitic Rocks
- Metasedimentary Rocks
- Metavolcanic Rocks

Figure 2.1. Drill Hole Positions. Drill hole positions are shown as blue circles, outcrop positions are shown as green circles.

The Sibley Group now includes five Formations (Figure 2.2). The Pass Lake Formation is the basal unit, consisting of the Loon Lake and Fork Bay Members. Cheadle (1986a) noted that sandstones, correlated with the Pass Lake Formation, have been found intercalated with rhyolites of the English Bay intrusion. The Rossport Formation, comprising the Channel Island, Middlebrun Bay, and Fire Hill Members, overlies the Pass Lake Formation. The Kama Hill Formation is unsubdivided and overlies the Rossport Formation. These three Formations were formerly defined by Franklin (1970, 1980) and Cheadle (1986a,b). Drill holes in Lake Superior have intersected upper units not previously recognized on the mainland. This has resulted in the identification of two new formations. The Outan Island Formation overlies the Kama Hill Formation and has been divided into two members: the Lyon Member and the Hele Member. This Formation is overlain by the Nipigon Bay Formation, which is not subdivided.

Some problems occur when attempting to describe the Sibley Group within the confines of these Formations due to overlap of lithofacies associations among them. This is particularly evident when trying to distinguish the Channel Island Member from the Fire Hill Member of the Rossport Formation, as defined by Cheadle (1986a) and Franklin (1980). Therefore, the Sibley Group will be described here by Formation and subdivided into lithofacies associations, some of which are similar to those described by Cheadle (1986b). These will later be put into the context of the Members and Formations formerly defined by Cheadle (1986a).

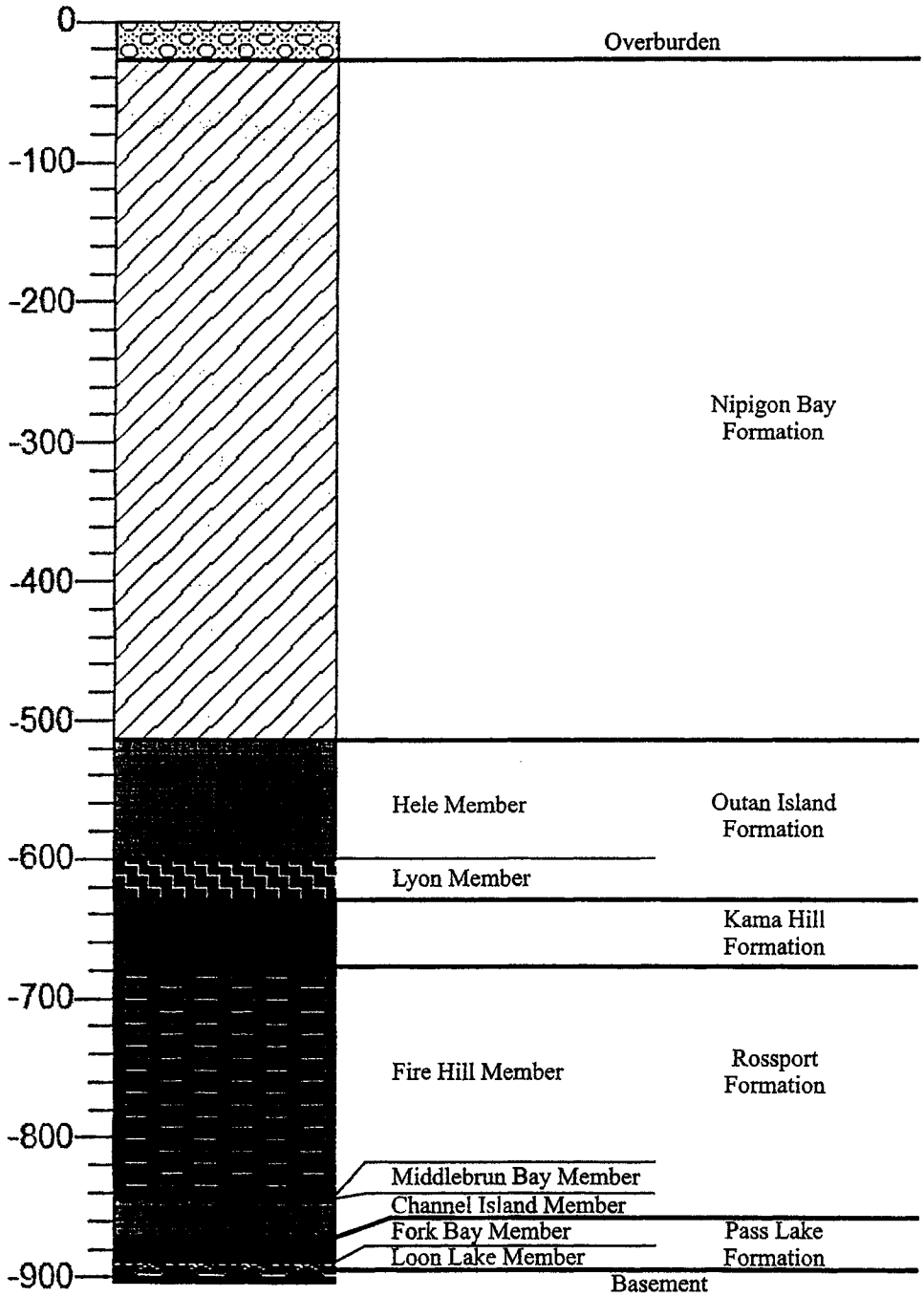

Figure 2.2. Generic Stratigraphic Column. This is a generic stratigraphic column, showing the organization and relative unit thicknesses (m) for the Members and Formations of the Sibley Group.

2.1 Pass Lake Formation

The Pass Lake Formation crops out sporadically throughout the Sibley Basin, with the thickest accumulations occurring in the central part of the basin. It thins towards the southeast. When present, the Formation can reach a thickness of 100 m, although it is more typically 5 to 25 m thick. Paleocurrents trend towards the southeast (Cheadle, 1986a).

The Pass Lake Formation consists of the Loon Lake Member and the Fork Bay Member. Cheadle (1986a) described the Loon Lake Member as a basal conglomerate facies, which is also the definition applied here. The Fork Bay Member was divided into three facies: heterolithic, cross-bedded, and plane-bedded sandstone facies. However, the large-scale features that these associations are based on are difficult to identify in drill core so these facies descriptions will be slightly modified to take this into account. The division between these Members is defined as the point where the conglomerates of the Loon Lake Member give way to the sandstones of the Fork Bay Member. This transition is typically sharp, although some gradational pebbly sandstone do occur. These pebbly sandstones have been included with the Fork Bay Member, in accord with Cheadle (1986a). The Loon Lake Formation can reach a thickness of 15 m, and the Fork Bay Member is 0 to 80 m thick.

2.1.1 Basal Conglomerate Lithofacies

The basal conglomerate occurs sporadically in drill core and outcrops in a patchy semicircle along the southern margin of the basin, filling topographic lows. Its thickest accumulation is in the southeast. The conglomerate can reach a thickness of 15 m, but is more typically only a few metres thick.

The basal conglomerate appear tabular to lensoid, and may be matrix-support to clast-support, with well-rounded clasts up to 40 cm in diameter (Figure 2.3). Some outcrops may be clast-support at the base and matrix-support at the top. An outcrop on La Grange Island in Lake Superior shows large-scale cross-stratification. Clasts are predominantly jasper, taconite, and shale derived from the underlying Gunflint Formation. Where the conglomerate overlies Archean granites, clasts of granite and quartzite dominate with some metavolcanic clasts (Cheadle, 1986b).

Cheadle (1986a) noted that cross-bedded medium-grained sandstone and dolomitic mudstone lenses are present in some outcrops. These are typically erosively cut by large scour and fill structures by overlying conglomerate. Caliche crusts and clast-coatings were also observed by Cheadle (1986a).

2.1.2 Sandstones

The sandstone lithofacies association is divided into several types of individual lithofacies based on drill core analysis, including well-sorted massive sandstone, poorly-sorted massive sandstone, silty sandstone, laminated siltstone/sandstone, and rippled sandstone. These units commonly grade into each other. Combinations of these lithofacies would be correlative with Cheadle's (1986a) plane-bedded (Figure 2.4), cross-bedded (Figure 2.5), and heterolithic facies. These facies seem to be organized with the heterolithic facies at the bottom, overlain by the cross-bedded facies, which is overlain by the plane-bedded facies (Cheadle, 1986a).

Figure 2.3 Basal Conglomerate Lithofacies. This picture shows the contact of the basal conglomerate lithofacies association with the sandstone lithofacies association at Pass Lake. Note the roundness, size, and lack of sorting of the clasts. A lens cap, outlined in white, is shown for scale.

Figure 2.4 Sandstone Lithofacies Association at Pass Lake. These plane-bedded sandstones overlie the basal conglomerate shown in Figure 2.1. Notice the upward thinning of the sandstone beds.

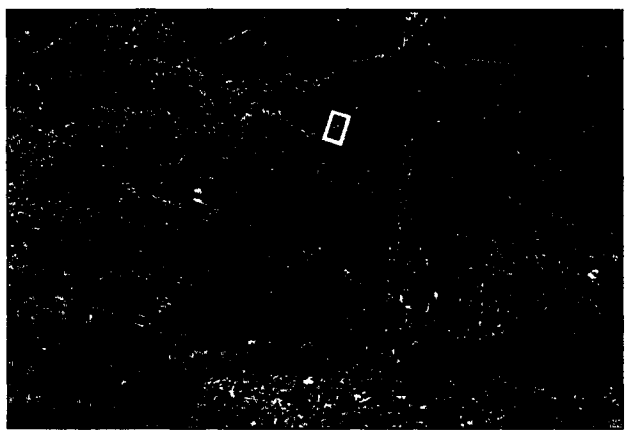

Figure 2.5 Large-scale Cross-stratification at Quarry Island. Large-scale cross-stratification of the sandstone lithofacies association of the Pass Lake Formation is shown in an outcrop from Quarry Island. GPS for scale, outlined in white.

Cheadle (1986a) described the plane-bedded facies as being primarily composed of horizontal laminae and thin beds, with secondary planar cross-beds and oscillation ripples. He also noted that, at Silver Islet, these are accompanied by scour and fill structures with coarser sandstone deposited within them. These structures are erosively overlain by the sandstones of the plane-bedded facies. Interbeds of calcareous and dolomitic mudstone and siltstone can also be found there. The well-sorted sandstone, horizontally-laminated sandstone/siltstone, and silty sandstone facies may be representative of the plane-bedded facies.

The cross-bedded facies described by Cheadle (1986a) consists of a 5-30 m thick unit of large-scale planar cross-beds. These cross-beds can be wedge-shaped or tabular, with individual sets reaching thicknesses of 1-10 m. Cheadle (1986a) noted that, at Channel Island, the cross-beds are interbedded with the plane-bedded facies, which partially overlies scour surfaces with pebbly sandstone infills.

The heterolithic facies of Cheadle (1986a), which only crops out on Channel Island, is composed of interbedded medium to very coarse-grained feldspathic wackes, arenites, and black shale. This facies may correlate with the poorly-sorted sandstone facies.

Based on drill core, the lower Fork Bay Member is dominated by interbedded, well-sorted and poorly-sorted, massive sandstone facies. The upper portion of the Fork Bay Member contains interbeds of the well-sorted, massive sandstone facies, the horizontally laminated siltstone/sandstone facies, and the ripple-laminated sandstone facies.

2.1.2.1 Well-sorted Sandstone Lithofacies

This facies is the most abundant unit of the Pass Lake Formation. It is a relatively well-sorted, purplish brown, medium-grained sandstone that appears to be faintly horizontally laminated. Some larger feldspar grains occur that range from 1-3 mm in diameter. Rare ripple laminae are also present. Series of well-sorted massive sandstone beds range from 10 cm to 600 cm in thickness. This lithofacies is interbedded with the poorly-sorted massive sandstone lithofacies.

2.1.2.2 Horizontally-laminated Sandstone/Siltstone Lithofacies Association

This lithofacies association is predominantly sandstone layers; composed of medium to fine-grained sandstone that may be graded, or have horizontal or low angle laminae. These beds can range from 1-600 cm in thickness. Massive siltstone beds, intercalated with the sandstone units, range from 1-50 cm in thickness. Areas of finely, horizontally laminated siltstone to sandy siltstone also occur. Individual layers of sandy siltstone are well-sorted and range from 1 to 100 cm thick.

2.1.2.3 Poorly-sorted Sandstone Lithofacies Association

This unit typically consists of purplish brown to buff medium-grained sandstone, although coarse to very coarse sandstone layers are present. Reduced spots, layers and areas are abundant. The sandstone contains copious amounts of small, elongate mudchips, 2 mm to 3 mm in length. Occasionally, mudchips may reach 1 cm to 2 cm in length. The poorly-sorted sandstone beds vary in thickness from 5 cm to 10 m, averaging 1 m.

2.1.2.4 Ripple-laminated Sandstone Lithofacies Association

This unit consists of ripple-laminated medium to fine-grained sandstone. Some ripple forms are preserved and laminae are covered with mudstone drapes. Individual laminae have a maximum thickness of 1 cm, although a series of ripple-laminated sandstones can range from 5-40 cm thick, although tend to be between 35 cm and 40 cm thick. This facies is interbedded with the well-sorted sandstone lithofacies association and the horizontally laminated siltstone/sandstone lithofacies association.

2.2 Rossport Formation

The Rossport Formation is the most complex of the Formations. The thickest accumulations of this Formation occur in the central portion of the basin, with the most prominent thinning towards the east. Cheadle (1986a) measured paleocurrents trending towards the east. The thickest accumulation of the Rossport Formation is 100 m.

The lower contact of the Rossport Formation is designated as the point in the stratigraphy where the sandstones of the Pass Lake Formation become less significant than the dolomitic mudstones of the Channel Island Member. Thus, there is commonly a transitional contact between the Pass Lake and Rossport Formation lithologies.

The Rossport Formation has been subdivided into ten facies associations: massive siltstone/sandstone, cyclic siltstone-dolomite, dolomitic mudstone, stromatolitic chert-carbonate, intraformational conglomerate, graded medium sandstone/siltstone, mudstone, sandy siltstone, thinly laminated fine sandstone/siltstone, and siltstone lithofacies associations. The lower portion of the Rossport Formation has a well-defined facies sequence. Above the contact with the Pass Lake Formation contact, there is typically a

sequence of lithofacies associations consisting of massive siltstone, sandstone, and dolomitic mudstone, followed by the cyclic siltstone-dolomite. The massive siltstone/sandstone lithofacies association may not be present if the Rossport Formation directly overlies the basement. The distribution of facies tends to be more varied above the cyclic siltstone-dolomite lithofacies association. The most common sequence begins with the dolomitic mudstone lithofacies association overlying the cyclic facies. This is followed by the sandstone/mudstone lithofacies association, stromatolitic lithofacies association, and a return to the sandstone/mudstone lithofacies association. The mudchip conglomerate lithofacies association, and sometimes the conglomerate lithofacies association, is interbedded with the upper sandstone/mudstone lithofacies association. Both of these lithofacies associations are overlain by interbeds of the sandy siltstone, laminated fine sandstone/siltstone, and siltstone lithofacies associations, but there is often an interbedded transition between them. Although the sandy siltstone, laminated fine sandstone/siltstone, and siltstone lithofacies associations interbed, there tends to be a general progression from sandy/siltstone dominated to siltstone-dominated lithofacies associations.

The main variations of the above sequence centre on the first introduction of the sandstone/mudstone lithofacies association (Appendix A). In some instances the sandstone/mudstone lithofacies association is first introduced in the middle of the cyclic siltstone-dolomite lithofacies association. In this case, there is the cyclic siltstone-dolomite lithofacies association, usually with the dolomitic mudstone lithofacies association accompanying it, occurring both below and above the first sandstone/siltstone layers. The sandstone/mudstone lithofacies association may also first occur below or above the stromatolitic lithofacies association. The mudchip conglomerate lithofacies association and

conglomerate lithofacies association may occur near the introduction of the sandstone/mudstone lithofacies association or farther up in the sequence.

2.2.1 Massive Siltstone/Sandstone Lithofacies Association

This lithofacies association is dominated by massive siltstone. The siltstone layers tend to be light to medium brick red with some reduction spots. In some cases dolomitic siltstone is present, mixing with non-dolomitic siltstone in swirly wisps. The siltstone may also contain coarser horizons of medium, coarse and very coarse sandstone. Mudstone units can be 45 cm to 450 cm thick, and are interbedded with poorly sorted, medium sandstone units that are 1 cm to 31 cm thick. Sandstone units are buff to greyish, with some pinkish tinges. Some of the layers contain coarser grains, whereas others are dominantly coarse-grained sandstone. A few of these sandstone layers are dolomitic, particularly when they are near the contact with the cyclic siltstone-dolomite lithofacies association.

2.2.2 Cyclic Siltstone-Dolomite Lithofacies Association

The cyclic siltstone-dolomite lithofacies association is unique within the Sibley Group. It consists of variations between two end members that are intimately interbedded (Figure 2.6a and 2.6c). For the purpose of logging, the cyclic siltstone-dolomite lithofacies association is generally divided into intervals dominated by one end member or the other, or by approximately even amounts of each. One end member is a red shale to siltstone, and the other is a dolomitic mudstone or dolomitic fine sandstone that is typically a shade of pink. The dolomitic fine sandstone member usually occurs in marginal areas of the basin.

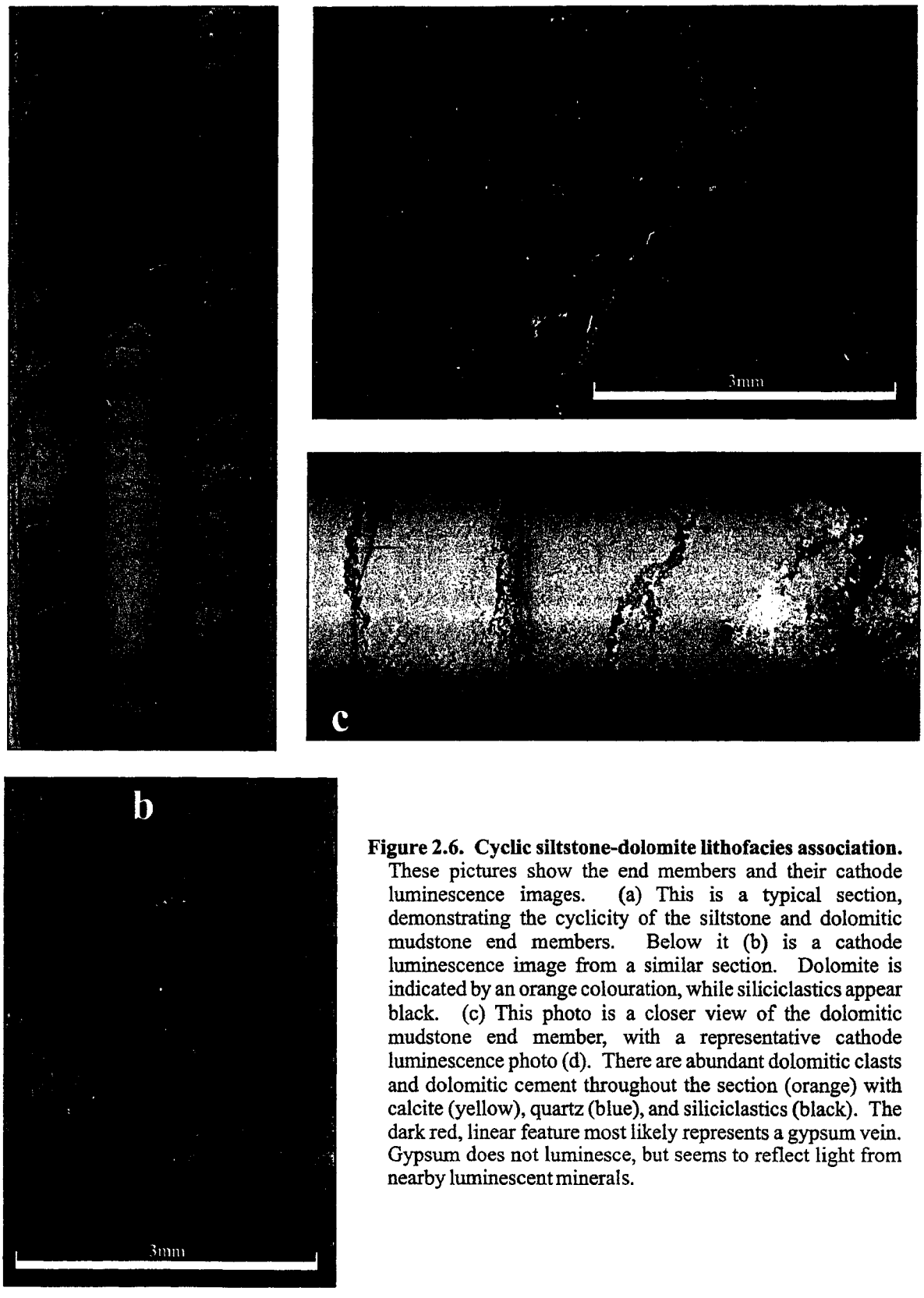

Figure 2.6. Cyclic siltstone-dolomite lithofacies association. These pictures show the end members and their cathode luminescence images. (a) This is a typical section, demonstrating the cyclicity of the siltstone and dolomitic mudstone end members. Below it (b) is a cathode luminescence image from a similar section. Dolomite is indicated by an orange colouration, while siliciclastics appear black. (c) This photo is a closer view of the dolomitic mudstone end member, with a representative cathode luminescence photo (d). There are abundant dolomitic clasts and dolomitic cement throughout the section (orange) with calcite (yellow), quartz (blue), and siliciclastics (black). The dark red, linear feature most likely represents a gypsum vein. Gypsum does not luminesce, but seems to reflect light from nearby luminescent minerals.

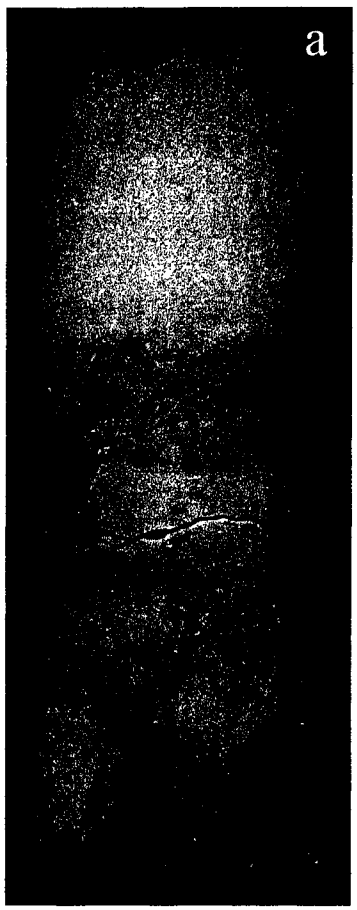

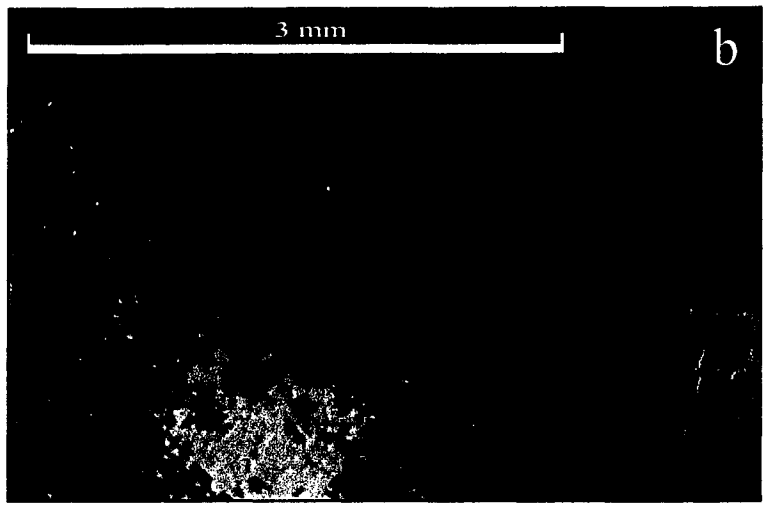

Figure 2.7 Gypsum, Dolomite, and Calcite Occurrences within the Cyclic Siltstone-Dolomite Lithofacies Association. (a) Gypsum layers can occasionally be found within this lithofacies association, ranging between 1 and 5 cm in thickness. This layer is 5 cm thick. (b) This photo shows a cathode luminescence picture of dolomitic mudstone (orange) with calcite (yellow). The elongate grains in the upper portion of this photo are gypsum. The growth patterns suggest that they formed after the dolomite. (c) This photo is a close-up of a dolomite and calcite vein in mudstone (black) under luminescence. It shows the intergrowths of calcite and dolomite, as well as the infiltration of dolomite into the mudstone. Below (d) is a siltstone conglomerate that has been cemented by gypsum (white).

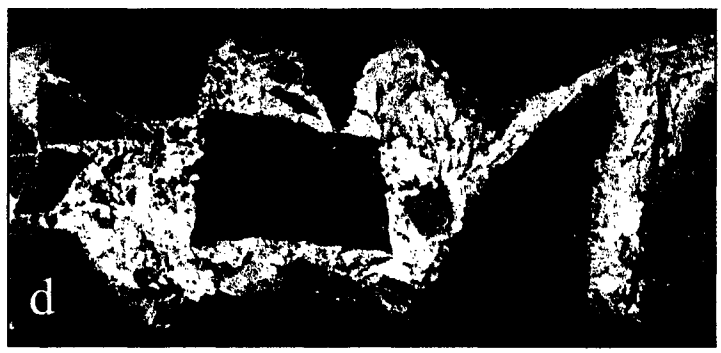

The shale/siltstone end member is commonly well consolidated, although thicker areas have friable sections. It is usually represented by a medium brick red silty shale, although both siltstone and shale do occur. Rare areas of very coarse sandstone may occur. Laminae within this member are seldom flat and are often disrupted by carbonate layers, and diagenetic carbonate and gypsum veins (Figure 2.6a). Shale/siltstone layers tend to be distorted around carbonate blobs and sink into cracks in the intercalated dolomitic mudstone laminae. Individual layers range from mm-scale to approximately 15 cm thick. Sections dominated by the shale/siltstone end member average 10-30 cm thick, but may be up to 130 cm thick.

The dolomitic mudstone end member is dark to medium brick red in colour, while the dolomitic fine sandstone end member tends to be buff. These layers frequently contain diagenetic calcite blobs and stringers, as well as gypsum nodules. Cathode luminescence photos show gypsum crystals growing off of a calcite vein, suggesting that these are early diagenetic processes (Figure 2.7b). Gypsum also seems to form 1cm to 5 cm layers within the dolomitic mudstone layers (Figure 2.7c). Mud stringers and granular looking bands may also be found within individual layers, probably indicating that they are actually multiple layers. The granular bands are typically found in dolomitic mudstone and consist of medium-sized quartz grains, although some coarse to very coarse grains also occur. The dolomitic mudstone fines away from these coarse bands. A few dolomitic mudstone layers near the bottom of the assemblage also have coarse siliciclastic horizons at the tops of the layers. In these cases, the extrabasinal granules can reach 5 mm in diameter and may be clast supported.

2.2.3 Dolomitic Mudstone Lithofacies Association

This lithofacies association seems to be restricted to directly below or directly above the cyclic siltstone-dolomite lithofacies association. It is often similar in appearance to the cyclic siltstone-dolomite lithofacies association in that it often has both light brick red to pink dolomitic mudstone and dark to medium brick red mudstone layers. However, it is completely dominated by mudstone, at times exclusively mudstone or shale in composition, and lacks the periodicity of the true cyclic siltstone-dolomite lithofacies association. The mudstone or shale beds typically range from 10 to 230 cm in thickness and averaging 50 cm thick, although they may occur on a mm-scale, and are interbedded with dolomitic or carbonaceous mudstone in sections up to 75 cm thick. Some shale layers have increasing carbonate content up through them. The dolomitic mudstone beds range from mm-scale laminae to 60 cm beds, averaging approximately 20 cm in thickness. Dolomitic mudstone layers increase as the cyclic siltstone-dolomite lithofacies association is approached.

2.2.4 Stromatolitic Chert-Carbonate Lithofacies Association

This lithofacies association is dominated by stromatolitic chert and carbonate laminae. It was thought to be a fairly continuous layer, and hence a marker bed, by Franklin (1980) and Cheadle (1986a,b). However, while it occurs locally as laterally extensive layers in outcrop, it has proven to be quite sporadic in drill core. Cheadle (1986a) divided this lithofacies association into four lithological elements: massive interbedded black chert and light grey carbonate, chert-carbonate sharpstone conglomerates, chert-carbonate crypt-algal laminites and columnar stromatolites, and evaporite minerals. The crypt-algal laminites have been identified as Stratifera (Cheadle, 1986a) and the columnar

stromatolites have been identified as Conophyton metula (Cheadle, 1986a). Cheadle (1986a) also identified pseudomorphs of sulphate minerals and halite within the crinkly laminae, and also observed that the chert appears to be an early replacement of carbonate, as well as noting the presence of pyrite and organic carbon within the chert.

All of Cheadle's (1986a) lithological elements have been found in drill core and outcrops. The crypt-algal laminites and columnar stromatolites are the most easily identifiable elements in drill core. The crypt-algal laminites (Figure 2.8) are usually not silicified, while the columnar stromatolites (Figure 2.8d) frequently are. Both gypsum crystals and halite pseudomorphs have been found. The stromatolitic facies is 0.8-1.4 m thick. Fine carbonate sandstone layers are interbedded with the crypt-algal laminites and limestone units.

An outcrop on Channel Island in Lake Superior (Figure 1.1) preserves the facies contacts between the stromatolitic lithofacies association and underlying units. The sequence begins with laminated medium-grained sandstone, with laminations fining upwards (Figure 2.8a). Draping foresets of trough cross-stratification indicate large wave ripples (Figure 2.8b). Areas within the laminated medium-grained sandstone unit are gradational from coarse to medium sandstone. Paleocurrents were also measured, giving 224°, 275°, and 100°.

Above this unit is a fine-grained sandstone unit, characterized by low angle cross-stratification and undulatory surfaces. One paleocurrent from the cross-stratification was measured as 132°. The layers are not graded, but often have thin, fissile mud caps. Overall the fine-grained sandstone unit increases its siltstone content upwards. The siltstone unit is

trough cross-stratified near the base, with paleocurrents at 130°, 160°, and 130°. Some layers are internally stratified, but overall become blocky, and more massive upwards.

The stromatolitic limestone unit lies directly above the siltstone unit. It is dominated by crinkly mat structures (Figure 2.8c), and some tepee structures have been observed. The stromatolitic layers are several millimetres thick, but may occur in packages of layers up to 2 cm thick. These layers and packages of layers are intercalated with very fine-grained carbonate sandstone layers that are mm-scale to 15 cm thick. Around the point of Channel Island, stratigraphically above the stromatolitic unit, is an intraformational conglomerate consisting of sandstone and siltstone clasts with caliche layers. A single eroded boulder was found containing large clasts of carbonaceous fine sandstone and marl, re-cemented by chert.

Another outcrop of the stromatolitic facies, on Black Sturgeon Road (Figure 1.1), preserves an intraformational conglomeratic unit in close proximity to the stromatolite unit. Both outcrops are low and rubbly and occur on opposite sides of the road from each other, making precise stratigraphic positioning difficult. The conglomeratic unit appears to consist of marly fine sandstone and some stromatolitic pieces with a chert matrix. The intact stromatolitic chert-carbonate lithofacies association consists of stromatolitic layers, and packages of layers, intercalated with very fine-grained carbonate sand lenses and layers. These are similar to the sections at Channel Island (Figure 2.8c), only they tend to be more silicified and less well preserved.

Figure 2.8. Stromatolitic Chert-Carbonate Lithofacies Association. The Channel Island sequence consists of upward thinning sandstone beds (a) and rippled fine sandstone (b), overlain by the crinkly laminae of the stromatolitic carbonate lifthofacies association (c). The crinkly laminae are intercalated with fine sandstone laminae. A silicified stromatolite from drill hole HE-02-02 is also shown (d).

2.2.5 Intraformational Conglomerate Lithofacies Association

The intraformational conglomerate lithofacies association consists of two slightly different conglomeratic facies, although these differences are not significant enough to preclude them being considered one lithofacies association. For descriptive purposes, one facies is referred to as a mudchip conglomerate (2.9b) and the second is simply termed conglomerate (2.9a).

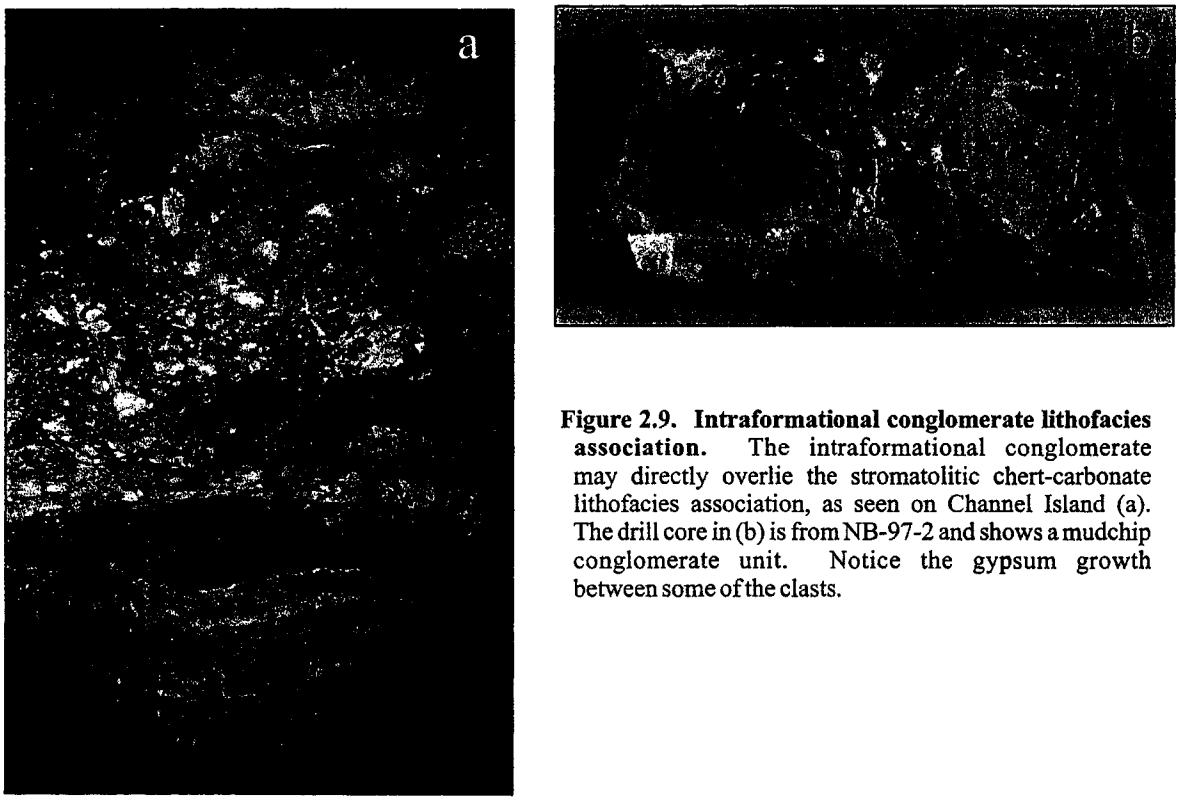

Figure 2.9. Intraformational conglomerate lithofacies association. The intraformational conglomerate may directly overlie the stromatolitic chert-carbonate lithofacies association, as seen on Channel Island (a). The drill core in (b) is from NB-97-2 and shows a mudchip conglomerate unit. Notice the gypsum growth between some of the clasts.

The mudchip conglomerate facies is relatively rare compared to most of the facies, although it is more common than the stromatolitic and conglomeratic facies. The mudchip conglomerate usually has a mudstone matrix and is matrix supported, although clast supported areas can be found. It consists predominantly of mud chips and blocks, but may

also contain dolomitic and gypsiferous clasts, as well as an occasional semi-lithified clast from the sandstone units. Blocks within the conglomerate are rounded and often elongate, although they tend to be less elongate when sandstone clasts are present. Some of the clasts have preserved layering within them. When present, they are crumpled and deformed, indicating soft sediment deformation. The mudchip conglomerate layers are 10 to 25 cm thick and may occur as isolated layers are in a series of layers. Individual clasts are mm-scale to 2 cm in diameter. The mudchip conglomerate may also appear in close proximity to the conglomeratic lithofacies association.

The conglomerate facies is an intraformational conglomerate, consisting of clasts of siltstone, fine sandstone, shale, and dolomite. Many clasts have preserved laminations within them. Clasts sizes are quite varied, ranging from pebble-size to boulder-size. Boulder-size clasts are extremely difficult to distinguish in drill core, but are clearly seen in an outcrop on Black Sturgeon Road, stratigraphically above the stromatolitic chert-carbonate lithofacies association. Here, the conglomerate beds reach tens of centimetres to one metre in thickness. The matrix is generally composed of sandy siltstone. Overall, sorting is quite poor. Many of the conglomerates are matrix-supported, although some may be locally clast-supported and a few of beds become matrix-supported upwards.

2.2.6 Graded Medium Sandstone/Siltstone Lithofacies Association

This lithofacies association is dominated by buff to pinkish red, massive, medium-grained sandstone. Sandstone units may also be fine, coarse, or very coarse grained and may be graded and massive or cross-stratified. Massive graded beds constitute the majority of the sandstone beds. Some climbing ripples have been found at the base of, and grading

into, the cross-stratified units. Many of the sandstones have carbonate cements, particularly those sandstones near the contact with the cyclic facies. The sandstone beds range from 5 to 400 cm in thickness, averaging approximately 40 cm thick. Successive sandstone layers may reach thicknesses of several metres before being interrupted by a siltstone bed. This lithofacies association is interbedded with siltstone beds of the siltstone lithofacies association, as well as the dolomitic mudstone lithofacies association and, to a lesser degree, the silty shale lithofacies association. The sandstone/siltstone lithofacies association is confined to the section of the Rossport Formation directly above the cyclic siltstone-dolomite or dolomitic mudstone lithofacies associations and below the mudstone, sandy siltstone and laminated fine sandstone/siltstone lithofacies associations.

2.2.7 Mudstone Lithofacies Association

The mudstone lithofacies association is relatively rare in the stratigraphy, but quite distinct. It consists of dark purplish brick red shale and mudstone intercalated with calcite layers. Individual layers within it are on the mm-scale, and the entire unit averages only 5 cm, although it can be up to 30 cm in thickness. The mudstone lithofacies association is interbedded with the siltstone and sandy siltstone lithofacies association.

2.2.8 Sandy Siltstone Lithofacies

The sandy siltstone lithofacies is typically massive, although some areas have vague horizontal laminae preserved. These laminae are obliterated by extensive mottling from reduced areas and distortion related to carbonate crystallization within the sediment. The reduced areas tend to cover large areas, with only some constrained to reduction spots.

There are abundant carbonate nodules, ranging from mm-scale up to 5 cm thick. Many areas of the sandy siltstone lithofacies association have high carbonate contents. Portions of this unit appear to have sections that may represent soil horizons. These sequences begin with a carbonate-rich sandy siltstone that progresses upward to sandy siltstone with nodular carbonate layers, topped with friable, dark purple shaley siltstone. The sandy siltstone lithofacies ranges from 30 cm to 400 cm thick, and is interbedded with the siltstone, mudstone, and laminated siltstone/fine sandstone lithofacies associations. Some conglomerate and mudchip conglomerate beds may extend up into this lithofacies.

2.2.9 Thinly Laminated Fine Sandstone/Siltstone Lithofacies Association

This lithofacies association is composed of fine sandstone layers that often grade to siltstone and are capped by dark red mudstone. The fine sandstone layers are lighter in colour, often contain some dolomite, and may be associated with carbonate nodules. Intervals of laminated fine sandstone/siltstone are generally 5 to 90 cm thick. Individual beds of fine sandstone and siltstone are cm-scale. This unit is predominantly interbedded with the siltstone facies, and occurs at approximately 3 m intervals throughout the siltstone section above the sandy siltstone lithofacies association.

2.2.10 Siltstone Lithofacies

All of the lithofacies associations above the cyclic siltstone-dolomite, dolomitic mudstone and stromatolitic lithofacies associations are interbedded with the siltstone lithofacies. The siltstone facies is composed of siltstone to silty shale, and is generally massive or contains fine laminae. Areas with relatively high shale content tend to be highly

friable, although the majority of this facies has limited friability. Reduction spots are relatively abundant, although reduced areas may spread out into large mottles. The siltstone facies commonly reaches a thickness of 300 cm, but may range from 50 cm to 10 m thick. This facies is gradational with the facies of the Kama Hill Formation.

2.3 Kama Hill Formation

The Kama Hill Formation is approximately 10 m to 50 m thick. According to Cheadle (1986a), the paleocurrents for this Formation trend towards the east. It is thickest in the central portion of the basin, thinning towards the east. The Kama Hill Formation is divided into four lithofacies associations, and is dominated by the horizontally-laminated fine sandstone/siltstone lithofacies association and the mudcracked fine sandstone lithofacies association. The rippled fine sandstone/siltstone lithofacies association and horizontally-laminated mudstone lithofacies association are less common, with the latter being the least common. The lithofacies associations tend to form sequences of horizontally-laminated fine sandstone/siltstone, rippled fine sandstone, and rippled siltstone with mud drapes. Occasionally, intervals of thick silt, horizontally-laminated shale/mudstone, and friable siltstone/shale layers occur. In some of the drill core, intervals of mudcracked sandstone/siltstone and horizontally-laminated mudstone are prevalent directly above the Rossport Formation, while the rippled sandstone facies dominates the top of the Kama Hill Formation.

2.3.1 Horizontally-laminated Fine Sandstone/Siltstone Lithofacies Association

This lithofacies association consists of layers of horizontally laminated fine sandstone and fine sandstone grading to siltstone, which commonly have horizons of very fine mudchips (Figure 2.10a). Some siltstone layers are contorted, have disruptive mottling, or contain contorted or folded mud wisps in them. Layers may have distinct boundaries or may be only distinguishable by slight changes in grain size. The individual fine sandstone to siltstone layers range from 1-2 cm in thickness. Units of horizontally-laminated fine sandstone/siltstone range from 5-800 cm, but are more typically 60 cm thick.

2.3.2 Mudcracked Fine Sandstone/Siltstone Lithofacies Association

This lithofacies association is dominated by fine sandstone to siltstone, with layers separated by thin mm-scale purple mud laminae. Individual fine sandstone and siltstone laminae are typically 3-5mm thick. Some thicker muddy siltstone layers do occur. The mudcracked fine sandstone lithofacies association has extensive mudcracks that often extend through multiple sediment layers (Figure 2.10a,b), obscuring the original layering. Mudcracked areas often extend for 2-10 cm. Elongate mudchips, 1-20 mm in diameter, tend to occur in a roughly horizontal alignment at the bases of some sandy layers. Units of the mudcracked fine sandstone/siltstone lithofacies association range from 3-95 cm thick, but are more commonly 5-10 cm thick.

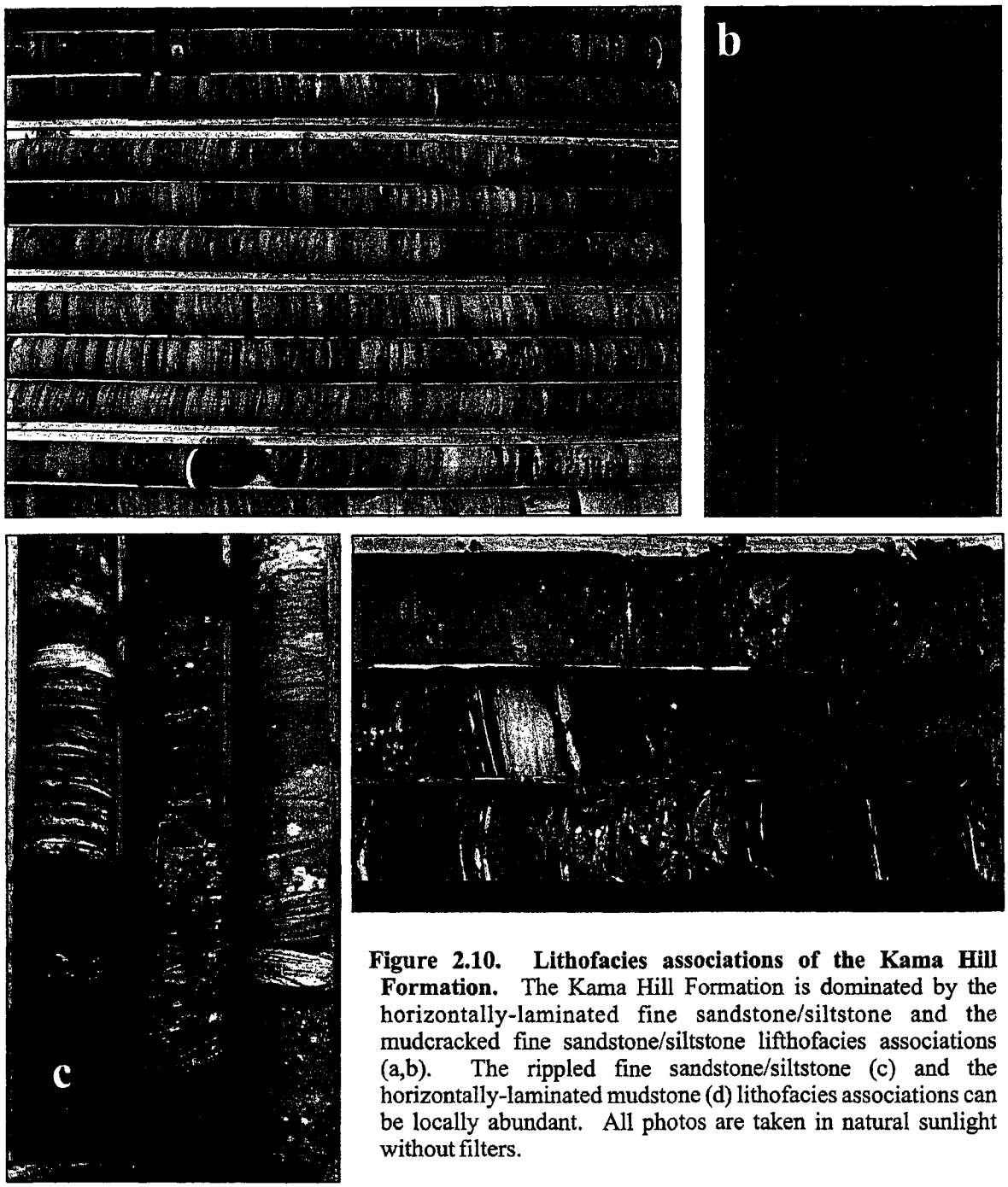

Figure 2.10. Lithofacies associations of the Kama Hill Formation. The Kama Hill Formation is dominated by the horizontally-laminated fine sandstone/siltstone and the mudcracked fine sandstone/siltstone lifthofacies associations (a,b). The rippled fine sandstone/siltstone (c) and the horizontally-laminated mudstone (d) lithofacies associations can be locally abundant. All photos are taken in natural sunlight without filters.

2.3.3 Rippled Fine Sandstone/Siltstone Lithofacies Association

Ripples may be found in units up to 25 cm thick, as individual layers, or isolated ripples of fine sandstone or siltstone in mudstone (Figure 2.10c). Packages of rippled sandstone/siltstone may dominate over sections up to 120 cm thick. Individual layers are generally 1-2 cm thick. The ripples tend to be fine sandstone lower in the Kama Hill Formation, becoming rippled siltstones higher in the sequence. The thickness of the mud caps on the ripples also increases upwards, from several mm to 2 cm thick.

2.3.4 Horizontally-laminated Mudstone Lithofacies

This facies consists of thin laminated to massive mudstone, with individual laminae typically on the mm-scale, although they may range from 2-10 cm thick. Many of these layers are extremely fissile (Figure 2.10d), while others are contorted or folded.

2.4 Outan Island Formation

The Outan Island Formation is a new addition to the Sibley stratigraphy. It has only been identified in five drill cores in the southeastern area of the Sibley Basin. One of the drill cores that sample this Formation was drilled in Hele Township, while the other holes are located in Nipigon Bay. However, the Nipigon Bay Formation has already been used to describe the topmost Formation of the Sibley Group, so this Formation is named after Outan Island, the closest named feature to a complete representation of the Formation.

There have been no paleocurrents measured for the Outan Island Formation as it has only been recognized in drill core. This Formation has a maximum thickness of 250 m.

The Outan Island Formation has been divided into five lithofacies associations: the mudstone, laminated sandstone/mudstone, siltstone, sandstone, and conglomerate lithofacies associations. The lower Outan Island Formation is dominated by the siltstone, mudstone and laminated sandstone/mudstone lithofacies associations, in decreasing order of importance. Some units of the sandstone lithofacies association occur in the lower Outan Island Formation as well, but are typically only 10 cm and rarely reach 150 cm, whereas they are 100 cm to 1500 cm thick in the upper Outan Island Formation.

The upper Outan Island Formation is dominated by thick units of the sandstone lithofacies association with minor alternations of the siltstone, mudstone, and laminated sandstone/ mudstone lithofacies associations. The conglomerate lithofacies association is only found alternating with the sandstone lithofacies association, and seems to occur both above and below the transition between the upper and lower Outan Island Formation.

2.4.1 Mudstone Lithofacies

The mudstone lithofacies consists of very finely laminated light red to peach shale and bright red mudstone alternating with massive mudstone. Within the laminated units, some of the mudstones grade vertically into shale laminae, while other mudstone and shale laminae are distinctly separated. Individual layers may have shale chips floating at the base and some have silicifed carbonate nodules near the tops of the layers. These units range from 6 cm to 35 cm in thickness.

2.4.2 Laminated Sandstone/Mudstone Lithofacies Association

This unit consists of fining upward layers of buff fine sandstone to reddish siltstone capped with brick red mudstone (Figure 2.11). The sandstone and mudstone layers are approximately the same thickness throughout most of the laminated sandstone/mudstone lithofacies association, although the mudstone laminae may be shaley partings instead. Very small rip-up mudstone clasts are frequently found at the base of the sandstone layers. Deep mudcracks are occasionally found penetrating through several layers.

2.4.3 Siltstone Lithofacies Association

The siltstone lithofacies association is dominated by brick red siltstone with abundant reduction spots. It is typically massive with rarer muddy areas, consisting of horizontal laminae and shale, mud wisps, and layers of mud blocks. Sections of the siltstone lithofacies association also have very fine sandstone that commonly exhibits ripple lamination. Siltstone ripple lamination can also be found. These facies of the siltstone lithofacies association can generally occur in two specific sequences. One sequence begins with sandy siltstone with ripple lamination and is overlain by horizontally laminated mudstone, while the other sequence is sandy siltstone with ripple lamination, overlain by ripple laminated siltstone, overlain by massive siltstone with mud wisps. Contacts are sharp at the base of these sequences, often containing mud rip-up clasts from underlying layers, although sandy areas sometimes have soupy contacts. The siltstone sequences are several metres thick, but individual layers within it are no more than 2 cm thick.

2.4.4 Sandstone Lithofacies

The sandstone lithofacies consists of coarse and medium-grained sandstones with muddier areas defining layer boundaries. The sandstones are predominantly massive, some of which are normally or reversely graded. Horizontal laminations and rarer ripple laminations also occur. Some of the sandstones contain large blocks of mudstone and mudchips. The mud blocks fall into three categories based on differences between them and their position within the sandstone units. The first category, consisting of basal mudchips, appears to be rip-up clasts from underlying layers. They are angular and blocky and some of the mud laminae remain intact. The second category is mudchips that appear to float in the centre of a sandstone layer. These mudchips are angular and elongate to blocky with no mud laminae associated with them. The third mudchip category seems to be restricted to the tops of the sandstone units. In these cases, there are mudstone layers overlying the sandstone unit. Here, sections of the lower mudstone laminae appear to have been delaminated and sunk into the sandstone surface. Some mudstone layers have been pulled apart or contorted, while other mudstone layers simply have wispy tendrils that penetrate into the underlying sandstone layer. The sandstone layers often have wavy mud caps. Some of the sandstone units are associated with thin laminae of very coarse sandstone that ranges in thickness from that of a single very coarse sand grain to 1 cm thick. The sandstone lithofacies association can reach 16 m, but is more typically 1 to 2 m thick. Individual sandstone layers are 16 cm to 100 cm thick.

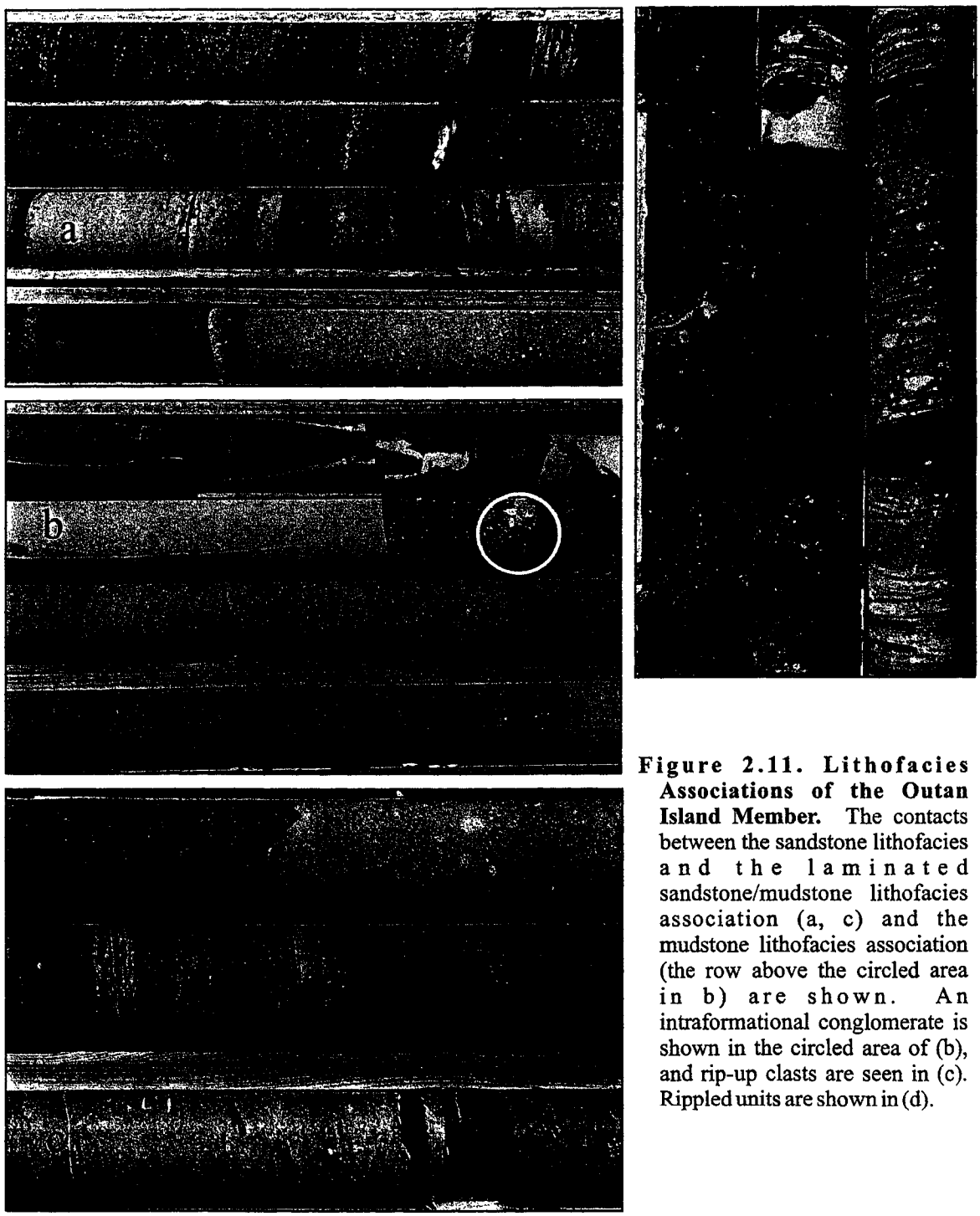

Figure 2.11. Lithofacies Associations of the Outan Island Member. The contacts between the sandstone lithofacies and the laminated sandstone/mudstone lithofacies association (a, c) and the mudstone lithofacies association (the row above the circled area in b) are shown. An intraformational conglomerate is shown in the circled area of (b), and rip-up clasts are seen in (c). Rippled units are shown in (d).

2.4.5 Conglomeratic Lithofacies

The conglomeratic lithofacies is intraformational, usually consisting of matrix-supported clasts of mudchips and blocks grading upward to a clast-supported conglomerate with clasts of mudstone and sandstone. A few of the conglomerates are not intraformational and contain mafic and granitic clasts. The basal mudchips are angular, while the larger mud fragments are rounded. The matrix is siltstone grading upward to medium sandstone. The matrix may have faint laminations, particularly around the basal mud blocks. Clasts range from mm-scale to 5 cm in diameter, and are commonly poorly sorted. Some conglomerates may have fining or coarsening upward trends in clast size. Other conglomerates strictly consist of mm-scale clasts, while another type are isolated occurrences of large, 5 cm diameter clasts at the contacts between sandstone layers (Figure 2.11). In these cases the sandstone layers are depressed around the clasts. The conglomerate lithofacies ranges between 5 cm and 45 cm, and averages 20 cm thick.

2.5 Nipigon Bay Formation

The Nipigon Bay Formation is also a relatively new addition to the Sibley stratigraphy. It is only present in two drill holes in Nipigon Bay and one outcrop on a small part of Simpson Island. The total thickness appears to be 450-500 m, based on drill core analysis. It has been divided into two lithofacies associations: the cross-stratified sandstone lithofacies association and the horizontally-laminated sandstone lithofacies association. The cross-stratified lithofacies association dominates the Nipigon Bay Formation.

2.5.1 Cross-stratified Sandstone Lithofacies

The cross-stratified sandstone lithofacies consists of alternating units of high-angle and low-angle cross-stratified medium-grained quartzarenite (Figure 2.12). Occasionally, some of the sandstone layers show reverse grading. Individual cross-stratified laminae are distinguished by faint colour variations, and are typically 1 cm to 3 cm thick. The surfaces of cross-sets are often oxidized to a reddish purple colour, while the majority of the sandstones are buff. Some mottling may occur across layers. Individual sets of high-angle cross-stratification dominate this lithofacies, and range from 50 cm to 350 cm thick, averaging approximately 100 cm thick. Unoriented cross-stratification in drill core contains ripple layers within the high-angle facies that are completely reversed relative to one another. These sets are typically stacked in 4 m to 40 m thick units, but are generally 10 m thick. The low-angle cross-stratified facies ranges from 13 cm to 230 cm thick, and averages approximately 30 cm thick. Stacked sets of this facies are usually 10 m thick, but can reach a thickness of 70 m. Occasionally, ripple forms are preserved along layer contacts. There is a gradational sequence from the horizontally laminated sandstone to the low-angle cross-stratified sandstone to the high-angle cross-stratified sandstone.

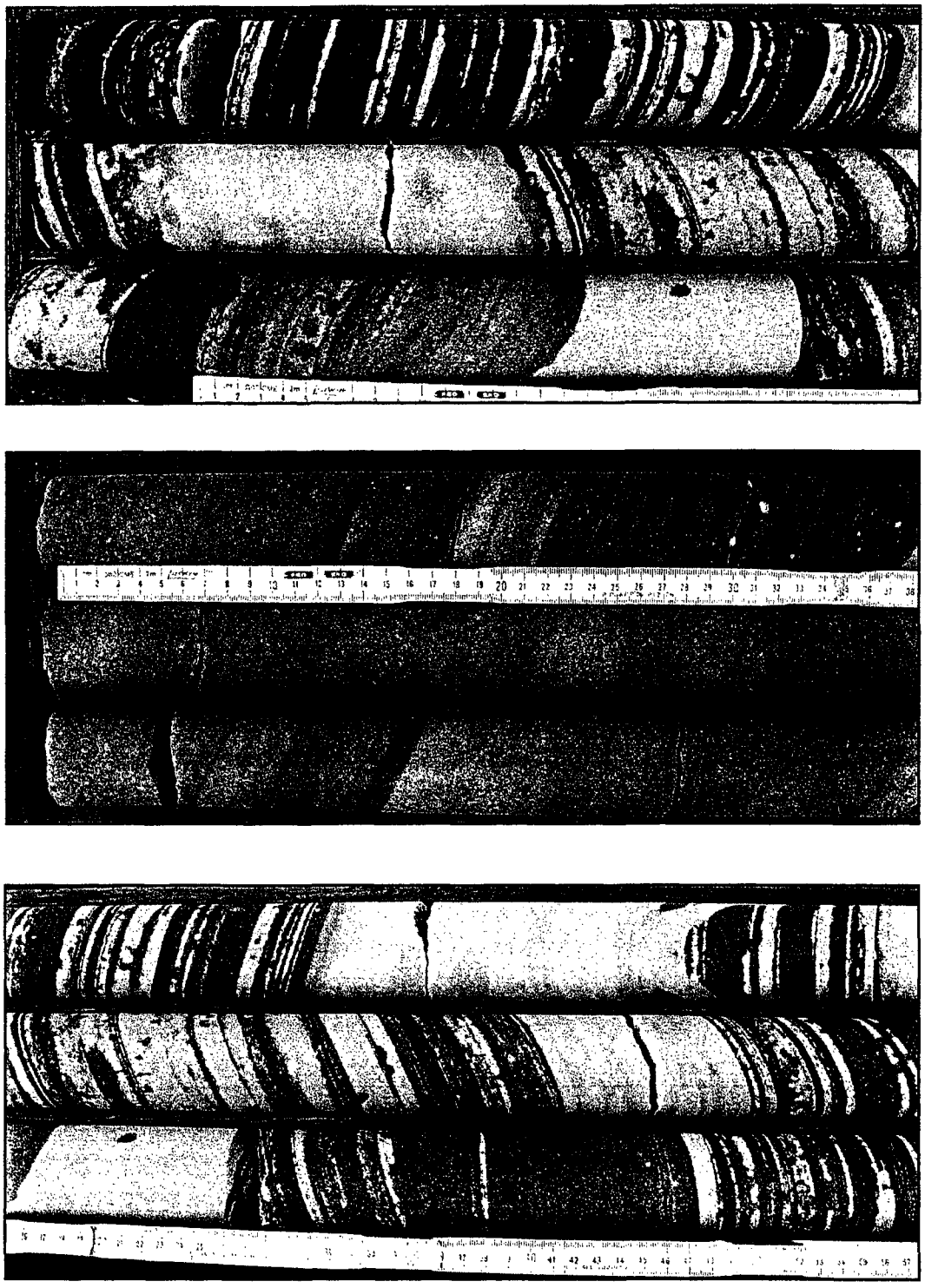

Figure 2.12. Lithofacies of the Nipigon Bay Formation. Three photographs are shown, representing the cross-stratified sandstone lithofacies. A ruler is provided for scale.

The one outcrop of the Nipigon Bay Formation, on Simpson Island, preserves a large-scale dune-form. This dune-form is approximately 15 m in height and is comprised of medium-grained sandstone cross-beds ranging from 10 cm to 50 cm thick. A toe-set wedge is preserved within the outcrop. Paleocurrents were measured to be 125°, 178°, 145°, 135°, 108°, 130°, and 110°.

2.5.2 Horizontally-laminated Sandstone Lithofacies Association

This lithofacies association is dominated by medium-grained sandstone, although coarse sandstones and some muddy sandstones are not uncommon. These units are 1 m to 80 m thick, but are commonly 3 m thick. Individual laminae are a few millimetres to a couple of centimetres thick. Muddy sandstone laminae tend to be slightly thinner, have a reddish colouration, and may be fissile. Massive sandstone beds may also be interbedded, ranging from decimetres to 3 m thick. The horizontally-laminated sandstone lithofacies association is more likely to be mottled than the cross-stratified sandstone lithofacies association.

2.6 Depositional Environments

Cheadle (1986a,b) gave interpretations for the Loon Lake and Fork Bay Members of the Pass Lake Formation, the Channel Island, Middlebrun Bay and Fire Hill Members of the Rossport Formation, and the Kama Hill Formation. Here, the depositional environments are examined by Formation to maintain continuity with the previous section,

although sub-environment divisions will become apparent and be assigned to a Member. Some of his interpretations are still valid, while others have been modified in light of the new three-dimensional understanding of the Sibley Basin derived from drill core. Depositional environment interpretations for the Outan Island and Nipigon Bay Formations will also be discussed. This new analysis of depositional environments should assist in reconstructing the basin architecture and history of the Sibley Group.

2.6.1 Pass Lake Formation

Cheadle (1986a,b) suggested that the Pass Lake Formation represents an alluvial fan. He identified the Loon Lake Member as a debris flow deposit. This was based on the basal conglomerate's muddy matrix, disrupted framework, and lack of stratification. However, Cheadle (1986a,b) also noted that some of the Loon Lake conglomerates were graded from clast-supported to matrix-supported, which he took to indicate water-lain bedload deposits. Miall (1996) noted that matrix-supported and graded conglomerates indicate debris flows, while clast-supported and stratified conglomerates suggest fluvial influences. Cheadle suggested that these latter conglomerates were episodic sheet-floods rather than forming in alluvial channels, due to the lack of internal cross-stratification and the presence of caliche crusts.

Cheadle (1986a,b) considered the heterolithic facies of the Fork Bay Member to be laterally equivalent to the Loon Lake Member. Because of this, as well as the textural immaturity of the sandstones and the existence of medium-scale cross-beds, ripple cross-stratification, and plane-bedded structures, Cheadle (1986a,b) interpreted the heterolithic facies to be turbidites. These would have formed in a lacustrine environment, proximal to

the alluvial fan. However, no sedimentological evidence has been found to support the presence of turbidites.

The cross-bedded and plane-bedded facies of Cheadle (1986a,b) were thought to have formed on the alluvial fan under different flow conditions during sheet-floods. The cross-bedded facies was thought to indicate an ephemeral braided stream deposit based on the association of horizontally-laminated sandstones, low-angle cross-sets, and a coarse pebble lag. Cheadle (1986a) also noted that the ripple-form laminations that are present within the cross-bedded facies suggest a subaqueous environment, as they are seldom preserved in aeolian dunes. He envisioned the horizontally-laminated sandstones developing during the initial ebbing of a flood, under upper flow regime conditions. With continued ebbing, low-angle cross-beds would form in transverse bars. Later reworking in a subaerial environment that prevailed in between flood events would result in a deflation pebble lag, which Cheadle (1986a) hypothesized to be a relict desert pavement.

The plane-bedded facies represents rapid deceleration of unchannelled sheet-floods and the formation of alluvial fan sand flats (Cheadle, 1986a), which produced sequences of scoured bases, planar laminations, planar cross-beds, ripple cross-laminations, oscillation ripples and a suspension cap. This sequence records a cycle that progresses from upper flow regime to lower flow regime to standing water (Cheadle, 1986a; Collinson, 1996), similar to the sand-flat cycles of the Upper Triassic red beds in Nova Scotia (Hubert and Hyde, 1982). The presence of desiccation cracks, halite casts, and caliche layers suggest subaerial exposure in a semi-arid environment (Collinson, 1996). The plane-bed facies becomes more abundant basin-ward, as would be expected from other braided rivers, such as the Platte River (Smith, 1970). Suspension deposits become more evident further

towards the basin centre and up-section. Cheadle (1986a) suggested that the Silver Islet outcrop represents reworking of the distal alluvial fan by an expanding lacustrine body.

The original interpretation of these units by Franklin (1970) and Franklin *et al.* (1980) seems more plausible. Franklin (1970) hypothesized that the basal conglomerate was derived from weathering and wave action against Archean basement or an uplifted fault scarp of Gunflint Formation rocks. He suggested the presence of a fault scarp based on the extreme angularity of the Gunflint clasts, very poor sorting, and concentration of the coarsest material in the southwest conglomerates. The maturity of the conglomeratic material in the Lake Nipigon area was thought to indicate a low-energy weathering environment. Franklin *et al.* (1980) believed that the conglomerate lenses were deposited during rapid, fluvial sedimentation in topographic lows of the pre-Sibley surface. Franklin (1970) interpreted the presence of ripple marked and cross-bedded strata interbedded with the conglomerate as indicating a littoral zone, similar to that of some shallow clastic seas (Johnson and Baldwin, 1996). Wave action prevents coarse-grained sediment from being transported into the basin. In a transgressive sequence, the coarse material is over-lapped by sand sheets that become reworked by waves (Johnson and Baldwin, 1996), similar to the sequence seen in the Sibley Group where the conglomerate lenses are overlain, and partially destroyed, by the sandstone lithofacies association.

The most convincing evidence to support the lacustrine model proposed by Franklin (1970) and Franklin *et al.* (1980) is in the sedimentary structures of the sandstone lithofacies association. Franklin *et al.* (1980) notes the presence of very low-angle cross-beds within the lower 5 m of the sandstone units and the dominance of oscillation ripples throughout the Pass Lake Formation. These features seem to indicate the existence of a

beach at the base of the sandstone lithofacies association, overlain by subaqueous sheet flows, interpreted as turbidites by Cheadle (1986a), over a shallow lacustrine basin. Franklin *et al.* (1980) thought the upward decrease in bed thickness was due to progressive expansion of the lake during a northward strandline migration. They originally hypothesized a northern transport direction based on the presence of chert grains with algal microfossils, similar to those in the Gunflint Formation, found in northern outcrops of the Pass Lake Formation. However, Cheadle (1986a) showed that paleocurrent directions indicate a transport direction towards the southeast. Franklin (1970) thought that the Silver Islet (Figure 1.1) outcrop was proximal to the shore, deposited during rapid sedimentation, while the greater maturity of the outcrop at the Enterprise Mine (Figure 1.1), where oscillation ripples are particularly common, was due to reworking by wave action.

In summary, Cheadle (1986a) envisioned an alluvial fan forming off of topographic lows and thinning towards the basin centre, where it encountered an expanding water body. Franklin (1970) and Franklin *et al.* (1980) thought that most of the conglomerates were formed near fault scarps and reworked by waves, while some of them were deposited in fluvial deposits in topographic lows. These are overlain by subaqueous sand sheets that were deposited in a lake, thinning upward as the water mass expanded.

2.6.2 Rossport Formation

Cheadle (1986a,b) interpreted the Rossport Formation as representing a lacustrine environment. The cyclic siltstone-dolomite lithofacies association is common to many ancient saline lake deposits, reflecting the cyclic variations in lake hydrology (Talbot and Allen, 1996). The calcitic blebs, chert nodules, evaporite minerals (gypsum), and pseudomorphs found within the cyclic siltstone-dolomite lithofacies and overlying dolomitic mudstone lithofacies are common in playa lakes, such as the Ebro Basin in Spain (Salvany *et al.*, 1994), and the Officer Basin in Australia (White and Youngs, 1980). The presence of the sandstone facies indicates basin margins and areas proximal to rivers or alluvial fans, while finer grained facies occur towards the basin centre (Smoot and Castens-Seidell, 1994). It is common for sand sheets to develop in broad unconfined channels on plains bordering playa lakes, and would have been particularly predominant over channelized flows in the absence of vegetation (Schumm, 1963; Miall, 1985, 1996).

Desiccation cracks, gypsum nodules, adhesion ripples, and friable mudstones become prevalent above the cyclic siltstone-dolomite lithofacies association, which has been interpreted as a damp mudflat by Cheadle (1986b), but may more accurately be compared to a sabkha. The dolomitic mudstones above the cyclic siltstone-dolomite lithofacies association contain solution load structures, growth faults and polygonal deformation structures associated with evaporite crusts on mud flats surrounding playa lakes (Smoot and Castens-Seidell, 1994) and appears similar to sabkha sediments (West *et al.*, 1979). The presence of gypsum and chert nodules, as well as hematitic soil and caliche layers, also supports the sabkha interpretation. Hematitic soils form in arid environments, appearing as brownish-yellow horizons overlying red, brown or ochre clay that is commonly illuviated (Collinson, 1996). In semi-arid environments, fersiallitic soils

dominate. The weathering in these soils is less complete than in ferruginous soils, and may produce calcitic nodules, similar to those found in the Rossport Formation. These nodules are caliche horizons and may occur as veins or elongate nodules, forming nearly continuous layers as maturity increases (Machette, 1985).

Cheadle (1986a) speculated that the dolomitic mudstones were deposited in ephemeral playa lakes, and the mudstones settled out during flash flood events. The overall paucity of coarse sediments through these units, except around marginal zones may indicate that the basin was shallow with low relief, similar to the Mercia Mudstone Group of Great Britain (Talbot and Allen, 1996). The Mercia Mudstone is dominated by dolomitic red mudstone, containing vague horizontal laminae, desiccation structures, and nodular gypsum horizons. Silt-sized grains have been found within dolomitic mudstone layers and been interpreted as wind-blown sediment. Further away from the cyclic siltstone-dolomite lithofacies association, there is an abundance of sand patch fabric, which has been interpreted as aeolian lags by Smoot and Castens-Seidell (1994). These sediments closely resemble the units of the Rossport Formation, suggesting that they also were deposited in a shallow, semi-arid basin with wide alluvial plains.

Above this succession of clastic and chemical sabkha deposits, there is a sudden influx of massive sand beds, which may occur directly below, but more commonly above, the stromatolitic facies of the Middlebrun Bay Member. Based on the distribution of these sandstone units in drill core, they have been used to distinguish the lower boundary of the Fire Hill Member. This boundary is different from that of Cheadle (1986a), who preferred to include the sandstones with the Channel Island Member.

Cheadle (1986a,b) thought that the stromatolite lithofacies occurred during a period when clastic input was restricted. He believed that there was one shallow lake that may have reached pH of 9-10, based on the early silicification of the stromatolites. Cheadle (1986b) also pointed to halite pseudomorphs to indicate alkalinity fluctuations. However, the stromatolitic facies is much more isolated than Cheadle (1986a,b) speculated. It is probable that the stromatolites occurred along the shorelines of partially restricted bays where alkalinity reached optimal conditions rather than throughout the entire shallow lake. These restricted conditions could have been caused by the influx of sand sheets into the basin, which initially occurred around the same time and may have provided the barriers to isolate parts of the lake, where the stromatolites would have formed during periods of low sedimentation between sheet floods. This would also account for the stromatolites occurring at slightly different stratigraphic horizons. Truc (1978) described a similar sequence of an isolated stromatolite unit found above an evaporitic sequence during the final fill stages of the basin. He suggested that this was due to the decreasing rate of subsidence and the near-full stage of the basin.

According to Cheadle (1986b), clastic sedimentation resumed, due to the onset of a wetter climate or uplift. He pointed to the lack of coarse sediment fractions and the absence of evidence for subaerial exposure as suggesting deposition away from lacustrine margins. Cheadle (1986b) suggested that the conglomerates within the upper portion of the Rossport Formation could represent intrusive sedimentary breccias.

However, the examination of drill core reveals that Cheadle's (1986a,b) observation about the lack of coarse sediment is not quite correct. Thick sand beds can be found extending vertically all the way to the Kama Hill Formation, although the drill core shows

that the majority of the sand sheets are confined to directly above the stromatolitic facies. These sand sheets are also interbedded with the mudchip and conglomerates that Cheadle (1986b) noticed in the Fire Hill Member and proposed to be intrusive sedimentary breccias. However, many of them appear to be debris flows, particularly in the case of the extensive outcrop on Black Sturgeon Road, described previously. The poor sorting, matrix-support, and lack of stratification in the conglomerates indicate a debris flow deposit (Collinson, 1996; Rust, 1978). The mudchip conglomerates sometimes include dolomitic and gypsiferous mud blocks, and indicate reworking of the basinal strata by slump events.

Cheadle (1986a) was also mistaken about the lack of subaerial exposure. Soil horizons, preserved as caliche layers and diagenetic gypsum nodules, attest to subaerial exposure. Perhaps the best example of subaerial exposure is the sequence on Channel Island (Figure 2.8), which progresses from subaqueous rippled sandstone to the stromatolitic carbonate unit to subaerial caliche layers and conglomerates. Some of the stromatolites contain tepee structures, as well as gypsum and halite casts, that are suggestive of hypersaline conditions shortly after deposition.

Some of the conglomerates noticed by Cheadle (1986a) and Franklin *et al.* (1980) were true sedimentary breccias and sand sills south of Pass Lake. Cheadle (1986a) suggested that these formed due to abnormally high fluid pressures associated with lithological barriers. He hypothesized that the mudstones and dolomites of the Channel Island Member, as well as the chert-carbonates of the stromatolitic lithofacies association, would have trapped water within the Pass Lake Formation. Fluid expulsion would then be triggered by earthquake activity creating conduits through the overlying barrier. These sedimentary breccias are frequently found within fault zones (Cheadle, 1986a) and

microfaults have been noticed in the mudstones of the Fire Hill Member and Kama Hill Formation.

2.6.3 Kama Hill Formation

Cheadle (1986a,b) suggested that the Kama Hill Formation represented a change from a lacustrine environment to a subaerial mudflat, where deposition occurs in a similar way to floodplains although there is a distinct lack of channel deposits. Some channel deposits are interbedded with the Kama Hill Formation near the contact with the Outan Island Formation, but the majority of the Kama Hill Formation is a result of unchannelized sheet flows and settling out of suspension. Cheadle (1986a) based his interpretation on the abundance of desiccation cracks and the absence of carbonates. The horizontally-laminated mudstone lithofacies association was interpreted as a suspension deposit primarily associated with mudflat ponds. The lack of carbonates and quartz nodules indicates a change in hydrological conditions (Cheadle, 1986a).

Most of the sediment on a floodplain is deposited during flood events. Commonly, intense precipitation or increased fluvial discharge causes the water table to rise, thus forming floodplain lakes (Collinson, 1996). In between these wet intervals, floodplains may dry out and develop subaerial indicators, such as mudcracks (Allen, 1964). Miall (1985) described a floodplain as consisting of mud or silt and thin laminae of silt or fine sand. These siltstones and mudstones are often interbedded with thin sharp-based sandstones, which may be graded or have parallel lamination, ripple cross-lamination, or climbing ripple cross-lamination and are associated with ephemeral streams or crevasse

splays on the floodplain (Collinson, 1996). Laminated muds of floodplain ponds, sand sheets denoting crevasse splays, and calcrete horizons may also be present (Miall, 1985). Flooding by sheet flows cause similar facies to form on the mudflat of the Kama Hill Formation.

The Kama Hill Formation is dominated by horizontally-laminated fine sandstone/siltstone and mudcracked fine sandstone/siltstone, similar to the floodplain along the Beatton River (Nanson, 1980). This represents sheet-flood and suspension deposits followed by subaerial exposure. The rippled fine sandstone/siltstone lithofacies association formed during flood events (Nanson, 1980). Laminated muds, some associated with wave rippled siltstone, are found in the Kama Hill Formation, representing mudflat ponds that periodically covered parts of the basin. The presence of thicker units of laminated shale and siltstone, sometimes associated with wave ripples and no subaerial indicators, such as mudcracks, suggests that some of these ponds remained for an extended period of time.

2.6.4 Outan Island Formation

Interpretations of depositional environments for the Outan Island Formation are hindered by the lack of surface exposure and the limited amount of drill core that intersected it. The lower Outan Island Formation is thought to represent a deltaic environment, and has been designated the Lyon Member. This unit is restricted to Nipigon Bay and has been named after nearby Lyon Township. The upper Outan Island Formation corresponds with a fluvial environment and has been named the Hele Member, after the township it was found in.

The Lyon Member coarsens upward and is dominated by siltstone and mudstone laminae with some sandstone beds. Small coarsening and thickening upwards sequences are common, grading from thin mud laminae to thick silt laminae or from mud laminae to fine sandstone to medium sandstone, with some cross-stratification present. Many of these laminae are normally graded. These sequences are interspersed with small fining upward units near the top of the Lyon Member. In some drill core, low-angle cross-stratification occurs between the Lyon Member and the Hele Member. This combination of lithofacies associations resembles a muddy deltaic environment, similar to the Upper Carboniferous Westphalian deltaic unit described by Haszeldine (1984), and the Acheloos delta in Greece (Piper and Panagos, 1981).

The siltstone and laminated siltstone and mudstone are similar to the fine-grained turbidites deposited in interdistributary areas during floods and in distal delta deposits (Piper and Panagos, 1981; Haszeldine, 1984; Reading and Collinson, 1996). Haszeldine (1984) interpreted the fining-upward sandstone sequences as channel-fill deposits and the coarsening-upward units as deposition in interdistributary areas subsequent to the breaching of delta channels during flood events, similar to crevasse splays (Reading and Collinson, 1996). The low-angle cross-stratified sandstones are, most likely, beach deposits (Reading and Collinson, 1996). In summary, the Lyon Member displays a typical coarsening-upward, prograding deltaic sequence from the muds and silts in the distal portions of the delta and deeper interdistributary areas to the interbedding of fining-upward channel deposits and coarsening-upward crevasse splay lobes in interdistributary areas. In some areas, thin beach deposits cap the sequence.

The majority of the Hele Member is dominated by cross-stratified sandstone and normal or inverse graded sand beds, topped with mud caps. Mudchip horizons and broken, contorted mud laminae are common. Many of these sandstones are incorporated into fining upward sequences from massive or parallel-laminated sandstone to rippled fine sandstone, rippled siltstone, and laminated mudstone. Intraformational conglomeratic units containing sub-rounded mud blocks are present at the base of some sandstone units, and midway through others.

Allen (1970) described six facies in a typical fluvial deposit: conglomeratic, large-scale cross-stratified sandstones, flat-bedded sandstones, small-scale cross-stratified sandstones, alternating beds of siltstone and sandstone, and siltstone facies. All but the large-scale cross-stratified sandstones have been identified in the Hele Member, although lack of the latter may only be due no outcrop exposure. Channel sequences have erosive bases and, generally, a channel lag of matrix-supported intraformational conglomerates (Allen, 1970; Miall, 1977). In the Hele Member, the fining-upward sequence overlies the channel lag and corresponds to waning flow conditions, similar to abandoned channel sediments (Allen, 1970). The siltstones and laminated siltstone-mudstone units, with some ripple laminae, were deposited on a floodplain. The presence of mudchips and small mudcracks suggests subaerial exposure on the floodplain (Nanson, 1980). Massive sandstones, that may be normal- or reverse-graded, are interbedded with the siltstones of the floodplain. These represent crevasse splay deposits (Allen, 1964; Miall, 1985), caused by a river breaking through its levee and carrying bedload sediment onto the floodplain. Occasionally, laminated shales are found interbedded with the siltstone lithofacies association, representing floodplain ponds.

The Hele Member resembles a meandering river system rather than a braided stream, although distal sand-dominant braided rivers can be difficult to distinguish from meandering rivers (Rust, 1978). It is particularly difficult to differentiate between the two when outcrops are not available to examine large-scale bedforms, as is the case in the Hele Member.

2.6.5 Nipigon Bay Formation

The Nipigon Bay Formation is believed to be an aeolian system. This is suggested by several factors. Most striking is the one outcrop of the Nipigon Bay Formation, on Simpson Island (Figure 1.1), which preserves a distinct, large-scale, remnant dune topography. This dune feature is approximately 15 m in height, which is excessive for most fluvial environments (Collinson, 1996; Miall, 1977) although large-scale cross-beds can be found in fluvial systems, such as the giant cross-beds of Jones and McCabe (1980) that reached a thickness of 35 m. Kocurek (1996) stresses the importance of the identification of paleo-topographic features for identifying aeolian dune systems. In drill core, the Nipigon Bay sets tend to be 50 cm to 400 cm thick, with co-sets ranging from 4 m to 40 m thick. The very large-scale cross-beds and high-angle sets indicate an aeolian environment (Clemmensen and Abrahamsen, 1983; Bigarella, 1972).

Besides the initial, large-scale dune feature, smaller sedimentary features within the outcrop and in drill core accentuated the similarities between the Nipigon Bay Formation and aeolian systems. Most aeolian dunes are primarily composed of steeply-dipping, concave upward laminae with plane or curved bounding surfaces (Bigarella, 1972). The

drill core contains 450 m to 500 m of predominantly high-angle cross-stratification, interbedded with some low-angle and horizontally laminated beds. The Simpson Island outcrop contains curved and planar bounding surfaces. The angle of dip on the dune surface should decrease downslope (Bigarella, 1972), which is seen in the outcrop and could possibly be indicated by the gradual change from high- to low-angle cross-stratification in drill core.

Another criterion for aeolian sand deposits is the high degree of sorting relative to subaqueous sandstones (Bigarella, 1972), which is also seen in the Nipigon Bay Formation. However, in some cases, coarse grains are present in the sandstones, which is not typically associated with aeolian sand dunes. Clemmensen and Abrahamsen (1983) observed coarsening upward, granule-rich horizons and incipient granule ripples interbedded with plane-bed laminae near the margins of the Arran Basin. They suggest that the coarse-fraction is related to very high wind velocities and note that inverse grading is well known in migrating wind ripples. However, the coarse grains here are more often interbedded with the high-angle cross-strata. This indicates that the coarse horizons represent a deflation lag, which is typically found at the bottom-sets of dunes (Kocurek, 1996; Clemmensen and Abrahamsen, 1983). One unusual feature is the rare, preserved ripple-forms in the Nipigon Bay Formation. These are typically absent in aeolian dunes, but have been noted in Paleozoic and Mesozoic sandstones of the Colorado Plateau (Bigarella, 1972) and the Arran Basin (Clemmensen and Abrahamsen, 1983).

The horizontally laminated beds represent the interdune areas. Bigarella (1972) showed that the flat-lying laminae of the interdune area were gradational with low-angle laminae as the base of a dune is approached. The Nipigon Bay horizontal laminae are

sometimes associated with silty material, suggesting that they were deposited in low-lying areas that were probably occasionally moist. Kocurek (1996) notes that interdune-flat accumulations are seldom preserved in dry environments, and this would be particularly true in the Mesoproterozoic with no vegetation to stabilize interdune areas. Therefore, the Nipigon Bay Formation was probably a semi-arid desert.

2.6.6 Summary of Depositional Environments

The Loon Lake Member represents transgressive reworking of a beach deposit. The heterolithic facies of the Fork Bay Member was considered by Cheadle (1986a) to be chronologically equivalent, denoting the subaqueous continuation of debris flows in the form of turbidites. However, these should not be considered true turbidites, but should be termed subaqueous sheet flows. Cross-bedded and plane-bedded facies, which are the deposits of braided streams along the lacustrine margins, may be found underlying these facies. The sand beds thin basin-ward and become interbedded with mud and shale beds accumulating during quiet periods in the shallow lake that was forming within the basin.

The lacustrine sandstones of Pass Lake Formation interfinger with the mudflat and marginal saline lake shales and mudstones of the Rossport Formation. Cyclic siltstone-dolomite beds formed within the saline lake, cycling with lake level fluctuations. Clastic material was restricted to fine sediment settling out during flash-flood events that recharged the basin, while sabkha-like sequences formed in the surrounding mudflats. After a prolonged period, the shallow saline lake began to dry further, forming extensive damp sabkha-like mudflats and allowing sand sheet incursions to penetrate farther into the basin

centre. During the initial incursions, these sand sheets isolated parts of the playa lake, producing water conditions that were favourable for stromatolite growth.

The periodically subaerial mudflat of the Fire Hill Member became predominantly subaerial during the onset of Kama Hill Formation deposition. The Kama Hill Formation represents a floodplain system, which is occasionally covered by ponds. Some of these ponds seem to remain for prolonged periods of time. In the eastern portion of the Sibley Basin, damp mudflat facies, similar to the Kama Hill Formation, can be found interbedded with both the deltaic and fluvial members of the Outan Island Formation, although the fluvial member can be found further towards the centre of the basin. The Kama Hill Formation and the lower member of the Outan Island Formation form a prograding deltaic system into a basin that was dry for part of the time, followed by fluvial deposition. There was a hiatus between the Outan Island Formation and the Nipigon Bay Formation, after which a thick sequence of aeolian sand dunes was deposited.

Chapter 3:

CHEMOSTRATIGRAPHY

One of the main purposes of this study was to increase the understanding of processes acting on and within the Sibley Basin. Geochemistry reflects the sedimentary processes, diagenesis, weathering history, and source material. By comparing different elements at various points in the stratigraphy, inferences can be made about the evolution of the Sibley Basin, such as changes in sedimentology, carbonate precipitation, weathering, and variations in source rock lithologies. To that end, samples of medium-grained sandstones, covering the entire sequence from the Pass Lake Formation to the Nipigon Bay Formation, were collected at approximately 20 m intervals from drill-core NB-97-4. Samples were also taken from NB-97-2 for further investigation of the Outan Island Formation.

3.1 Theoretical Considerations

Only medium-grained sandstones were chosen for sampling, as suggested by Johnsson (1993), in an effort to minimize the effect of grain-size on geochemistry. This bias is produced by the natural separation of certain minerals into different grain-size fractions. For example, amphiboles have a tendency to form clay-sized particles upon weathering, whereas quartz concentrates in the sand-sized fractions. However, it should be noted that the sandstones have been subjected to differing degrees of sorting, thus causing some geochemical differences even amongst samples with the same average grain-size (Johnsson, 1993).

One of the more pressing concerns when using geochemistry is the potential for changes in elemental abundances due to alteration and weathering. Alteration is particularly important for the Pass Lake Formation, as well as sections of the Sibley Group that are proximal to the many intruding diabase sills. In some cases the alteration is due to metamorphism induced by sills and intrusions (Rogala, 2000), while in other instances diagenesis and carbonate cementation cause post-depositional changes in mobile element abundances. The degree and effects of thermal alteration have not been examined in depth in this study, and sampling was restricted to sandstones that appeared to be free of the metamorphic effects of the sills. It should be noted that the Pass Lake Formation has secondary concentrations of barite (Franklin *et al.*, 1986), which indicate some redistribution of mobile elements.

The geochemical characteristics of the sandstones can be used to make some inferences about the source material. Elements were tested for immobility using the techniques of Fralick and Kronberg (1997). A variety of element ratios were adapted from this work for the study of the clastic material. Ratios, such as Zr/TiO_2, can indicate whether the source is mafic or felsic and Nb/Y can be used to show the alkalinity of the source rock. The provenance of the Sibley Group sediments can be determined by comparing a variety of element ratios with potential source materials and by employing discrimination diagrams. Since paleocurrent directions are different between Formations, the geochemistry should reflect changes in source materials.

3.2 Methodology

Samples of medium-grained sandstones were collected at approximately 20 m intervals spanning the Sibley Group from the Pass Lake Formation up to, and including, the Nipigon Bay Formation. These samples were pulverized using a steel mortar and pestle, then powdered to a maximum grain-size of 30 microns using a ball mill. The chemical digestion process began by applying a mixture of 5 mL HNO_3 and 10 mL of double distilled water (DDW) to the samples in Teflon beakers, then allowing them to sit overnight at a temperature of 90°C. The samples were then subjected to a combination of 5 mL HF and 10 mL HNO_3 and were left to digest overnight at 90°C. This step was repeated twice more in order for all of the silica to be digested. On the last night, the samples were digested at 150°C instead of 90°C, and evaporated until dryness. Once dry, 5 mL of HCl was added to the samples and allowed to simmer for 20 minutes at a temperature of 90°C. After 20 minutes, 10 mL of DDW was added and allowed to simmer for a further 10 minutes. At this point the digested samples were transferred to 100 mL volumetric flasks and kept at 90°C for 2 hours. The flasks were then topped up to 100 mL, using DDW, to produce a 5% HCl solution. The digested samples were then transferred into plastic bottles and sent to the Lakehead University Instrumentation Laboratory for analysis on a Varian Vista Pro Radial ICP-AES, with a Cetac autosampler operating at 1100 watts, with a 10 second read-time. Blank samples and geological standards were also analyzed. Carbon and hydrogen were analysed using an Elemental Analyzer, model 240A, with a lower detection limit of 0.04 wt% for carbon and 0.05 wt% for hydrogen. The data are summarized in Tables B-1 and B-2 in Appendix B.

3.3 Stratigraphic Variation

A variety of elements and ratios were plotted against depth and stratigraphy to examine geochemical changes in the Sibley Group. These graphs provide information about the weathering history of the basin and changes in source material, such as mafic versus felsic trends and alkalinity trends.

3.3.1 Sedimentary Trends

Sedimentary trends reflect changes in geochemistry caused by grain-size, evaporite precipitation, and cementation of the samples. Geochemical variation due to grain-size has been kept to a minimum by solely sampling medium-grained sandstones. However, some differences in geochemistry may arise due to varying degrees of sorting. This would primarily be conveyed by the SiO_2 content of the sandstones. The presence of early carbonate precipitates or later cements would be reflected in the CaO and CO_2 concentrations of the sandstones.

The Sibley Group shows an increase in SiO_2 content up-section on the SiO_2 content versus depth plot (Figure 3.1). The Pass Lake sandstones, between 800 m and 900 m, have SiO_2 concentrations averaging approximately 74%. At a depth of 800 m, the SiO_2 content drops to 55%, and gradually increases to 90% over the next 150 m. This section coincides with the Rossport and lower Kama Hill Formations. Between 450 m and 650 m, correlated with the Kama Hill and Outan Island Formation, the SiO_2 values are relatively consistent, averaging approximately 83%. There is a sharp increase in SiO_2 to an average of 90% at 550 m, marking the boundary between the Outan Island Formation and Nipigon Bay Formation.

The changes in SiO_2 content can be accounted for by the sedimentology of the individual formations. The Pass Lake Formation is dominated by poorly-sorted quartz and feldspathic sandstones with some carbonate cements. The Rossport Formation contains abundant carbonates and clay that mix with the sandstones, diluting their SiO_2 contents. This dilution decreases upwards in the sequence, causing the rebound in SiO_2 values. The SiO_2 values remain relatively stable in the Kama Hill and Outan Island Formations, but increases sharply at the contact with the Nipigon Bay Formation. The Nipigon Bay Formation is an extremely well-sorted sandstone, dominated by quartz grains.

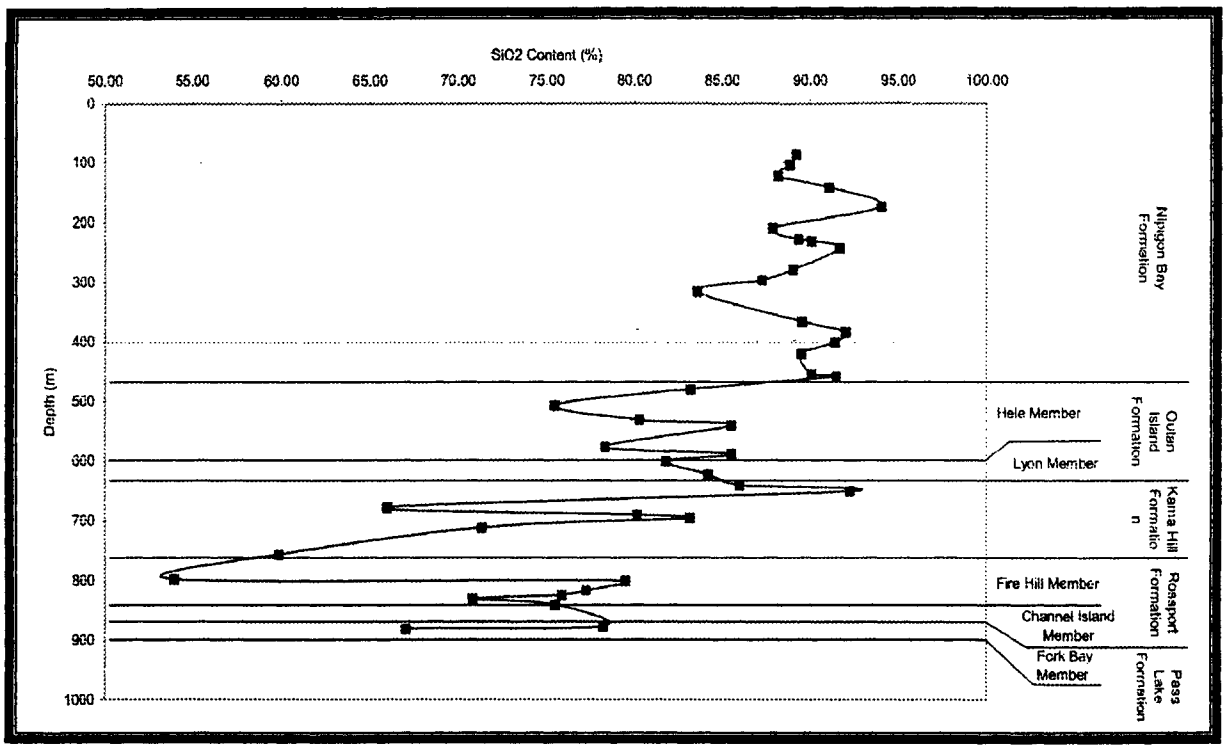

Figure 3.1. SiO_2 Content vs. Depth. There is an overall increase in SiO_2 content upwards through the Sibley stratigraphy. For comparison, immature Neoarchean sandstones eroded from the same source region have an average SiO_2 content of 64 wt% (Fralick and Kronberg, 1997), moderately mature Paleoproterozoic sandstones of the basal Huronian Supergroup have an average of 86 wt% SiO_2 (personal communication, P. Fralick), and super-mature Paleoproterozoic sandstones of the Baraboo Quartzite have an average of 98 wt% SiO_2 (this study).

The differences in SiO_2 content pose some problems when attempting to compare the geochemistry of the five Formations. When the proportion of SiO_2 is high, the trace elements become diluted and it is difficult to determine whether a trend is real or simply an artifact of this dilution. Therefore, ratios are used for the majority of the geochemical comparisons.

The presence of carbonates within the Sibley Group can be shown by graphs of CaO against depth and CO_2 against depth. The CaO versus depth graph (Figure 3.2) shows values between 6.0% and 16.0% CaO for the section between the depths of 900 m and 700 m, which correlates with the Pass Lake and Rossport Formations. Intermediate values between 0.1% and 6.0% characterize the Kama Hill and Outan Island Formations. The Nipigon Bay Formation has the lowest CaO content, less than 2%. It should be noted that these are absolute values and do not take SiO_2 dilution into account. However, when Al_2O_3 is used to normalize the dilution (Figure 3.3), the trend is maintained, although the trends for the Rossport, Kama Hill, and Outan Island Formations are less pronounced.

The CO_2 against depth diagram (Figure 3.4) should show a more accurate picture of the carbonate distribution as the carbonate is primarily in the form of dolomite, and hence not fully accounted for by the CaO content. However, the CO_2 concentrations provide a slightly more confusing picture. The Pass Lake has a variable CO_2 content, although it appears to be increasing as the Rossport Formation is approached at a depth of ~800 m. The CO_2 content is consistently high throughout the Rossport Formation (~700 m – 800 m depths), and then becomes variable again through the Kama Hill and Outan Island Formations, decreasing slightly up-section. The Nipigon Bay Formation (450 m to surface) has uniformly low CO_2 concentrations of less than 2%.

When Al_2O_3 is used to normalize the CO_2 values, a more coherent graph results (Figure 3.5). This diagram shows a fairly consistent variability of the CO_2 content for the Pass Lake, Kama Hill and Outan Island Formations. There is a CO_2 peak around a depth of 800 to 850 m that is associated with the high carbonate content of the Rossport Formation. The low CO_2 trend for the Nipigon Bay Formation (450 m to surface) becomes smoother.

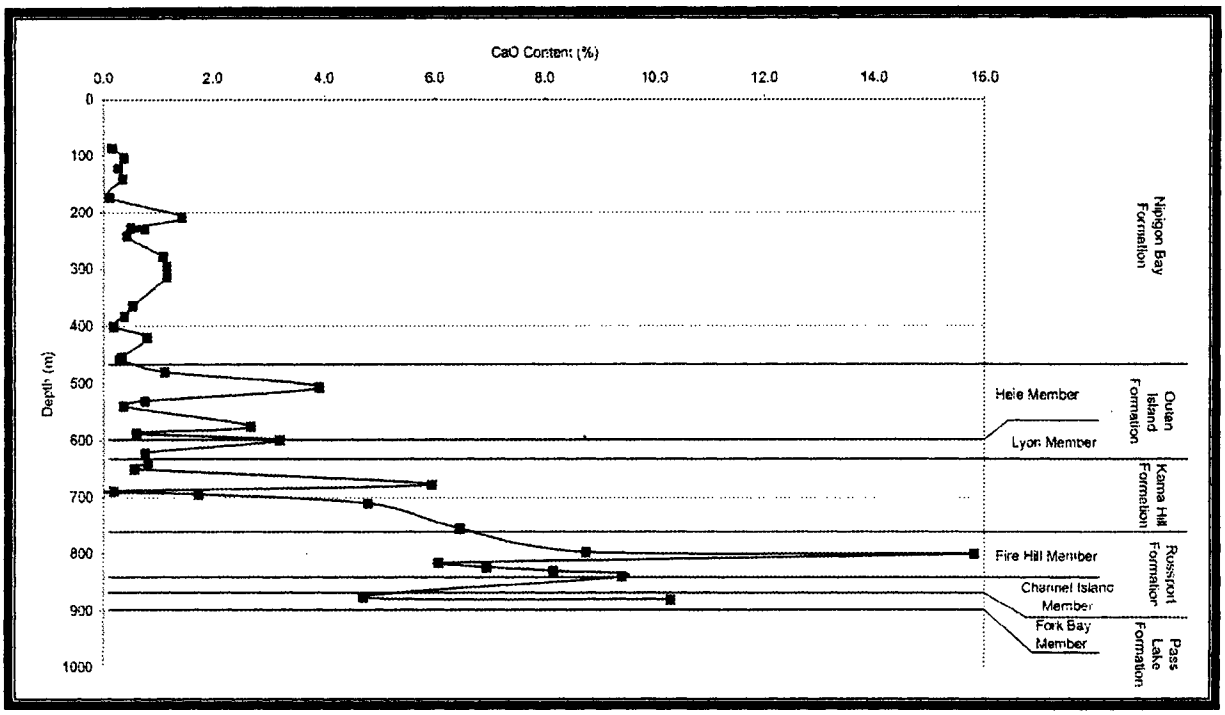

Figure 3.2. CaO Content vs. Depth. There is a decrease of CaO content up through the Sibley stratigraphy. Higher CaO values below 700 m are associated with the Rossport and Pass Lake Formations, due at least in part to the presence of carbonates in the sandstones.

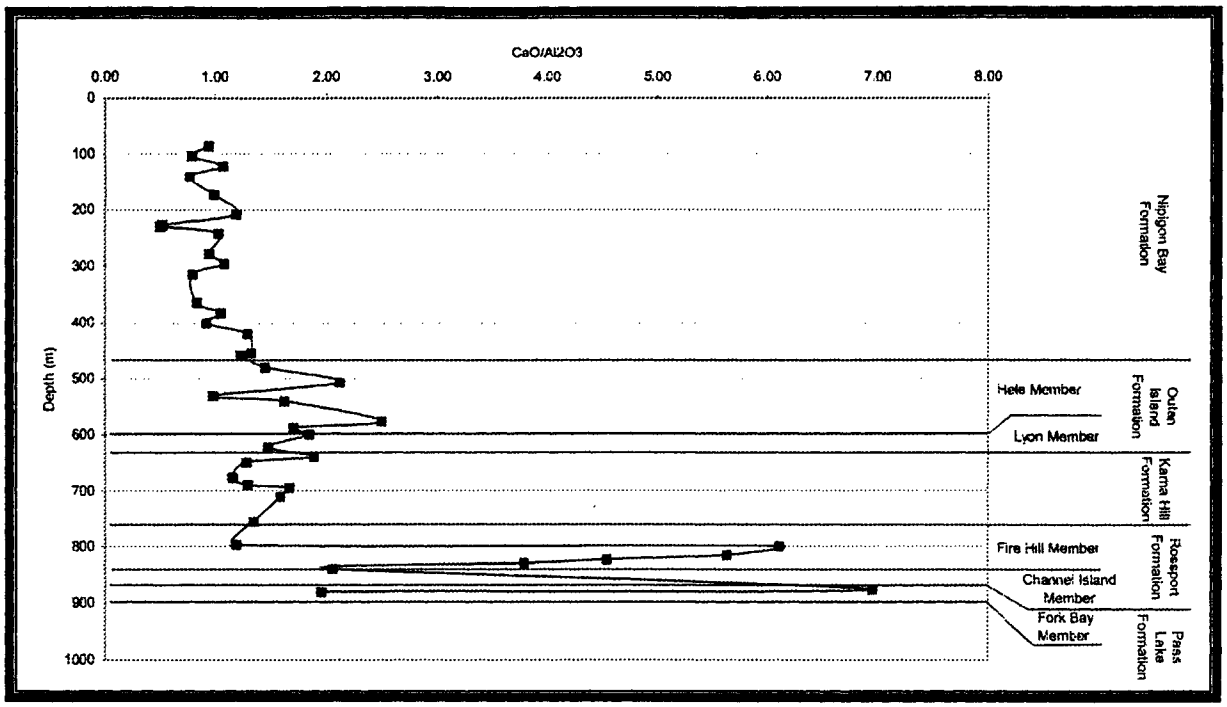

Figure 3.3. CaO/Al_2O_3 vs. Depth. The Al_2O_3 has been used to normalize the CaO content to eliminate the dilution effect of SiO_2. There is significantly more CaO within the lower 100 m, correlated with the lower Rossport Formation and the Pass Lake Formation. Above this, there is a general decrease in CaO content through the remainder of the Sibley stratigraphy.

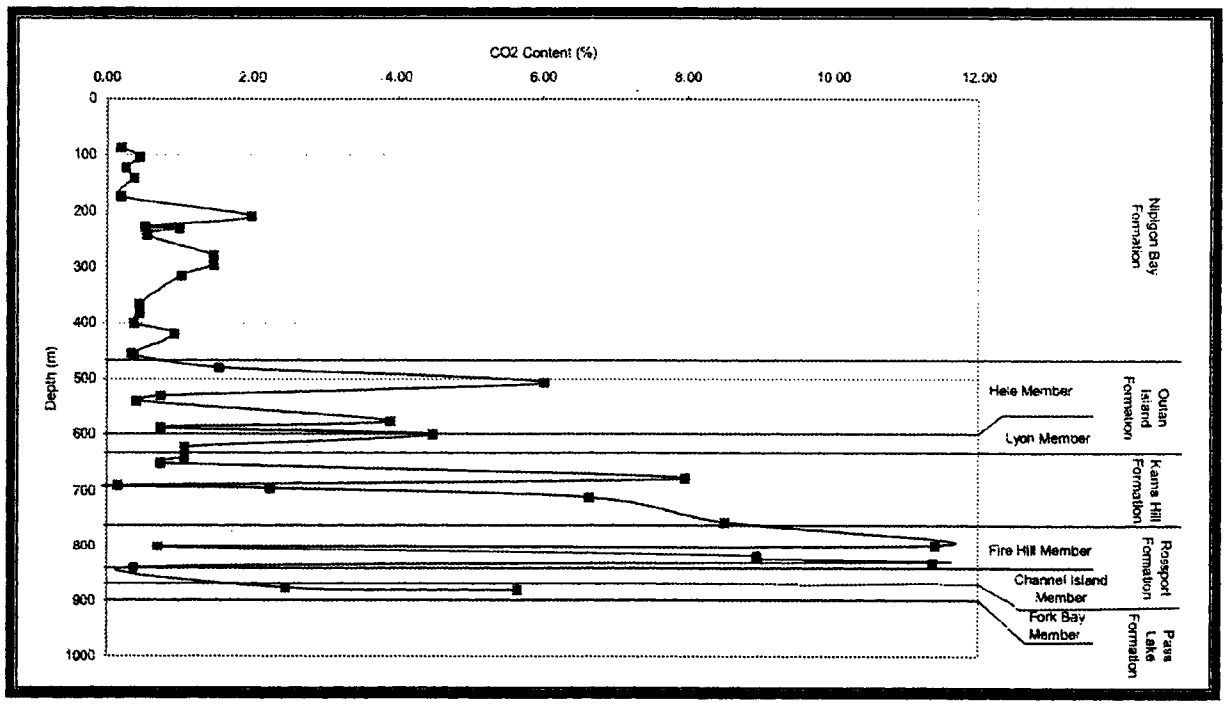

Figure 3.4. CO_2 Content vs. Depth. The CO_2 content appears to be quite variable, particularly throughout the lower 450 m of the sequence. Particularly high CO_2 contents occur between 700 m and 850 m, associated with the Rossport Formation. The abundance of CO_2 within the upper 450 m (the Nipigon Bay Formation) is significantly reduced.

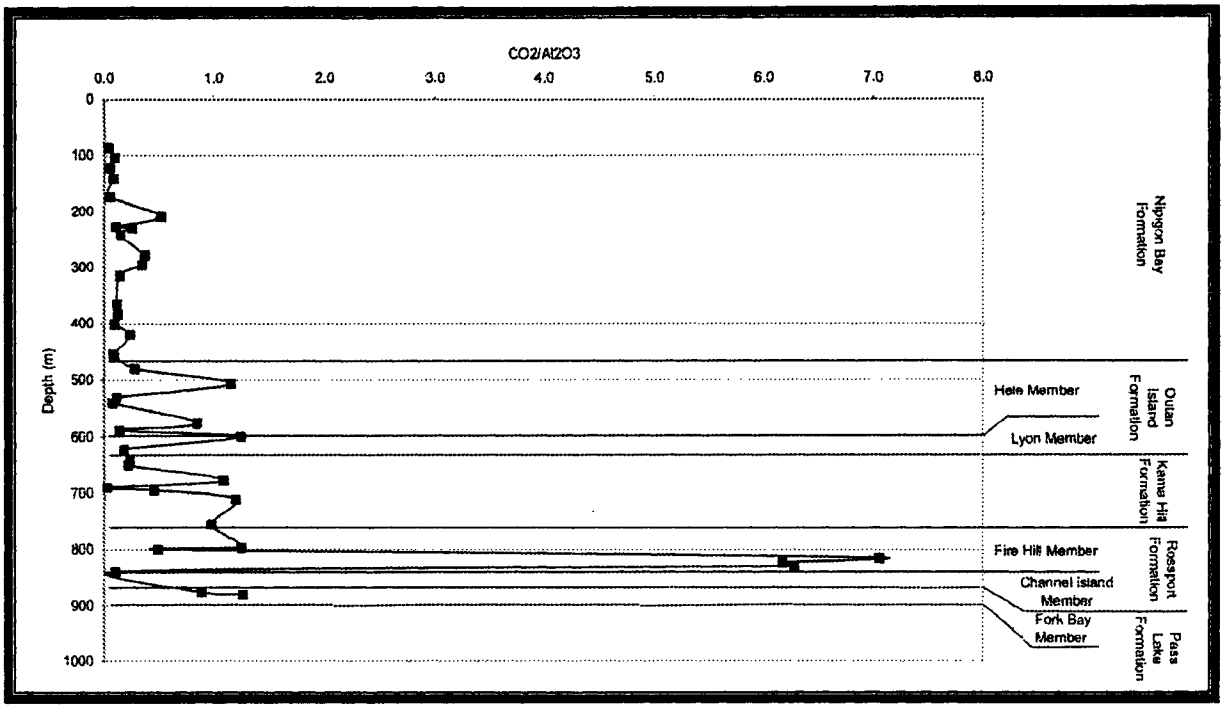

Figure 3.5. CO_2/Al_2O_3 vs. Depth. This ratio has been used to eliminate differences between the sandstone samples due to SiO_2 dilution effects. Note the CO_2 peak around 800 m to 850 m, associated with the Rossport Formation. Sporadic high values persist through the Kama Hill and Outan Island Formation (between 450 m and 900 m). The CO_2 content shows a consistent decrease above 450 m, correlated with the Nipigion Bay Formation.

3.3.2 Weathering and Alteration Trends

The main elements affected by weathering are Na, K, and Ca due to their relatively high mobility. Ratios of Na_2O/ K_2O, CaO/K_2O, and MgO/Fe_2O_3, as well as the Chemical Index of Alteration (CIA) were plotted against depth to investigate weathering trends. These graphs form Figures 3.6, 3.7, 3.8, and 3.9, respectively.

During the weathering process, Na_2O and CaO are initially removed faster than K_2O. This initial stage is followed by a decrease in the K_2O content. The Na_2O/K_2O ratio (Figure 3.6) is interesting when compared with the Sibley stratigraphy, showing a shallow trend of Na_2O depletion relative to K_2O, with two enrichment peaks. The lower 100 m, the Pass Lake Formation, has relatively high Na_2O concentrations relative to K_2O, including a

peak at 877 m, followed by a gradual decrease up to the lower Rossport Formation. There is also a Na_2O peak at 507 m, near the transition between the Outan Island and Nipigon Bay Formations. The elevated Na_2O in the Pass Lake Formation is probably a result of the influence of less weathered, more source-proximal material at the base of the section, with the detritus becoming progressively more weathered upwards until a steady state of Na_2O and K_2O depletion is developed in the lower Kama Hill Formation. The Na_2O peak at the base of the Nipigon Bay Formation may be related to salt pan development in inter-dune areas. It should also be noted that the Na_2O values average 0.15%, much lower than any source rock. This indicates that the sediment has either been exposed to chemical weathering for a prolonged amount of time or climatic conditions and atmospheric composition have promoted intense chemical weathering.

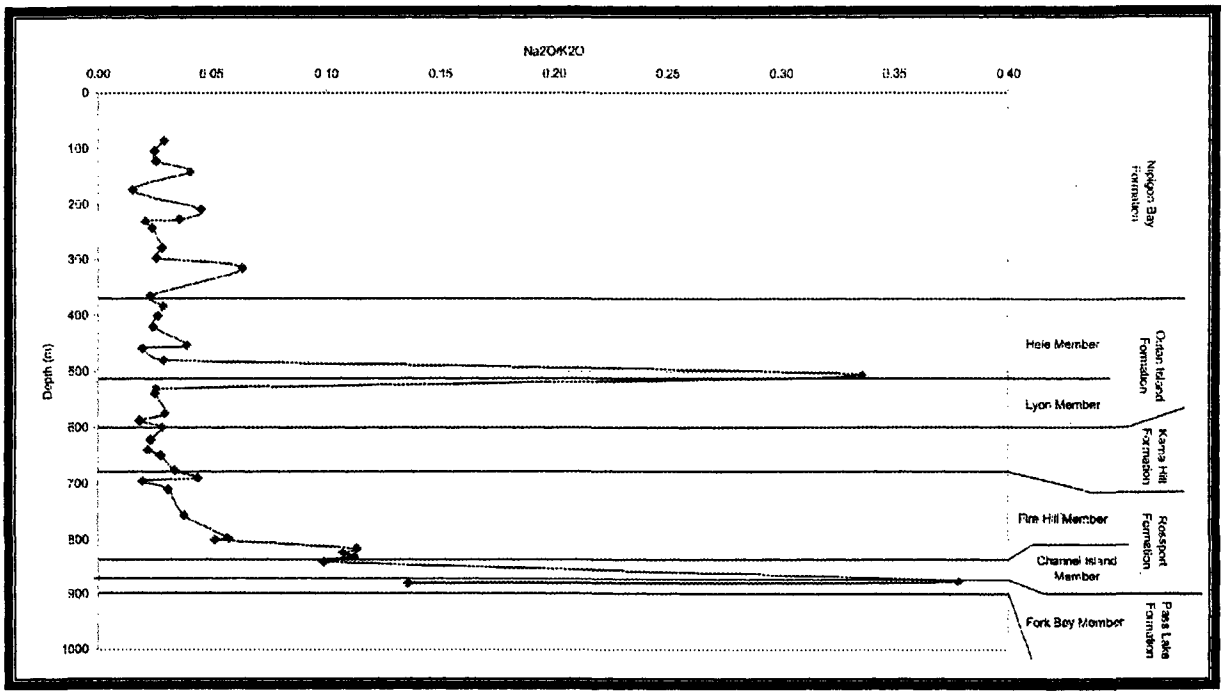

Figure 3.6. Na_2O/K_2O vs. Depth. There is a relatively smooth weathering trend shown by Na_2O/K_2O, with the exception of the anomalously high Na_2O content in one sample of the Pass Lake Formation at a depth of 877 m and one in the Outan Island Formation at a depth of 480 m, near the contact of the Nipigon Bay Formation.

The CaO/K_2O versus stratigraphic depth (Figure 3.7) shows two trends. The first trend is an increase in CaO/K_2O from the Pass Lake Formation through the Rossport Formation. This is due to the presence of calcite, dolomite, and gypsum in the sandstones, as well as carbonate cements. The second trend covers the rest of the sequence, and is distinctly offset from the first trend. The second trend begins with much lower CaO/K_2O values than the first trend, and shows a slight decrease upward in CaO relative to K_2O.

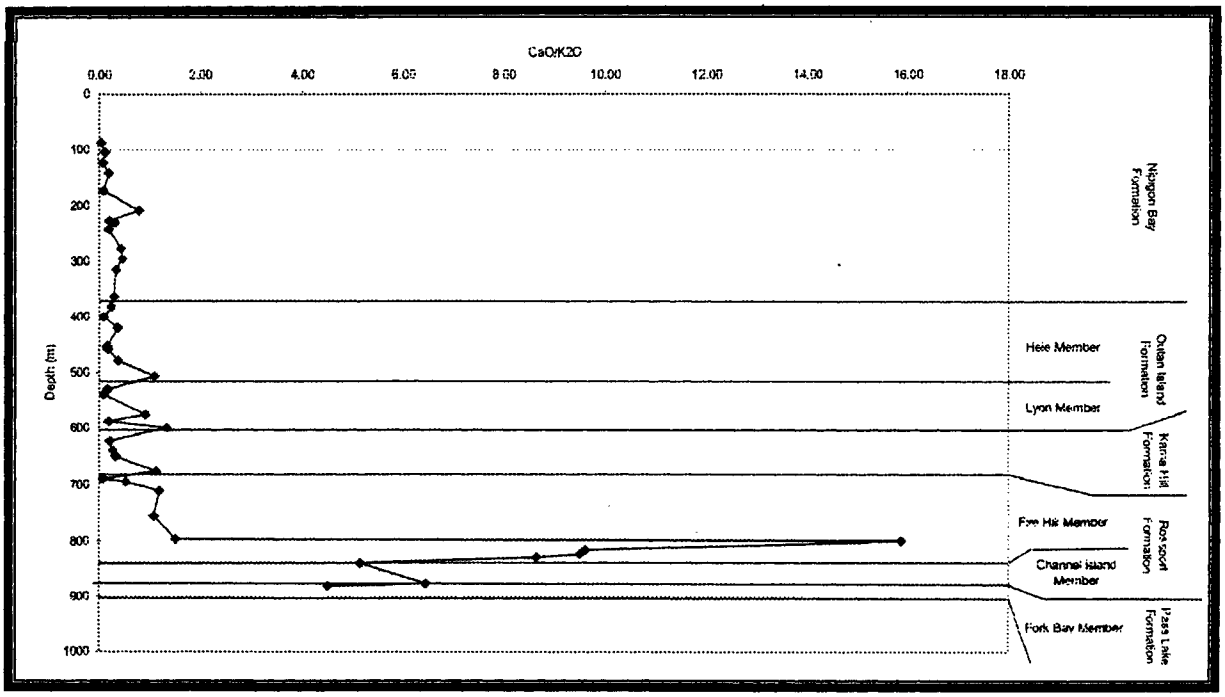

Figure 3.7. CaO/K_2O vs. Depth. There are two distinct trends shown by this weathering ratio. There is initially an increase in CaO content from the Pass Lake Formation to the Rossport Formation. This is a secondary enrichment associated with carbonate cementation. The rest of the sequence has significantly lower CaO/K_2O values, with a very slightly decreasing value upwards.

Another ratio that can be used for examining weathering trends is MgO/Fe_2O_3. Theoretically, MgO should be lost more rapidly during the initial weathering stages. As amphiboles and micas are altered Mg is removed, whereas Fe forms insoluble oxides (Johnsson, 1993). Figure 3.8 shows the MgO/Fe_2O_3 trend for the Sibley Group. Overall, this ratio shows an upward decrease in MgO content relative to Fe_2O_3, although the trend is not smooth. Sharp peaks throughout the lower 200 m of the sequence might be explained by the incorporation of MgO into dolomite and dolomitic cements within the Pass Lake and Rossport Formations. Reworking of the lower carbonate units may cause the high value at 680 m.

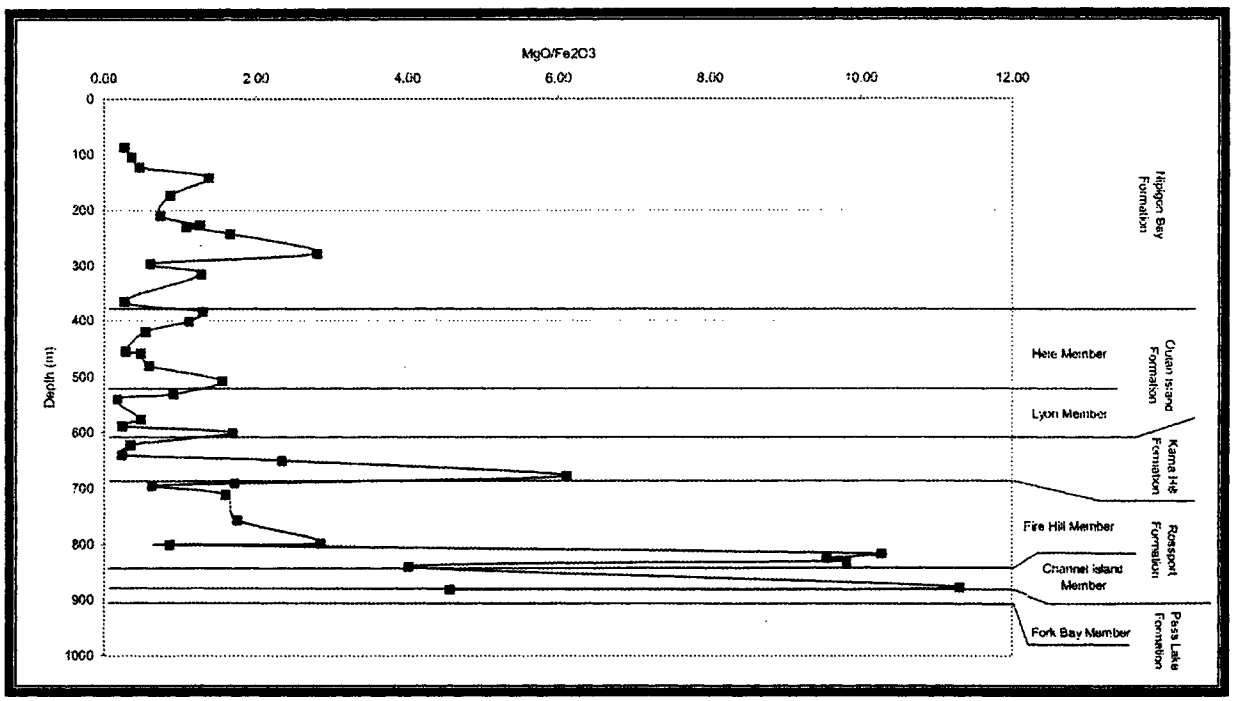

Figure 3.8. MgO/Fe_2O_3 vs. Depth. The MgO/Fe_2O_3 ratio provides information about the weathering of the Sibley Group. MgO should initially be lost more rapidly during weathering, thus a lower number indicates material that has been more extensively weathered or reworked.

The Chemical Index of Alteration (CIA) is defined as $Al_2O_3/(Na_2O + K_2O + CaO + Al_2O_3)*100$ (Nesbitt and Young, 1982), and is a common indicator of the degree of weathering in shales. This typically results in a number between 50 and 100, with 50 indicating a fresh sample and a value of 100 indicating a total removal of Na, K, and Ca (McLennan *et al.*, 1993). However, here the CIA was used on sandstones, which would cause the CIA values to be lowered. Three CIA graphs have been plotted. The first graph (Figure 3.9) shows a CIA (uncorrected for the presence of carbonates) against depth, while Figure 3.10 assumes that the carbonate is all dolomite and corrects for it, and Figure 3.11 corrects for the carbonate assuming that it is all calcite. Carbonate cements, either calcite or dolomite in this case, cause a CaO enrichment in the rock, which lowers the CIA. This is corrected by using the amount of CO_2 to calculate the equivalent amount of CaO that would be used by either calcite or dolomite, and then subtracting it from the total CaO. The lowermost 100 m of the Sibley stratigraphy, correlated with the Pass Lake and lower Rossport Formations, shows anomalously low CIA values on Figures 3.9 and 3.10. One concern about using an uncorrected CIA is the potential influence of secondary CaO content, although the CaO/K_2O and CaO/Al_2O_3 ratios (Figures 3.6 and 3.3, respectively) indicate that calcium values are not elevated above a depth of 800 m.

The Rossport Formation is characterized by an abundance of dolomite layers and dolomitic mudstones; therefore the CIA was corrected for the presence of dolomite (Figure 3.10). This has the effect of decreasing the off-set between the central section and the top section. The dolomite adjustment also brings many of the anomalous values below 800 m closer to the CIA value of 50.

Because this did not seem to account for all of the effects, a correction for calcite was made (Figure 3.11). This removed the off-set between the central section and the top section, creating a relatively smooth curve of increasing CIA values. However, there wasn't a significant change between the calcite and dolomite corrections below 800 m.

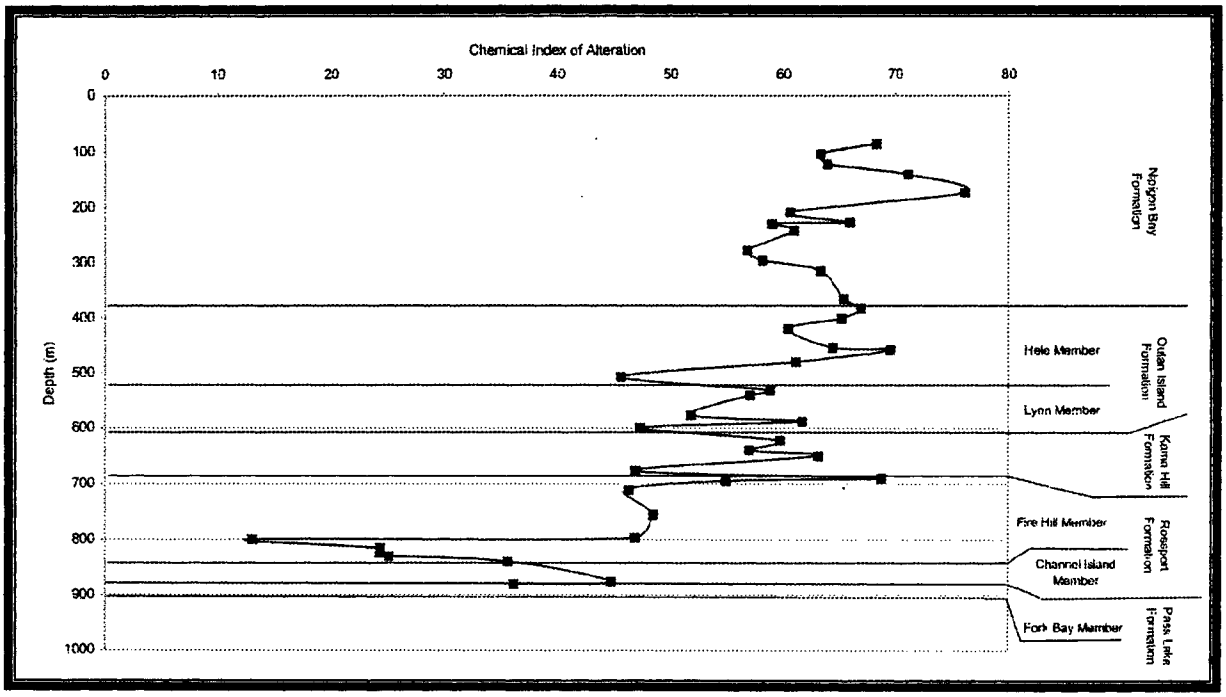

Figure 3.9. Chemical Index of Alteration vs. Depth. The CIA should fall between 50 and 100. However, the Pass Lake and lower Rossport Formation (from depths of 800 to 900 m) do not follow this. The rest of the sequence seems to show an increase in the amount of weathering upwards. For comparison, other sandstones with similar source rocks have CIA values of 1) immature Beardmore-Geraldton assemblage, CIA=51 (Fralick and Kronberg, 1997); 2) moderately mature lower Huronian Supergroup, CIA=59 (personal communication, P. Fralick); super-mature Baraboo Quartzite, CIA=76 (data, this study).

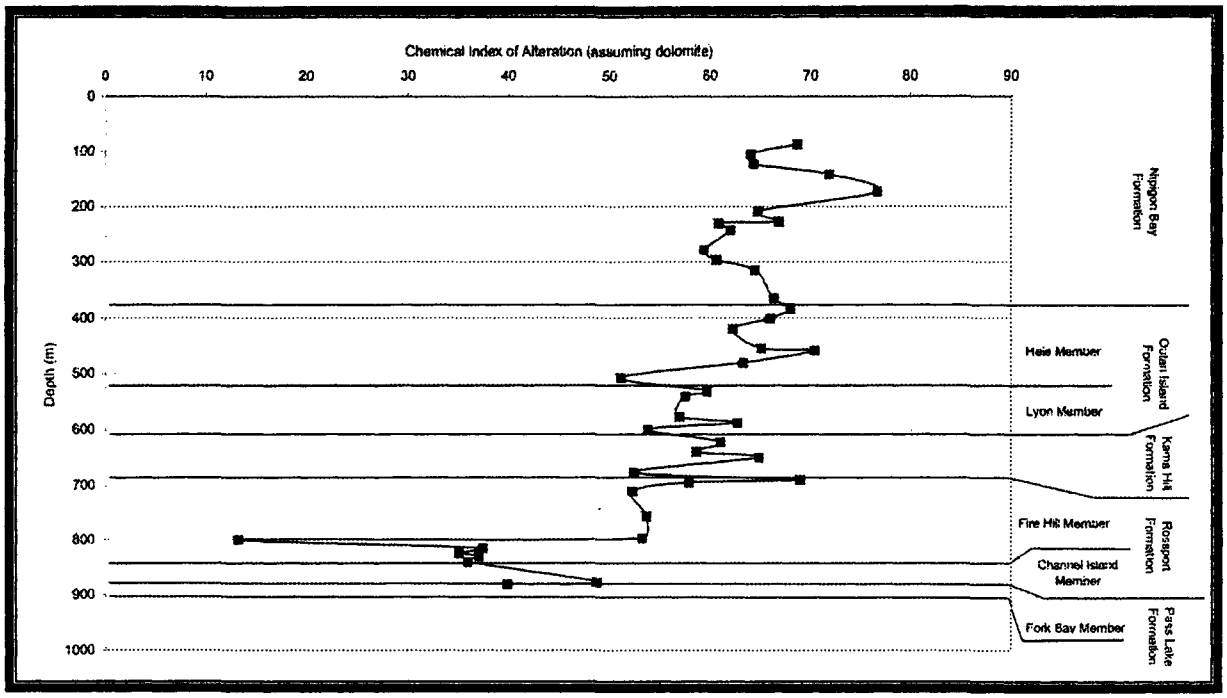

Figure 3.10. Chemical Index of Alteration, correcting for dolomite. Values for the section between 800 m and 900 m are still anomalously low. This correction appears to reduce the off-set between the 450-800 m section and the Nipigon Bay Formation (above 450 m).

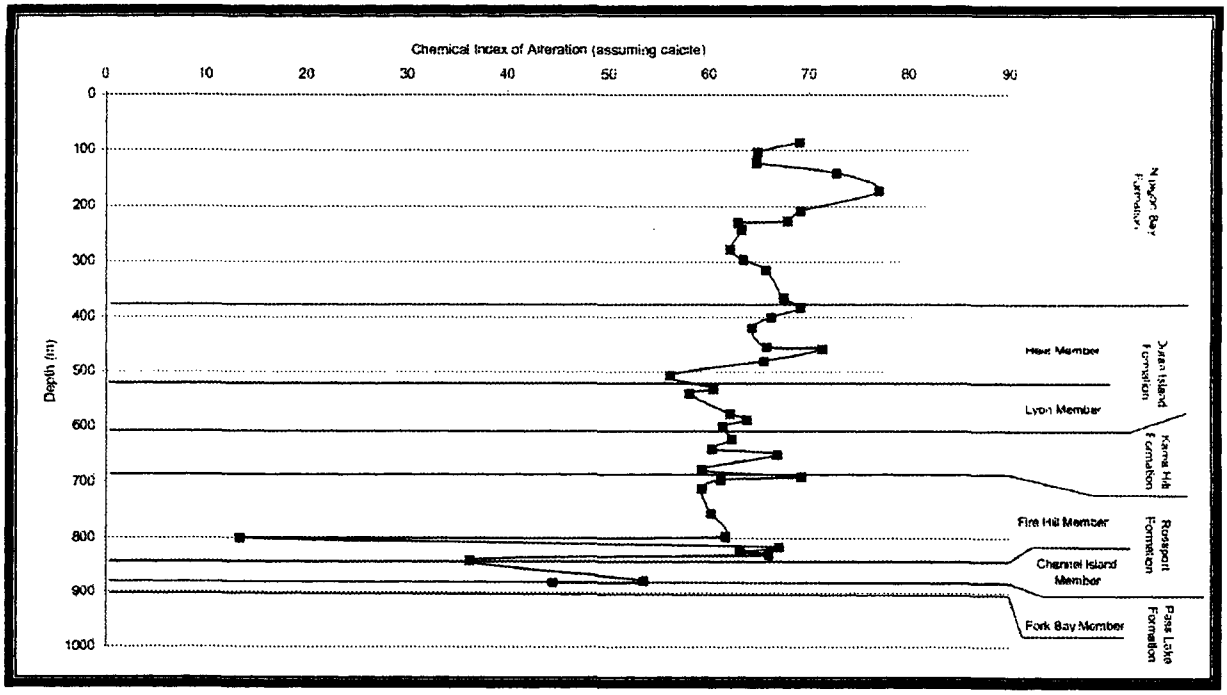

Figure 3.11. Chemical Index of Alteration, correcting for calcite. More of the anomalous CIA values are accounted for by assuming that the carbonate is calcite, although there are still some anomalous points below 800 m.

The Chemical Index of Alteration graphs indicate that there is an increase in the degree of weathering from the base of the Sibley Group up to the top of it. The CIA values below 800 m appear to be anomalous, even when dolomite or calcite corrections are made. Therefore these values are possibly a reflection of the source material (ie. Al-poor calc-silicate rocks in the source terrane) and an extremely low degree of weathering (McLennan *et al.*, 1993), although some of the anomalous CaO may be incorporated into gypsum. Sulphur values were not reliable enough to test this hypothesis and it is not believed that gypsum could account for the entire anomaly, based on the low abundance of gypsum in the sandstones.

Values above 800 m fall within the typical CIA range, and show an increase in the degree of weathering up to the top of the sequence. There is a distinct smoothing in the weathering curve when dolomite and calcite corrections are made. This suggests that calcite cementation, and to a lesser degree dolomite cementation, is important between 450 m and 800 m. The CIA values above 450 m were minimally affected by the corrections.

3.3.3 Source Rock Trends

Sedimentary geochemistry can also reveal stratigraphic trends other than those associated with weathering and alteration. For example, Zr/TiO_2, Zr/V, and V/Al_2O_3 can be used to identify the dominance of a mafic source over a felsic source (Fralick and Kronberg, 1997). For the first two ratios, higher numbers indicate more felsic material in the sediment and lower numbers denote more mafic material, while in the latter ratio the opposite is true. Other ratios, such as Nb/Y can provide information about the alkalinity of the source rocks (Fralick and Kronberg, 1997).

When the Zr/TiO_2 and Zr/V against depth graphs are analyzed individually they appear to depict clear trends. However, when compared to each other, the results for the base of the section are dissimilar. The Zr/TiO_2 ratio, shown in Figure 3.12, initially appears to be complex, but when the sequence is separated into the five formations trends begin to appear. There is an increase in Zr relative to TiO_2 from the base of the Pass Lake Formation up to the Channel Island Member of the Rossport Formation, suggesting an increasingly felsic source influence. There is a sudden decrease in Zr relative to TiO_2 within the Channel Island Member, which could be a change to a source richer in mafic material, followed by a second trend of increasing Zr relative to TiO_2 up to the base of the Nipigon Bay Formation at approximately 450 m. The Zr/TiO_2 ratio fro the Nipigon Bay Formation is high, but also quite variatble.

The Zr/V ratio (Figure 3.13) indicates a slightly different trend than the trend shown on the Zr/TiO_2 graph. Overall, there is an increase in felsic material up through the Sibley stratigraphy. The lower half of the stratigraphy is moderately variable and apparently random. The upper portion, corresponding with the Nipigon Bay Formation has, on average, a higher Zr/V ratio and seems to have a series of mafic to felsic trends within it.

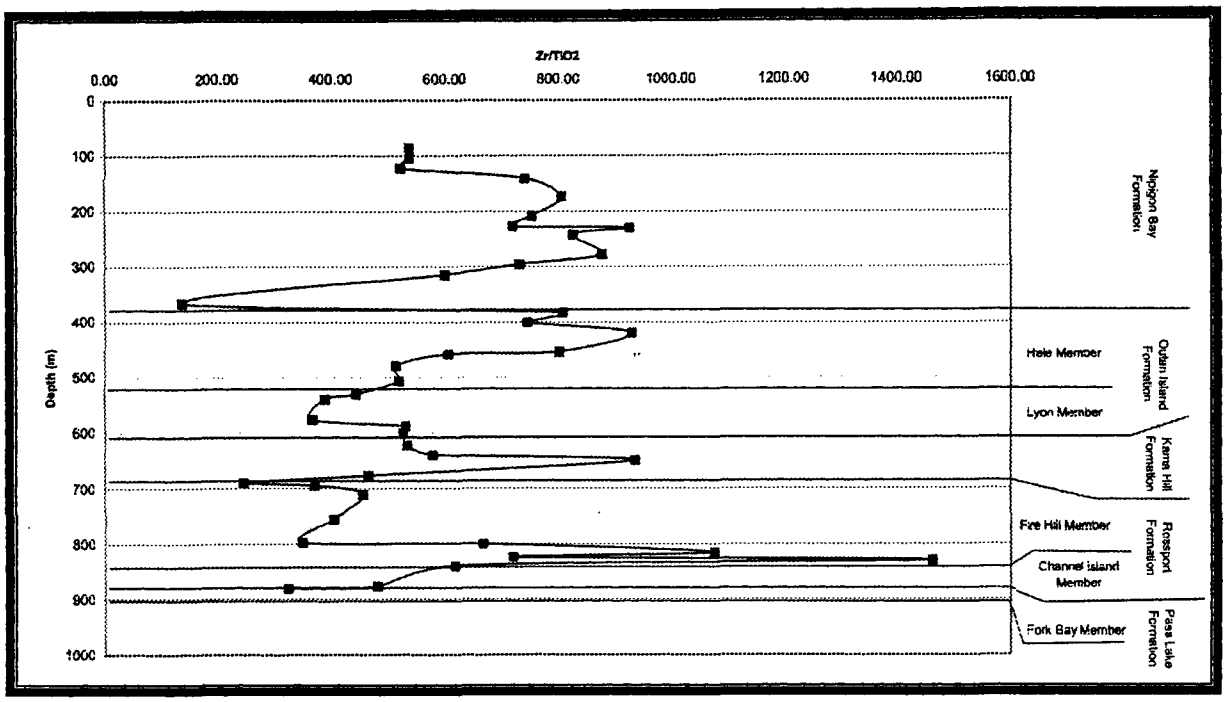

Figure 3.12. Zr/TiO_2 vs. Depth. The Zr/TiO_2 ratio is an indication of whether the source material is more mafic or felsic. A higher number indicates that the material is more felsic, while a lower number indicates a more mafic source.

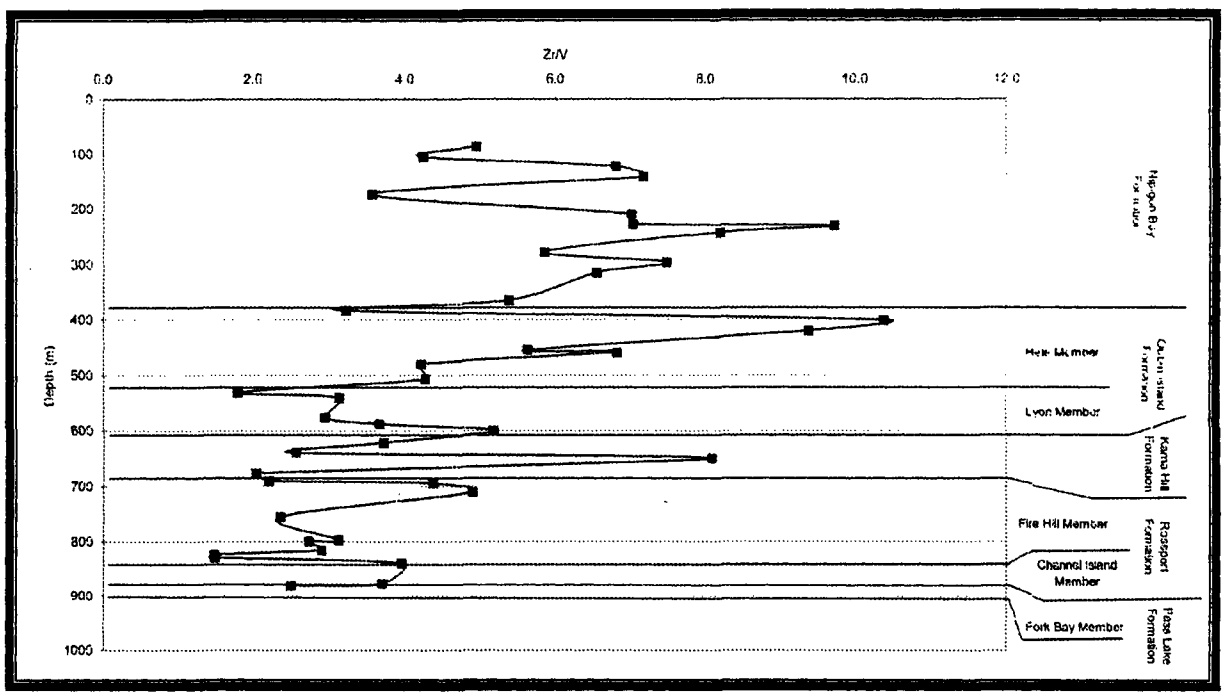

Figure 3.13. Zr/V vs. Depth. The Zr/V ratio is an indication of whether the source material is more mafic or felsic. A higher number indicates that the material is more felsic, while a lower number indicates a more mafic source.

The inconsistencies among the Zr/TiO_2, and Zr/V graphs suggest that there is a complex interplay of mafic and felsic source material throughout the depositional history of the Sibley Basin. These results could be caused by the zircon concentrating in the sand fraction as a resistate, and the TiO_2 and V concentrating in the clay fraction. Thus, increased weathering up-section increases the Zr value in the sandstones relative to the Al_2O_3, TiO_2, and V. This, interacting with changes in the source terrane creates a complex pattern. Therefore, since V and Al_2O_3 both concentrate in the clay-sized fraction, V/Al_2O_3 was plotted against depth (Figure 3.14) in an attempt to clarify the trends.

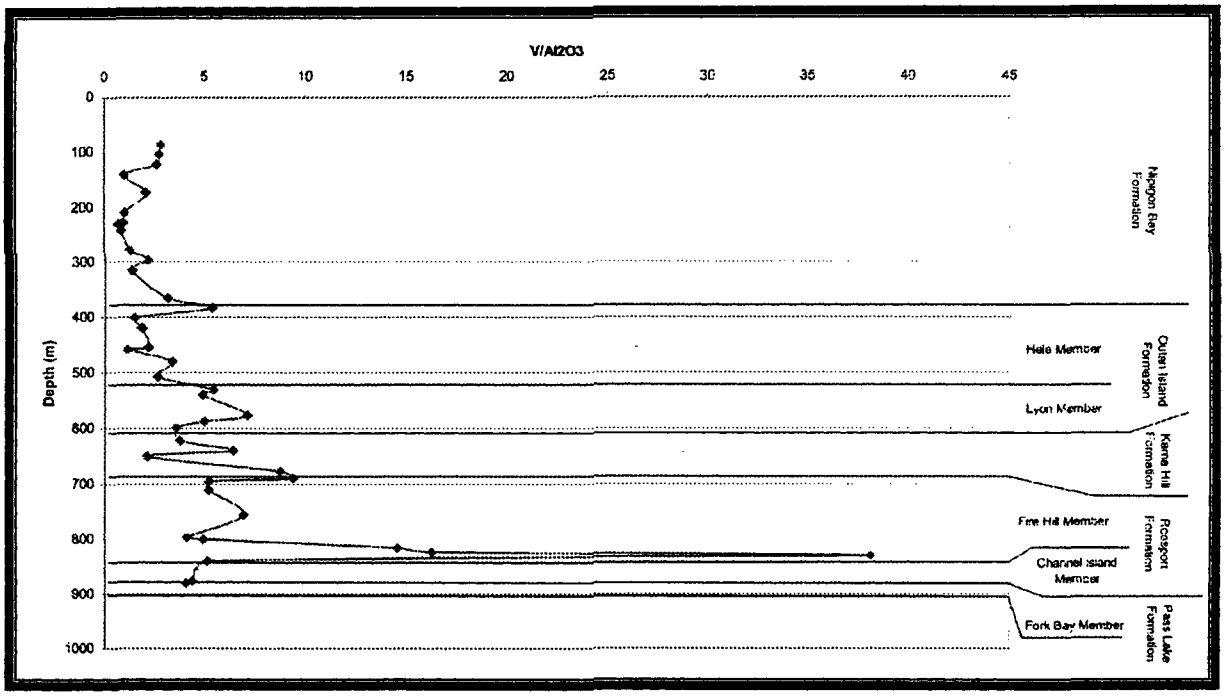

Figure 3.14. V/Al_2O_3 vs. Depth. The V/Al_2O_3 ratio is an indication of whether the source material is more mafic or felsic. A lower number indicates that the material is more felsic, while a higher number indicates a more mafic source.

The V/Al_2O_3 versus depth graph (Figure 3.14) indicates an overall increase in the amount of felsic material up-section. There is one significant mafic peak within the Rossport sandstones (lower 100 m), which gradually becomes more felsic as 800 m is

approached. Between 800 m and 450 m there are smaller variations within the sequence, which may be a random scatter. As the base of the Nipigon Bay Formation is approached, at 450 m, there is an increase in felsic material. This is followed by a relatively consistently high amount of felsic material throughout the majority of the Formation until the top 75 m to 100 m, where there is an increase in mafic material.

Variations in the alkalinity of the source rocks can be explored by looking at Nb/Y against the stratigraphic depth (Figure 3.15). There is a decrease in the amount of Nb relative to Y up-section, indicating a decrease in the alkalinity of the source rocks. This trend is explored more in relation with Zr/TiO_2 under source modelling.

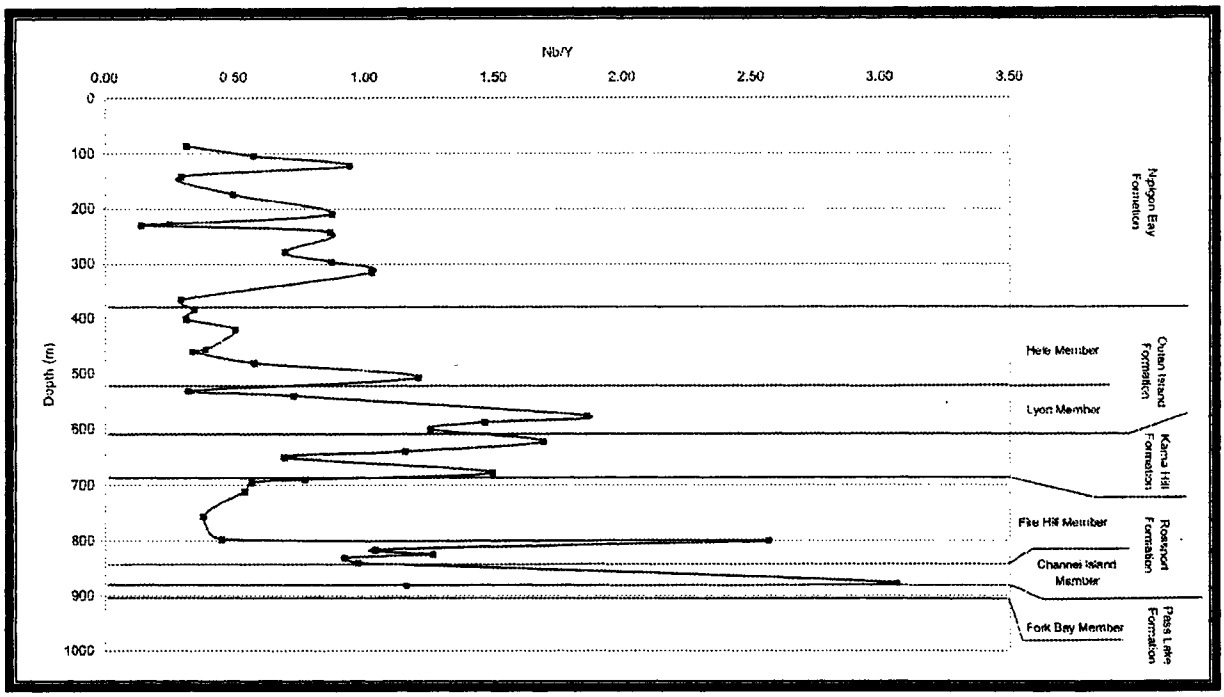

Figure 3.15. Nb/Y vs. Depth. The Nb/Y ratio is used to examine changes in alkalinity within the Sibley Group. A higher number indicates higher alkalinity.

3.4 Source Modelling

Variations in the geochemistry of the Sibley Group up through the stratigraphy indicate that there are distinct changes in the source material of the sediment. The variations can be used to divide the Sibley into three groups: 1) the Pass Lake and Channel Island Member of the Rossport Formation; 2) the remaining Rossport Formation, the Kama Hill Formation, and Outan Island Formation; and 3) the Nipigon Bay Formation. There is a gradual geochemical transition through the Rossport Formation, with most elemental trends changing within the Channel Island Member (at 800 m) (Figures 3.3, 3.6, and others not shown), while other elemental trends, such as total CaO (Figure 3.2) and CO_2 (Figure 3.4), change at the Rossport/Kama Hill boundary.

In order to examine source rock relationships, analyses of potential source rocks were obtained and plotted, with the Sibley Group analyses, on discrimination diagrams and ratio graphs. Potential source material included material found within the conglomerates of the Loon Lake Member of the Pass Lake Formation, such as Archean granites and metasediments and material derived from the Gunflint and Rove Formations. Analyses from Archean granites (Richardson, 2003a,b) and the English Bay granite (Fralick, unpublished data) were also used as potential sources. In order to facilitate comparisons between the Sibley Group and the source rocks, the Sibley was divided into the three groups defined by the stratigraphic geochemical variations. The first group includes the lower 100 m, the second group is between 800 m and 450 m, and the third group covers the sequence above 450 m.

Richardson (2003a) conducted a more detailed provenance study of the Pass Lake Formation. He determined that the Pass Lake Formation had been derived from the enriched English Bay Granite and un-enriched regional granites. A similar process has been followed here to compare the entire Sibley Group to his work. The ratios used here were chosen because they showed Richardson's (2003a) trends most clearly.

Figure 3.16 shows Y/TiO_2 against Nb/TiO_2 and Figure 3.17 shows Zr/TiO_2 against Nb/TiO_2. Both of these graphs indicate that the samples of the Sibley Group sediments appear to be derived from the same type of material, simply mixed in differing amounts. The lower group (dark blue squares), correlated with the Pass Lake Formation and Channel Island Member of the Rossport Formation, seems to form a similar trend on the Y/TiO_2 against Nb/TiO_2 plot to that seen in Richardson (2003a). Here, this unit has a sub-horizontal trend between the English Bay granite and a sandstone that has been proven to be derived from the English Bay Granite (Fralick and Kronberg, 1997), and they are situated between the English Bay Granite and the regional Archean granites. Richardson (2003a) also showed that the Pass Lake sandstones form a mixing line between the English Bay granite and these regional granites.

However, the middle (medium blue squares) and upper (light blue squares) groups do not fall along this mixing line. These groups appear to be related to each other, lying along the same mixing line. These sandstones have a steeper trend than the one given by the English Bay granite-Archean granite trend, suggesting that there is another source rock contributing to them.

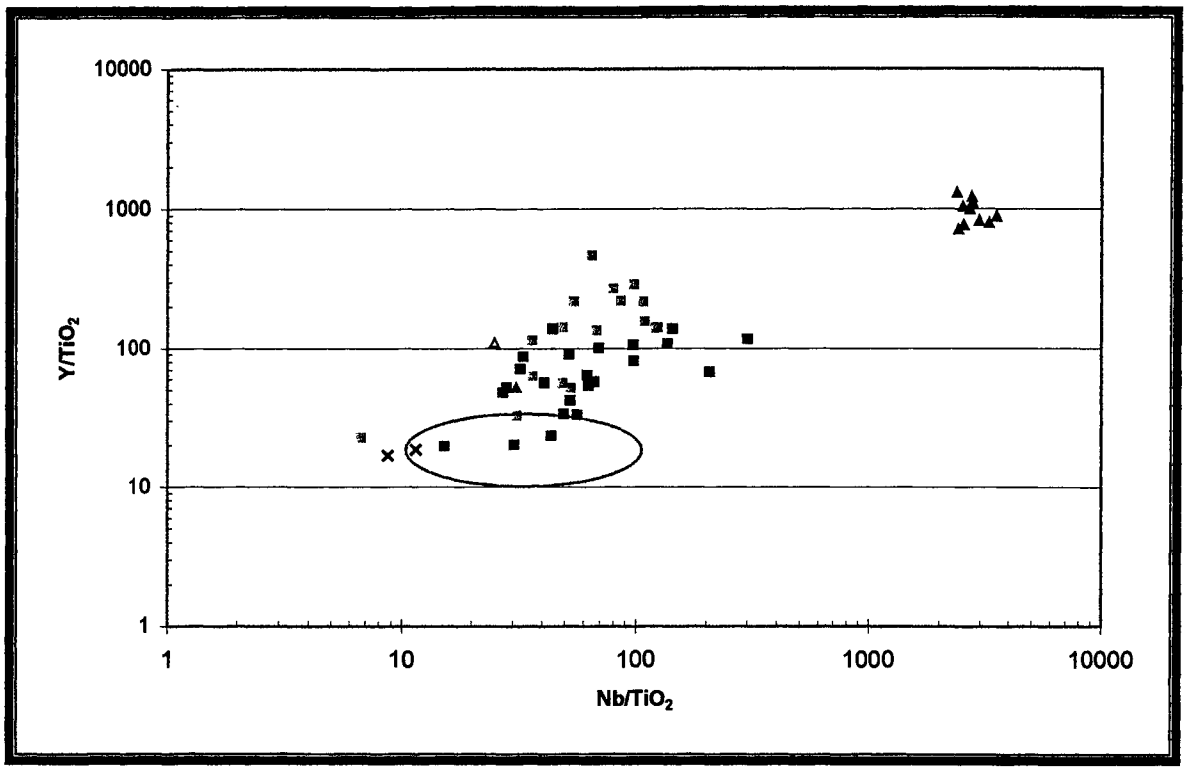

Figure 3.16. Y/TiO_2 vs. Nb/TiO_2. The Sibley Group is divided into three sections based on the stratigraphic variation section. Dark blue squares represent the Pass Lake and Channel Island Member of the Rossport Formation, medium blue squares represent the remainder of the Rossport Formation and the Kama Hill and Outan Island Formations, and the light blue squares represent the Nipigon Bay Formation. The green triangle represents an average Pass Lake sandstone, the open red triangle represents Pass Lake sandstones from English Bay, the filled red triangles are English Bay granites, and the black "X"s represent Quetico sediments. The outlined area denotes regional granites from Richardson (2003).

The Zr/TiO_2 vs. Nb/TiO_2 graph (Figure 3.17) has slightly different results. The upper and middle group samples are parallel and above the trend of the Archean granites, suggesting a stronger regional granite influence than the Y/TiO_2 vs. Nb/TiO_2 graph, although some influx from a more enriched source is also required. The sandstones from the lower sample group are clustered near the top of the Archean granite trend, extending sub-horizontal to the English Bay granite. This reinforces the idea that these sandstones are a result of mixing material from Archean and English Bay granites.

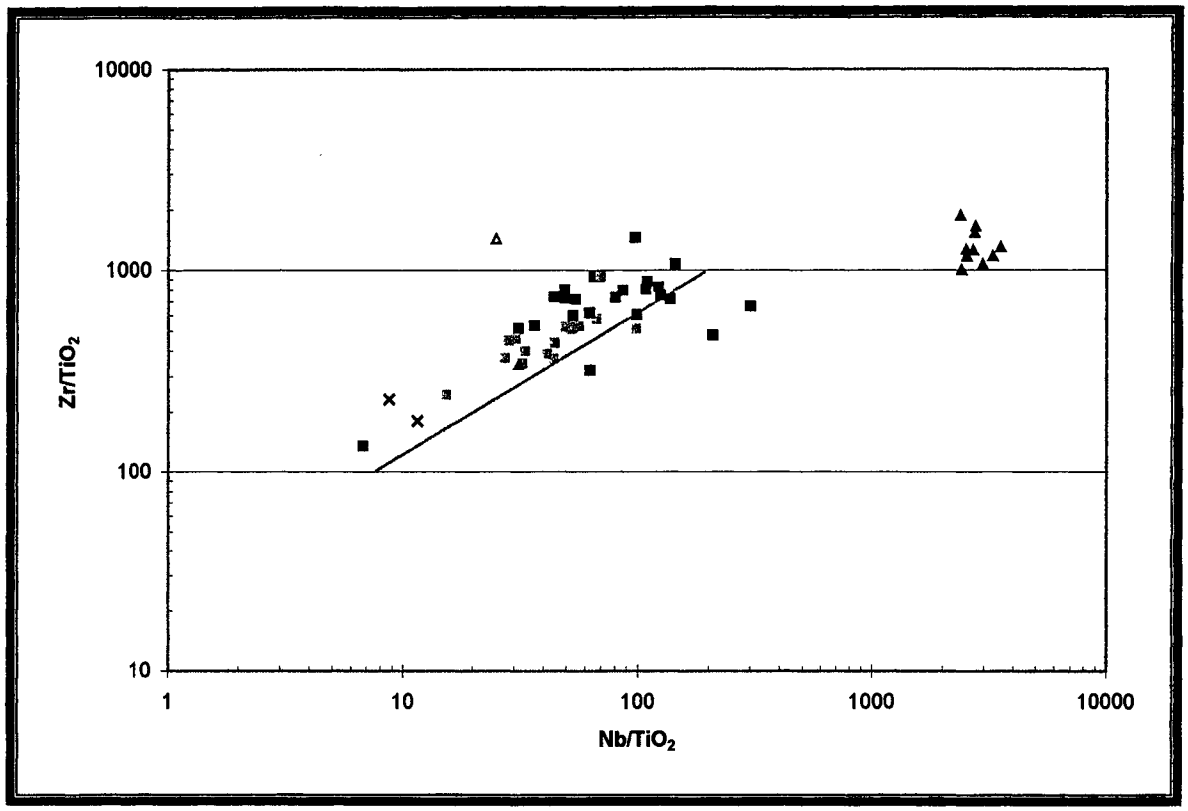

Figure 3.17. Zr/TiO_2 vs. Nb/TiO_2. The Sibley Group is divided into three sections based on the stratigraphic variation section. Light blue squares represent the Pass Lake and Channel Island Member of the Rossport Formation, medium blue squares represent the remainder of the Rossport Formation and the Kama Hill and Outan Island Formations, and the dark blue squares represent the Nipigon Bay Formation. The green triangle represents an average Pass Lake sandstone, the open red triangle represents Pass Lake sandstones at English Bay, the closed red triangles represent the English Bay granite, and the "X" represent Quetico sediments. The grey line denotes regional Archean granites, from Richardson (2003).

3.4 Conclusions

Geochemistry is a valuable tool in analysing the Sibley Group as it reflects the sedimentary and weathering processes affecting the basin and source rock composition. SiO_2, CaO, and CO_2 exhibit sedimentary trends that indicate a general increase in SiO_2 content upwards in the basin fill and the presence of carbonates in sandstones throughout the lower half of the sequence, as was expected from the lithologies of the units.

The Pass Lake Formation averages approximately 74% SiO_2, followed by an increase from 55% to 85% SiO_2 from the Rossport Formation through to the Kama Hill Formation. Above this there is a decreased SiO_2 content from 85% to 75% in the Outan

Island Formation, overlain by a sharp off-set at the Nipigon Bay Formation, which has an average of 90% SiO_2. These trends reflect the feldspathic sandstones and carbonates within the Pass Lake Formation, the presence of carbonates and muddy material within the Rossport, Kama Hill, and Outan Island Formations, and the extreme maturity of the Nipigon Bay sandstones.

The CaO and CO_2 trends show an increase from the Pass Lake Formation to the Channel Island Member of the Rossport Formation, followed by intermediate amounts of carbonate from the Rossport to the Outan Island Formation and a sharp decrease in carbonates within the sandstones of the Nipigon Bay Formation.

Weathering trends are more complex to decipher than sedimentary trends. All of the ratios used to examine weathering indicated a general increase in the degree of weathering upwards through the sequence. The CaO/K_2O graph indicated the presence of secondary carbonate enrichment within the Pass Lake and Rossport Formations. The CIA graphs were particularly interesting, stressing the importance of calcite and dolomite in grains and cements throughout the sandstones of the Rossport, Kama Hill, and Outan Island Formations. The presence of carbonates was also somewhat important in the Pass Lake Formation, but appears to be secondary to the influence of the degree of weathering of its source material.

Attempts at examining source rock trends produced some conflicting results. There seemed to be an overall increase in the amount of felsic material from the Pass Lake Formation to the Nipigon Bay Formation. There appears to be an increase in V/Al_2O_3 near the Pass Lake-Rossport Formation boundary, followed by a series of small-scale mafic to felsic trends between the Rossport Formation and the base of the Nipigon Bay Formation.

As the base of the Nipigon Bay Formation is approached, at 450 m, there is an increase in felsic material. This is followed by a relatively consistently high amount of felsic material throughout the majority of the Formation until the top 75 m to 100 m, where there is a slight increase in mafic material. There also appears to be a decrease in the alkalinity of the source material up-section.

Comparisons between the Sibley Group sediments and potential source rocks were made using Y/TiO_2 - Nb/TiO_2 and Zr/TiO_2 - Nb/TiO_2 graphs. These graphs indicate that the sandstones of the Pass Lake Formation and Channel Island Member of the Rossport Formation (lower 100 m) are derived from the English Bay Granite and regional Archean granites. The middle and upper groups are derived from regional Archean granites and an unidentified enriched source, although minor influence from the English Bay Granite may be a factor.

Chapter 4:

MAGNETOSTRATIGRAPHY

This preliminary paleomagnetic study of the Sibley Group has two foci. The first aspect involved assessing the differences between the paleopoles of the Pass Lake, Kama Hill, and Nipigon Bay Formations. By comparing these Formations, it was hoped that the paleopoles would reveal an apparent polar wander path (APWP) similar to the Proterozoic APWP, which would indicate differences in the age and geographic location between the lower, middle, and upper units of the Sibley Group.

The second aspect of this study involves secular variation within the cyclic siltstone-dolomite lithofacies association of the Rossport Formation. By examining the periodicity of the secular variation, estimates might be made about the sedimentation rates for the Rossport Formation.

4.1 Theoretical Considerations

There are two main types of magnetization: induced magnetization and remanent magnetization. Induced magnetization occurs during exposure to a magnetic field, such as the Earth's. This type of magnetization lasts only as long as the field is in place, and therefore is only able to express the *present* magnetic field (Butler, 1998). Remanent magnetization is capable of recording *past* magnetic fields and is used for paleomagnetic studies. It arises in several ways. Primary natural remanent magnetization (NRM) is established in ferromagnetic minerals, such as hematite and magnetite, at the time of mineral formation by processes such as chemical remanent magnetization (CRM), created

during diagenetic mineral growth. Detrital remanent magnetization (DRM) is formed when ferromagnetic minerals are deposited in sedimentary environments (Butler, 1998). In the case of detrital magnetization, the grains are already magnetized. They align themselves with the geomagnetic field as they settle out of the water column, thus recording the position of magnetic north at the time of deposition (Tauxe, 1998).

Secondary remanent magnetizations may overprint the characteristic or primary remanent magnetization, due to subsequent long-term interaction with the geomagnetic field (Butler, 1998). These overprints may or may not be related to distinct geological remagnetization events. Over time, the initial remanent magnetization of a ferromagnetic mineral weakens. More precisely, the initial magnetization is subject to randomization as individual particles gradually acquire sufficient thermal energy to overcome the older signal (Tauxe, 1998). The randomized particles tend to orient themselves with the geomagnetic field, thus recording magnetic north at various locations through time. Complete overprinting of the initial remanent magnetization occurs, for example, when a ferromagnetic mineral is exposed to temperatures above the mineral's Curie or Blocking Temperature of the earlier remanence (Butler, 1998).

Due to the effects of secondary magnetization, a remanent magnetization vector is composed of one or more vector components. It is important to isolate any individual components, by incremental demagnetization, to obtain meaningful paleomagnetic data. For example, by heating specimens incrementally, the magnetic vectors of a specimen can be randomized. The most recently acquired magnetic vectors are removed first at low temperature. Then, with each successive heating, older magnetic vectors are removed

(Butler, 1998; Tauxe, 1998). A mineral's magnetic components are completely demagnetized when the rock is heated to that mineral's Curie temperature.

Red bed sequences, such as the Sibley Group, are one of the most useful types of sediments for paleomagnetic studies. However, they also have problems associated with them. Therefore, it is important to consider whether the hematite in the Sibley is detrital or diagenetic in origin, as well as the degree to which it has been exposed to secondary magnetizations. The dominant ferromagnetic mineral is hematite, with specularite and minor magnetite occurring in some samples (Franklin, 1970). Hematite and specularite are among the more stable of the magnetic minerals (Elston *et al.*, 2002), and should, therefore, reliably record the paleomagnetization. Some of the sedimentary units, particularly in the Nipigon Bay Formation, indicate that at least some of the magnetization is a result of detrital processes. For example, some hematite occurrences are restricted to individual sandstone laminae. Most of the source rocks for the Sibley Basin, such as the iron formations of the Proterozoic Gunflint Formation and Archean rocks, readily provide magnetic minerals (Franklin, 1970). However, much of the basin shows signs of diagenetic alteration. This is seen as hematite coatings on grains and irregular oxidized and reduced blotches that do not mirror the sedimentary layering. Franklin (1970) also notes the formation of platy specularite hematite in vugs. Nevertheless, the red pigmentation probably formed early, preserving a record of the magnetism near the time of deposition. The sediments were deposited in subaerial to shallow lacustrine environments, indicating conditions conducive for the oxidation of ferromagnetic minerals. Clasts of altered Sibley sediments can also be found in conglomerates and breccias in the upper sections of the sequence, suggesting that diagenetic processes were at work roughly coeval with

deposition. A paleosecular variation has also been observed in a section of the Rossport Formation, once again signifying rapid formation of diagenetic hematite.

4.2 Previous work

Robertson and Fahrig (1971) and Robertson (1973a) were responsible for most of the early paleomagnetic work on the Sibley Group, although the credit for this work is commonly erroneously given to Hinze and Wold (1982). Robertson and Fahrig (1971) also conducted paleomagnetic studies on other rocks found within the Sibley region. Many of these studies used rocks with known ages, such as dikes and Logan sills (Robertson and Fahrig, 1971), and Keweenawan samples (Robertson, 1973b).

Robertson (1973a) collected samples from three of the seven units defined by Franklin (1970). He noted that the sediments could have either a normal or reversed component acquired during deposition, as well as potentially having a magnetic component produced during baking from the intrusion of Logan Sills. Robertson (1973a) determined that the paleopole position for the Sibley Group is 215°E, 20° S, and determined that the Sibley Basin was within equatorial latitudes at the time of deposition. This position was paired with the 1339 Ma Rb-Sr age (Franklin, 1978) the Sibley Group was given at the time and used as a reference point on the Logan Loop.

Unfortunately, there were several points that were not taken into account. The first problem arises from the sampling procedure. The samples were taken without a good stratigraphic control. The samples cover only three of the five Formations (Robertson, 1973a), excluding the two new Formations that comprise over half of the Sibley stratigraphy. Therefore, the samples cannot be used for magnetostratigraphy since the

samples are not assigned to lithofacies units. A problem also arises from averaging the paleopoles to form a generic paleopole for the Sibley Group as Robertson (1973a) did. While this is a common technique, Robertson (1973a) only used the lower half of the stratigraphy. Therefore, if there is a large difference in paleopole positions between the bottom and top of the Sibley, Robertson's average will not be valid. The last problem with paleomagnetic work on the Sibley is related to advances in age dating techniques and new stratigraphic discoveries within the Sibley. Evidence seems to indicate that the Sibley is older than previously thought. Regrettably, the Sibley Group has been used on the Logan Loop as a defining point at 1339 Ma when this age is a diagenetic overprint (Franklin, 1978), rather than its depositional age.

This study attempts to resolve some of these problems. Enough work has been done that it is possible to constrain the samples in a stratigraphic framework. Samples were taken from four of the five Formations. These are the Pass Lake, Rossport, Kama Hill and Nipigon Bay Formations. The Outan Island Formation is only found in one un-oriented drill hole and does not lend itself to useful paleomagnetic research at this point. The resulting paleopoles should provide a polar wander path for the Sibley Group. The pole positions may assist in indicating an age for the Sibley Group, as well as potentially giving some insight into the period of time it covers.

4.3 Methodology

Oriented samples were taken from the Pass Lake Formation and units transitional to the Rossport Formation, Kama Hill and Nipigon Bay Formations for paleomagnetic analysis. The Pass Lake Formation was sampled from an outcrop at Pass Lake and from

Quarry Island and Copper Island on Lake Superior. These samples provided a total of 17 specimens. Another 10 samples were also taken from islands in Lake Superior, representing units that were transitional to the Rossport. Seventeen specimens were drilled from 3 samples from a Kama Hill outcrop, although only 15 provided useable data. The Kama Hill Formation presents a problem for paleomagnetic sampling due to the highly fissile nature of the sedimentary rocks, both during the sample preparation process and during heating. The Nipigon Bay Formation has only been found to crop out on one corner of Simpson Island in Lake Superior. Fifteen specimens were acquired from four samples from this location. Samples of the cyclic siltstone-dolomite lithofacies association of the Rossport Formation were obtained from unoriented drill core recovered from the NB-97-4 hole.

The oriented specimens were found to have bimodal magnetic intensities, where the Kama Hill specimens averaged 700 mA/m and the Pass Lake and Nipigon Bay samples had less than 10 mA/m. This meant that two machines were required to properly measure the paleomagnetism. The Kama Hill specimens were measured using a Molspin and the Pass Lake and Nipigon Bay samples were measured using a JR5a Spinner Magnetometer. This group of samples was initially measured then thermally demagnetized to 150°C. The samples were then heated at 50°C intervals to 500°C, followed by 25°C intervals until 700°C was reached. The final temperature was chosen because hematite has a Curie temperature of 680°C (Butler, 1998). Paleomagnetic measurements were taken after each heating. Samples from the Rossport Formation were measured on a Molspin for their initial magnetic signature, followed by thermal demagnetization by heating at 50°C intervals from 150°C to 700°C. Measurements were acquired after each heating.

Paleomagnetic poles were determined and plotted using Spin01 software for all sample sets.

4.4 Stratigraphic Variation

4.4.1 Results

All of the sample groups showed distinctly different primary and secondary component vectors, summarized in Table 4.1. The Pass Lake samples initially appeared to be the most complex. They have been divided into the Pass Lake outcrop (PLO), Quarry Island (QI), and Transitional to Rossport (T) groups. The Quarry Island and Transitional groups typically exhibit steadily decaying intensity-demagnetization curves, as shown in Figure 4.1. The PLO group has a sharp peak on the intensity decay graph (Figure 4.2d) at approximately 500°C, related to a change in the direction of the vector components.

Thermal demagnetization revealed two components in all of the samples. The earliest vector (A) shows differences between the groups, seen in the stereonets in Figure 4.3. The PLO Group paleopole is found at 185.1°E/10.6°N, although the stereonet for this group shows that there is too much scatter for it to be reliably used. Therefore, the PLO Group is omitted from the paleopole maps. The Transitional Group and Quarry Island Group paleopoles are found at 1.0°E/189.4°N and 15.4°E/30.8°N (Figure 4.5), respectively. However, the alternate paleopole for the Quarry Island Group, found at 195.4°E/30.8°S, is used for the discussion on stratigraphic variation because it lies on the Mesoproterozoic apparent polar wander path. A second, later component, designated B, is shared by all of the samples and is tightly constrained at 255.7°E/64.6°N, as shown by the clustering on the stereonet depicted in Figure 4.4. It is also plotted on the map in Figure 4.5.

Table 4.1. Summary of Paleomagnetic Results

Site	N	n	Site Lat.	Site Long.	Site Paleolat	Decl.	Incl.	α_{95}	κ	Pole Lat.	Pole Long.	Demag Temp
Nipigon Bay A Component	4	13	48.8	272.3	55.2	253.9	70.9	14.7	8.9	30.9	232.6	250°C
Nipigon Bay B Component	4	7	48.8	272.3	32.2	44.4	51.6	12.0	26.3	53.0	12.1	350°C
Nipigon Bay C Component	4	12	48.8	272.3	22.9	303.3	40.3	4.4	98.3	22.9	173.2	450°C
Kama Hill A Component	3	8	49.0	271.7	-23.7	52.6	-41.2	18.7	9.7	-3.6	224.8	400°C
Kama Hill B Component	3	13	49.0	271.7	-43.7	138.4	-62.3	5.4	59.7	61.1	186.9	500°C
Pass Lake Outcrop A Component	1	6	48.8	272.3	9.8	274.9	19.2	62.0	2.1	10.6	185.1	350°C
Pass Lake Quarry Island A Component	2	11	48.8	272.3	-14.9	239.9	-28.0	11.9	15.7	30.8	15.4	400°C
Pass Lake Transition A Component	4	10	48.8	272.3	5.5	265.3	11.0	18.8	6.9	1.0	189.4	450°C
Pass Lake B Component	7	26	48.8	272.3	71.8	337.0	80.7	7.0	17.3	255.7	64.6	500°C

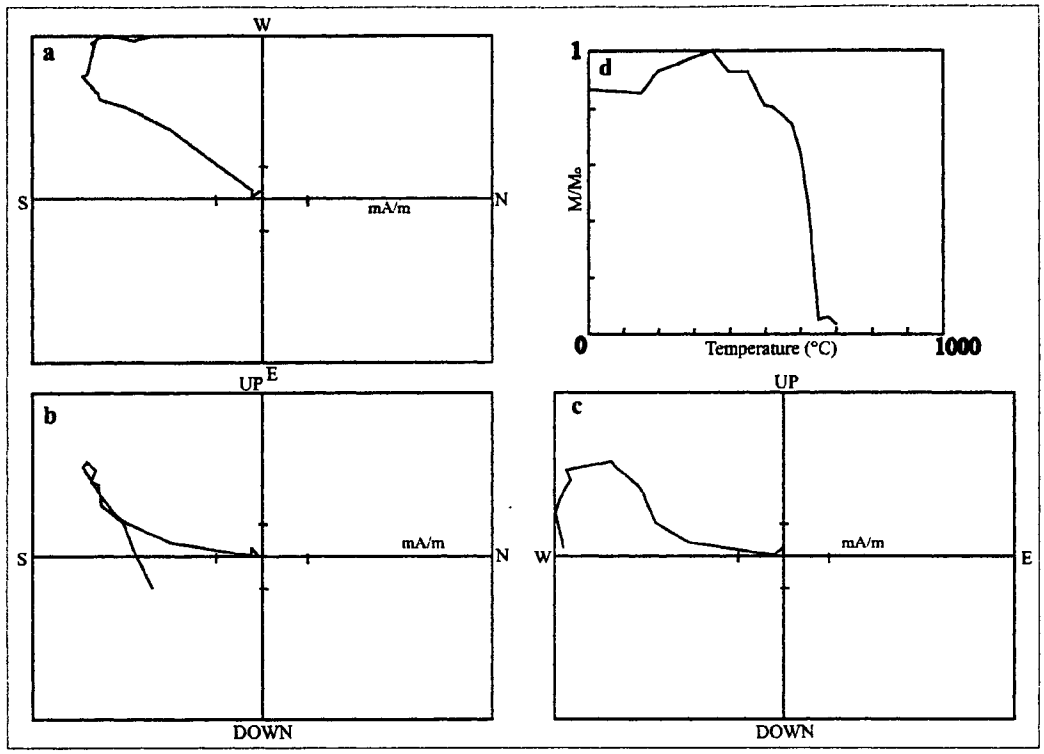

Figure 4.1. Demagnetization Vectors for the Pass Lake Formation. Graphs a, b, and c show typical two-dimensional vector plots for the Quarry Island and Transitional Groups of the Pass Lake Formation. Ticks indicate 1 mA/m. Graph d is an intensity decay plot.

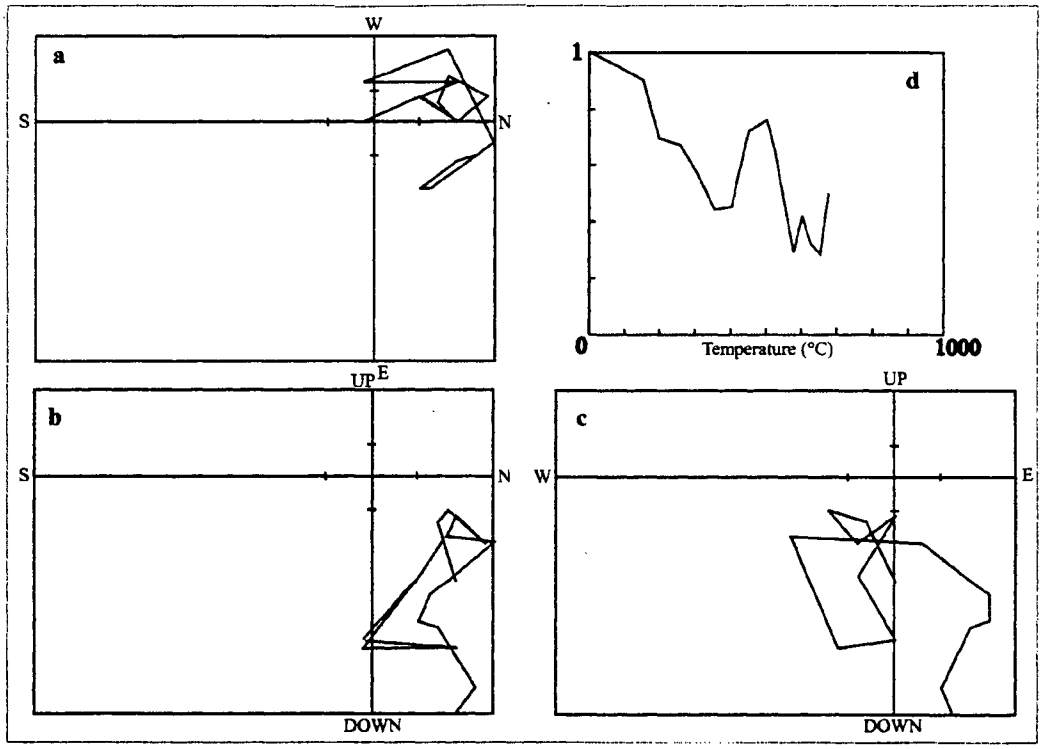

Figure 4.2. Demagnetization Vectors for the Pass Lake Outcrop Group. Graphs a, b, and c show typical two-dimensional vector plots for the Pass Lake Outcrop Group of the Pass Lake Formation. Ticks indicate 1 mA/m. Graph d is an intensity decay plot.

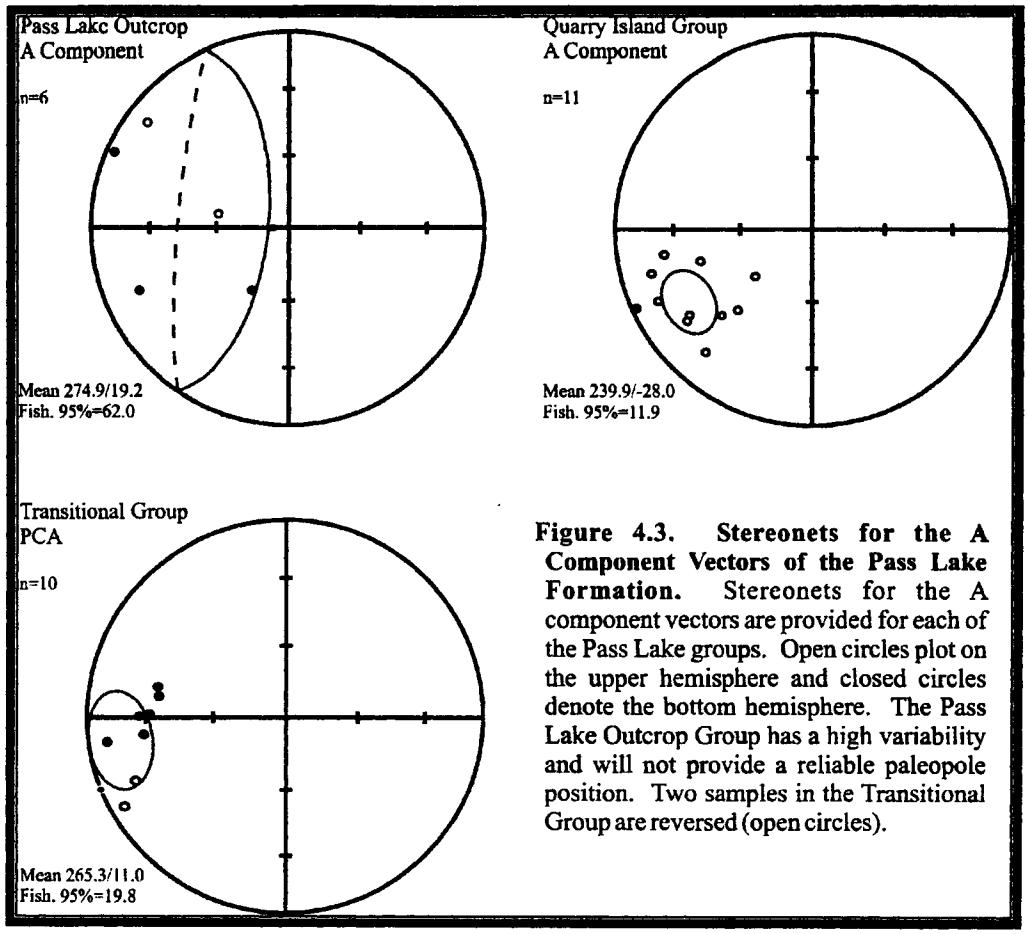

Figure 4.3. Stereonets for the A Component Vectors of the Pass Lake Formation. Stereonets for the A component vectors are provided for each of the Pass Lake groups. Open circles plot on the upper hemisphere and closed circles denote the bottom hemisphere. The Pass Lake Outcrop Group has a high variability and will not provide a reliable paleopole position. Two samples in the Transitional Group are reversed (open circles).

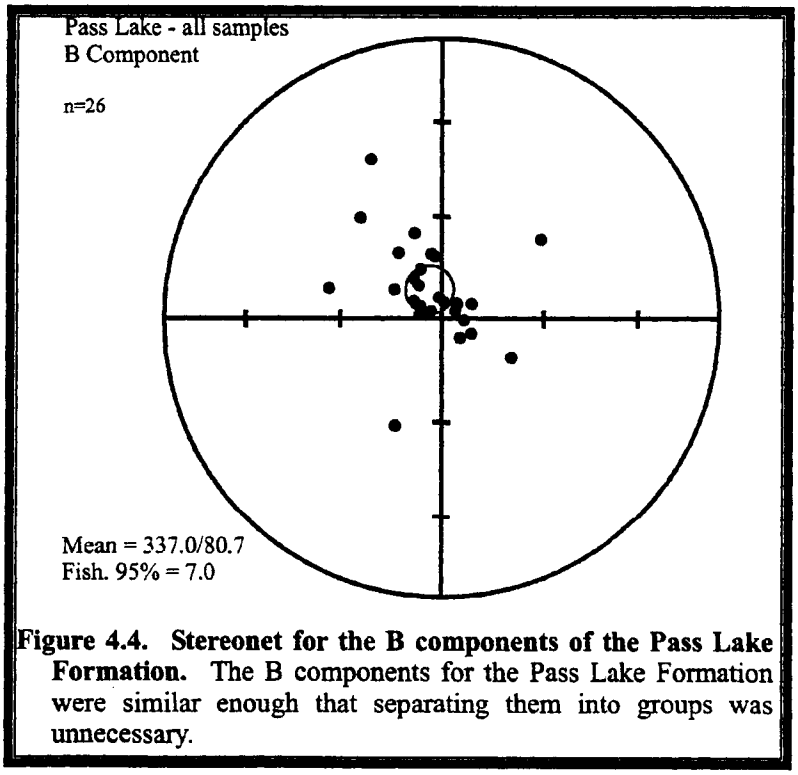

Figure 4.4. Stereonet for the B components of the Pass Lake Formation. The B components for the Pass Lake Formation were similar enough that separating them into groups was unnecessary.

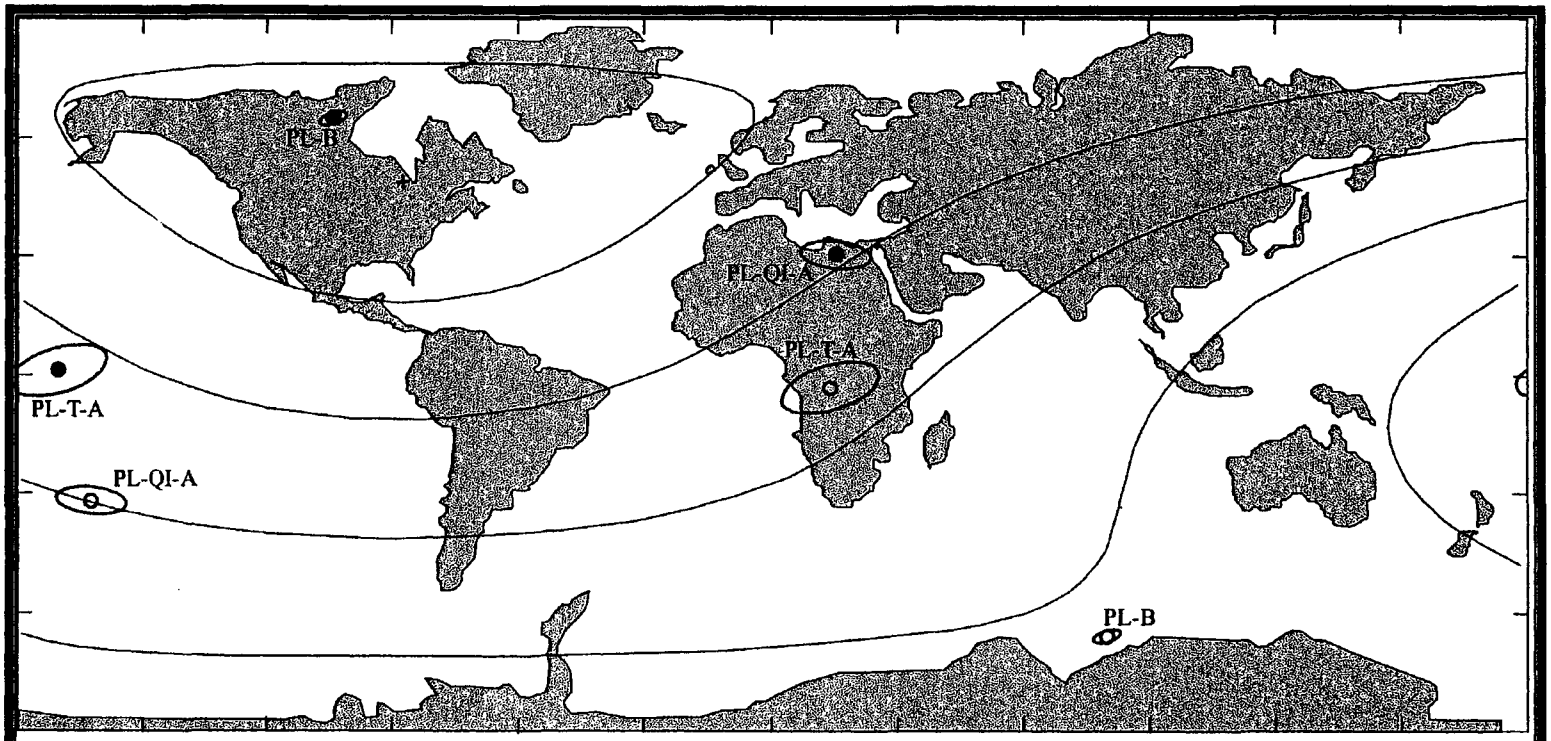

Figure 4.5. Composite Paleopole Map of the Pass Lake Formation. The samples for the Pass Lake Formation have been divided into three groups based on their A component paleopoles. The Quarry Island Group (QI) and the Transitional Group (T), which are samples taken from the transitional area between the Pass Lake and Rossport Formations, are shown. The A component of the Pass Lake Outcrop Group (O) was too scattered to generate a reliable paleopole position. All three of the sample groups had the same B component. The paleopole positions are shown as closed circles and alternate paleopoles are shown as open circles. The sample site is located at 272.3°E, 48.8°N.

The specimens of the Kama Hill Formation typically show two component demagnetization curves, with smooth intensity decay curves (Figure 4.6), although some of the samples only have one component. Stereonet projections are shown for both the primary and secondary components in Figure 4.7. The primary magnetic component reveals a paleopole at 186.9°E/61.1°N, and the secondary component has a paleopole located at 224.8°E/3.6°S. Both of these paleopoles and their alternate poles are shown in Figure 4.8).

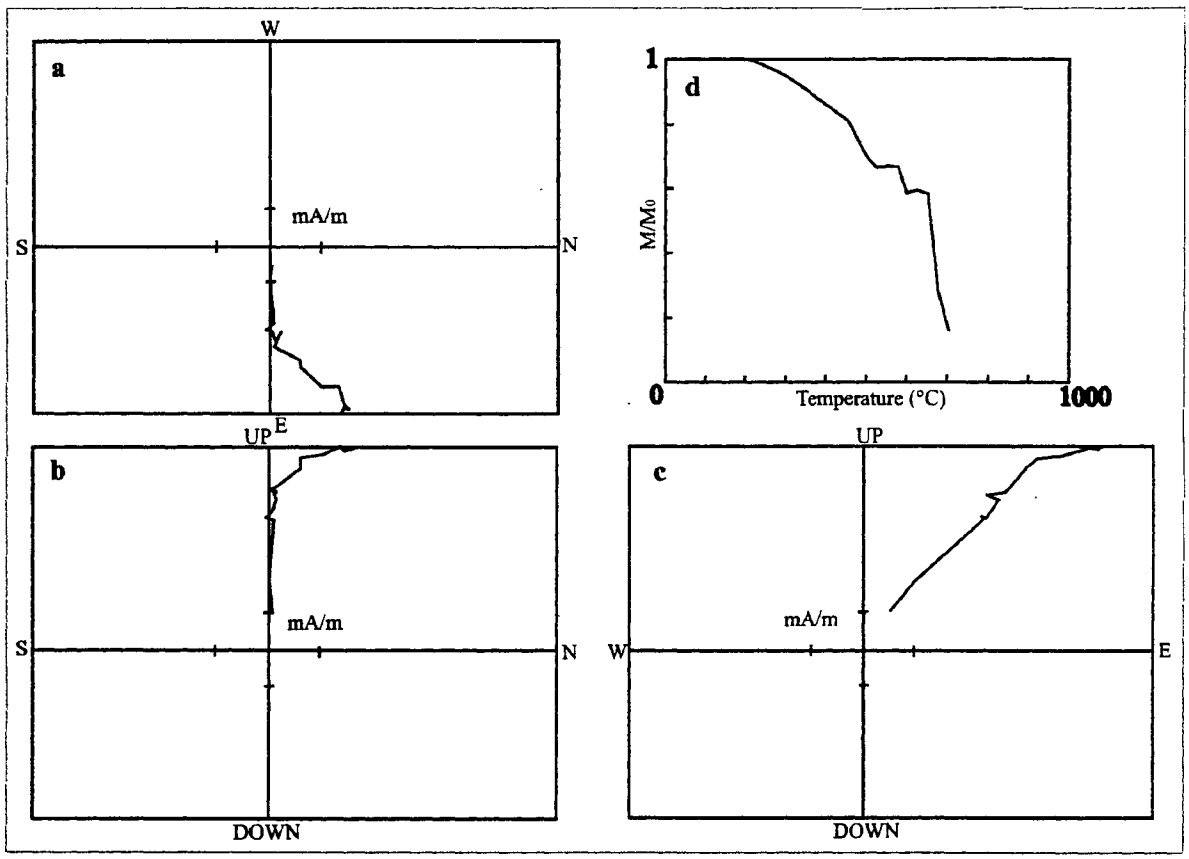

Figure 4.6. Demagnetization Vectors for the Kama Hill Formation. Graphs a, b, and c show typical two-dimensional vector plots for the Kama Hill Formation. Ticks indicate 1 mA/m. Graph d is an intensity decay plot.

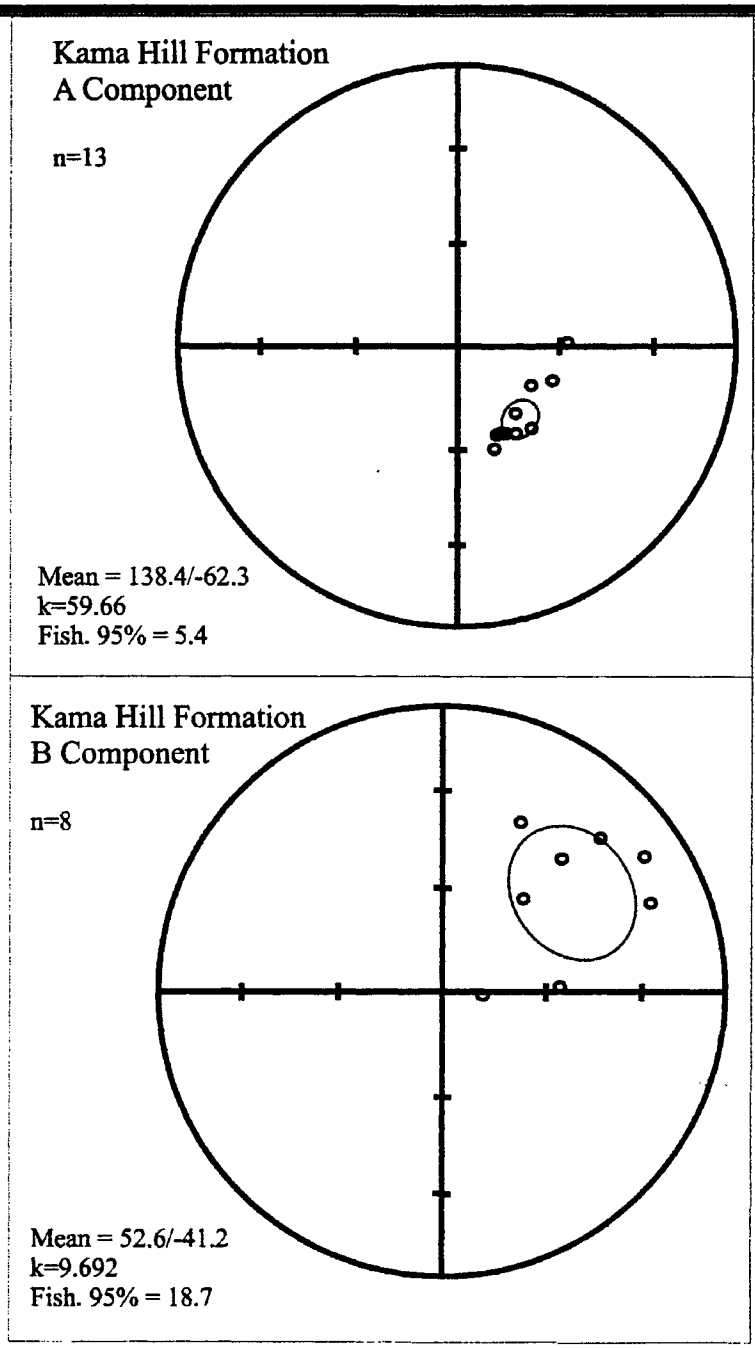

Figure 4.7. A and B Component Stereonets for Kama Hill. Stereonets for the A and B vector components derived from the Kama Hill Formation are shown. In both the A and B Component stereonets, all samples plotted on the upper hemisphere, indicated by open circles. The grey circle indicates the 95% confidence cone.

Figure 4.8. Composite Paleopole Map of the Kama Hill Formation. The A and B component paleopoles (closed circles) and alternate paleopoles (open circles) are shown for the Kama Hill Formation. The sample site is located at 272.3°E, 48.8°N.

The Nipigon Bay samples also typically show smooth intensity curves and two component demagnetization curves (Figure 4.9), although three components are sometimes present. All three principal components were found in only four samples, although seven samples showed the A and C components, two showed the A and B components, one showed the B and C components, and one showed only the C component. The stereonets for the A, B and C components are depicted in Figure 4.10. The paleopoles for A, B, and C are located at 232.6°E/30.9°N, 53.0°E/32.2°N, and 173.2°E/38.8°N, respectively, and, along with the alternate poles, are plotted on the map in Figure 4.11.

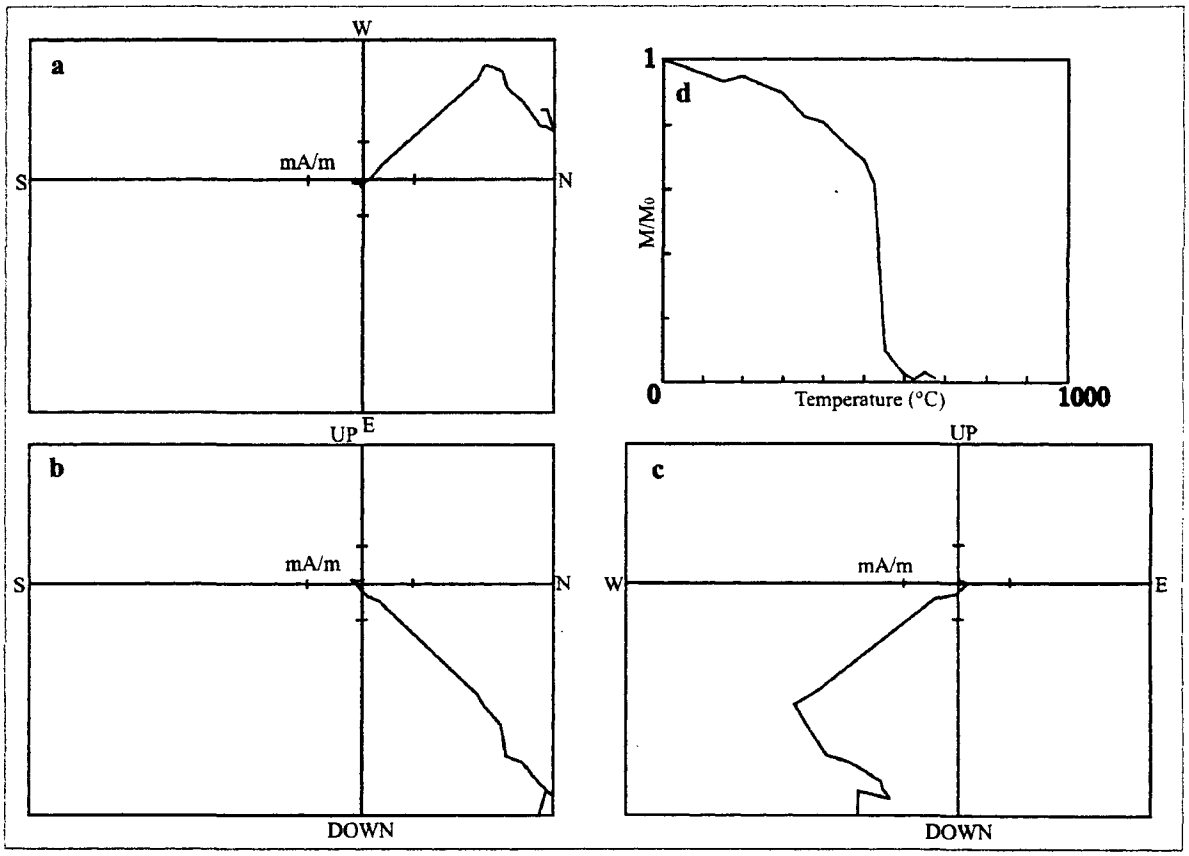

Figure 4.9. Demagnetization Vectors for the Nipigon Bay Formation. Graphs a, b, and c show typical two-dimensional vector plots for the Nipigon Bay Formation. Ticks indicate 1 mA/m. Graph d is an intensity decay plot.

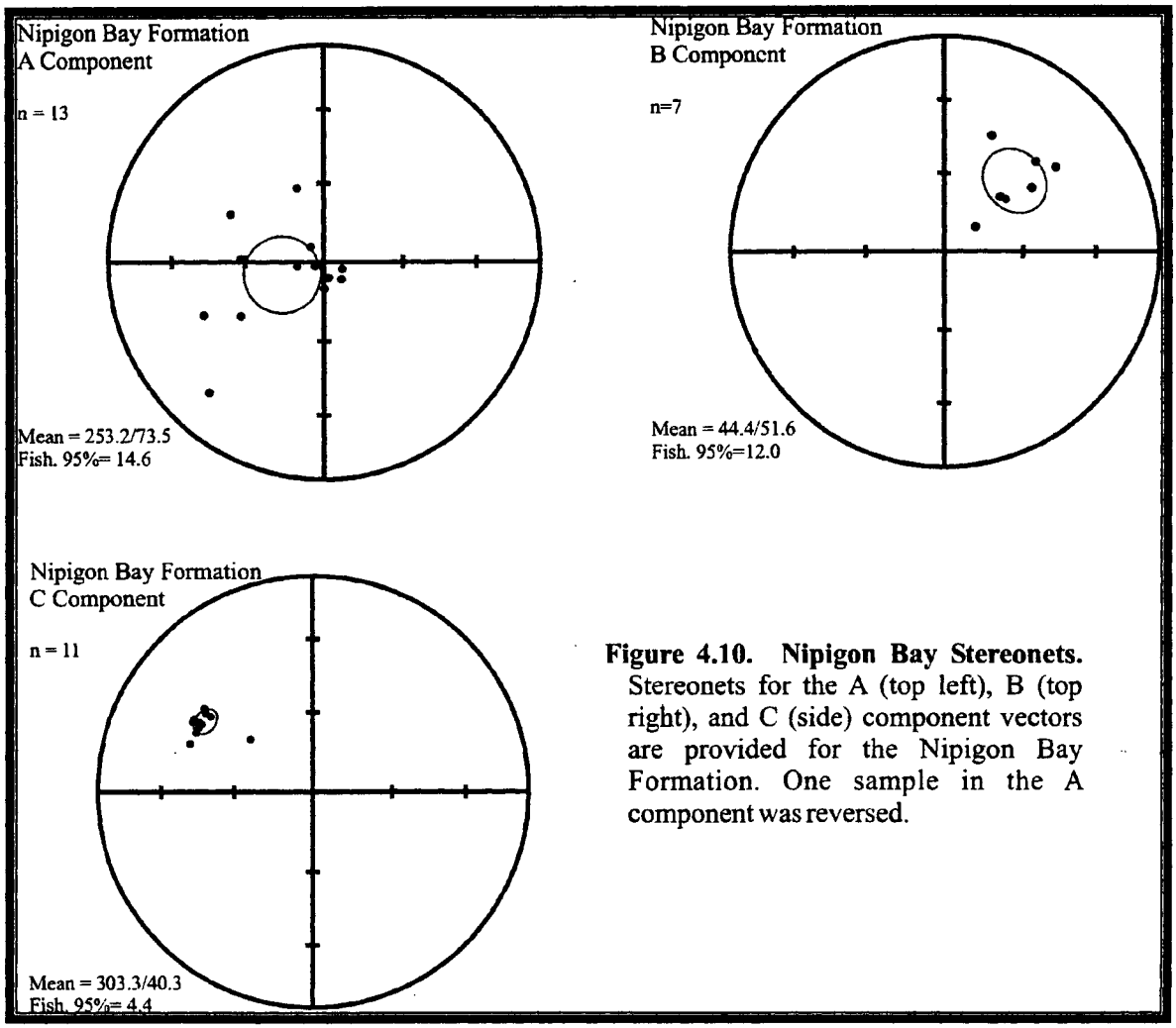

Figure 4.10. Nipigon Bay Stereonets. Stereonets for the A (top left), B (top right), and C (side) component vectors are provided for the Nipigon Bay Formation. One sample in the A component was reversed.

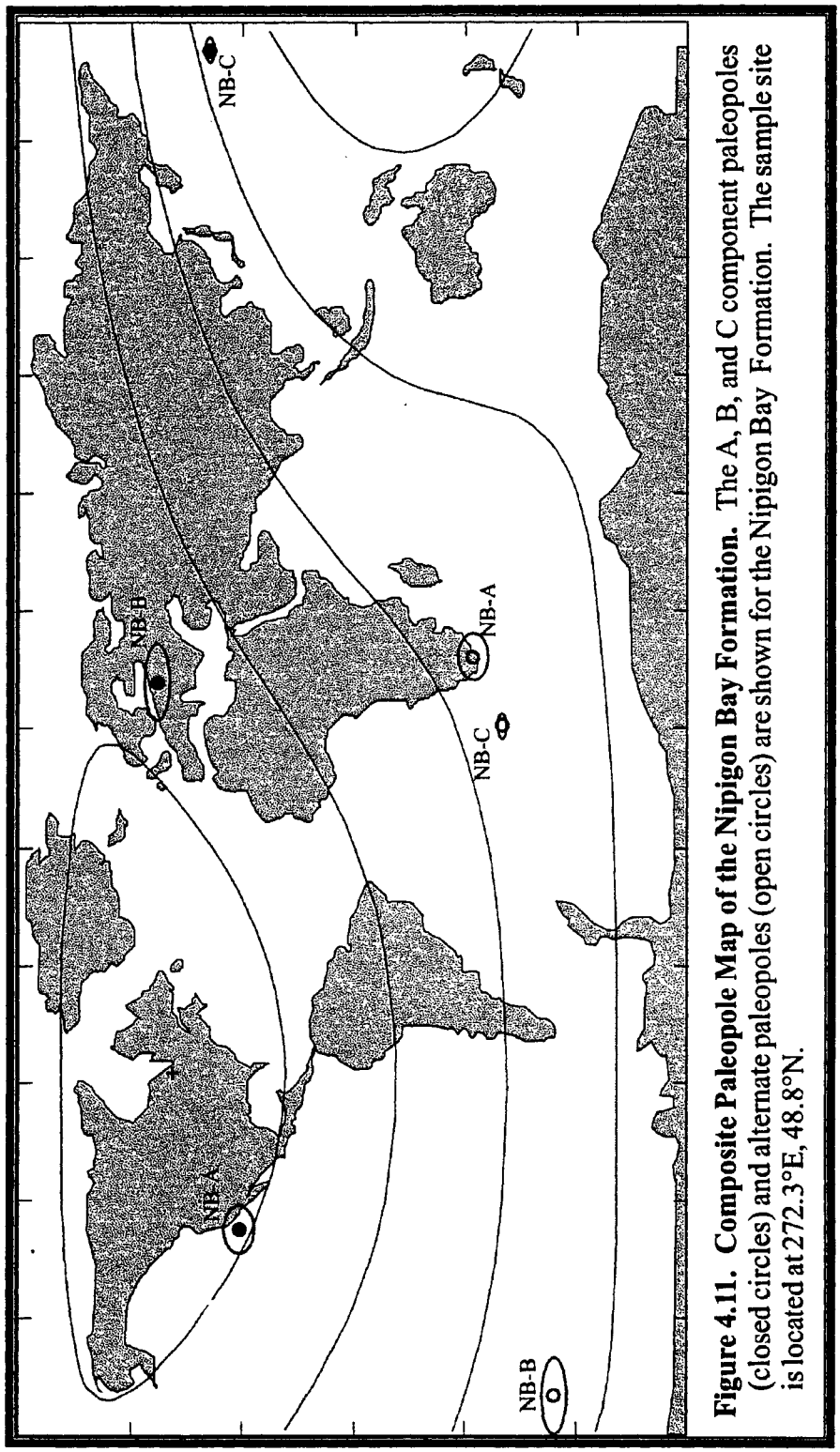

Figure 4.11. Composite Paleopole Map of the Nipigon Bay Formation. The A, B, and C component paleopoles (closed circles) and alternate paleopoles (open circles) are shown for the Nipigon Bay Formation. The sample site is located at 272.3°E, 48.8°N.

4.4.2 Interpretation

Magnetostratigraphy can be very useful for basin analysis. It can provide information about the geographic location where the sediments were deposited, as well as changes in latitude over time. The paleopole position on an apparent polar wander path (APWP) will imply the approximate age of the Sibley Group. With more detailed studies of reversals and paleopole positions, another method for stratigraphic correlation of the Sibley Group could be possible.

To facilitate interpretations of paleomagnetic data, they are compared with an APWP. An APWP is unique to each continent or terrane, and is constructed from the paleopole positions of rocks with well-constrained ages (Butler, 1998). However, some poles plot away from the expected APWP. These are known as discordant poles (Tauxe, 1998). Discordant poles have not been completely explained, but in some cases may be related to independent rotation or translations as experienced by terranes and microplates (Tauxe, 1998), excursions, and non-dipole field anomalies (Butler, 1998).

The results of paleomagnetic analysis of the Sibley show distinct differences among the Formations (Figures 4.4, 4.8, 4.11). These data have been plotted in Figure 4.12 against a Proterozoic APWP for the North American Craton, which Elston *et al.* (2002) used to examine Belt Supergroup. The Pass Lake Formation appears to record several events, none of which seem to be related to the time of deposition. The alternate paleopole for the Quarry Island Group plots off of the APWP near the 1400 Ma interval, which may be related to a diagenetic event at 1339±33 Ma, defined by the Rb-Sr age determination of Franklin (1978). The Transitional Group plots between 1300 Ma and 1400 Ma and is very likely associated with diagenetic alteration represented by Franklin's (1978) age

determination. All of the Pass Lake sample groups have the same B component (PL-B on Figure 4.12). This pole does not match the present magnetic pole position, but is younger than the other Pass Lake paleopoles.

The Kama Hill paleopoles are particularly interesting. The oldest paleopole (KH-A on Figure 4.12) is not near the APWP, but is found off the coast of Alaska. This pole is most likely a discordant pole. The younger Kama Hill pole (KH-B) is near the 1500 Ma section of the APWP, most likely representing the time of deposition or a diagenetic event closely related to it. Because the Kama Hill is in the middle of the stratigraphic sequence, it can be hypothesized that the Sibley deposition began prior to this time. The intercalation of English Bay rhyolites (1537 Ma) and Sibley Group sediments that was observed by Cheadle (1986a) further supports this theory.

The Nipigon Bay Formation is more complex than the other Formations because it is a three-component system. The A-component paleopole is the oldest and is not situated near the APWP, probably representing a discordant pole. The C-component paleopole is clearly related to resetting by the thermal event of the Osler Volcanics at 1100 Ma. This is reasonable since the samples were collected from an outcrop that was only meters below the 10s of kilometres thick succession of Keweenawan mafic volcanics. The Nipigon Bay B-component paleopole is reversed, and is situated off of the 1400 Ma to 1450 Ma section of the APWP near the reversed pole of the Quarry Island Group of the Pass Lake Formation. The Nipigon Bay paleopole may be related to Franklin's (1978) 1339 Ma Rb-Sr age on diagenetic alteration or it may be a depositional pole.

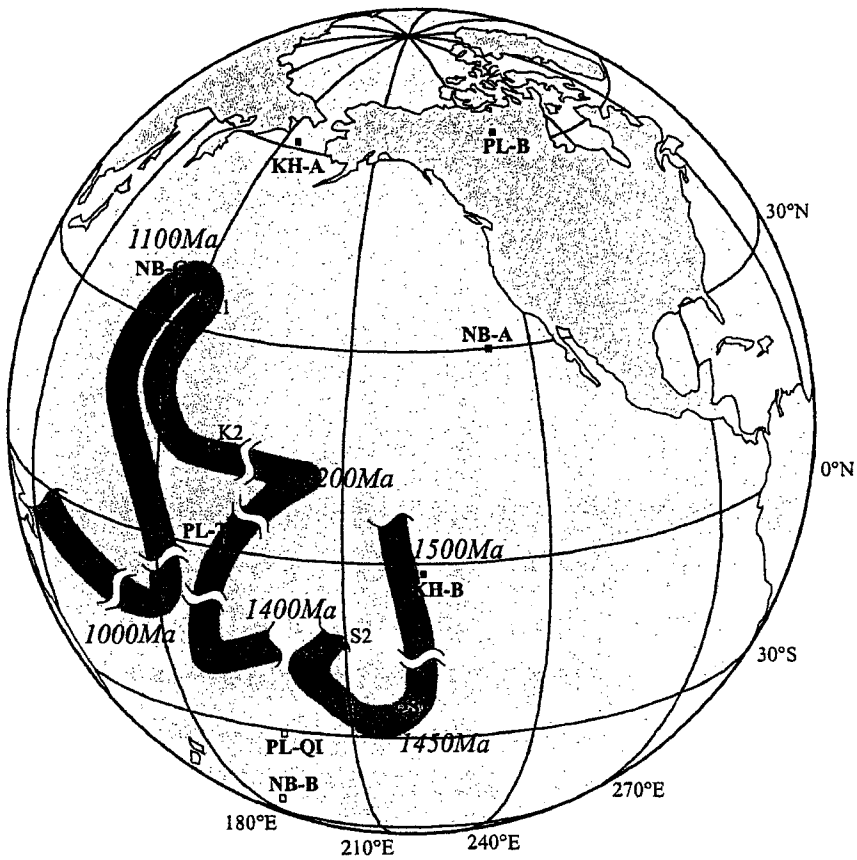

Figure 4.12. A Comparison of Sibley Group Paleopoles and a Mesoproterozoic Apparent Polar Wander Path. A well-defined Proterozoic Apparent Polar Wander Path (APWP) is plotted (after Elston *et al.*, 2002). The A components for the Pass Lake Formation(PL) are designated with QI and T to indicate the Quarry Island and Transitional Groups. The Kama Hill Formation is designate KH and the Nipigon Bay Formation is NB. The A, B, and C components are denoted respectively by A, B or C after the Formation short form. The A and B components of the Nipigon Bay Formation are somewhat problematic for the Mesoproterozoic APWP and may actually be the reverse of the paleopoles shown. Elston *et al.* (2002) has provided a lower (S1) and upper (S2) Sibley Group pole based on data from Robertson (1973a), as well as a pole for the Keweenawan Osler Group (K1) and lower Powder Mill Volcanics (K2).

4.6 Secular Variation

4.6.1 Results

The surface expression of the Earth's geomagnetic field changes over time. This change is known as secular variation, and is typically associated with a periodicity of 1 to 10^5 years (Butler, 1998). The majority of paleo-secular variation curves reported from lacustrine sediment represent 2500-3000 years over a 1 m interval. The periodicity of the paleo-secular variation curve for the Sibley Group will be estimated here by counting the number of turning points in the paleo-inclination records and using estimated sedimentation rates. These rates were obtained from the literature for sedimentation rates in similar sedimentary environments.

A 90 cm section of the cyclic siltstone-dolomite lithofacies association of the Rossport Formation in Noranda's NB-97-4 drill hole was sampled to study secular variation in the Sibley Group. This section was chosen because it appears to represent a period of continuous deposition of fine-grained material. Unfortunately, the drill core was not oriented so the specimens can not be used to determine a paleopole position. Since samples were kept oriented to one another, the variation in relative declination can be shown (Figure 4.13a), as well as variations in inclination (Figure 4.13b). The average inclination was determined to be 1.06° by using the following calculation, where n is the number of samples and T is the average angle of inclination:

$$\tan\left[\left({}^{1}/_{n}\right)\sqrt{\Sigma\theta^{2}}\right]=2\tan T$$

An example of a secular variation curve is provided for comparison in Figure 4.14. This particular curve is for unconsolidated Holocene sediments from Fish Lake in southern

Oregon. This set of curves typically has two inclination peaks for every declination peak, which is not seen as clearly in the Sibley.

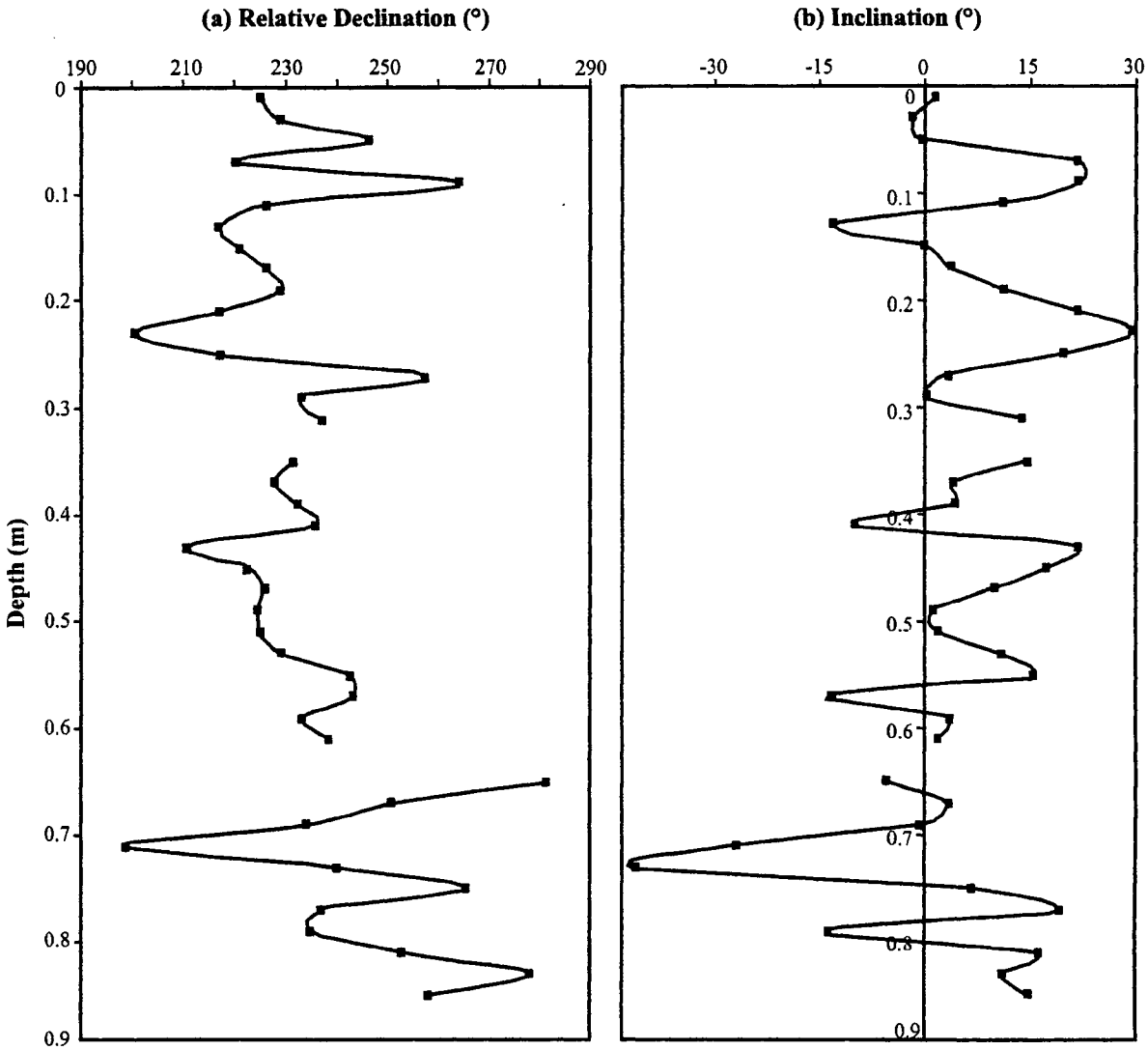

Figure 4.13. Paleosecular variation of a section from the Rossport Formation, drill hole NB-97-4. (a) The left graph shows relative declination against depth. The core was unoriented but the samples are oriented to one another. (b) The graph on the right shows inclination against depth. Gaps in the curve are where samples failed to provide enough data points for analysis due to breakage.

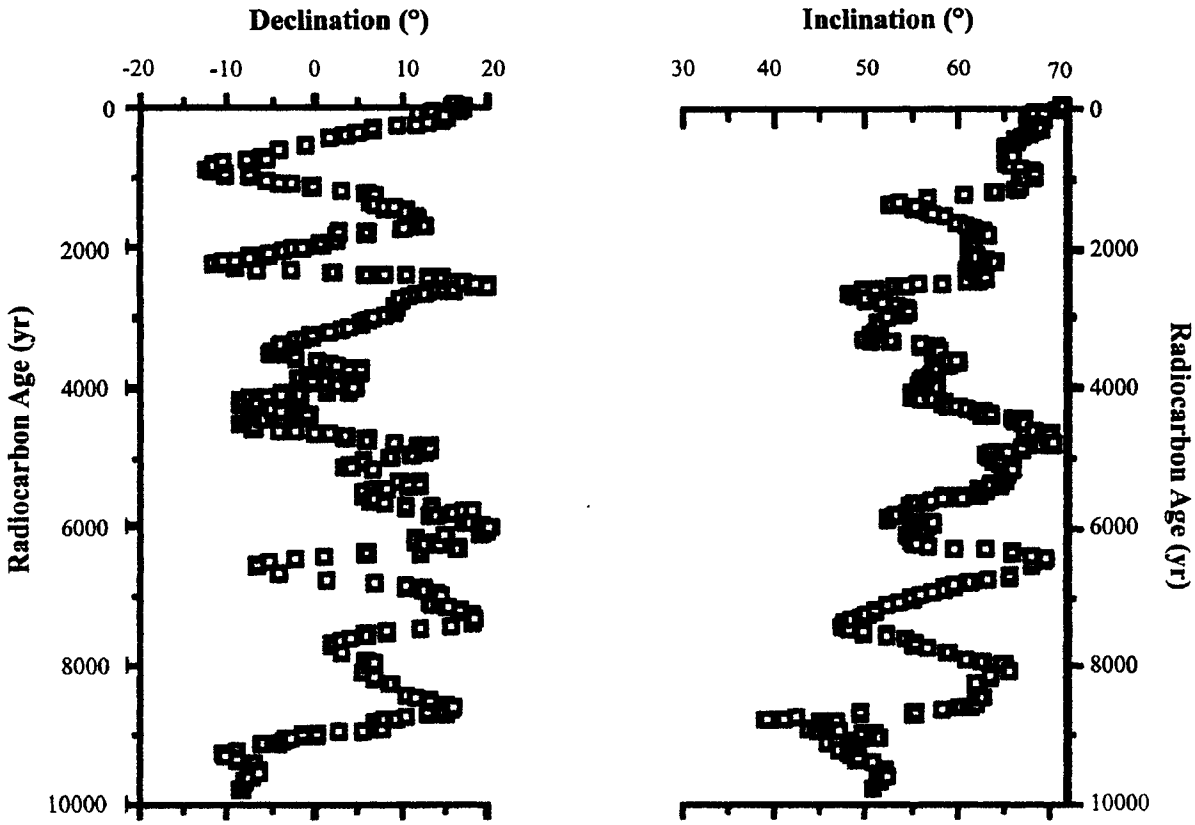

Figure 4.14. Example of a Paleo-Secular Variation Curve. This example of a secular variation curve is derived from unconsolidated Holocene sediments from Fish Lake, southeastern Oregon (from Butler, 1998).

4.6.2 Interpretation

The Channel Island Member of the Rossport Formation, the unit that was sampled for the secular variation study, is a relatively continuous record of deposition from a playa lake to lacustrine environment. While there are many factors governing sedimentation rate, it can be hypothesized that the cyclic siltstone-dolomite lithofacies association should have a sedimentation rate similar to other playa lake deposits, such as Lake Amadeus in central Australia. This method of estimating sedimentation rates is quite speculative because of the many factors affecting the preservation of sediments and apparent sedimentation rates. For example, sedimentation rates should have been higher during the Proterozoic due to the

lack of vegetation. Problems can also arise when comparing sedimentation rates between different sample scales, because rates of deposition can appear high over a short interval, such as when flood events are recorded.

Sedimentation rates for Lake Amadeus have been calculated to be 0.002 mm/a to 0.015 mm/a (Chen and Barton, 1991). Kruiver *et al.* (2000) estimated a much higher rate of deposition for a Permian red bed sequence in France, inferring a rate of 0.118 mm/a. However, they compared the number of peaks in their secular variation curve to a modern secular variation curve in order to estimate the sedimentation rate. In fact, their sedimentation rate is close to that of Holocene lacustrine sediments, which are characterized by very high rates of deposition. Hartshorn and Lewkowicz (2000) calculated a deposition rate of 0.13 mm/a to 0.22 mm/a for a high-energy lake in the Sawtooth Range, Ellesmere Island. The red beds of the Mesoproterozoic Belt Supergroup have produced estimates of 0.05 to 0.84 mm/a (Evans *et al.*, 2000), although the higher sedimentation rates incorporate tuff deposits as well. Extremely high rates of deposition can occur when high relief is present, such as in the Amazon where sedimentation rates have been calculated to be 1.1 mm/a to 300 mm/a (Kronberg *et al.*, 1998).

Ten inclination peaks have been observed over an 85 cm section of Noranda core (Figure 4.13). If the lowest estimate for the Amadeus Basin is used to calculate a periodicity for the section of the Channel Island Member, a periodicity of approximately 42,500 years is reached. The higher sedimentation rate for the Amadeus Basin gives a periodicity of approximately 5,700 years. Typical playa lakes are subject to very low sedimentation rates because they are usually closed systems in arid to semi-arid environments where the majority of the sediment enters the basin during rare flood events.

The Permian and Mesoproterozoic red bed estimates produce periodicities of 720 and 1700 years, respectively. Extremely high sedimentation rates, such as in the Sawtooth range, while unlikely, would give a periodicity of only 400-650 years, similar to contemporary paleosecular variation cycles. It is thought that the Channel Island Member should have sedimentation rates near the higher range of sedimentation rates from the playa lake in the Amadeus Basin or the lower rate from the red beds of the Belt Supergroup.

When these periodicity estimates are compared to other secular variation curves, such as those of Lund (1988), it can be determined whether these periodicity estimates are reasonable. Lund (1988) calculated a periodicity of 3000-4000 years for Quaternary lacustrine sediments and Barton and McElhinny (1982) estimated a periodicity of 1000-5000 years for recent lacustrine sediments in Australia, while recent lacustrine secular variation curves for western North America have been assigned a periodicity of a few hundred years (Hanna and Verosub, 1989). The periodicity estimates for the core from Channel Island Member agree with the estimates from Lund (1988) and Barton and McElhinny (1982) if the sedimentation rate is 0.02-0.03 mm/a, which is reasonable for playa lake and lacustrine deposition rates.

4.7 Conclusions

While the magnetostratigraphy study did not show conclusive depositional ages for all of the Formations, the paleopole for the Kama Hill Formation might indicate that deposition of the Sibley Group began before approximately 1500 Ma. The poles for the Transitional Group of the Pass Lake Formation, and possibly the Quarry Island Group and

B-component of the Nipigon Bay Formation, can be explained by resetting during a 1339 Ma diagenetic event. It is unclear whether the B-component of the Nipigon Bay Formation is a reset age related to the 1339 Ma diagenetic event or a true depositional age. The youngest of the Nipigon Bay Formation paleopoles (C-component) can be accounted for by a Keweenawan remagnetization.

The cyclic siltstone-dolomite lithofacies association of the Rossport Formation has preserved paleosecular variation. By using a range of sedimentation rates between 0.15 mm/a and 0.5 mm/a, which were calculated for other playa lake (Chen and Barton, 1991) and red bed (Evans *et al.*, 2000) units, the periodicity of the secular variation can be estimated at 1700 to 5700 years. This range corresponds with the typical range of 2500 to 3000 years per cycle (Butler, 1998). The documentation of paleosecular variation in the Mesoproterozoic Sibley Group provides one of the oldest records of this phenomenum known.

This study was only meant as a preliminary analysis of the magnetostratigraphy and paleosecular variation within the Sibley Group. A more detailed study is required to attempt to address some of the problems encountered here. First of all, sampling should be conducted on a much larger scale. This has inherent difficulties due to the limited exposure and quality of outcrops for some of the units. An effort should also be made to sample beds with relatively high mudstone contents, as these lithofacies appear to be more resistant to resetting. This is most likely due to the low porosity of mudstones compared to sandstones, which effectively reduces the amount of fluid movement through them. Low temperature demagnetization techniques should also be used to reduce any VRM components.

Chapter 5:

THE SIBLEY BASIN

The previous chapters have been leading up to a large-scale examination of the strata occupying the Sibley Basin in order to create a better understanding of the controls on the sedimentary depositional system imposed by tectonism and climate. The lithostratigraphy of the Sibley Basin has been modelled using Rockworks99 software, which incorporated 25 complete drill logs, as well as outcrop data. Collar elevations and UTM coordinates were used to place the drill-core logs in the correct spatial positions relative to one another. Models and projected sections have been generated using north-south directional weighting. This modelling technique was chosen because the Sibley Basin is elongate along a north-south trend. The model covers the southern half of the Sibley Basin, as no data was available for the far northern reaches around Lake Nipigon.

5.1 Basin Architecture

Three-dimensional data plots of the Sibley Basin (Figures 5.1, 5.2, and 5.3) were constructed using Formation thicknesses obtained from drill core logs and some outcrop data. The models show an elongate depression near the eastern margin that runs the length of the modelled area. This feature is characterized by steep, sharp walls, which seem to imply a fault-bounded basin, although the paleocurrent directions (Cheadle, 1986a) and the thickness of the units indicate that the southern part of this depression was originally a deeper area of the basin. This fault, possibly the Black Sturgeon Fault, could easily have reactivated during the Keweenawan. More drill core is needed from this area to determine

whether the linear extent of this depression is true or merely an artifact of the modelling program. The southern portion of this depression is deeper and preserves the Outan Island and Nipigon Bay Formations.

Figure 5.1 depicts the Pass Lake Formation data plot, based on the Fork Bay Member. The Loon Lake Member is too sporadic to be used in the modelling program, but blue circles indicate the drill core and outcrop locations where it was found. The thickest occurrences of this Member are along the exposed southern portion of the basin. The Fork Bay Member has a relatively uniform thickness across the basin, although slightly thicker accumulations occur in the topographic lows of the basement.

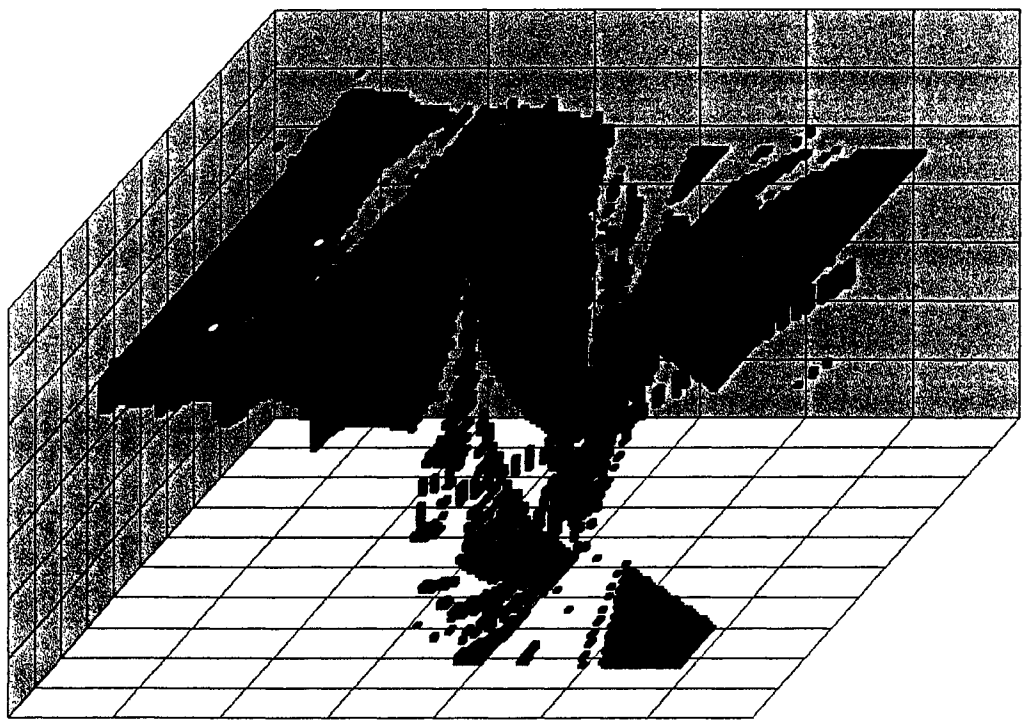

Figure 5.1. Three-dimensional Data Plot of the Pass Lake Formation. The drill hole positions (circles) are overlain on a three-dimensional data plot of the Rossport Formation. The blue circles denote the positions of the Loon Lake Member of the Pass Lake Position and the green circles signify the positions of the Middlebrun Bay Member of the Rossport Formation.

The three-dimensional data plot for the Rossport Formation is show in Figure 5.2. The Channel Island Member has a relatively uniform thickness, although it is slightly thicker over topographic lows. The Middlebrun Bay Member is only found as discrete occurrences and is indicated by green circles. The Member is observed near the eastern and western margins of the basin. The Fire Hill Member constitutes the majority of the Rossport Formation, and is thickest in the northern part of the linear depression.

The distribution of the Kama Hill Formation is shown in Figure 5.3. It is the thickest along the western to northwestern margin of the Sibley Basin, and becomes progressively thinner towards the centre in the basin. The Outan Island Formation laps onto the Kama Hill Formation within the centre of the basin and the linear depression. The Nipigon Bay Formation is restricted to the southern portion of the linear depression.

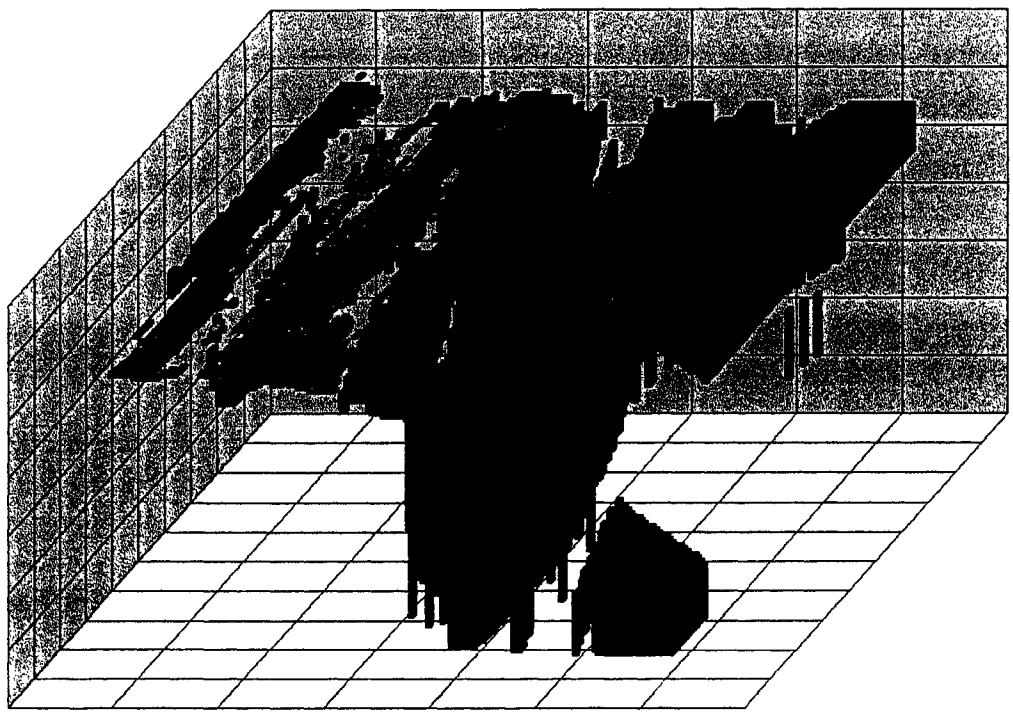

Figure 5.2. Three-dimensional Data Plot of the Rossport Formation. The drill hole positions are overlain on a three-dimensional data plot of the Rossport Formation. The pink/grey layer represents the Channel Island Member and the red layer is the Fire Hill Member. The blue circles denote the positions of the Loon Lake Member of the Pass Lake Formation and the green circles signify the positions of the Middlebrun Bay Member of the Rossport Formation.

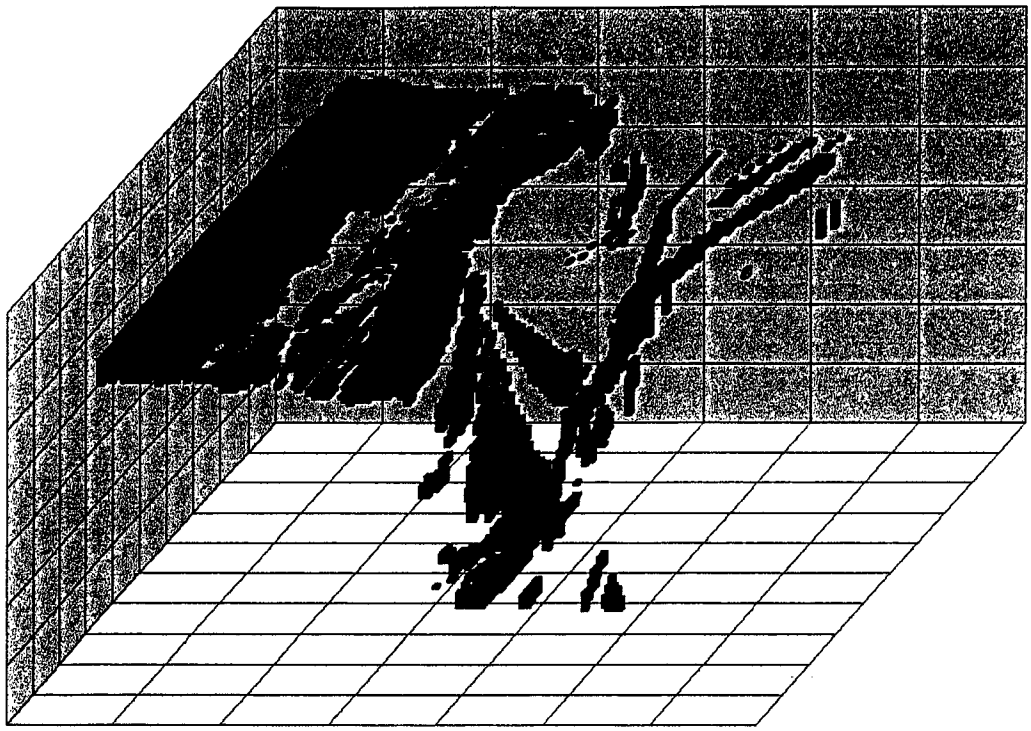

Figure 5.3. Three-dimensional Data Plot of the Kama Hill Formation. The drill hole positions are overlain on a three-dimensional data plot of the Rossport Formation. The blue circles denote the positions of the Loon Lake Member of the Pass Lake Formation and the green circles signify the positions of the Middlebrun Bay Member of the Rossport Formation.

The basin architecture can also be shown using a series of cross-sections. A map of the Sibley Basin (Figure 5.4) shows the lines used for the projected stratigraphic sections depicted in Figures 5.5, 5.6, and 5.7. These sections illustrate the relationships between the members of the Sibley Group along west-east, northwest-southeast, and north-south section lines. The Loon Lake Member of the Pass Lake Formation and the Middlebrun Bay Member of the Rossport Formation are not included due to their sporadic and limited extent. The Hele Member causes some problems in the modelling program in the western part of the basin because it is primarily found within the linear depression and only has one occurrence in the west, which the program interprets as a relatively uniform member across the entire western section.

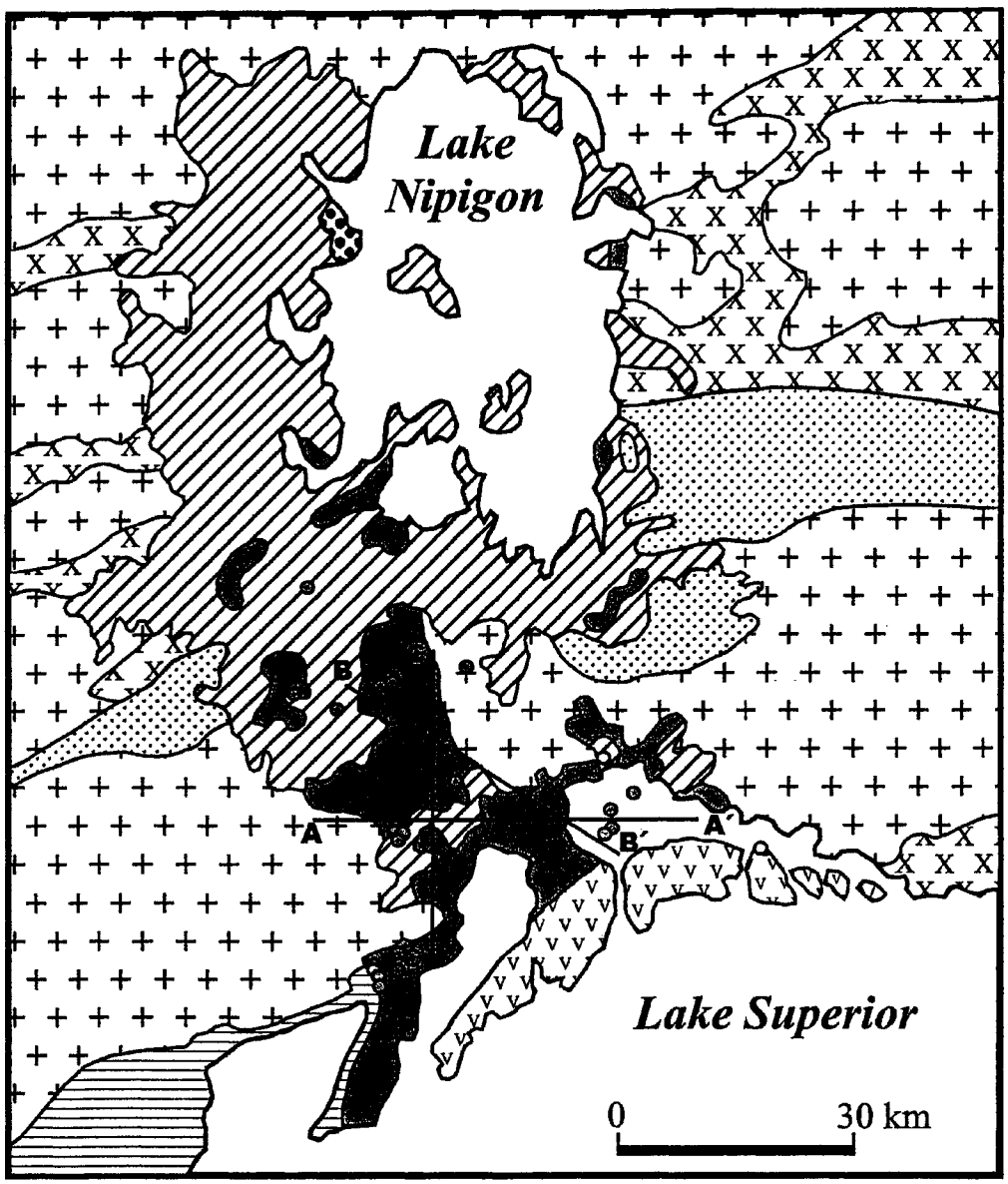

LEGEND

Proterozoic

1097 Ma
Osler Group

1110 Ma
Diabase

> 1339 Ma
Sibley Group

1537 Ma
Granite and Rhyolite

1900 Ma
Animikie Group

Archean

Granitic Rocks

Metasedimentary
Rocks

Metavolcanic
Rocks

Figure 5.4. Locations of projected stratigraphic sections. Three projected stratigraphic sections were produced along lines A-A′, B-B′, and C-C′. The positions of the drill holes (blue circles) and outcrops (green circles) used are shown in relation to these lines.

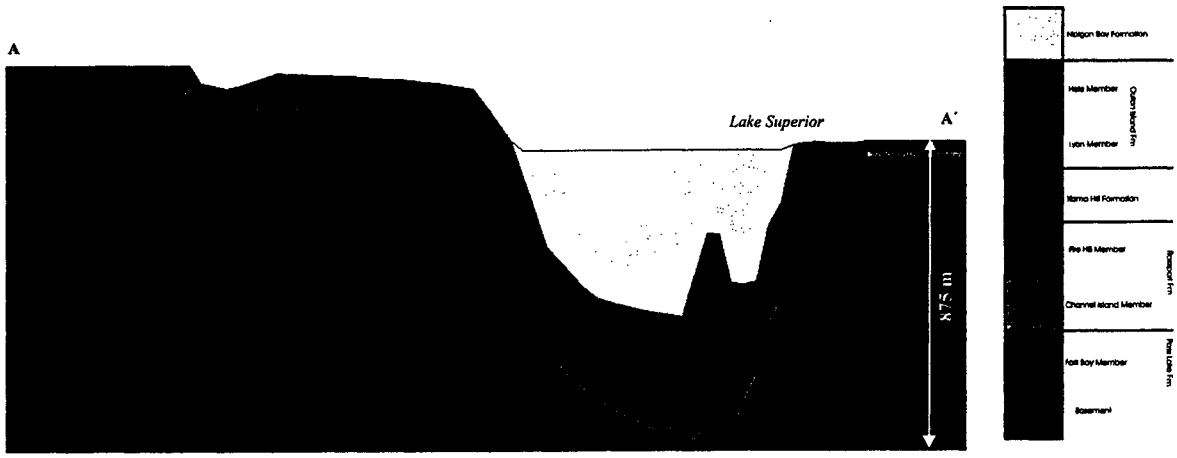

Figure 5.5. West-East Projected Stratigraphic Section. This section corresponds with the A-A′ line on Figure 5.4 and shows the relationship among the members of the Sibley Group across the basin from west to east.

Figure 5.6. Northwest-Southeast Projected Stratigraphic Section. This section corresponds with the B-B′ line on Figure 5.4 and shows the relationship among the members of the Sibley Group across the basin from northwest to southeast. The colours are the same as in the generic stratigraphic column (Figure 2.2) and as above.

Figure 5.7. North-South Projected Stratigraphic Section. This section corresponds with the C-C' line on Figure 5.4 and shows the relationship among the members of the Sibley Group across the basin from north to south. The colours are the same as in the generic stratigraphic column (Figure 2.2) and as above.

The west-east and northwest-southeast projected stratigraphic sections clearly demonstrate the relationship that the Fork Bay Member has with a topographic high of basement rock in the north. The northwest-southeast and north-south sections reveal a similar relationship for the Channel Island Member. The Fire Hill Member seems to be thicker in some of the topographic lows, although it is thickest in the large linear depression in the east, which might indicate that it was the deeper part of the Sibley Basin during deposition. This is also supported by the distribution of paleocurrent directions of the Pass Lake and Rossport Formations Cheadle (1986a) that shows transport directions converging towards this area, and is seen more readily when the projected stratigraphic sections are hung on a datum. Two horizons were selected, the first at the base of the Fire Hill Member (Figure 5.8), and the second at the top of the Fire Hill Member (Figure 5.9). These were selected to emphasize the change in basin dynamics during the deposition of the Fire Hill Member. Prior to the deposition of the Fire Hill Member, the basin had a relatively uniform depth, with some deeper areas in the east. However, during the Fire Hill Member, subsidence is much greater in the east, coinciding with the position of the linear depression. The Kama Hill Formation primarily occurs as a thin veneer across the basin with little topographic variability, except within the linear depression. The Lyon Member is restricted to the margins on either side of the eastern linear depression, while the Hele Member can be found overlying the Kama Hill Formation beyond it.

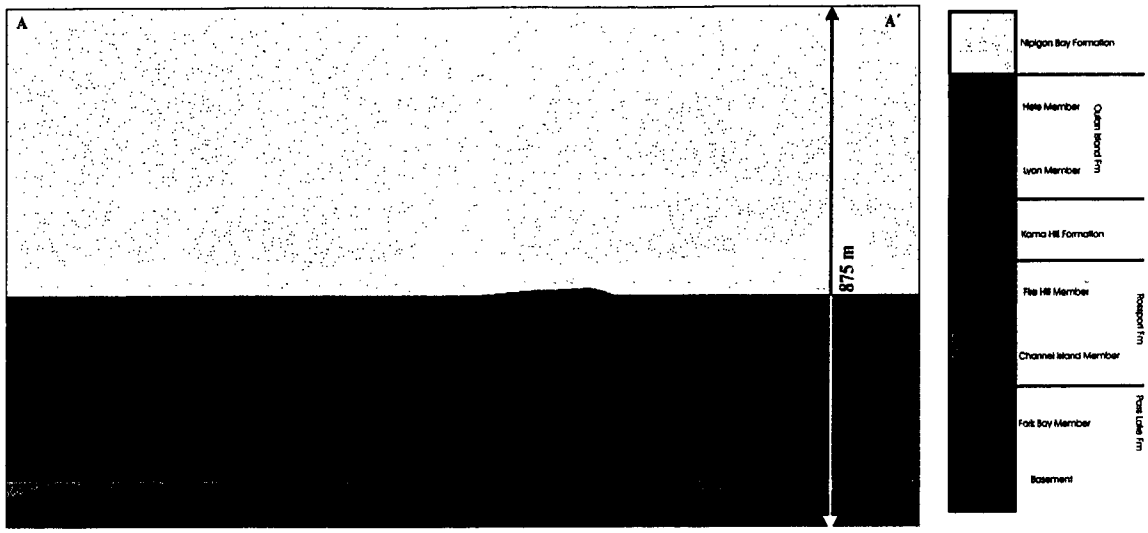

Figure 5.8. West-East Projected Stratigraphic Section hung on the Base of the Fire Hill Member. This section corresponds with the A-A′ line on Figure 5.4 and shows the relationship among the members of the Sibley Group across the basin from west to east. The Outan Island and Nipigon Bay Formations are distorted due to the lack of data points on this projection.

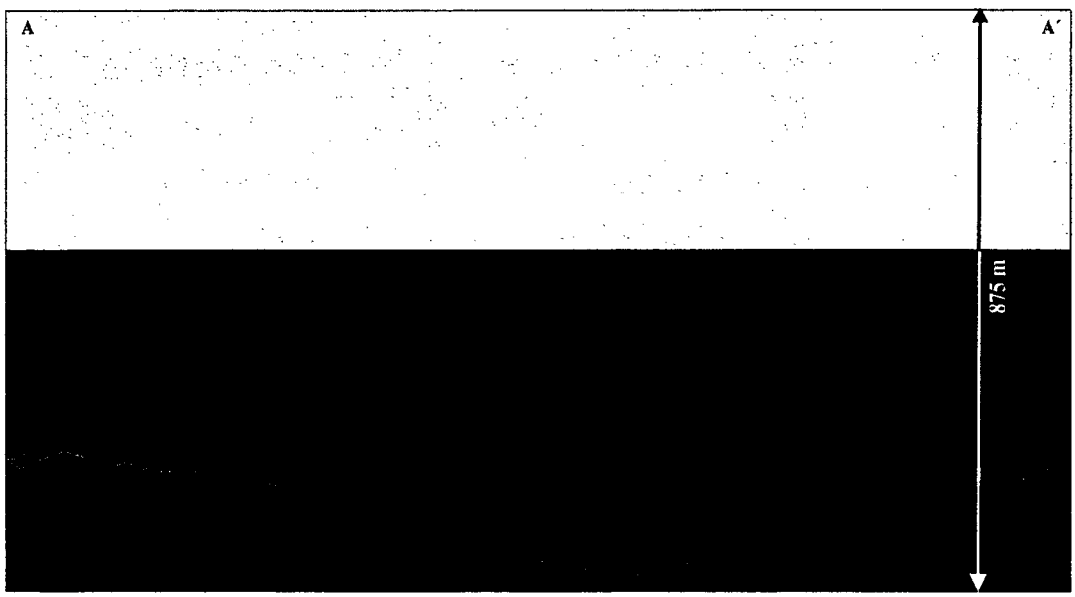

Figure 5.9. West-East Projected Stratigraphic Section hung on the Top of the Fire Hill Member. This section corresponds with the A-A′ line on Figure 5.4 and shows the relationship among the members of the Sibley Group across the basin from west to east. Formation colours same as above. The Outan Island and Nipigon Bay Formations are distorted due to the lack of data points on this projection.

This has some implications for the formation and depositional history of the basin. The original surface of the Sibley Basin was irregular with the greatest topographic variability occurring in the southern section, while the central portion was relatively flat. This variability does not include the linear depression, which was accentuated by rifting. The basin was relatively flat during the initiation of Sibley sedimentation, and then deepened during the time of the Fire Hill Member. Basement variability for the northern Sibley Basin, around Lake Nipigon, is unknown. The conglomeratic facies of the Loon Lake Member was deposited in depressions, and onlapped local topographic highs. The Fork Bay Member blanketed the topography, aside from the occasional basement hill that shows through. The sediment was transported as sheet flows from the northwest (Cheadle, 1986a), possibly from the English Bay region of Lake Nipigon. The geochemical interpretations from this study and Richardson (2003) imply an enriched felsic igneous source, similar to the granite-rhyolites of the English Bay intrusion. The climate was semi-arid during this time, as suggested by caliche layers and halite casts.

The Channel Island Member represents the saline lake of the Rossport Formation. This member appears continuous in Figure 5.8, although it may not have been laterally continuous for this entire time span. It could possibly have occurred as a couple of medium-sized saline lakes or it could have been one lake that became divided into many during prolonged arid periods. The stromatolitic facies of the Middlebrun Bay Member occurs above the Channel Island Member, forming as the individual basins were isolated by the influx of sand sheets. Unfortunately, paleocurrents have not been found to give transport directions for these sandstones, although geochemical comparisons suggest that they are derived more from regional Archean granites than English Bay granites, implying

a decreasing influence of southeast-trending transport directions. The incursion of sand sheets and debris flow intraformational conglomerates, as well as the injection of sedimentary breccias and change in basin hydrology (Cheadle, 1986a), could indicate tectonic activity within the basin. This is also supported by the increased subsidence seen during the Fire Hill Member in Figure 5.9. This series of events is probably related to the change in paleocurrent direction seen in the Kama Hill Formation. The beginning of the Rossport Formation period is characterized by a semi-arid environment, as suggested by carbonate and gypsum precipitation, caliche layers, and desiccation features. The Fire Hill Member appears to be associated with a slightly more humid climate, although this may simply be due to the ability of external fluvial systems to enter the basin as subsidence of the thermal welt that created the basin margins progressed.

This moderately humid environment was maintained through the Kama Hill Formation, as a floodplain-like mudflat with unchannelized sheet flows developed across the basin. The thickest accumulations of this unit occur in the west and pinch out towards the east. In places, the Kama Hill Formation is interbedded with the Outan Island Formation, suggesting that they were, at least partly, coeval. Paleocurrents for the Kama Hill Formation trend towards the northwest, a complete reversal from the Pass Lake and Rossport Formations. Cheadle (1986a) suggests that this reversal is related to either uplift in the south or subsidence in the north, although he found no compelling geologic evidence to support either theory. Some subsidence did occur in the north due to intrusion of diabase sills, but not until after the Sibley was deposited (Cheadle, 1986a). He advocates southern uplift possibly related to doming related to Keweenawan volcanism. However, there is a large time gap between this unit and the Keweenawan events, and it would conflict with the

stratigraphic distribution of the Outan Island Formation. There is no paleocurrent data available for the Outan Island Formation, but the distribution of the deltaic Lyon Member (Figure 5.5, 5.6) appears to indicate that flow directions should have been towards the northwest. It seems illogical for a delta to form onto a subaerial mudflat rather than into a basin, and similarly for a river to flow away from that topographic low, referring to the deepest part of the basin located in the southeast prior to the faulting event. The deltaic unit is more prevalent along the eastern margin of the linear depression, therefore it is possible that a river entered the pre-faulting depression (shown by the Fire Hill Member in Figure 5.9) on the east and in discrete locations around the low and then flowed out in rivers across the floodplain towards the northwest, as indicated by Kama Hill paleocurrent directions. Outcrop exposures of the Outan Island Formation and more paleocurrent measurements are needed.

There is a hiatus between the Outan Island Formation and the Nipigon Bay Formation. The Nipigon Bay Formation is an aeolian sand dune system and seems to indicate a return to an arid environment. This unit is restricted to the southern area of the linear depression, has southeast-trending paleocurrent directions, and seems to be deriving some of its source material from the English Bay granites, as well as the regional Archean granites.

It is not known precisely when the linear depression was created. The thickness of the Rossport Formation seems to indicate that the area was a low-lying area at the time of deposition, although its present depth is dramatically exaggerated. The sharpness of the sides of the depression suggests that it is fault-bounded and it could easily have been reactivated during Keweenawan events.

5.2 Tectonic History

It has been hypothesized that the Sibley Basin formed as an intracratonic basin (Fralick and Kissin, 1996), rather than in a rift basin, as suggested by Franklin (1980). Cheadle (1986a) questioned whether the Sibley Group was deposited in a rift basin based on the limited areal extent of the alluvial fans of the Pass Lake Formation, which suggests that normal faulting was not controlling basin formation. The alluvial fan interpretation has been rejected here, but the lack of abundant coarse clastic material still argues against extensive fault-bounded margins. Cheadle (1986a) also rejected the rift hypothesis because the lacustrine facies of the Sibley Group was shallow and unstratified, as opposed to most rift lakes (Hentz, 1985). He suggested that the basin formed due to broad subsidence during lithospheric stretching prior to the development of the Mid-Continental Rift. Fralick and Kissin (1996) disagree with the Sibley Group being related to the Mid-continental Rift, mentioning that the paleodrainage pattern of the Sibley Group conflicts with the possibility of a mantle plume being situated beneath the rift during the time of deposition. The presence of the plume would cause up-doming and drainage away from the area, the opposite of what is seen in the lower Sibley Group. The Sibley Group also predates the earliest Keweenawan volcanics by at least 200 my.

The distribution of the units of the Sibley Group indicate that the basin was broad and relatively shallow, with the majority of the subsidence occurring in the southeast corner of the study area. Paleocurrents (Cheadle, 1986a) and geochemical analyses indicate that the sediment of the Pass Lake Formation was transported from the north. The dominance of an internal sediment source indicates a physical barrier along the northern margin of the Sibley Basin. However, the northern outcrops were not included in this study and no other

inferences can be made about the northern margin. It appears that basement topographic relief was more pronounced in the south than the central basin area, although the limited areal extent of the alluvial fans seems to argue against abundant pre- or syndepositional faulting (Cheadle, 1986a). The southernmost extent of the Sibley Basin lies beneath Lake Superior, hindering further inferences about the nature of that margin. Fralick and Kissin (1996) suggest that the basin was due to the existence of a thermal welt in the region, produced by a mantle plume, at approximately 1550 Ma. They suggest that the basin was formed due to subsidence early in the cooling history, driven by excess mass in the upper crust or rapid cooling in the hot, central zone of the thermal welt. The shape of the basin, the presence of pre-Sibley anorogenic granites, and the lack of volcanics in the Sibley Basin correspond with the early phases of a passive-rift intracratonic basin, such as in the Belt-Purcell Basin (Chandler, 2000; Höy *et al.*, 2000).

There appears to have been differential subsidence within the basin. Cheadle (1986a) observed igneous rocks associated with the English Bay Intrusion intercalated with the sandstones of the Pass Lake Formation. Fralick and Kissin (1996) noted that there had not been significant unroofing of the English Bay Granite prior to Sibley deposition, and that associated hydrothermal processes were affecting the sediment of the Pass Lake Formation during transport. This indicates that the area of the English Bay Intrusion was still relatively elevated during initial deposition of the Sibley Group. Subsidence of this area may have reached a maximum during deposition of the Fire Hill Member when the paleoslope changed direction, although the depression illustrated by the Fire Hill Member in Figure 5.9 could indicate that this slope change was more localized than previously thought. Further study is required in the northern part of the basin to resolve this. A

southern uplift could also produce a change in paleoslope. Greenberg and Brown (1984) have described uplift south of Lake Superior at approximately 1500 Ma. Although this uplift event may have been too far away to affect the Sibley Group, there is a possibility that it could be the uplift mechanism that changed the paleoslope if Cheadle (1986a) was correct in identifying English Bay rhyolites, which are 1537+10-2 Ma (Davis and Sutcliffe, 1985), as being intercalated with Sibley sediment.

The paleoslope probably began to change during the Fire Hill Member, rather than the Kama Hill Formation as indicated by Cheadle (1986a). This is suggested by a sedimentological change, microfaults, intrusive sedimentary breccias and sills, the disruption of basin hydrology, and an apparent increase in subsidence. The Fire Hill Member includes a number of sand beds and intraformational conglomerates, which represent sheet flows and debris flows. The presence of these units probably indicates an increase in local topographic relief, driven by tectonic uplift in the south. Montgomery and Brandon (2002) proposed that landslides and debris flows are driven more by active, tectonically driven uplift rather than simple local relief variations. Microfaults have been found cutting sediment layers in the Channel Island and Fire Hill Members of the Rossport Formation, as well as the Kama Hill Formation.

Further evidence of tectonic activity comes from the intrusive sedimentary breccias and sills identified by Cheadle (1986a) and Franklin (1980). Cheadle (1986a) noted that some of the conglomerates in the Fire Hill Member were composed of red dolomitic mudstone blocks, derived solely from the underlying strata and often accompanied by high-angle normal faults. These breccia plugs flare outward toward the top and at least one was seen to bifurcate into two smaller bodies upward. Cheadle (1986a) took this to indicate that

sedimentary breccias intrude upwards into the overlying sediment. He also noted that sand dikes and sills cut through some of the breccias, indicating multiple phases of intrusion driven by high fluid pressures. Because the Sibley Group lacks evidence for rapid or deep burial, Cheadle (1986a) proposed that the sandstones of the Pass Lake and parts of the Channel Island Member acted as groundwater reservoirs that were capped by impermeable dolomitic mudstones and chert-carbonate units, creating an aquifer. The impermeable layers would have been breached during earthquake activity throughout the early part of the Fire Hill Member. Cheadle (1986a) suggested that the initial aquifer breaches caused the intrusion of breccias from underlying strata, and the later sandstone sills and dikes were derived from rupturing deeper, Pass Lake reservoirs. The presence of sedimentary breccias and sills and associated changes in basin hydrology, debris flows, and microfaults supports that tectonic uplift began during the time of deposition of the Fire Hill Member, rather than the Kama Hill Formation as Cheadle (1986a) hypothesized.

5.3 Basin Hydrology

Cheadle (1986a) observed that there was a hydrological change between the Rossport Formation and the Kama Hill Formation. The Sibley Basin was a closed system during the deposition of the Rossport Formation, with rainfall being the primary source of water. Evaporation caused the concentration of solutes in the groundwater, creating a saline brine. Yechieli and Brown (2002) calculated that a saline brine could take anywhere from 4000 years to evolve in an open water-body playa to 600,000 years in a groundwater playa system. The concentration of the brines is controlled by the thermodynamic activity

of water, where increased concentrations of solutes decrease the ability of the water to evaporate (Yechieli and Wood, 2002). Both dolomite and gypsum are stable at relatively moderate solute concentrations and evaporation levels (Yechieli and Wood, 2002), although the presence of halite casts indicates that higher evaporation levels were reached. Around the time of the Middlebrun Bay and Fire Hill Members, the brine became silica over-saturated (Cheadle, 1986a), as seen by the presence of chert in the stromatolitic lithofacies association and the displacive growth of quartzine nodules within the Fire Hill Member.

During deposition of the Kama Hill Formation, the Sibley Basin was hydrologically open. This change is seen in the absence of carbonate facies, other than in rare post-lithification veins, and the lack of sulphate and quartz nodules. The introduction of externally derived source water allows the groundwater to be replenished before a brine can evolve (Cheadle, 1986a). Cheadle (1986a) alternatively offered that the water table might have become so deep during Kama Hill times that evaporites could no longer form near the surface. The presence of the closely related deltaic and fluvial units of the newly discovered Outan Island Formation seems to suggest that this was not the case.

The presence of the sedimentary breccias in the Fire Hill Member (Cheadle, 1986a) is interpreted as liquefaction structures caused by breaches in Channel Island and Pass Lake aquifers. Presumably, mixing with the aquifer brines would cause changes in the groundwater above the aquifer. The presence of sand sheet deposits also indicates a more significant supply of external water entering the basin. Most likely, the groundwater experienced salinity fluctuations between recharges from the aquifer and surface drainage, as it progressed to a completely open hydrological system.

The preliminary paleomagnetic study conducted here suggests that the Pass Lake and Nipigon Bay sandstones have acted as fluid conduits, while the mudstones of the Kama Hill Formation were not reset by these events. The sandstones have had two periods of resetting, the first between 1350 Ma and 1450 Ma, and the second between 1100 Ma and 1200 Ma. The first could be related to the 1339 Ma Rb-Sr age given by Franklin (1978). Age determination using apparent polar wander paths have a fair degree of error involved and the Rb-Sr system may have remained open beyond the hematite resetting. The second remagnetization event appears to be related to the Keweenawan. The Nipigon Bay Formation is in close proximity to Osler Group volcanics, but the Pass Lake samples are not, which suggests that a medium was required to transport heat through these sandstones to cause remagnetization. It is common for fluid migration to cause diagenetic resetting of hematite, such as some of the Carboniferous strata in the Rocky Mountains (Geissman and Harlan, 2002) and the Mississippian Turner Valley Formation in Alberta (Cioppa *et al.*, 2000), and is most likely to be the case here. There are no indications that the Sibley Group was buried to significant depths (Cheadle, 1986a). The demagnetization temperatures indicate that the resetting occurred between 200 °C and 450 °C.

5.4 Conclusions

The Sibley Basin was formed as a broadly subsiding intracratonic basin, as suggested by the lack of faulting and igneous intrusions and is similar to the basal Formations of the Belt Supergroup (Chandler, 2000; Höy *et al.*, 2000). Fralick and Kissin (1996) hypothesized that the presence of a mantle plume, at approximately 1550 Ma,

caused lithospheric stretching. Subsidence occurred over the plume focus during the early cooling history and the regional thermal welt formed the basin margins. Initial basin relief shows a broad, relatively flat basin. Differential subsidence produced a depression in the eastern part of the basin during the deposition of the Fire Hill Member, which was later accentuated by faulting. This depression presently has sharp, steep edges and seems to geographically correspond with the Black Sturgeon Fault.

Sedimentation of the Sibley Group began with the basal conglomerates and sandstone unit of the Pass Lake Formation. Coarse sediment was focussed along the shoreline of a lacustrine water body, with subaqueous sand sheets being deposited on the bottom of the basin. As subsidence progressed, the lake became isolated from external influences and changed to the playa lake and sabkha/mudflat environment of the Rossport Formation. There was a change in paleoslope during the Fire Hill Member of the Rossport Formation, causing a disruption to basin hydrology and a change in sedimentation patterns. The Kama Hill Formation overlies the Rossport Formation, representing a subaerial mudflat characterized by unchannelized sheet flows. The Kama Hill Formation grades into the coarsening upward deltaic sequence of the Lyon Member of the Outan Island Formation, which is then erosively cut and overlain by the fluvial facies of the Hele Member of the Outan Island Formation. After a hiatus, a thick succession of aeolian sandstones was deposited, known as the Nipigon Bay Formation.

Robertson (1973a) estimated that the Sibley Group was deposited within 10° south of the paleo-equator, based on his paleomagnetic work. The inclination derived from the Rossport Formation, averaging 1.06°, substantiates this claim. The paleomagnetic analysis of the Kama Hill, which appears to be close to a true depositional pole, indicates a

paleolatitude near 20° south. Present day climatic regimes throughout these latitudes are arid to semi-arid, although 20° latitude is dominated by arid environments and between 10° north and south of the equator is dominated by semi-arid to humid climates (Hidore and Oliver, 1993).

The environments within the Sibley Basin appear to change from a semi-arid environment to a moister environment, followed by a return to arid conditions. The important question is whether this cycle is because of localized climatic change or due to a tectonic influence. The key to answering this question lies in understanding reasons for the hydrological changes during the Fire Hill Member. Prior to the Fire Hill Member, the Sibley Basin was a closed hydrological system with an evolved alkaline brine, but the basin became an open system by the time of the Kama Hill Formation (Cheadle, 1986a). These hydrological changes coincide with the renewed introduction of coarse sediment into the basin, the presence of debris flows, and sedimentary breccias and sills, which indicate that this was also a period of tectonic activity, most likely uplift in the south. The sedimentary breccias are the result of extreme liquefaction, possibly attributed to earthquakes, which disrupted the aquifers that held the saline brine (Cheadle, 1986a). At the same time, sheet flows and debris flows entered the basin, indicating topographic changes. The tectonic events that caused these changes may also have opened the hydrological regime by making it more accessible for fluvial influences from the south.

Chapter 6:

DISCUSSION – COMPARISON WITH MESOPROTEROZOIC NORTH AMERICAN BASINS & CONTINENTAL IMPLICATIONS

There were other North American basins active during the same time as the Sibley Basin. The largest of these is the Belt-Purcell Basin, outcropping in northern Idaho, western Montana, and southern Alberta and British Columbia. The Belt-Purcell Supergroup is a 15-20 km thick unit, spanning approximately 70 million years (Evans *et al.*, 2000). Evans *et al.* (2000) used SHRIMP U-Pb analysis to determine the geochronology of tuffs near the bottom and top of the sequence, assigning them ages of 1454 ± 9 Ma and 1401 ± 6 Ma, respectively. Anderson and Parrish (2000) suggest an earlier age for the beginning of sedimentation within the basin, between 1543 Ma and 1497 Ma. These ages agree with a paleomagnetic study done on the Belt-Purcell Supergroup by Elston *et al.* (2002), which shows the Sibley Group as having similar paleopole positions. Many of the Belt rocks experienced a metamorphic event associated with the intrusion of sills around 1352-1341 Ma (McFarlane and Pattison, 2000). This is very close to the age of the 1339 ± 33 Ma diagenetic event that Franklin *et al.* (1980) determined for the Sibley Group.

The Belt-Purcell Basin initially formed as a result of a passive rift, with continued subsidence due to regional sag during thermal decay (Chandler, 2000; Höy *et al.*, 2000), similar to the scenario hypothesized for the Sibley Basin. Chandler (2000) uses the sedimentology of the Neihart, Fort Steele, Waterton, and Altyn Formations, as well as the absence of volcanism, to support this theory. Höy *et al.* (2000) note extensional faults

along the basin margins, rift-axis faults that produced graben and half-graben basins, hydrothermal flow along the rift axis, sedimentary fragmentals, and gabbroic dikes. Anorogenic magmatism, at 1543-1512 Ma (Anderson and Parrish, 2000) seems to have preceded sedimentation.

There is a controversy about whether the Belt-Purcell Basin was a lacustrine (Winston, 1990) or a restricted marine setting (Hall and Veizer, 1995; Lyons *et al.*, 1999; Höy *et al.*, 2000; Pratt, 2001). Winston (1990) thought that the stratigraphy and sedimentary features of the Belt-Purcell Supergroup fit a lacustrine setting. Hall and Veizer (1995) suggest that $^{87}Sr/^{86}Sr$ values for the Lower and Middle Belt carbonates fit with Proterozoic seawater, supported by the consistency of the $\delta^{18}O$ and $\delta^{13}C$ of the limestones. Lyons *et al.* (1999) state that $\delta^{34}S$ values can only have formed in a restricted marine setting. Chandler (2000) comments that, while the sandstone facies, mudcracks and presence of shortite in the Prichard-Aldridge Formation indicate alluvial sedimentation, the Ravalli Group, Middle Belt carbonate, and Missoula Group appear to be distinctly shallow-marine and interprets all four groups as marine.

The Prichard-Aldridge Formation and equivalents, the Ravalli Group, the Middle Belt carbonate, and the Missoula Group comprise the four Groups of the Belt-Purcell Supergroup (Chandler, 2000), shown in Figure 6.1. Figure 6.2 depicts the Sibley Group stratigraphy for comparison. The Prichard-Aldridge Group is dominated by turbidites. The eastern part of the basin is composed of basin-margin quartzites (Neihart and Fort Steele Formations), overlain by large fining-upward cycles that Höy *et al.* (2000) interpreted to indicate basin extension and sudden basin subsidence. These are overlain by thin-bedded turbidites, peritidal carbonates (Waterton and Altyn Formations), a progression from

shallow to deep-water shales, and carbonates (Newland, Chamberlain, and Greyson Formations) (Chandler, 2000). The LaHood Formation, an arid alluvial fan-delta complex, is found in the west (Chandler, 2000).

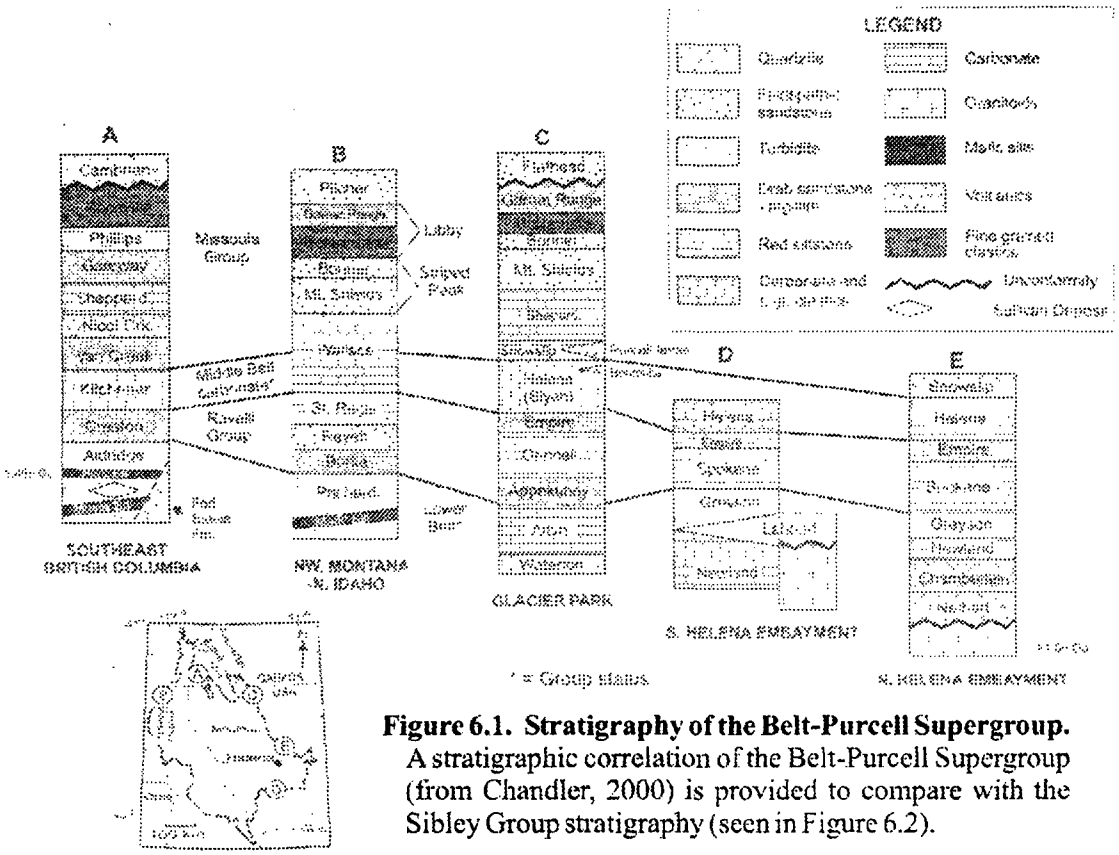

Figure 6.1. Stratigraphy of the Belt-Purcell Supergroup. A stratigraphic correlation of the Belt-Purcell Supergroup (from Chandler, 2000) is provided to compare with the Sibley Group stratigraphy (seen in Figure 6.2).

Slack and Höy (2000) show that the sediments in the lower Prichard-Aldridge Group were derived from a single source, whereas later units, with similar environments, have sediments derived from multiple sources, possibly indicating that the lower units were deposited in a restricted basin environment. Chandler (2000) maintains that the Belt Basin was restricted during the Prichard-Aldridge Group, and remained at least partially restricted

through deposition of the Ravalli Group. Lyons *et al.* (1999) use $\delta^{18}O$ and $\delta^{13}C$ values to support the restricted aspect of the Belt Basin.

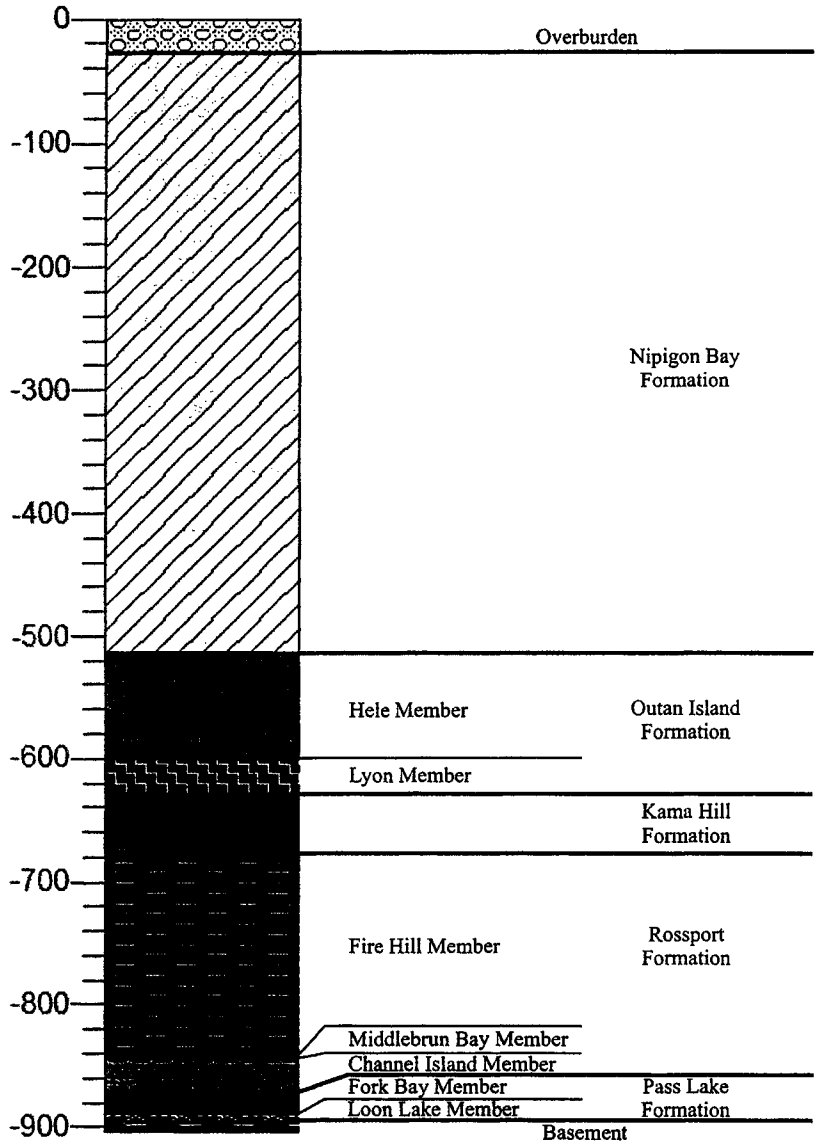

Figure 6.2. Generic Stratigraphic Column of the Sibley Group. This is a generic stratigraphic column, showing the organization and relative unit thicknesses for the Members and Formations of the Sibley Group.

The Ravalli Group is dominated by fine-grained red beds and represents a major regressive cycle. The units represent inland sea playas, braided streams, submerged tidal mudflats, supra-tidal to shallow marine deposits, overlain by subtidal carbonates (Chandler,

2000). Winston (1990) had a slightly different interpretation, beginning with braided streams overlain by sand flats, playa mudflats, and perennial playa lake deposits.

Chandler (2000) considers the Middle Belt carbonate to be a transgressive sequence with deep-water facies (Wallace Formation) in the west, a mixed facies (Helena Formation) in the centre, and a shallow-water facies (Kitchener and Van Creek Formation) in the east. There does not seem to be much agreement about the depositional environment of this unit, and the Helena Formation is particularly controversial. Winston (1990) maintains that it is a lacustrine environment, Pratt (2001) has determined it to be a marine unit, while Chandler (2000), usually a proponent for a restricted marine setting, does not commit one way or the other. The Missoula Group has been interpreted as being deposited in a sandy alluvial apron, progressing upwards to a marginal marine sandflat, mudflat, and a mixed shallow-marine environment.

Regardless of which side of the lacustrine versus marine debate was taken, the majority of the researchers recognized the influence of a semi-arid environment. This is seen in the abundant desiccation cracks and mudchips, sabkha/playa evaporates, casts of halite cubes and hoppers, the replacement of gypsum by barite and relict chickenwire structure (Winston, 1990; Chandler, 2000; Pratt, 2001). The Belt-Purcell Supergroup was deposited between 10°S and 35°S latitude (Chandler, 2000; Elston *et al.*, 2002), similar to the Sibley Group.

Winston (1990) also discusses several other basins that formed in the southwestern United States between 1400 Ma and 700 Ma, including the Unkar Group and the Apache Group that were deposited between 1300 Ma and 1200 Ma. Both of these basins contain sedimentary features attributable to a semi-arid climate and seem to have been deposited in

intracratonic basins. The Unkar Group consists of the Bass Limestone, Hakatai Shale, Shinumo Quartzite, and Dox Sandstone, which is predominantly a redbed sequence. The Bass Limestone contains very fine-grained dolomicrite, cryptalgal laminae and stromatolites, and interbedded shale, conglomerate, sandstone, and evaporite breccias (Winston, 1990). Abundant mudcracks, molar tooth structure, caliche horizons, and salt casts are also found, similar to the Belt-Purcell Supergroup, indicating a semi-arid environment (Pratt, 2001). The Hakatai Shale contains red mudstone and fine-grained sandstone, with some dolomitic mudstones and subaerial features, such as caliche horizons, mudcracks, and salt casts (Winston, 1990). The Shinumo Quartzite is dominated by fluvial and deltaic deposits with minor salt-casts and mudcracks, and is overlain by the Dox Sandstone, which represents a deltaic and sabkha/mudflat environment (Winston, 1990). Paleoenvironmental variations within the Unkar Group have been attributed to minor sea level fluctuations related to subsidence and basin filling (Hendricks and Stevenson, 1990).

The Apache Group consists of the Pioneer Formation, the Dripping Spring Quartzite, and the Mescal Limestone, and was overlain by the Troy Quartzite. The Pioneer Formation consists of tuffaceous mudstone, sandstone, and cross-bedded sandstone lenses with a local basal conglomerate (Winston, 1990). These have been interpreted to be an alluvial fan complex (Middleton and Trujillo, 1984) or braided stream deposits (McConnell, 1975). The Dripping Spring Quartzite consists of fluvial channels, tabular sandstone beds, and interbedded mudcracked mudstone, although Winston (1990) believed that this unit had remained subaqueous. The Mescal Limestone is dominated by dolomicrite, cherty dolomicrite, evaporites, halite molds, and chert nodules with some crypt-algal laminites deposited during a time when the basin became restricted, similar to

the Helena Formation of the Belt-Purcell Supergroup (Winston, 1990). This suggests that the Apache Group was also deposited in a semi-arid environment capable of producing these features when water conditions were restricted enough for evaporation to be efficient. The Apache Group is overlain by the Troy Quartzite, which consists of well-sorted cross-bedded aeolian sandstones interbedded with braided fluvial sandstones and conglomerates (Winston, 1990).

The Sibley Group, Belt-Purcell Supergroup, Unkar Group, and Apache Groups are spread out across the North American continent and are approximately coeval. All of these basins show evidence for semi-arid environments, although wetter periods of deposition seem to have occurred. However, the number of large-scale wet-dry cycles within each basin is variable. In the Belt-Purcell Supergroup, Chandler (2000) attributes this to strongly seasonal tropical climate and Hendricks and Stevenson (1990) believe that, in the Unkar Group, these variations are due to subsidence and basin filling. Local conditions seem to govern this seemingly climatic variatiability for each basin. Overall, the North American continent experienced a hot, semi-arid environment during the Mesoproterozoic, with local controls imprinting regional cyclicity on top of continental climatic cyclicity. The influence of local controls is particularly evident in the distribution of the thick aeolian sequences, which are only present in the upper units of the Sibley Group and the Troy Quartzite, overlying the Apache Group. These thick sandstone sequences seem to be restricted to basins formed in continental interiors between 10° and 30° latitude, which would be more prone to arid conditions suitable for desert formation (Hidore and Oliver, 1993; Kocurek, 1996).

The Sibley Group, Belt-Purcell Supergroup, Unkar Group, and Apache Groups also seem to have formed in the same type of tectonic setting, exhibiting similar lithofacies trends. These trends reflect alluvial fan or lacustrine environments, overlain by sediment deposited in restricted lacustrine or marine basins and on restricted coastal and playa sabkhas (Winston, 1990; Chandler, 2000). Chandler (2000) describes this succession as a typical passive rift sedimentation pattern, reflecting initial isolation of the basin by the presence of a thermal welt, followed by a change to longitudinal sediment transport after the subsiding basin is partially filled.

REFERENCES

Allen, J.R.L. 1964. Studies in fluviatile sedimentation: six cyclothems from the lower Old Red Sandstone, Anglo-Welsh Basin. *Sedimentology*, **3**, 163-198.

Allen, J.R.L. 1970. Studies in fluviatile sedimentation: a comparison of fining-upward cyclothems, with special reference to coarse-member composition and interpretation. *Journal of Sedimentary Petrology*, **40** (1), 298-323.

Anderson, H.E. and Parrish, R.R. 2000. U-Pb Geochronological evidence for the geological history of the Belt-Purcell Supergroup, southeastern British Columbia. *In*: J.W. Lydon, T. Höy, J.F. Slack, and M.E. Knapp (eds.), The Geological Environment of the Sullivan Deposit, British Columbia, *Geological Association of Canada, Mineral Deposits Division, Special Publication* **1**, 113-126.

Anglin, C.D., Franklin, J.M., Loveridge, W.D., Hunt, P.A., Osterberg, S.A. 1988. Use of zircon U-Pb ages of felsic intrusive and extrusive rocks in eastern Wabigoon Subprovince, Ontario, to place constraints on base metal and gold mineralization. *In*: Radiogenic Age and Isotopic Studies, Report 2, *Geological Survey of Canada*, Paper **88-2**, 109-115.

Baker, P.A. and Kastner, M. 1981. Constraints on the formation of sedimentary dolomite. *Science*, **213**, 214-216.

Barnett, P.J. 1991. Quaternary geology of Ontario. *In:* P.C. Thurston, H.R. Williams, R.H. Sutcliffe, and G.M. Stott (eds.), Geology of Ontario, *Ontario Geological Survey*, Special **4** (1), 303-381.

Barrett, T.J. and Fralick, P.W. 1985. Sediment redeposition in Archean iron formation: examples from the Beardmore-Geraldton greenstone belt, Ontario. *Journal of Sedimentary Petrology*, **55** (2), 205-212.

Barrett, T.J. and Fralick, P.W. 1989. Turbidites and iron formations, Beardmore-Geraldton, Ontario: application of a combined ramp/fan model to Archean clastic and chemical sedimentation. *Sedimentology*, **36**, 221-234.

Barton, C.E. and McElhinny, M.W. 1982. Time series analysis of the 10 000 yr geomagnetic secular variation record from SE Australia. *Geophysical Journal, Royal Astronomical Society*, **68** (3), 709-724.

Bigarella, J.J. 1972. Eolian environments: their characteristics recognition and importance. *In:* Rigby, J.K. and Hamblin, W.K. (eds.), Recognition of Ancient Sedimentary Environments, *Society of Economic Paleontologists and Mineralogists*, Special Publication **16**, 13-62.

Blackburn, C.E., Johns, G.W., Ayer, J., and Davis, D.W. 1991. Wabigoon Subprovince. *In:* P.C. Thurston, H.R. Williams, R.H. Sutcliffe, and G.M. Stott (eds.), Geology of Ontario, *Ontario Geological Survey*, Special 4 (1), 303-381.

Butler, R.F. 1998. Paleomagnetism: magnetic domains to geological terranes, Department of Geosciences University of Arizona, http://www.geo.arizona.edu/Paleomag/book/ (originally published by Blackwell Scientific Publications in 1992)

Chandler, F.W. 2000. The Belt-Purcell Basin as a low-latitude passive rift: implications for the geological environment of Sullivan type deposits. *In*: J.W. Lydon, T. Höy, J.F. Slack, and M.E. Knapp (eds.), The Geological Environment of the Sullivan Deposit, British Columbia, *Geological Association of Canada, Mineral Deposits Division, Special Publication* **1**, 82-112.

Cheadle, B.A. 1986a. Stratigraphy and sedimentation of the Middle Proterozoic Sibley Group, Thunder Bay District, Ontario. *Unpublished PhD. Thesis*, The University of Western Ontario, London, 434 p.

Cheadle, B. 1986b. Alluvial-playa sedimentation in the lower Keweenawan Sibley Group, Thunder Bay District, Ontario. *Canadian Journal of Earth Sciences*, **23**, 527-541.

Chen, X.Y. and Barton, C.E. 1991. Onset of aridity and dune building in central Australia: sedimentological and magnetostratigraphic evidence from Lake Amadeus. *Paleogeography, Paleoclimatology, Paleoecology*, **84** (1-4), 53-73.

Ciopa, M.T., Al-Asam, I.S., Symons, D.T.A., Lewchuk, M.T., and Gillen, K.P. 2000. Correlating paleomagnetic, geochemical, and petrographic evidence to date diagenetic and fluid flow events in the Mississippian Turner Valley Formation, Moose Valley, Alberta, Canada. *Sedimentary Geology*, **131**, 109-129.

Coates, M.E. 1972. Geology of the Black Sturgeon River area, District of Thunder Bay. *Ontario Department of Mines and Northern Affairs Geological Report* **98**, 41 p.

Clemmensen, L.B. and Abrahamsen, K. 1983. Aeolian stratification and facies association in desert sediments, Arran basin (Permian), Scotland. *Sedimentology*, **30**, 311-339.

Collinson, J.D. 1996. Alluvial sediments. *In:* H.G. Reading (ed.), Sedimentary Environments: processes, facies, and stratigraphy, 3rd edition, Blackwell Science, 37-82.

Davis, D.W. and Sutcliffe, R.H. 1985. U-Pb ages from the Nipigon Plate and Northern Lake Superior. *Geological Society of America Bulletin*, **96**, 1572-1579.

Davis, D.W., Poulsen, H.K., and Kamo, S.L. 1989. New insights into Archean crustal development from geochronology in the Rainy Lake area, Superior Province, Canada. *Journal of Geology*, **97**, 379-398.

De Deckker, P. and Last, W.M. 1988. Modern dolomite deposition in continental, saline lakes, western Victoria, Australia. *Geology*, **16**, 29-32.

Devaney, J.R. and Williams, H.R. 1989. Evolution of an Archean subprovince boundary: a sedimentological and structural study of part of the Wabigoon-Quetico boundary in northern Ontario. *Canadian Journal of Earth Sciences*, **26** (5), 1013-1026.

Elston, D.P., Enkin, R.J., Baker, J. and Kisilevsky, D.K. 2002. Tightening the Belt: paleomagnetic-stratigraphic constraints on deposition, correlation, and deformation of the Middle Proterozoic (ca. 1.4 Ga) Belt-Purcell Supergroup, United States and Canada. *Geological Society of America Bulletin*, **114**, 619-638.

Eriksson, K.A., Krapez, B. and Fralick P.W. 1994. Sedimentology of Archean greenstone belts: signatures of tectonic evolution. *Earth-Science Reviews*, **37**, 1-88.

Eriksson, K.A., Krapez, B. and Fralick P.W. 1997. Sedimentological aspects. *In*: M.J. De Wit and L.D. Ashwal (eds), Greenstone Belts, Clarendon Press, Oxford, 33-54.

Evans, K.V., Aleinikoff, J.N., Obradovich, J.D. and Fanning, C.M. 2000. SHRIMP U-Pb geochronology of volcanic rocks, Belt Supergroup, western Montana: evidence for rapid deposition of sedimentary strata. *Canadian Journal of Earth Sciences*, **37**, 1287-1300.

Folk, R.L. and Land, L.S. 1975. Mg/Ca ratio and salinity: two controls over crystallization of dolomite. *The American Association of Petroleum Geology Bulletin*, **59** (1), 60-68.

Fralick, P., Jinhua, W., and Williams, H.R. 1992. Trench and slope basin deposits in an Archean metasedimentary belt, Superior Province, Canadian Shield. *Canadian Journal of Earth Sciences*, **29** (12), 2551-2557.

Fralick, P.W. and Barrett, T.J. 1995. Depositional controls on iron formation associations in Canada. *In*: A.G. Plint (ed.), Sedimentary facies analysis. International Association of Sedimentologists, Special Publication **22**, 137-156.

Fralick, P.W. and Kissin, S.A. 1996. Mesoproterozoic basin development in central North America: Implications of Sibley Group volcanism and sedimentation at Redstone Point. *Unpublished manuscript*

Fralick, P.W. and Kronberg, B.I. 1997. Geochemical discrimination of clastic sedimentary rock sources. *Sedimentary Geology*, **113**, 111-124.

Fralick, P.W., Davis, D.W., Kissin, S.A. 2002. The age of the Gunflint Formation, Ontario, Canada: single zircon U-Pb age determinations from reworked volcanic ash. *Canadian Journal of Earth Sciences*, **39**, 1085-1091.

Franklin, J.M., McIlwaine, W., Poulsen K. and Wanless, R. 1980. Stratigraphy and depositional setting of the Sibley Group, Thunder Bay District, Ontario, Canada. *Canadian Journal of Earth Sciences*, **17**, 633-650.

Franklin, J.M. 1970. Metalogeny of the Proterozoic rocks of Thunder Bay District, Ontario. *Unpublished PhD. Thesis*, University of Western Ontario, London, 317 p.

Franklin, J.M., Kissin, S.A., and Smyk, M..C. 1986. Silver deposits associated with the Proterozoic rocks of the Thunder Bay District, Ontario. *Canadian Journal of Earth Sciences*, **23** (10), 1576-1591.

Franklin, J.M. 1978. The Sibley Group, Ontario, *in:* Wanless, R.K. and Loveridge, W.D. (eds.), Rubidium-strontium isotopic age studies, report 2. *Geological Survey of Canada Paper* **77-14**, 31-34.

Geissman, J.S. and Harlan, S.S. 2002. Late Paleozoic remagnetization of Precambrian crystalline rock along the Precambrian/Carboniferous nonconformity, Rocky Mountains: a relationship among deformation, remagnetization, and fluid migration. *Earth and Planetary Science Letters*, **203**, 905-924.

Greenberg, J.K. and Brown, B.A. 1984. Cratonic sedimentation during the Proterozoic: an anorogenic connection in Wisconsin and the upper Midwest. *Journal of Geology*, **92**, 159-171.

Hall, S.M. and Veizer, J. 1995. Geochemistry of Precambrian carbonates: VII. Belt supergroup, Montana and Idaho, USA. *Geochimica et Cosmochimica Acta*, **60** (4), 667-677.

Hanna, R.L. and Verosub, K.L. 1989. A review of lacustrine paleomagnetic records from western North America: 0-40 000 years BP. *Physics of the Earth and Planetary Interiors*, **56** (1-2), 76-95.

Hartshorn, J. and Lewkowicz, A.G. 2000. Lacustrine record of high energy events lake in the Sawtooth Range, Ellesmere Island, Canadian High Arctic. *Zeitschrift fur Geomorphologie*, **44** (4), 417-434.

Haszeldine, R.S. 1984. Muddy delta in freshwater lakes, and tectonism in the Upper Carboniferous Coalfield of NE England. *Sedimentology*, **31**, 811-822.

Hendricks, J.D. and Stevenson, G.M. 1990. Grand Canyon Supergroup: Unkar Group. *In:* S.S. Beus (ed.), Grand Canyon Geology, Oxford University Press, 29-47.

Hentz, T.F. 1985. Early Jurassic sedimentation of a rift-valley lake: Culpeper basin, northern Virgina. *Geological Society of America Bulletin*, **96**, 92-107.

Hidore, J.J. and Oliver, J.E. 1993. Climatology: an Atmospheric Science. Maxwell MacMillan Canada: Toronto, 423 p.

Höy, T., Anderson, D., Turner, R.J.W., and Leitch, C.H.B. 2000. Tectonic, magmatic, and metallogenic history of the early synrift phase of the Purcell Basin, southeastern British Columbia. *In*: J.W. Lydon, T. Höy, J.F. Slack, and M.E. Knapp (eds.), The Geological Environment of the Sullivan Deposit, British Columbia, *Geological Association of Canada, Mineral Deposits Division, Special Publication* **1**, 32-60.

Hubert, J.F. and Hyde, M.G. 1982. Sheet-flow deposit of graded beds and mudstones on an alluvial sandflat – playa system: Upper Triassic Blomidon redbeds, St. Mary's Bay, Nova Scotia. *Sedimentology*, **29**, 457-474.

Johnson, H.D. and Baldwin, C.T. 1996. Shallow clastic seas. *In:* H.G. Reading (ed.), Sedimentary Environments: processes, facies, and stratigraphy, 3rd edition, Blackwell Science, 232-280.

Johnsson, M.J. 1993. The system controlling the composition of clastic sediments. *In:* M.J. Johnsson and A. Basu (eds.), Processes Controlling the Composition of Clastic Sediments, *Geological Society of America, Special Paper* **284**, 1-19.

Jones, C.M. and McCabe, P.J. 1980. Erosion surfaces within giant fluvial cross-beds of the Carboniferous in Northern England. *Journal of Sedimentary Petrology*, **50**, 613-620.

Kronberg, B.I., Fralick, P.W., and Benchimol, R.E. 1998. Late Quaternary sedimenation and palaeohydrology in the Acre foreland basin, SW Amazonia. *Basin Research*, **10**, 311-323.

Logan, Sir W.E. (1863). *Geological Survey of Canada*, Report of Progress from its commencement to 1863.

Lund, S.P., Liddicoat, J.C., Lajoie, K.R., Henyey, T.L., and Robinson, S.W. 1988. Paleomagnetic evidence for long-term (10^4 year) memory and periodic behaviour in the Earth's core dynamo process. *Geophysical Research Letters*, **15** (10), 1101-1104.

Lydon, J.W., Walker, R., and Anderson, E.H. 2000. Lithogeochemistryof the Aldridge Formation and the chemical effects of burial diagenesis. *In:* J.W. Lydon, T. Höy, J.F. Slack, and M.E. Knapp (eds.), The Geological Environment of the Sullivan Deposit, British Columbia. *Geological Association of Canada, Mineral Deposits Division,* **Special Publication 1**, 136-179.

Lyons, T.W., Luepke, J.J., Schreiber, M.E., and Zieg, G.A. 2000. Sulfur geochemical constraints on Mesoproterozoic restricted marine deposition: lower Belt Supergroup, northwestern United States. *Geochimica et Cosmochimica Acta*, **64** (3), 427-437.

Kocurek, G.A. 1996. Desert aeolian systems. *In:* H.G. Reading (ed.), Sedimentary Environments: processes, facies, and stratigraphy, 3rd edition, Blackwell Science, 125-153.

Kruiver, P.P, Dekkers, M.J., Langereis, C.G. 2000. Secular variation in Permian red beds from Dome de Barrot, SE France. *Earth and Planetary Science Letters*, **179** (1), 205-217.

McConnell, R.I. 1975. Stratigraphy and depositional history of the Pioneer Formation (late Proterozoic) of Central Arizona. *Geological Society of America, Abstracts with Programs*, **7**, 344 p.

McFarlane, C.R.M. and Pattison, D.R.M. 2000. Geology of the Matthew Creek metamorphic zone, southeast British Columbia, a window into Middle Proterozoic metamorphism in the Purcell Basin.

McLennan, S.M., Hemming, S., McDaniel D.K., and Hanson, G.N. 1993. Geochemical approaches to sedimentation, provenance, and tectonics. *In:* M.J. Johnsson and A. Basu (eds.), Processes Controlling the Composition of Clastic Sediments, *Geological Society of America, Special Paper* **284**, 21-40.

Machette, M.N. 1985. Calcic soils of the southwestern United States. *Geological Society of America, Special Paper*, **203**, 1-21.

Montgomery, D.R. and Brandon, M.T. 2002. Tectonic controls on erosion rates in tectonically active mountain ranges. *Earth and Planetary Science Letters*, **201**, 489-489.

Miall, A.D. 1977. A review of the braided-river depositional environment. *Earth Science Reviews*, **13**, 1-62.

Miall, A.D. 1985. Architectural-element analysis: a new method of facies analysis applied to fluvial deposits. *Earth-Science Reviews*, **22**, 261-308.

Miall, A.D. 1996. The Geology of Fluvial deposits: sedimentary facies, basin analysis, and petroleum geology. Springer: New York, 422-451.

Middleton, L.T. and Trujillo, A.P. 1984. Sedimentology and depositional setting of the Upper Proterozoic Scanlan Conglomerate, central Arizona. *In:* E.H. Koster and R.J. Steele (eds.), Sedimentology of Gravels and Conglomerates, *Canadian Society of Petroleum Geologists*, Memoir **10**, 189-201.

Nanson, G.C. 1980. Point bar and floodplain formation of the meandering Beatton River, northeastern British Columbia. *Sedimentology*, **27**, 3-29.

Nesbitt, H.W. and Young, G.M. 1982. Early Proterozoic climates and plate motions inferred from major element chemistry of lutites. *Nature*, **299**, 715-717.

Ojakangas, R., Morey, G.B, and Green, J.C. 2001. The Mesoproterozoic Midcontinent Rift System, Lake Superior Region, USA. *Sedimentary Geology*, **141-142**, 421-442.

Ojakangas, R., Morey, G.B., and Southwick, D.L. 2001. Paleoproterozoic basin development and sedimentation in the Lake Superior region, North America. *Sedimentary Geology*, **141-142**, 319-341.

Piper, D.J.W. and Panagos, A.G. 1981. Growth patterns of the Acheloos and Evinos deltas, western Greece. *Sedimentary Geology*, **28**, 111-132.

Pratt, B.R. 2001. Oceanography, bathymetry and syndepositional tectonics of a Precambrain intracratonic basin: integrating sediments, storms, earthquakes and tsunamis in the Belt Supergroup (Helena Formation, ca. 1.45 Ga), western North America. *Sedimentary Geology*, **141-142**, 371-394.

Pufahl, P. and Fralick, P. 2000. Depositional environments of the Paleoproterozoic Gunflint Formation. *In:* Proceedings of the Institute on Lake Superior Geology, **46**(2).

Reading, H.G. and Collinson, J.D. 1996. Clastic coasts. *In:* H.G. Reading (ed.), Sedimentary Environments: processes, facies, and stratigraphy, 3rd edition, Blackwell Science, 154-231.

Richardson, A.J. 2003a. Pass Lake Formation sediment provenance. Unpublished undergraduate thesis, Lakehead University, 40 p.

Richardson, A.J. 2003b. Sibley Basin sediment provenance using zircon and whole rock geochemical methods: possible source areas of the Pass Lake Formation. *49th Annual Institute of Lake Superior Geology, Proceedings and Abstracts.*

Robertson, W.A. and Fahrig, W.F. (1971). The great Logan Paleomagnetic Loop – the polar wandering path from Canadian Shield rocks during the Neohelikian Era. *Canadian Journal of Earth Sciences*, **8**, 1355-1372.

Robertson, W.A. 1973a. Pole position from thermally cleaned Sibley Group sediments and its relevance to Proterozoic magnetic stratigraphy. *Canadian Journal of Earth Sciences*, **10**, 180-193.

Robertson, W.A. 1973b. Pole positions from the Mamainse Point Lavas and their bearing on a Keweenawan Pole Path and Polarity Sequence. *Canadian Journal of Earth Sciences*, **10**, 1541-1555.

Rogala, B. 2000. A metamorphosed evaporite sequence from the Sibley Basin. Unpublished undergraduate thesis, Lakehead University, 38 p.

Rust, B.R. 1978. Depositional models for braided alluvium. *In:* A. Miall (ed), Fluvial Sedimentology, Canadian Society of Petroleum Geologists Memoir **5**, 605-625.

Salvany, J.M., Muñoz, A., and Pérez, A. 1994. Nonmarine evaporitic sedimentation and associated diagenetic processes of the southwestern margin of the Ebro Basin (Lower Miocene), Spain. *Journal of Sedimentary Research*, **A64** (2), 190-203.

Schneider, D.A., Bickford, M.E., Cannon, W.F., Schulz, K.J., and Hamilton, M.A. (2002). Age of volcanic rocks and syndepositional iron formations, Marquette Range Supergroup: implications for the tectonic setting of Paleoproterozoic iron formations of the Lake Superior Region. *Canadian Journal of Earth Sciences*, **39**, 999-1012.

Schumm, S.A. 1963. Speculations concerning paleohydrologic controls of terrestrial sedimentation. *Geological Society of America Bulletin*, **79**, 1573-1588.

Slack, J.F. and Höy, T. 2000. Geochemistry and provenance of clastic metasedimentary rocks of the Aldridge and Fort Steele Formations, Purcell Supergroup, southeastern British Columbia. *In*: J.W. Lydon, T. Höy, J.F. Slack, and M.E. Knapp (eds.), The Geological Environment of the Sullivan Deposit, British Columbia, *Geological Association of Canada, Mineral Deposits Division, Special Publication* **1**, 82-112.

Smith, N.D. 1970. The braided stream depositional environment: comparison of the Platte River with some Silurian clastic rocks, North-Central Appalachians. *Geological Society of America*, **81**, 2993-3014.

Smoot, J.P. and Castens-Seidell, B. 1994. Sedimentary features produced by ellforescent salt crusts, Saline Valley and Death Valley, California. *Sedimentology and Geochemistry of Modern and Ancient Saline Lakes, SEPM Special Publication*, **50**, 73-90.

Sutcliffe, R.H. 1991. Proterozoic Geology of the Lake Superior Area. *In:* P.C. Thurston, H.R. Williams, R.H. Sutcliffe, and G.M. Stott (eds.), Geology of Ontario, *Ontario Geological Survey*, Special **4** (1), 627-658.

Talbot, M.R. and Allen, P.A. 1996. Lakes. *In:* H.G. Reading (ed.), Sedimentary Environments: processes, facies, and stratigraphy, 3rd edition, Blackwell Science, 154-231.

Tanton, T.L. 1931. Fort William and Port Arthur, and Thunder Cape map-area, Thunder Bay District, Ontario. *Geological Survey of Canada*, **Memoir 167**, 222 p. + maps.

Tauxe, L. 1998. Paleomagnetic principles and practice, *Kluwer Academic Publishers*, Netherlands, 299 p.

Thomas, M.D. and Teskey, D.J. 1994. An interpretation of gravity anomalies over the Midcontinent Rift, Lake Superior, constrained by GLIMPCE seismic and aeromagnetic data. *Canadian Journal of Earth Sciences*, **31**, 682-697.

Tomlinson, K. 1983. Chrono-stratigraphic correlation of the late Quaternary lacustrine sediments from Lake Erie. *Unpublished undergraduate thesis*, 72p.

Truc, G. 1978. Lacustrine sedimentation in an evaporitic environment: the Ludian (Palaeogene) of the Mormoiron basin, southeastern France. *Special Publication of the Internation Association of Sedimentology*, **2**, 189-203.

Van Hise, C.R. and Leith, C.K. 1909. Precambrian geology of North America. *United States Geological Survey Bulletin* **360**, 939 p.

West, I.M., Ali, Y.A., and Hilmy, M.E. 1979. Primary gypsum nodules in a modern sabkha on the Mediterranean coast of Egypt. *Geology*, **7**, 354-358.

White, A.H. and Youngs, B.C. 1980. Cambrian alkali playa-lacustrine sequence in the northeastern Officer Basin, South Australia. *Journal of Sedimentary Petrology*, **50** (4), 1279-1286.

Williams, H.R. 1991. Quetico Subprovince. *In:* P.C. Thurston, H.R. Williams, R.H. Sutcliffe, and G.M. Stott (eds.), Geology of Ontario, *Ontario Geological Survey*, Special **4** (1), 303-381.

Wilson, A.W.G. 1910. Geology of the Nipigon Basin, Ontario. *Geological Survey of Canada*, **Memoir 1**, 152 p.

Winchester, J.A. and Floyd, P.A. 1977. Geochemical discrimination of different magma series and their differentiation products using immobile elements. *Chemical Geology*, **20**, 325-343.

Winston, D. 1990. Evidence for intracratonic, fluvial, and lacustrine settings of Middle to Late Proterozoic Basins of western U.S.A. *In:* C.F. Gower, T. Rivers, and A.B. Ryan (eds.), Mid-Proterozoic Laurentia-Baltica, *Geological Association of Canada, Special Paper* **38**, 535-564.

Yechieli, Y. and Wood, W.W. 2002. Hydrogeologic processes in saline systems: playas, sabkhas, and saline lakes. *Earth-Science Reviews*, **58**, 343-365.

Appendix A

DRILL LOGS

Drill logs are provided for all of the holes used in this study. Each stratigraphic column begins with a drill log, including the name and UTM co-ordinates for each hole, followed by a graphical representation of each drill hole.

SB-101 377950 E, 5383500N

		Kama Hill Fm	
0	5.29	Shale	extensive evaporite minerals at base
5.29	5.36	mudstone	finely laminated
5.36	8.6	Shale	
8.6	8.62	coarse sandstone	
8.62	8.76	cross-stratified sandstone	wave ripples
8.76	13.71	Shale	
13.71	13.85	fine sandstone	
13.85	14.68	Shale	
14.68	15.04	Fine Sandstone	slumped
15.04	31.84	Silty Shale	several horizons of extensive evaporite minerals
		Fire Hill Member	
31.84	34.28	Sandstone	
34.28	35.5	Sandstone	mudchip horizon through middle
35.5	35.88	Sandstone	
35.88	36.59	Sandstone	patchy with wispy mud
36.59	37.25	sandstone	
37.25	38.01	siltstone	extensive evaporite minerals at base, contorted bedding
38.01	38.63	Siltstone	
38.63	38.78	mudchip conglomerate	evaporite minerals
38.78	38.99	Shale	
38.99	41.28	Siltstone	
41.28	41.98	Mudchip Conglomerate	evaporite minerals throughout
41.98	42.14	Shale	
42.14	42.51		missing
42.51	43.16	Mudchip Conglomerate	
43.16	43.49	Shale	
43.49	45.8	Mudchip Conglomerate	
45.8	45.95	Shale	
45.95	46.09	breccia	
46.09	46.18	Shale	
46.18	46.33		missing
46.33	46.4	Siltstone	
46.4	46.43	Shale	
46.43	46.44	Mudchip Conglomerate	
46.44	46.55	Shale	
46.55	46.56	Mudchip Conglomerate	
46.56	46.69	Siltstone	
46.69	46.73	Shale	
46.73	46.77	Breccia	
46.77	46.84	Shale	
46.84	47.2	Fine Sandstone	cross-laminated at base
47.2	48.55	Shale	
48.55	48.61	cross-laminated fine sandstone	
48.61	50.22	Siltstone	
50.22	50.29	Sandstone	
50.29	50.99	reverse graded sandstone	gradational to sand
50.99	51.32		missing

51.32	51.39	Silty Shale	
51.39	51.46	Mudstone	finely laminated, green
51.46	52.17	Sandstone	
52.17	52.49	Shale	sandy at base
52.49	52.8	Sandstone	
52.8	53.27	Mudstone	mud and sand interlaminated
53.27	54.59	Sandstone	
54.59	55.06	Sandstone	mud-rich, evaporites at base
55.06	56.48	Sandstone	some evap minerals
56.48	56.76		missing
56.76	56.83	Sandstone	
56.83	56.89	Mudstone	
56.89	57.74	Sandstone	
57.74	57.94	Mudstone	mud/sand interlaminated
57.94	58.11	Sandstone	
58.11	59.17	Mudstone	mud/sand interlaminated
59.17	59.42	Sandstone	
59.42	59.5	Shale	
59.5	59.81		missing
59.81	60.28	Mudstone	mud/sand interlaminated
60.28	60.47	Sandstone	
60.47	60.61	Shale	
60.61	60.91	Sandstone	some irregular mud laminae
60.91	62.09	Sandstone	
62.09	62.35		missing
62.35	62.4	Sandstone	
62.4	62.6	Mudstone	some sandy spots
62.6	63.28	Sandstone	
63.28	63.73	Mudstone	mud/sand interlaminated
63.73	63.92	Sandstone	
63.92	64.1	Mudstone	mud/sand interlaminated
64.1	64.27	Sandstone	
64.27	64.59	Mudstone	some interbedded sand
64.59	65.1	Sandstone	
65.1	65.48	Mudstone	interbedded mud/sand
65.48	65.78		missing
65.78	66.55	Sandstone	with few shaley partings
66.55	67.51	Sandstone	with interbedded mud
67.51	67.7	Sandstone	massive
67.7	68.55	Sandstone	with interbedded mud
68.55	68.97	chickenwire structure	
68.97	69.06	Shale	evaporite minerals
69.06	69.17	dolomitic mudstone	
69.17	69.22	Shale	
69.22	69.43	pebbly sandstone	coarse clasts at base
Channel Island Member, Rossport Fm			
69.43	73.86	Shale	patch fabric with silt/sst, possible chickenwire
73.86	74.82	Shale	A-shale dominated with some dolomite
74.82	75.18		missing
75.18	76.49	Shale	A

76.49	76.52	dolomitic sandstone	
76.52	76.98	Siltstone	
76.98	77.34		missing
77.37	77.38	dolomitic mudstone	B-dolomite dominated with shale
77.38	80.42	Shale	A with some evaporite minerals
80.42	80.64	dolomitic mudstone	C-equal amounts of shale & dolomite
80.64	80.79	Shale	A
80.79	81.04		missing
81.04	81.94	Shale	A
81.94	82.06	dolomitic mudstone	B
82.06	82.7	Shale	A
82.7	82.76	dolomitic mudstone	C
82.76	83.03	Shale	A
83.03	83.23		missing
83.23	83.71	Shale	A
83.71	83.74	dolomitic mudstone	B
83.74	83.98	Shale	A
83.98	84.02	Shale	A
84.02	84.1	dolomitic mudstone	B
84.1	84.42	Shale	A
84.42	84.6	dolomitic mudstone	C
84.6	84.76	dolomitic mudstone	B- with evaporite minerals
84.76	84.96	Shale	A
84.96	85.07	dolomitic mudstone	C
85.07	85.4	Shale	A
85.4	85.49	dolomitic mudstone	B with evaporite minerals
85.49	85.73	Shale	A
85.73	85.81	dolomitic mudstone	B with evaporite minerals
85.81	85.86	Shale	A
85.86	85.96	dolomitic mudstone	B
85.96	86.23		missing
86.23	86.95	Shale	A
86.95	87.07	dolomitic mudstone	C
87.07	87.14	dolomitic mudstone	B with evaporite minerals
87.14	87.28	Shale	A
87.28	87.34	dolomitic mudstone	B
87.34	88.6	Shale	A with gypsum veins
88.6	88.68	dolomitic mudstone	B
88.68	89.25	Shale	A
89.25	89.52		missing
89.52	89.7	Shale	A
89.7	90.1	dolomitic mudstone	B
90.1	90.57	dolomitic mudstone	C
90.57	90.72	dolomitic mudstone	B
90.72	91.34	Shale	A
91.34	91.61	dolomitic mudstone	C with extensive evaporites at top
91.61	91.67	dolomitic mudstone	B
91.67	91.78	Shale	A
91.78	91.84	dolomitic sandstone	B with some coarse clasts
91.84	92.04	Shale	A

92.04	92.05	dolomitic mudstone	B
92.05	92.18	Shale	A
92.18	92.27	dolomitic mudstone	C with evaporites
92.27	92.53		missing
92.53	92.73	Shale	A
92.73	92.95	dolomitic mudstone	C
92.95	93.03	Shale	A
93.03	93.19	dolomitic mudstone	C
93.19	93.24	coarse sandstone	
93.24	94.3	Shale	A
94.3	94.36	dolomitic mudstone	B
94.36	94.64	Shale	A
94.64	94.85	dolomitic mudstone	B broken up
94.85	94.91	Shale	A
94.91	95.08	dolomitic mudstone	B with some evaporite minerals
95.08	95.38	Chickenwire Structure	
95.38	95.43	dolomitic mudstone	B broken up
95.43	95.75	Shale	A
95.75	95.85	dolomitic mudstone	B
95.85	96		missing
96	96.12	Shale	A
96.12	96.29	dolomitic mudstone	C
96.29	96.38	dolomitic mudstone	B
96.38	96.73	dolomitic mudstone	C
96.73	96.78	dolomitic mudstone	B
96.78	97	Shale	A
97	97.02	dolomitic mudstone	B
97.02	97.37	dolomitic mudstone	C
97.37	97.44	dolomitic mudstone	B
97.44	97.67	dolomitic mudstone	C
97.67	97.81	dolomitic mudstone	B
97.81	98.04	Shale	A
98.04	98.05	dolomitic mudstone	B
98.05	98.39	Shale	A
98.39	98.49	dolomitic mudstone	B
98.49	98.78		missing
98.78	98.87	Shale	A
98.87	99.11	dolomitic mudstone	C
99.11	99.4	dolomitic mudstone	B
99.4	99.46	Shale	A
99.46	99.62	dolomitic mudstone	B
99.62	100.25	Shale	A
100.25	100.39	dolomitic mudstone	B
100.39	100.95	Shale	A
100.95	101.19	dolomitic mudstone	C
101.19	101.59		missing
101.59	101.71	dolomitic mudstone	B
101.71	101.8	Shale	A
101.8	101.93	dolomitic mudstone	B
101.93	102.23	dolomitic mudstone	C

102.23	102.47	dolomitic mudstone	B
102.47	102.63	Shale	A
102.63	102.88	dolomitic mudstone	B
102.88	103.66	Shale	A
103.66	103.89	dolomitic mudstone	B
103.89	103.99	dolomitic mudstone	C
103.99	104.08	dolomitic mudstone	B
104.08	104.76	dolomitic mudstone	C
104.76	105.16		missing
105.16	105.46	dolomitic mudstone	
105.46	105.62	Siltstone	
105.62	105.63	dolomitic mudstone	
105.63	105.66	Shale	
105.66	105.8	dolomitic mudstone	
105.8	107.23	Siltstone	
107.23	107.24	dolomitic mudstone	
107.24	107.77	Shale	
107.77	107.82	dolomitic mudstone	
107.82	108.02	Siltstone	
108.02	108.06	dolomitic mudstone	
108.06	108.26	Shale	
108.26	108.27	dolomitic mudstone	
108.27	108.31	shale	
108.31	108.32	dolomitic mudstone	
108.32	108.54	Siltstone	evaporite minerals
108.54	108.83	dolomitic sandstone	coarse sandstone at base
108.83	111.36	Siltstone	shale at top, evaporites at base
111.36	111.38	dolomitic sandstone	coarse sand
111.38	112.64	Siltstone	
112.64	112.65	dolomitic sandstone	coarse sand
112.65	116	Siltstone	
116	116.04	dolomitic sandstone	dolomitic
116.04	118.54	Siltstone	
Fork Bay Member, Pass Lake Fm			
118.54	126.72	Fine Sandstone	few shale horizons
126.72	126.98	Shale	
126.98	127.01	Coarse Sandstone	
127.01	127.45	Shaley Siltstone	
127.45	127.66	Sandstone	
127.66	128.43	Siltstone	
128.43	128.58	Shale	
128.58	128.7	Sandstone	
128.7	129.04	Shale	
129.04	129.07	Sandstone	
129.07	129.57		missing
129.57	129.61	Shale	
129.61	130.1	Sandstone	
130.1	132.09	diabase	
132.09	148.16	Sandstone	mauve, gypsum veins, some coarse horizons, fines to shale at top
148.16	148.3	Mudstone	gypsum veins, parallel bedding

148.3	149.2	Sandstone	
149.2	165.31	gneiss	basement

SB-101

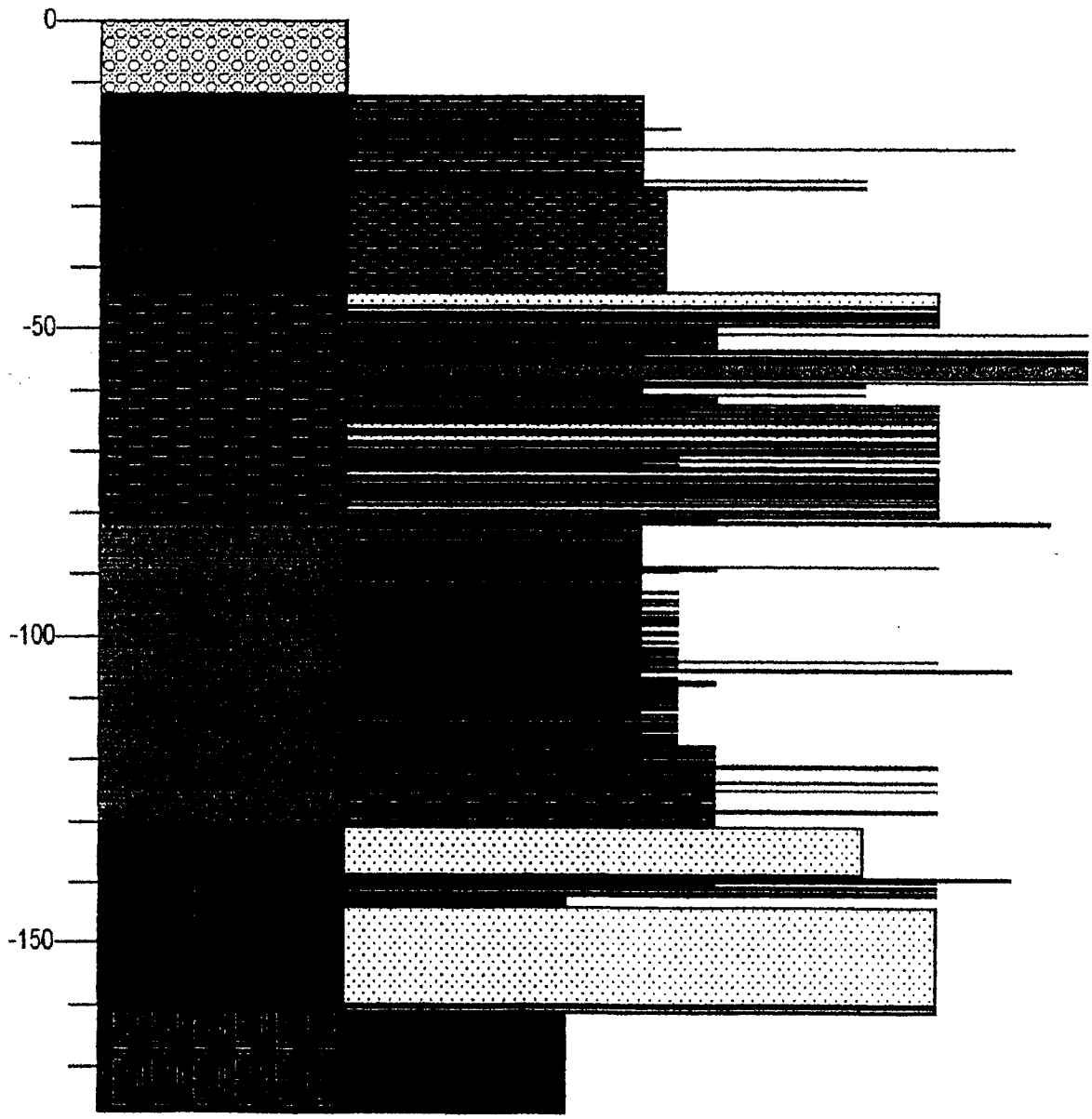

SB-102 377900 E, 5383300 N

Kama Hill Fm			
0	0.6	Shale	
0.6	0.68	Mudstone	finely laminated, green
0.68	0.81	Shale	crumbly
0.81	0.87	Mudstone	green, finely laminated
0.87	1.22	Shale	
1.22	1.31	Mudstone	green, broken
1.31	1.66	Shale	
1.66	2.02	Siltstone	shale wisps, fissile
2.02	6.69	Shale	silty in some areas, reductions spots, evaporites
6.69	6.92		missing
6.92	7.1	cross-stratified sandstone	green, finely laminated
7.1	8.89	Shale	with silt
8.89	8.96	Siltstone	green, finely laminated
8.96	9.4	Shale	
9.4	9.47	cross-stratified sandstone	sandy, green
9.47	11.73	Shale	with silt
11.73	11.8	Shale	green
11.8	14.84	Shale	fissile with some competent silt
14.84	14.91	cross-stratified siltstone	silty
14.91	14.99	Shale	fissile
14.99	15.08	horizontally laminated sandstone	silty, parallel laminated
15.08	15.2	Shale	fissile
15.2	15.54	mudcracked siltstone	extensive mudcracks
15.54	15.78		missing
15.78	15.89	Sandstone	silty
15.89	15.98	Sandstone	
15.98	21.27	Siltstone	some shale layers and evaporites
21.27	25.9	Shale	rare evaporites, reduced at bottom, red at top
25.9	26.32	Siltstone	interbedded shale layers with evaporites in them
26.32	26.58	Shale	
26.58	26.73	Shale with evaporites	
26.73	27.83	Shale	
27.83	28.82	Shale	abundant evaporites
28.82	35.18	Shale	crumbly, periodic evaporite growth
Fire Hill Member, Rossport Fm			
35.18	36.83	mudchip conglomerate	mudchips, few evaporites
36.83	37.11		missing
37.11	37.98	Fine Sandstone	silty
37.98	42.54		missing
42.54	42.72	Siltstone	
42.72	42.8	dolomitic mudstone	
42.8	43.17	Siltstone	evaporites near top
43.17	43.26	dolomitic mudstone	
43.26	43.95	Siltstone	evaporites cause brecciation in places
43.95	44.02	dolomitic mudstone	
44.02	44.25	Siltstone	
44.25	44.44	dolomitic mudstone	

44.44	44.7	Silstone	shale lam, evaporite veining
44.7	44.9	dolomitic mudstone	
44.9	45.45		missing
45.45	45.49	Sandstone	greenish grey
45.49	45.54	dolomitic mudstone	
45.54	45.63	Shaley Siltstone	some evaporites
45.63	45.75	dolomitic mudstone	
45.75	45.88	Siltstone	
45.88	45.94	dolomitic mudstone	
45.94	46.46	Shale with evaporites	
46.46	46.56	dolomitic mudstone	
46.56	47.81	Siltstone	
47.81	48.16		missing
48.16	48.86	Siltstone	extensive evaporites at bottom and top
48.86	49.04	Mudchip Conglomerate	
49.04	49.21	Siltstone	
49.21	49.63	Mudchip Conglomerate	extensive evaporites
49.63	49.79	Siltstone	
49.79	50.06	dolomitic mudstone	
50.06	50.15	Siltstone	
50.15	50.22	dolomitic mudstone	mudcracked, evap
50.22	50.33	Mudchip Conglomerate	
50.33	50.42	Siltstone	
50.42	50.48	dolomitic mudstone	
50.48	50.65	Siltstone	
50.65	50.7	Shale	evaporites
50.7	50.76	Shaley Siltstone	
50.76	50.94	dolomitic mudstone	evap
50.94	50.99	Shale	
50.99	51.1	Mudchip Conglomerate	
51.1	51.29		missing
51.29	51.58	Silty Shale	evaporites
51.58	51.72		missing
51.72	51.98	Mudchip Conglomerate	some lam pinched out around clasts
51.98	53.31		missing
53.31	53.46	dolomitic mudstone	some shale lam
53.46	53.86	Shale	few dolomite lam
53.86	53.9	dolomitic mudstone	
53.9	54.45	Shale	
54.45	54.63	Siltstone	
54.63	55.83	Shale	irregular layers
55.83	56.45	Siltstone	
56.45	56.63		missing
56.63	57.98	Shale	7 cm dolomite horizon and lots of evaporites
57.98	58.34	Sandstone	
58.34	58.82	Shale	sandy patches
58.82	59.31	Sandstone	2 mud partings
59.31	59.69		missing
59.69	59.96	Mudstone	mud, shale, sand interbedded/patchy
59.96	60.29	Sandstone	

60.29	60.69	Shale	irregularly interbedded shale/sandstone
60.69	61.53	Sandstone	massive
61.53	61.58	Shale	
61.58	62.04	Sandstone	
62.04	62.51	reverse graded sandstone	sand content increase upwards
62.51	62.85		missing
62.85	63.77	Mudstone	silty, evaporites
63.77	64.92	Sandstone	mud interlaminated at bottom
64.92	65.3	Silty Shale	
65.3	65.55	Sandstone	fine matrix, coarse floating granules
65.55	65.67	Sandstone	massive, grey
65.67	66.79	Fine Sandstone	silty with shale, evaporites, sandier upwards
66.79	66.89	Shale	
66.89	67.01	Mudstone	interbedded sand/mud
67.01	69.63	Sandstone	
69.63	69.71	Mudstone	green
69.71	70	Sandstone	interbedded sand/mud
70	70.56	Sandstone	few mud lam
70.56	70.83		missing
70.83	71.49	Sandstone	some shale partings
71.49	71.83	Shale	irregularly interbedded sand lam
71.83	75.86	Sandstone	some shale rich horizons, more near top
Channel Island Member, Rossport Fm			
75.86	76.5	Shale	floating coarse granules
76.5	76.78	chickenwire structure	shale
76.78	76.88	Shale	disrupted laminae
76.88	77.17		missing
77.17	77.25	dolomitic mudstone	with floating coarse quartz granules
77.25	79	Chickenwire Structure	silty shale
79	79.35	dolomitic mudstone	
79.35	79.59	dolomitic mudstone	
79.59	79.91		missing
79.91	81.13	Chickenwire Structure	popcorn, silty dolomite
81.13	85.73	Silty Shale	dolomite present, chickenwire structure at top
85.73	85.96		missing
85.96	86.04	Shale	A
86.04	86.3		missing
86.3	86.4	Siltstone	dolomitic with coarse granules
86.4	86.45	Shale	badly disrupted
86.45	86.5	Silty Shale	floating coarse granules
86.5	87.17	shale	A
87.17	87.26	dolomitic mudstone	disrupted layers
87.26	87.69	Shale	A-swirly bedding, dolomite clasts
87.69	87.72	dolomitic mudstone	B
87.72	89.02	Shale	A patchy at top and base
89.02	89.07	dolomitic mudstone	B
89.07	89.13	shale	A
89.13	89.15	dolomitic mudstone	B
89.15	89.4		missing
89.4	89.97	Shale	A

89.97	89.99	dolomitic mudstone	B
89.99	90.27	Shale	A
90.27	90.32	dolomitic mudstone	C
90.32	90.43	Shale	A
90.43	90.44	dolomitic mudstone	B
90.44	90.52	Shale	A
90.52	90.6	dolomitic mudstone	C
90.6	90.72	Shale	A
90.72	90.89	dolomitic mudstone	C
90.89	91.05	dolomitic mudstone	B
91.05	91.14	Shale	A
91.14	91.43	dolomitic mudstone	C
91.43	91.84		missing
91.84	91.85	dolomitic mudstone	B
91.85	92.15	Shale	A
92.15	92.24	dolomitic mudstone	B
92.24	92.36	dolomitic mudstone	C
92.36	92.42	dolomitic mudstone	B
92.42	92.44	Shale	A
92.42	92.45	dolomitic mudstone	B
92.45	92.6	Shale	A
92.6	92.75	dolomitic mudstone	C
92.75	93.04	Shale	A
93.04	93.14	dolomitic mudstone	B
93.14	93.26	Shale	A
93.26	93.33	dolomitic mudstone	C
93.33	93.38	Shale	A
93.38	93.48	dolomitic mudstone	B
93.48	93.56	Shale	A
93.56	93.57	dolomitic mudstone	B
93.57	94	Shale	A
94	94.09	dolomitic mudstone	C
94.09	94.22	Shale	A
94.22	94.25	dolomitic mudstone	B
94.25	94.41	dolomitic mudstone	C
94.41	94.73	Shale	A
94.73	94.8	dolomitic mudstone	B
94.8	94.84	Shale	A
94.84	95.06		missing
95.06	95.3	Shale	A
95.3	95.62	dolomitic mudstone	C
95.62	95.79	Shale	A
95.79	96.25	dolomitic mudstone	C
96.25	96.28	dolomitic mudstone	B
96.28	96.31	Shale	A
96.31	96.38	dolomitic mudstone	B
96.38	96.53	Shale	A
96.53	96.59	dolomitic mudstone	B
96.59	96.66	Shale	A
96.66	96.71	dolomitic mudstone	B

96.71	96.81	Shale	A
96.81	96.9	dolomitic mudstone	B
96.9	97.09	Shale	A
97.09	97.22	dolomitic mudstone	B
97.22	97.53		missing
97.53	97.7	dolomitic mudstone	C
97.7	97.74	dolomitic mudstone	B
97.74	98.04	Shale	A
98.04	98.07	dolomitic mudstone	B
98.07	98.17	Shale	A
98.17	98.23	dolomitic mudstone	B
98.23	98.86	Shale	A
98.86	98.96	dolomitic mudstone	C with floating quartz pebbles at base
98.96	99.31	Shale	A
99.31	99.4	Shale	A
99.4	99.47	dolomitic mudstone	C
99.47	99.49	dolomitic mudstone	B
99.49	99.5	Shale	A
99.5	99.54	dolomitic mudstone	B
99.54	99.56	Shale	A
99.56	99.64	dolomitic mudstone	B
99.64	99.82	Shale	A
99.82	99.84	dolomitic mudstone	B
99.84	100.1	Shale	A
100.1	100.26	dolomitic mudstone	B
100.26	100.28	Shale	A
100.28	100.35	dolomitic mudstone	B with evaporites
100.35	100.38	Shale	A
100.38	100.48	dolomitic mudstone	B with evaporites
100.48	100.52	Shale	A
100.52	100.76	dolomitic mudstone	B
100.76	101.08		missing
101.08	101.24	dolomitic mudstone	C
101.24	101.31	dolomitic mudstone	B
101.31	101.39	Shale	A
101.39	101.45	dolomitic mudstone	B
101.45	101.68	Shale	A
101.68	101.77	dolomitic mudstone	B
101.77	101.93	Shale	A
101.93	102.06	dolomitic mudstone	C
102.06	102.11	Shale	A
102.06	102.15	dolomitic mudstone	B
102.15	102.28	Shale	A contorted bedding at top
102.28	102.37	dolomitic mudstone	B
102.37	102.65	dolomitic mudstone	C
102.65	102.7	Shale	A
102.7	102.82	dolomitic mudstone	C
102.82	102.86	dolomitic mudstone	B, evap
102.86	102.96	dolomitic mudstone	C
102.96	103	Shale	A

103	103.07	dolomitic mudstone	B, evap
103.07	103.47	dolomitic mudstone	C
103.47	103.48	Shale	A
103.48	103.51	dolomitic mudstone	C
103.51	103.64	Shale	A
103.64	103.74	dolomitic mudstone	C
103.74	104.05		missing
104.05	104.41	Shale	A
104.41	104.42	dolomitic mudstone	B
104.42	104.5	Shale	A
104.5	104.53	dolomitic mudstone	B with coarse granules
104.53	104.79	Shale	A
104.79	104.9	dolomitic mudstone	B
104.9	105.11	Shale	A
105.11	105.13	dolomitic mudstone	B
105.13	105.18	Shale	A
105.18	105.26	dolomitic mudstone	B
105.26	105.39		missing
105.39	105.43	Shale	A
105.43	105.46	dolomitic mudstone	C brecciated
105.46	105.57	Shale	A
105.57	105.67	dolomitic mudstone	B
105.67	106.05	Shale	A
106.05	106.09	dolomitic mudstone	B
106.09	106.21	Shale	A
106.21	106.32	dolomitic mudstone	B, evap
106.32	106.33	Shale	A
106.33	106.36	dolomitic mudstone	B, evap
106.36	106.56	Shale	A
106.56	106.77		missing
106.77	106.89	dolomitic mudstone	C
106.89	106.99	dolomitic mudstone	B
106.99	107.14	dolomitic mudstone	C
107.14	107.19	Shale	A
107.19	107.35	dolomitic mudstone	B
107.35	107.66	dolomitic mudstone	C
107.66	107.71	Shale	A
107.71	108.06	dolomitic mudstone	C
107.71	108.14	dolomitic mudstone	B
108.14	108.71	Shale	A
108.71	108.98		missing
108.98	109	Shale	A
109	109.15	dolomitic mudstone	C
109.15	109.21	Shale	A
109.21	109.28	dolomitic mudstone	C
109.28	109.34	Shale	A
109.34	109.51	dolomitic mudstone	B
109.51	109.61	dolomitic mudstone	C
109.61	109.67	Shale	A
109.67	109.72	dolomitic mudstone	C

109.72	109.83	dolomitic mudstone	B
109.83	109.87	dolomitic mudstone	C
109.87	109.92	Shale	A
109.92	110.17	dolomitic mudstone	C
110.17	110.27	dolomitic mudstone	B
110.27	110.47	Shale	A
110.47	110.5	dolomitic mudstone	B
110.5	110.65	dolomitic mudstone	C
110.65	110.71	dolomitic mudstone	B, evap
110.71	110.84	Shale	A
110.84	110.85	dolomitic mudstone	B
110.85	110.89	Shale	A
110.89	110.98	dolomitic mudstone	B
110.98	111.02	Shale	A
111.02	111.1	dolomitic mudstone	B
111.1	111.43	dolomitic mudstone	C, evap
111.43	111.47	dolomitic mudstone	B
111.47	111.58	Shale	A
111.58	111.61	dolomitic mudstone	B, evap
111.61	111.63	Shale	A
111.63	111.86		missing
111.86	111.96	Shale	A
111.96	112.17	dolomitic mudstone	C
112.17	112.25	Shale	A
112.25	112.52	dolomitic mudstone	C
112.52	112.55	Shale	A
112.55	112.67		missing
112.67	112.88	dolomitic sandstone	C with coarse granules, pebbles, evaporites
112.88	114.31	Shale	A
114.31	114.32	dolomitic mudstone	B
114.32	114.65	Shale	A
114.65	114.68	dolomitic sandstone	B with coarse sand at bottom
114.68	114.95	Shale	A
114.95	114.96	dolomitic mudstone	B
114.96	115.22	Shale	A
115.22	115.23	dolomitic mudstone	B
115.23	115.36	Shale	A
115.36	115.87		missing
115.87	117.82	Siltstone	grades to shale at top
117.82	119.14	Siltstone	with dolomite, shalier at top, some coarse granules
119.14	119.16	Coarse Sandstone	
119.16	120.83	Chickenwire Structure	patchy siltstone with dolomite
120.83	120.85	Shale	
120.85	120.88	Coarse Sandstone	
120.88	121.9	Shale	dolomite rich at top, large evaporites
121.9	122.86	Siltstone	dolomite rich at top
122.86	123.14		missing
123.14	123.54	laminated siltstone	parallel lam
123.54	123.55	Shale	
123.55	123.57	Coarse Sandstone	

123.57	123.86	Siltstone	
123.86	124.52	Shale	brick red
124.52	125.67	Silty Shale	patch fabric
125.67	125.9	Sandstone	
125.9	126.15	Shale	
126.15	126.5	Sandstone	
126.5	127.57	Shale	well sorted
127.57	128.15	Sandstone	
128.15	128.38	Shale	
128.38	128.5		missing
128.5	128.59	horizontally laminated sandstone	parallel lam
128.59	129.11	Shale	lots of coarse granules
129.11	129.98	Sandstone	
Fork Bay Member, Pass Lake Fm			
129.98	130.8	graded sandstone	grades upwards, with coarse granules
130.8	131.08		missing
131.08	131.2	Sandstone	with evaporites
131.2	134.16	Sandstone	
134.16	134.26		missing
134.26	134.49	Shale	
134.49	134.83	Sandstone	
134.83	135	Shale	
135	135.62	Sandstone	
135.62	135.77	Shale	gypsum vein
135.77	135.85	Sandstone	
135.85	136.03	Conglomerate	silty shale
136.03	136.58	Sandstone	
136.58	136.7	Fine Sandstone	silty with shale bands
136.7	136.89	pebbly sandstone	with rock fragments
136.89	141.21	diabase	
141.21	141.32	Sandstone	altered
141.32	141.53		missing
141.53	141.59	Sandstone	
141.59	141.6	Silty Shale	
141.6	141.71	Sandstone	
141.71	141.77	Silty Shale	
141.77	141.93	Sandstone	
141.93	141.96	Silty Shale	
141.96	142.33	Sandstone	
142.33	142.62		missing
142.62	142.65	Siltstone	
142.65	142.71	Shale	
142.71	143.35	Sandstone	
1443.35	143.65		missing
143.65	145.31	diabase	
145.31	159.89	horizontally laminated sandstone	parallel bedding, mauve
159.89	163.8	Granite	basement

SB-102

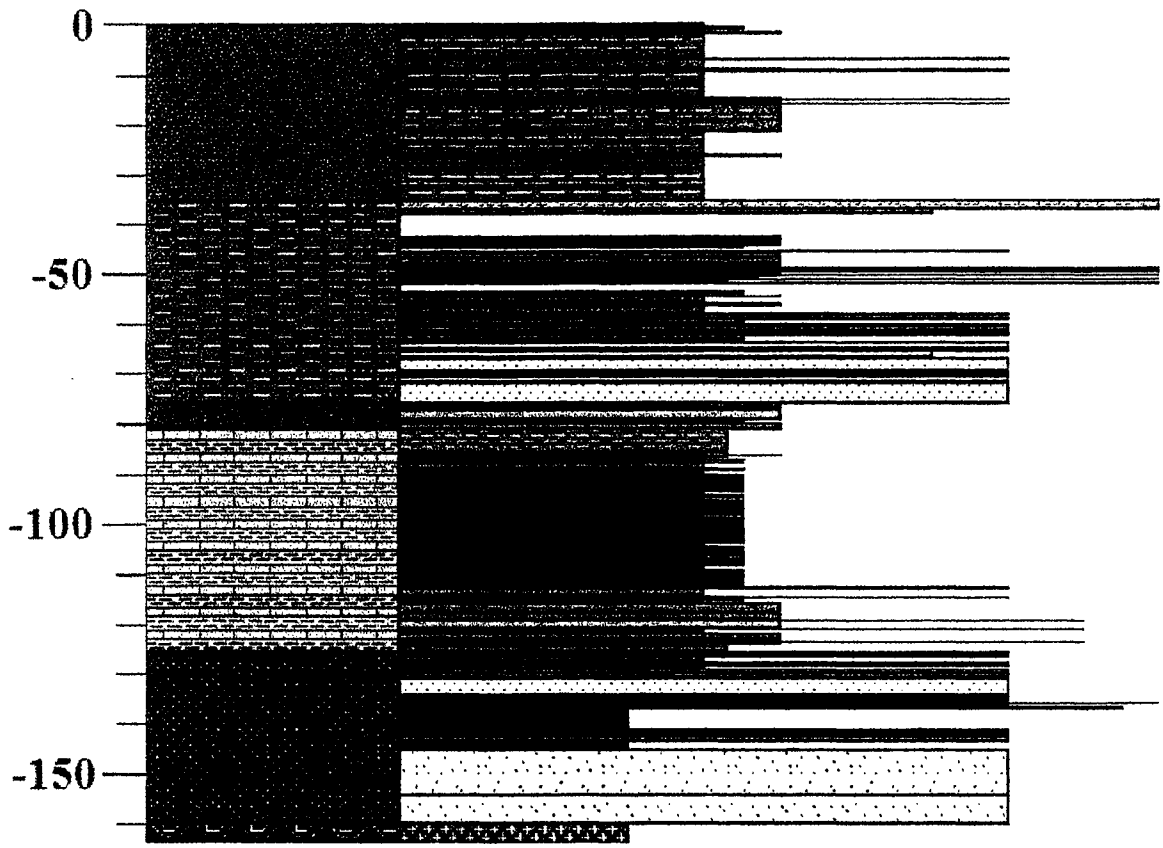

SO-1 384150 E, 5433950 N

Fire Hill Member, Rossport Fm			
0.00	4.16	Silty Shale	
4.16	4.68	Fine Sandstone	green & buff lam, mostly parallel lam, with some wavy
4.68	5.19	Silty Shale	
5.19	6.02	Fine Sandstone	small mudchips
6.02	6.98	Silty Shale	
6.98	8.23	cross-stratified sandstone	mudchips present, trough x-strat
8.23	8.65	cross-stratified sandstone	scours, loads, mudchips, trough x-strat
8.65	9.13	Silty Shale	reduction spots
9.13	10.16	Sandstone	fine parallel lam & x-lam
10.16	12.09	Shale	sandy, sand dikes, current ripples
12.09	12.28	cross-stratified sandstone	flame structure, x-trough
12.28	12.43	Shale	sandy wisps
12.43	12.59	Sandstone	
12.59	12.75	Shale	
12.75	13.19	cross-stratified sandstone	x-trough
13.19	13.51	Shale	
13.51	14.23	Sandstone	some shale lam, parallel lam
14.23	14.29	Shale	
14.29	14.40	Sandstone	
14.40	14.61	Shale	
14.61	14.64	Sandstone	
14.64	15.04	Shale	
15.04	15.08	Sandstone	
15.08	15.22	Shale	
15.22	15.83	Sandstone	
15.83	16.03	Shale	
16.03	16.35	cross-stratified sandstone	green, fsst
16.35	16.85	Siltstone	Sandy, rip-up layers, sand pillows
16.85	16.94	Fine Sandstone	green
16.94	17.74	Silty Shale	sandy
17.74	17.91	Sandstone	
17.91	18.21	Silty Shale	interlam with sand
18.21	18.33	Sandstone	rip-up clasts at base
18.33	18.45	Sandstone	
18.45	18.73	Silty Shale	interbedded with sand
18.73	19.20	Shale	
19.20	19.24	Shale	sandy
19.24	19.38	Shale	
19.38	19.45	Sandstone	interbedded with shale
19.45	19.71	Shale	
19.71	20.23	cross-stratified sandstone	rippled, green mudchips scattered in it
20.23	20.41	Shale	
20.41	20.44	Sandstone	
20.44	20.74	Shale	red, buff sand intercalated
20.74	21.80	Fine Sandstone	purple & white, mudchip horizons
21.80	22.08	Very Fine Sandstone	few mudchip and shale horizons
22.08	22.28	Silty Shale	buff, green & red lam

22.28	23.56	Siltstone	red, parallel lam, ripple lam, mudcracks
23.56	24.07	Sandstone	green & buff
24.07	28.37	Silty Shale	fine sandstone intercalated
Fork Bay Member, Pass Lake Fm			
28.37	28.77	Sandstone	lt. pink, floating mudchips
28.77	28.79	Shale	red
28.79	28.88	Sandstone	green mud horizons
28.88	28.90	Shale	red
28.90	29.08	Sandstone	parallel lam, some green mud lam
29.08	29.11	Shale	red
29.11	29.17	Sandstone	some green mud lam
29.17	29.37	Siltstone	
29.37	29.47	Fine Sandstone	with silt and shale interlam
29.47	29.76	Sandstone	green mud at base
29.76	29.78	Shale	
29.78	32.08	Sandstone	very few mudchips, lt. purple
32.08	32.10	Shale	red
32.10	32.16	Sandstone	with green mud
32.16	32.17	Sandstone	buff
32.17	32.30	Sandstone	purple, mudchip horizon
32.30	32.33	Sandstone	buff with green mud lam
32.33	32.58	Sandstone	
32.58	32.62	Shale	red
32.62	32.66	Sandstone	buff with green mud lam
32.66	32.69	Shale	red
32.69	32.71	Sandstone	buff with green mud lam
32.71	32.79	Shale	red
32.79	34.90	Siltstone	some sand, shale, mudchip horizons
34.90	34.98	Sandstone	buff with green mud lam
34.98	35.51	Siltstone	some sand, shale, mudchip horizons
35.51	36.14	Sandstone	green mud at base
36.14	36.42	Silty Shale	
36.42	36.45	Sandstone	
36.45	36.50	Shale	
36.50	36.52	Sandstone	
36.52	36.59	Shale	
36.59	36.61	Sandstone	
36.61	36.66	Shale	
36.66	36.78	Sandstone	
36.78	36.93	Interlaminated Sandstone and Shale	
36.93	36.97	Shale	
36.97	37.04	Sandstone	
37.04	37.12	Shale	
37.12	37.20	Sandstone	mudchips
37.20	37.42	Sandstone	silty
37.42	37.46	Sandstone	
37.46	39.96	Sandstone	purple, some mudchip horizons
39.96	40.14	Sandstone	buff with green mud lam
40.14	40.23	Shale	
40.23	40.65	Sandstone	mud-rich section

40.65	40.81	Siltstone	
40.81	40.88	Sandstone	
40.88	41.06	Siltstone	
41.06	41.73	Sandstone	silty
41.73	41.85	Silty Shale	
41.85	43.00	reverse graded sandstone	coarsens upward from silt
43.00	43.30	Shale	
43.30	44.01	Sandstone	silty
44.01	44.35	Sandstone	
44.35	44.44	cross-stratified siltstone	with fine sandstone, some x-lam near top
44.44	45.88	Sandstone	
45.88	45.89	Shale	red
45.89	46.00	Sandstone	
46.00	46.03	Shale	
46.03	47.08	Sandstone	
47.08	47.52	Fine Sandstone	interlam with silt
47.52	48.43	Shale	
48.43	48.62	Sandstone	buff
48.62	48.78	Shale	red & green
48.78	49.13	Sandstone	buff, mudchips at base
49.13	51.23	Siltstone	interlam with sst & shale
51.23	51.91	horizontally laminated sandstone	parallel lam
51.91	52.51	siltstone	
52.51	53.26	very fine sandstone	

SO-1

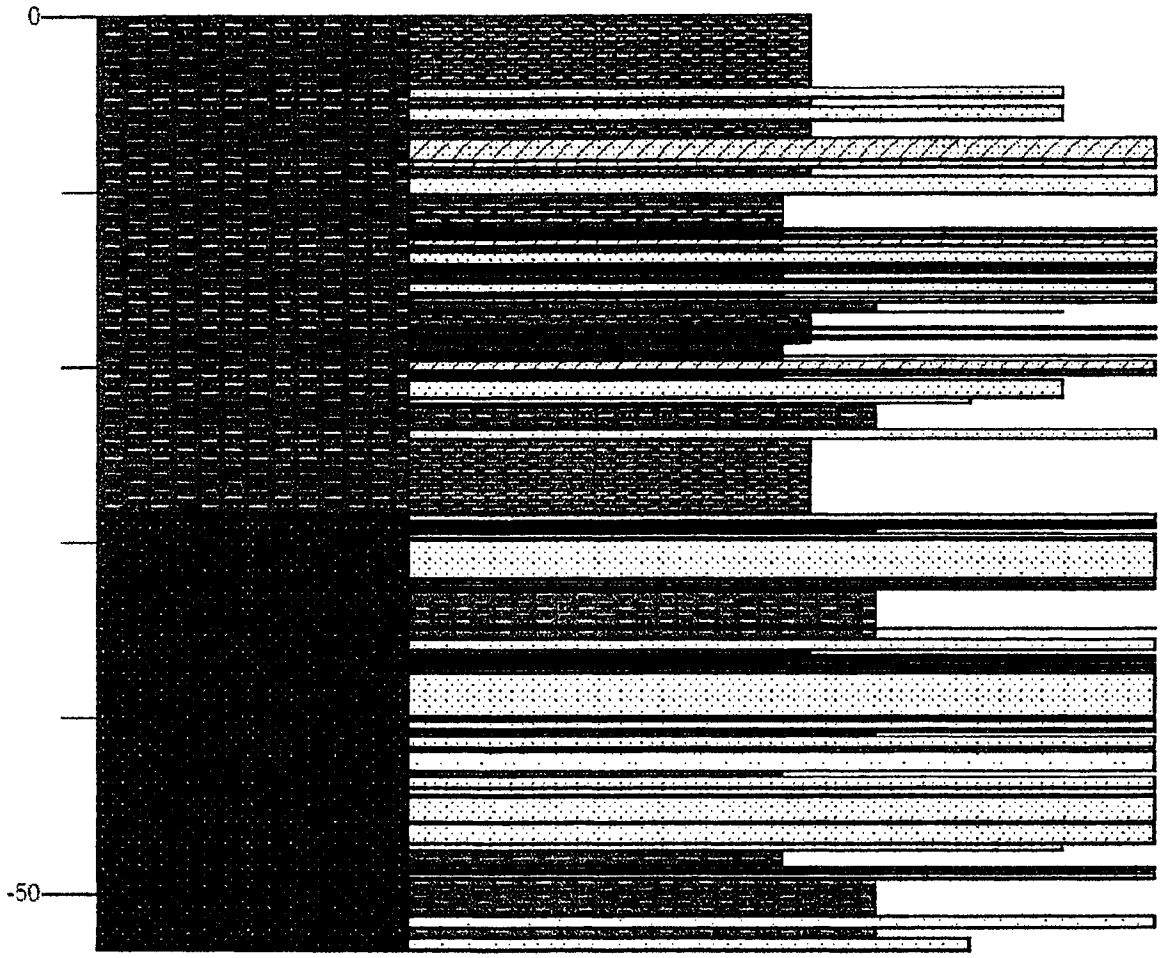

SO-2 384150 5433950

Kama Hill Fm			
0	0.32	laminated siltstone	
0.32	0.33	Sandstone	
0.33	0.36	Shale	
0.36	0.39	Shale	
0.39	0.46	Shale	
0.46	0.49	Shale	
0.49	0.53	Shale	
0.53	0.69	Shale	
0.69	0.71	Siltstone	
0.71	0.84	Shale	
0.84	0.86	Siltstone	
0.86	0.94	Shale	
0.94	0.96	Siltstone	
0.96	1.13	Shale	
1.13	1.15	Siltstone	
1.15	1.2	Shale	
1.2	1.22	Siltstone	
1.22	1.36	Shale	
1.36	1.38	Siltstone	
1.38	1.81	Shale	
Fire Hill Member, Rossport Fm			
1.81	1.88	Sandstone	
1.88	1.9	Shale	
1.9	1.91	Sandstone	
1.91	1.93	Sandstone	
1.93	1.99	Shale	
1.99	2.02	Sandstone	
2.02	2.2	laminated siltstone	
2.2	2.25	Sandstone	
2.25	2.44	laminated siltstone	
2.44	2.49	Sandstone	
2.49	2.59	Shale	
2.59	2.61	Sandstone	
2.61	2.62	Shale	
2.62	2.67	Sandstone	
2.67	2.68	Shale	
2.68	2.7	Sandstone	
2.7	2.77	Shale	
2.77	2.79	Sandstone	
2.79	2.87	Shale	
2.87	2.89	Sandstone	
2.89	2.91	Shale	
2.91	2.97	Sandstone	
2.97	2.99	Shale	
2.99	3.01	Sandstone	
3.01	3.03	Shale	
3.03	3.07	Sandstone	

3.07	3.2	Shale	
3.2	3.21	Sandstone	
3.21	3.26	Shale	
3.26	3.27	Sandstone	
3.27	3.31	Shale	
3.31	3.32	Sandstone	
3.32	3.33	Shale	
3.33	3.34	Sandstone	
3.34	3.39	Shale	
3.39	3.41	Sandstone	
3.41	3.73	Shale	thin lam
3.73	3.74	Sandstone	
3.74	3.94	Shale	thin lam
3.94	3.97	Sandstone	
3.97	4.16	Shale	thin lam
4.16	4.22	Sandstone	rip-up base
4.22	4.49	Shale	thin lam
4.49	4.52	Sandstone	
4.52	4.66	Shale	
4.66	4.68	Sandstone	
4.68	4.71	Shale	
4.71	4.77	Sandstone	
4.77	4.87	Shale	
4.87	4.92	Sandstone	
4.92	5	Shale	
5	5.07	Sandstone	
5.07	5.22	Shale	thin lam
5.22	5.24	Sandstone	
5.24	5.3	Shale	
5.3	5.36	Sandstone	
5.36	5.41	Shale	
5.41	5.46	Sandstone	
5.46	5.62	Shale	
5.62	5.66	Sandstone	
5.66	5.69	Shale	
5.69	5.7	Sandstone	
5.7	5.74	Shale	
5.74	5.79	Sandstone	
5.79	5.83	Shale	
5.83	5.87	Sandstone	
5.87	5.99	Shale	
5.99	6.01	Sandstone	
6.01	6.04	Shale	
6.04	6.05	Sandstone	
6.05	6.19	Shale	
6.19	6.21	Sandstone	
6.21	6.23	Shale	
6.23	6.25	Sandstone	
6.25	6.38	Shale	
6.38	6.4	Sandstone	

6.4	6.41	Shale	
6.41	6.43	Sandstone	
6.43	6.44	Shale	
6.44	6.5	Sandstone	
6.5	6.87	Shale	
6.87	6.89	Sandstone	
6.89	7.05	Shale	
7.05	7.07	Sandstone	
7.07	7.13	Shale	
7.13	7.15	Sandstone	
7.15	7.28	Shale	
7.28	7.31	Sandstone	
7.31	7.32	Shale	
7.32	7.35	Sandstone	
7.35	7.42	Shale	
7.42	7.44	Sandstone	
7.44	7.46	Shale	
7.47	7.48	Sandstone	
7.47	7.51	Shale	
7.51	7.52	Sandstone	
7.52	7.53	Shale	
7.53	7.54	Sandstone	
7.54	7.57	Shale	
7.57	7.58	Sandstone	
7.58	7.69	Shale	
7.69	7.71	Sandstone	
7.71	7.74	Shale	
7.74	7.76	Sandstone	
7.76	7.77	Shale	
7.77	7.83	Sandstone	
7.83	7.84	Shale	
7.84	7.86	Sandstone	
7.86	8.02	Shale	
8.02	8.06	Sandstone	
8.06	8.2	Shale	
8.2	8.86	Sandstone	
8.86	8.91	Shale	
8.91	8.93	Sandstone	
8.93	8.95	Shale	
8.95	8.97	Sandstone	
8.97	9	Shale	
9	9.14	Sandstone	
9.14	9.16	Shale	
9.16	9.24	Sandstone	
9.24	9.31	Shale	
9.31	9.54	Sandstone	
9.54	9.58	Shale	
9.58	9.98	Siltstone	
9.98	10.15	Shale	
10.15	10.19	Siltstone	

10.19	11.12	Shale	
11.12	11.41	Siltstone	
11.41	11.64	Shale	
11.64	11.68	Siltstone	
11.68	11.7	Shale	
11.7	11.72	Siltstone	
11.72	11.83	Shale	
11.83	12.14	Siltstone	
12.14	12.19	Shale	
12.19	12.21	Siltstone	
12.21	12.24	Shale	
12.24	12.25	Siltstone	
12.25	12.51	Shale	
12.51	12.52	Siltstone	
12.52	12.59	Shale	
12.59	12.73	Sandstone	
12.73	12.74	Shale	
12.74	12.78	Siltstone	
12.78	12.84	Shale	
12.84	12.88	Siltstone	
12.88	12.99	Shale	
12.99	13.02	Siltstone	
13.02	13.03	Shale	
13.03	13.05	Siltstone	
13.05	13.07	Shale	
13.07	13.18	Siltstone	
13.18	13.24	Shale	
13.24	13.57	Siltstone	
13.57	13.79	Shale	
13.79	13.86	Siltstone	
13.86	13.87	Shale	
13.87	13.88	Siltstone	
13.88	13.89	Shale	
13.89	13.9	Siltstone	
13.9	13.96	Shale	
13.96	13.97	Siltstone	
13.97	14.04	Shale	
14.04	14.05	Sandstone	
14.05	14.43	Shale	
14.43	14.45	Siltstone	
14.45	14.49	Shale	
14.49	14.54	Siltstone	
14.54	14.62	Shale	
14.62	14.66	Siltstone	
14.66	14.71	Shale	
14.71	14.75	Siltstone	
14.75	14.87	Shale	
14.87	15.29	Sandstone	
15.29	15.75	laminated siltstone	
15.75	15.82	Siltstone	

15.82	15.87	Shale	
15.87	15.9	Siltstone	
15.9	15.94	Shale	
15.94	16.12	Siltstone	
16.12	16.23	Shale	
16.23	16.25	Siltstone	
16.25	16.27	Shale	
16.27	16.32	Siltstone	
16.32	16.33	Shale	
16.33	16.34	Siltstone	
16.34	17.41	Silty Shale	thin lam
17.41	17.65	Shale	
17.65	17.72	Sandstone	
17.72	17.76	Shale	
17.76	17.77	Siltstone	
17.77	17.83	Shale	
17.83	17.84	Siltstone	
17.84	17.87	Shale	
17.87	17.88	Siltstone	
17.88	17.95	Shale	
17.95	17.96	Siltstone	
17.96	18.1	Shale	
18.1	18.11	Siltstone	
18.11	18.42	Shale	
18.42	18.47	Siltstone	
18.47	18.56	Shale	
18.56	18.59	Siltstone	
18.59	18.65	Shale	
18.65	18.7	Siltstone	
18.7	18.91	Shale	
18.91	18.94	Sandstone	
18.94	18.96	Shale	
18.96	19.14	Sandstone	
19.14	19.17	Shale	
19.17	19.2	Sandstone	
19.2	19.27	Shale	
19.27	19.28	Siltstone	
19.28	19.31	Shale	
19.31	19.33	Siltstone	
19.33	19.39	Shale	
19.39	19.4	Siltstone	
19.4	19.58	Shale	
19.58	19.59	Siltstone	
19.59	19.72	Shale	
19.72	19.8	Siltstone	
19.8	19.81	Shale	
19.81	19.9	Siltstone	
19.9	19.93	Shale	
19.93	19.95	Siltstone	
19.95	19.99	Shale	

19.99	20	Siltstone	
20	20.04	Shale	
20.04	20.05	Siltstone	
20.05	20.1	Shale	
20.1	20.11	Siltstone	
20.11	20.16	Shale	
20.16	20.17	Siltstone	
20.17	20.22	Shale	
20.22	20.25	Siltstone	
20.25	20.28	Shale	
20.28	20.32	Sandstone	
20.32	20.37	Shale	
20.37	20.39	Siltstone	
20.39	20.42	Shale	
20.42	20.48	Sandstone	
20.48	20.62	Shale	
20.62	20.63	Siltstone	
20.63	20.83	Shale	
20.83	20.87	Sandstone	
20.87	20.89	Shale	
20.89	20.94	Siltstone	
20.94	21	Shale	
21	21.01	Siltstone	
21.01	21.14	Shale	
21.14	21.2	Siltstone	
21.2	21.22	Shale	
21.22	21.23	Siltstone	
21.23	21.24	Shale	
21.24	21.28	Siltstone	
21.28	21.3	Shale	
21.3	21.31	Siltstone	
21.31	21.33	Shale	
21.33	21.34	Siltstone	
21.34	21.35	Shale	
21.35	21.36	Siltstone	
21.36	21.37	Shale	
21.37	21.41	Siltstone	
21.41	21.45	Shale	
21.45	21.46	Siltstone	
21.46	21.54	Shale	
21.54	21.58	Siltstone	
21.58	21.89	Shale	
21.89	21.91	Siltstone	
21.91	22.03	Shale	
22.03	22.17	Siltstone	
22.17	22.22	Shale	
22.22	22.24	Siltstone	
22.24	22.53	Shale	
22.53	22.54	Siltstone	
22.54	22.89	Shale	

22.89	22.91	Siltstone	
22.91	22.97	Shale	
22.97	22.98	Siltstone	
22.98	23.04	Shale	
23.04	23.06	Siltstone	
23.06	23.29	Shale	
23.29	23.31	Sandstone	
23.31	23.58	laminated siltstone	
23.58	23.88	Siltstone	
23.88	23.94	laminated siltstone	
23.94	23.95	Siltstone	
23.95	24	Shale	
24	24.02	Siltstone	
24.02	24.08	Shale	
24.08	24.12	Siltstone	
24.12	24.14	Shale	
24.14	24.17	Silstone	
24.17	24.19	Shale	
24.19	24.2	Siltstone	
24.2	24.29	Shale	
24.29	24.3	Siltstone	
24.3	24.34	Shale	
24.34	24.38	Breccia	
24.38	24.5	Shale	
24.5	24.52	Breccia	
24.52	24.71	laminated siltstone	
24.71	24.72	Siltstone	
24.72	24.91	Shale	
24.91	24.95	Siltstone	
24.95	25.02	Shale	
25.02	25.03	Siltstone	
25.03	25.35	Shale	
25.35	25.38	Siltstone	
25.38	25.47	Shale	
25.47	25.5	Siltstone	
25.5	25.68	Shale	
25.68	25.74	Siltstone	
25.74	25.83	Shale	
25.83	25.84	Siltstone	
25.84	26.1	Shale	
26.1	26.15	Sandstone	
26.15	26.21	Shale	
26.21	26.22	Sandstone	
26.22	26.45	Shale	
26.45	26.46	Sandstone	
26.46	26.53	Shale	
26.53	26.55	Siltstone	
26.55	26.61	Shale	
26.61	26.67	Siltstone	
26.67	26.82	laminated siltstone	

26.82	26.89	laminated siltstone	
26.89	26.9	Shale	
26.9	26.94	Siltstone	
26.94	26.99	Shale	
26.99	27	Siltstone	
27	27.11	Shale	
27.11	27.22	Siltstone	
27.22	27.27	Shale	
27.22	27.29	Siltstone	
27.29	27.3	Shale	
27.3	27.43	Siltstone	
27.43	27.47	Shale	
27.47	27.49	Siltstone	
24.49	27.53	Shale	
27.53	27.59	Siltstone	
27.59	27.81	Shale	
27.81	27.82	Siltstone	
27.82	27.84	Shale	
27.84	27.86	Siltstone	
27.86	28.04	laminated siltstone	
28.04	28.1	Siltstone	
28.1	28.32	Shale	
28.32	28.34	Siltstone	
28.34	28.39	Shale	
28.39	28.41	Siltstone	
28.41	28.49	Shale	
28.49	28.5	Siltstone	
28.5	28.54	Shale	
28.54	28.56	Siltstone	
28.56	28.59	Shale	
28.59	28.61	Siltstone	
28.61	28.63	Shale	
28.63	28.64	Siltstone	
28.64	29.53	Shale	
29.53	29.58	Siltstone	
29.58	29.81	laminated siltstone	
29.81	29.83	Siltstone	
29.83	29.97	Shale	
29.97	29.99	Sandstone	
29.99	30.51	Shale	
30.51	30.58	Sandstone	
30.58	30.63	Shale	
30.63	30.65	Siltstone	
30.65	30.73	Shale	
30.73	30.77	Siltstone	
30.77	30.83	Shale	
30.83	30.87	Siltstone	
30.87	30.93	Shale	
30.93	30.95	Siltstone	
30.95	31.01	Shale	

31.01	31.07	Siltstone	
31.07	31.15	Shale	
31.15	31.17	Siltstone	
31.17	31.2	Shale	
31.2	31.22	Siltstone	
31.22	31.26	Shale	
31.26	31.31	Siltstone	
31.31	31.33	Shale	
31.33	31.36	Siltstone	
31.36	31.37	Shale	
31.37	31.41	Siltstone	
31.41	31.59	Shale	
31.59	31.78	Sandstone	
31.78	31.86	Shale	
31.86	31.88	Siltstone	
31.88	31.9	Shale	
31.9	31.91	Siltstone	
31.91	31.93	Shale	
31.93	31.98	Siltstone	
31.98	31.99	Shale	
31.99	32.02	Siltstone	
32.02	32.13	Shale	
32.13	32.15	Siltstone	
32.15	32.33	Shale	
32.33	32.34	Siltstone	
32.34	33.06	Shale	
33.06	33.08	Sandstone	
33.08	33.45	Shale	
33.45	33.48	Sandstone	
33.48	33.54	Shale	
33.54	33.55	Siltstone	
33.55	33.74	Shale	
33.74	33.75	Siltstone	
33.75	33.84	Shale	
33.84	33.85	Siltstone	
33.85	33.99	Shale	
33.99	34	Siltstone	
34	34.01	Shale	
34.01	34.07	Siltstone	
34.07	34.08	Shale	
34.08	34.12	Sandstone	
34.12	34.14	Shale	
34.14	34.16	Siltstone	
34.16	34.17	Shale	
34.17	34.18	Siltstone	
34.18	34.19	Shale	
34.19	34.24	Siltstone	
34.24	34.25	Shale	
34.25	34.28	Siltstone	
34.28	34.38	Shale	

34.38	34.44	Breccia	
34.44	34.62	Shale	
34.62	34.65	Siltstone	
34.65	34.68	Shale	
34.68	34.69	Siltstone	
34.69	34.81	Shale	
34.81	34.82	Siltstone	
34.82	34.93	Shale	
34.93	35.02	Sandstone	
35.02	35.03	Shale	
35.03	36.12	Sandstone	
Channel Island, Rossport Fm			
36.47	37.51	Silty Shale	green & peach, interlam with sst
37.51	37.88	Mudstone	red
37.88	37.93	Shale	peach
37.93	38.49	Shale	
38.49	38.5	Sandstone	
38.5	38.9	Mudstone	massive, light and chalky
38.9	38.95	Sandstone	red
38.95	39.18	Silty Shale	irregular lam, green & peach
39.18	39.45	Shale	
39.45	39.46	Siltstone	
39.46	39.67	Shale	
39.67	39.68	Siltstone	
39.68	39.81	Shale	
39.81	39.82	Siltstone	
39.82	40.07	Shale	
40.07	40.08	Siltstone	
40.08	40.11	Shale	
40.11	40.12	Siltstone	
40.38	40.48	Shale	
40.48	40.5	Siltstone	
40.5	40.53	Shale	
40.53	40.54	Siltstone	
40.54	40.58	Shale	
Fork Bay Member, Pass Lake Fm			
40.58	40.64	Fine Sandstone	
40.64	40.73	Shale	
40.73	40.8	Fine Sandstone	
40.8	40.91	Shale	
40.91	40.95	Fine Sandstone	
40.95	41.04	Shale	
41.04	41.17	Fine Sandstone	
41.17	41.45	Shale	
41.45	41.46	Sandstone	
41.46	42.16	Shale	
42.16	42.34	Sandstone	
42.34	42.59	Shale	
42.59	42.61	Sandstone	
42.61	42.75	Shale	

42.75	42.78	Sandstone	
42.78	42.92	Shale	
42.92	42.98	Sandstone	
42.98	43.37	Shale	
43.37	43.4	Sandstone	
43.4	44.48	Sandstone	green & peach mud interlam
44.48	44.67	Shale	
44.67	45.52	Sandstone	
45.52	45.72	Shale	
45.72	45.76	Sandstone	
45.76	45.87	Shale	
45.87	45.88	Sandstone	
45.88	45.92	Shale	
45.92	45.96	Sandstone	
45.96	46.03	Shale	
46.03	46.09	Sandstone	
46.09	46.13	Shale	
46.13	46.3	Sandstone	
46.3	46.45	Shale	
46.45	46.6	Sandstone	
46.6	46.8	Shale	
46.8	46.86	Sandstone	
46.86	46.87	Shale	
46.87	47.89	Sandstone	
47.89	49.19	diabase	
49.19	49.27	Shale	
49.27	49.42	Siltstone	
49.42	49.47	Shale	
49.47	49.59	Siltstone	
49.59	49.8	Shale	
49.8	49.94	Sandstone	
49.94	49.99	Shale	
49.99	50	Sandstone	
50	50.02	Shale	
50.02	50.03	Sandstone	
50.03	50.06	Shale	
50.06	50.11	Sandstone	
50.11	51.46	Shale	peach & red, chalky
51.46	51.51	Sandstone	
51.51	51.52	Shale	
51.52	52.32	Sandstone	
52.32	52.38	Shale	
52.38	52.64	Sandstone	
52.64	53.06	Shale	
53.06	53.3	Sandstone	
53.3	53.31	Shale	
53.31	53.33	Sandstone	
53.33	53.34	Sandstone	
53.34	53.35	Shale	
53.35	53.36	Silty Sandstone	

53.36	53.38	Shale	
53.38	53.39	Silty Sandstone	
53.39	53.41	Shale	
53.41	53.46	Sandstone	
53.46	53.49	Shale	
53.49	53.63	Sandstone	
53.63	53.73	Shale	
53.73	53.76	Sandstone	
53.76	53.82	Shale	
53.82	53.83	Sandstone	
53.83	53.9	Shale	
53.9	53.91	Sandstone	
53.91	54.14	Shale	
54.14	56.84	Sandstone	
56.84	56.97	Shale	
56.97	57.31	Sandstone	
57.31	57.37	Shale	
57.37	57.95	Sandstone	
57.95	58.3	Shale	
58.3	59.55	Sandstone	
59.55	59.71	Shale	
59.71	61.61	Sandstone	
61.61	61.66	Shale	
61.66	61.68	Sandstone	
61.68	61.75	Shale	
61.75	61.76	Sandstone	
61.76	61.79	Shale	
61.79	61.8	Sandstone	
61.8	61.85	Shale	
61.85	61.86	Sandstone	
61.86	61.92	Shale	
61.92	61.93	Sandstone	
61.93	62.08	Shale	
62.08	62.09	Sandstone	
62.09	62.14	Shale	
62.14	62.61	Sandstone	
62.61	62.75	Shale	
62.75	63.95	Sandstone	
63.95	63.96	Shale	
63.96	64.05	Sandstone	
64.05	64.07	Shale	
64.07	64.09	Sandstone	
64.09	64.11	Shale	
64.11	64.14	Sandstone	
64.14	64.24	Shale	
64.24	64.69	Sandstone	
64.69	64.73	Shale	
64.73	64.87	Sandstone	
64.87	64.9	Shale	
64.9	65.06	Sandstone	

65.06	65.14	Shale	
65.14	65.16	Sandstone	
65.16	65.17	Shale	
65.17	65.19	Sandstone	
65.19	65.23	Shale	
65.23	65.26	Sandstone	
65.26	65.3	Shale	
65.3	65.5	Sandstone	
65.5	65.81	Shale	
65.81	65.84	Sandstone	
65.84	66.05	Shale	
66.05	66.06	Sandstone	
66.06	66.37	Shale	
66.37	66.38	Sandstone	
66.38	66.41	Siltstone	
66.41	66.45	Sandstone	
66.45	66.68	Shale	
66.68	66.77	Sandstone	
66.77	66.98	Shale	
66.98	67.01	Sandstone	
67.01	67.03	Shale	
67.03	67.11	cross-stratified sandstone	
67.11	67.13	Shale	
67.13	67.18	Sandstone	
67.18	67.19	Shale	
67.19	67.26	Sandstone	
67.26	67.31	Shale	
67.31	67.34	Sandstone	
67.34	67.37	Shale	
67.37	67.39	Sandstone	
67.39	68.04	Sandstone	
68.04	68.25	Shale	
68.25	68.26	Sandstone	
68.26	68.4	Shale	
68.4	68.41	Conglomerate	sst to shale up
68.41	68.43	Breccia	paleosol
68.43	68.47	Shale	
68.47	68.51	Sandstone	
68.51	68.56	Shale	
68.56	68.58	Sandstone	
68.58	68.59	Shale	
68.59	68.63	Sandstone	
68.63	68.83	Shale	
68.83	68.88	Sandstone	
68.88	68.9	Shale	
68.9	68.95	Sandstone	
68.95	69.2	Shale	
69.2	69.26	Sandstone	
69.26	69.79	Shale	
69.79	69.86	Sandstone	

69.86	69.96	Shale	
69.96	69.98	Sandstone	
69.98	70.8	Shale	
70.8	70.82	Sandstone	
70.82	71.54	Shale	
71.54	71.63	Sandstone	
71.63	71.64	Shale	
71.64	71.77	Silty Sandstone	
71.77	72.05	Shale	
72.05	72.12	Sandstone	
72.12	72.3	Shale	
72.3	72.43	Sandstone	
72.43	72.66	Shale	
72.66	72.73	Sandstone	
72.73	73.24	Shale	
73.24	73.28	Sandstone	
73.28	73.54	Shale	
73.54	73.59	Sandstone	
73.59	73.71	Shale	
73.71	73.72	Sandstone	
73.72	74.47	Shale	dark maroon, soil horizon
74.47	74.54	Breccia	green
74.54	75.53	mudcracked siltstone	mudcracks, thin lam shale
75.53	75.59	cross-stratified sandstone	some discontinuous ripple lam
75.59	76.07	mudcracked siltstone	mudcracks, mud/shale lam
76.07	76.19	cross-stratified sandstone	some discontinuous ripple lam
76.19	76.93	Mudstone	same as above
76.93	77.04	cross-stratified sandstone	same as above
77.04	78.3	Mudstone	same as above
78.3	78.38	cross-stratified sandstone	same as above
78.38	78.93	Mudstone	same as above, more sand
78.93	78.96	cross-stratified sandstone	same as above
78.96	92.88	Sandstone	mud horizons
92.88	93.73	Shale	well-laminated, sandy horizons
93.73	100.49	Sandstone	some shale horizons
100.49	101.58	diabase	
101.58	109.08	Fine Sandstone	patchy, reduction spots, parallel lam

SO-2

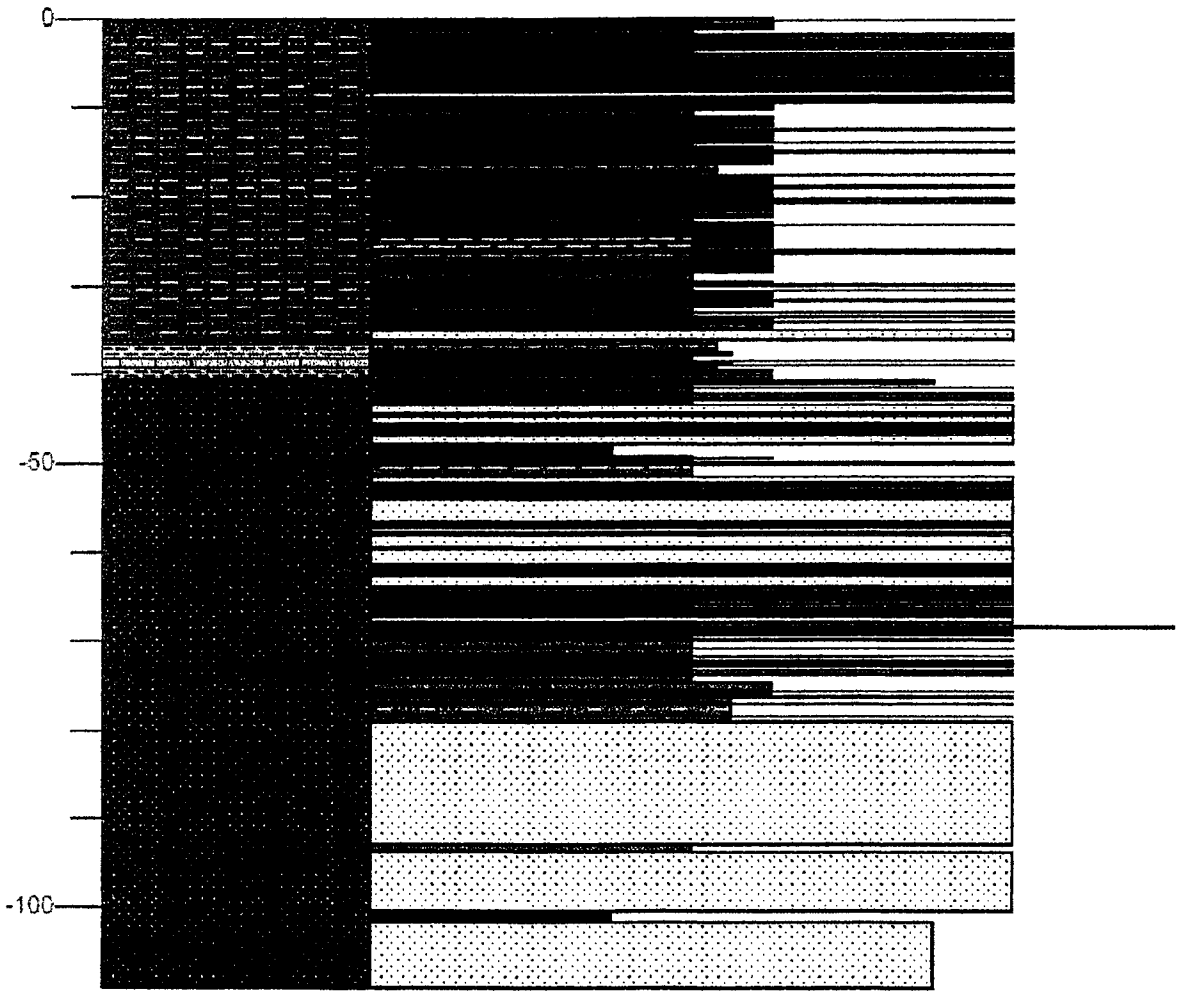

DO-82-1 377500 E, 5410100 N

Fire Hill Member, Rossport Fm			
0.00	2.00	Sandstone	
Channel Island, Rossport Fm			
2.00	2.23	Siltstone	
2.23	2.33	Sandstone	
2.33	2.58	Siltstone	
2.58	2.60	Sandstone	
2.60	3.37	Siltstone	light pink
3.37	5.17	Mudstone	light buff pink, massive
5.17	5.67		missing
5.67	5.90	Breccia	abundant calcite veins, angular fine-grained fragments
5.90	16.97	Granite	pink granitic basement

DO-82-2 377500 5410070

Fork Bay Member, Pass Lake Fm			
0.00	1.51	fine sandstone	
1.51	1.53	Sandstone	
1.53	2.04	Fine Sandstone	
2.04	2.05	Sandstone	
2.05	2.79	fine sandstone	
2.79	2.82	Sandstone	
2.82	4.36	Fine Sandstone	
4.36	4.38	Sandstone	
4.38	5.29	Fine Sandstone	
5.29	5.30	Sandstone	
5.30	5.35	Fine Sandstone	
5.35	5.40	Sandstone	
5.40	7.39	Fine Sandstone	
7.39	7.44		
7.44	8.77	Fine Sandstone	
8.77	8.82	Sandstone	
8.82	10.12	Fine Sandstone	
10.12	10.27	Sandstone	
10.27	12.47	Fine Sandstone	
12.47	12.57	Sandstone	
12.57	14.37	Fine Sandstone	
14.37	14.46	Sandstone	
14.46	15.93	Fine Sandstone	
15.93	20.91	Granite	basement

DO-82-1

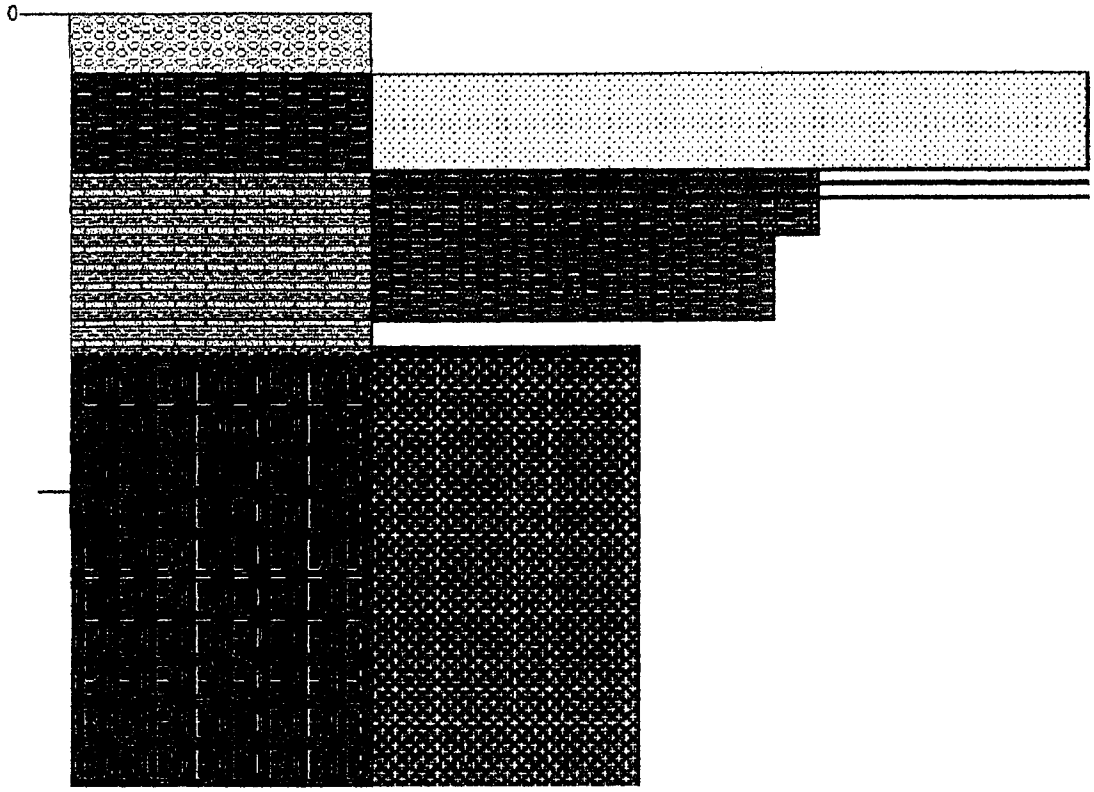

DO-82-2

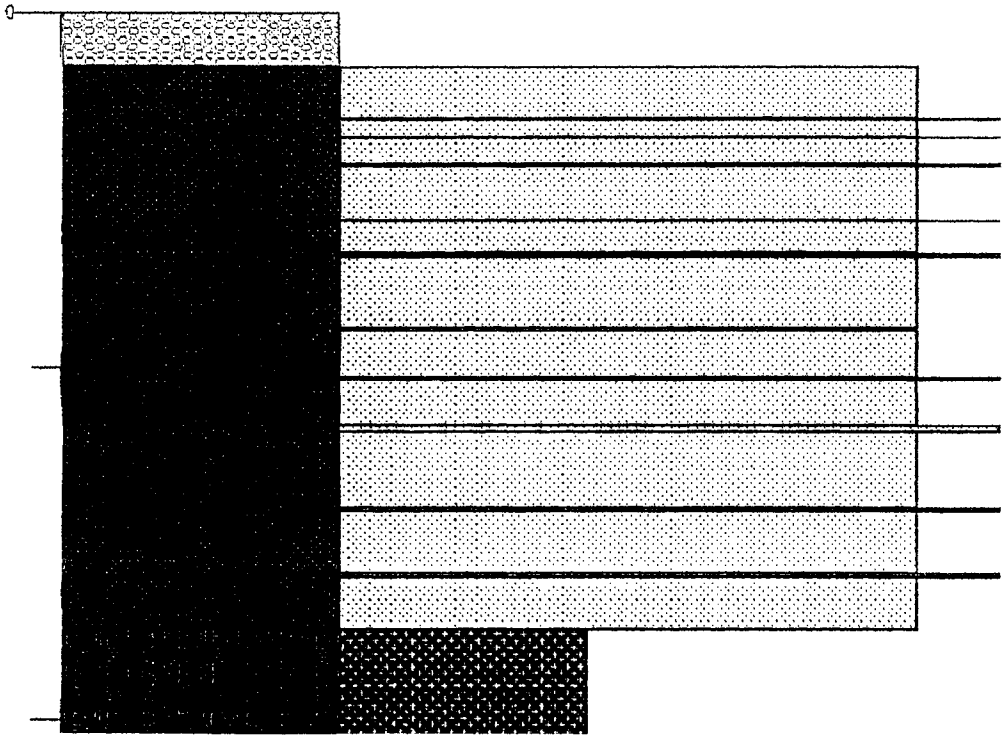

DO-82-3 377410 E, 5410900 N

Channel Island Member, Rossport Fm			
0.00	0.24	Shale	
0.24	0.26	Sandstone	
0.26	0.30	Shale	
0.30	0.34	Sandstone	
0.34	1.24	Shale	
1.24	1.25	Sandstone	
1.25	2.80	Shale	
2.80	2.81	Sandstone	
2.81	3.79	Shale	
3.79	3.82	Sandstone	
3.82	3.87	Shale	
3.87	3.89	Sandstone	
3.89	3.91	Shale	
3.91	3.94	Sandstone	
3.94	4.34	Shale	
4.34	4.35	Sandstone	
4.35	4.36	Shale	
4.36	4.38	Sandstone	
4.38	4.50	Shale	
4.50	4.51	Sandstone	
4.51	4.57	Shale	
4.57	4.58	Sandstone	
4.58	5.28	Shale	
5.28	5.29	Sandstone	
5.29	5.53	Shale	
5.53	5.54	Sandstone	
5.54	6.06	Shale	
6.06	6.09	Sandstone	
6.09	6.75	Shale	
6.75	6.85	Sandstone	
6.85	7.34	Shale	
7.34	7.37	Sandstone	
7.37	8.19	Shale	
8.19	8.21	Sandstone	
8.21	8.26	Shale	
8.26	8.29	Sandstone	clast support
8.29	8.99	Silty Shale	
8.99	9.00	Sandstone	medium to fine-grained, matrix support
9.00	16.30	Shale	red, silty, calcite veining
16.30	19.06	Granite	basement

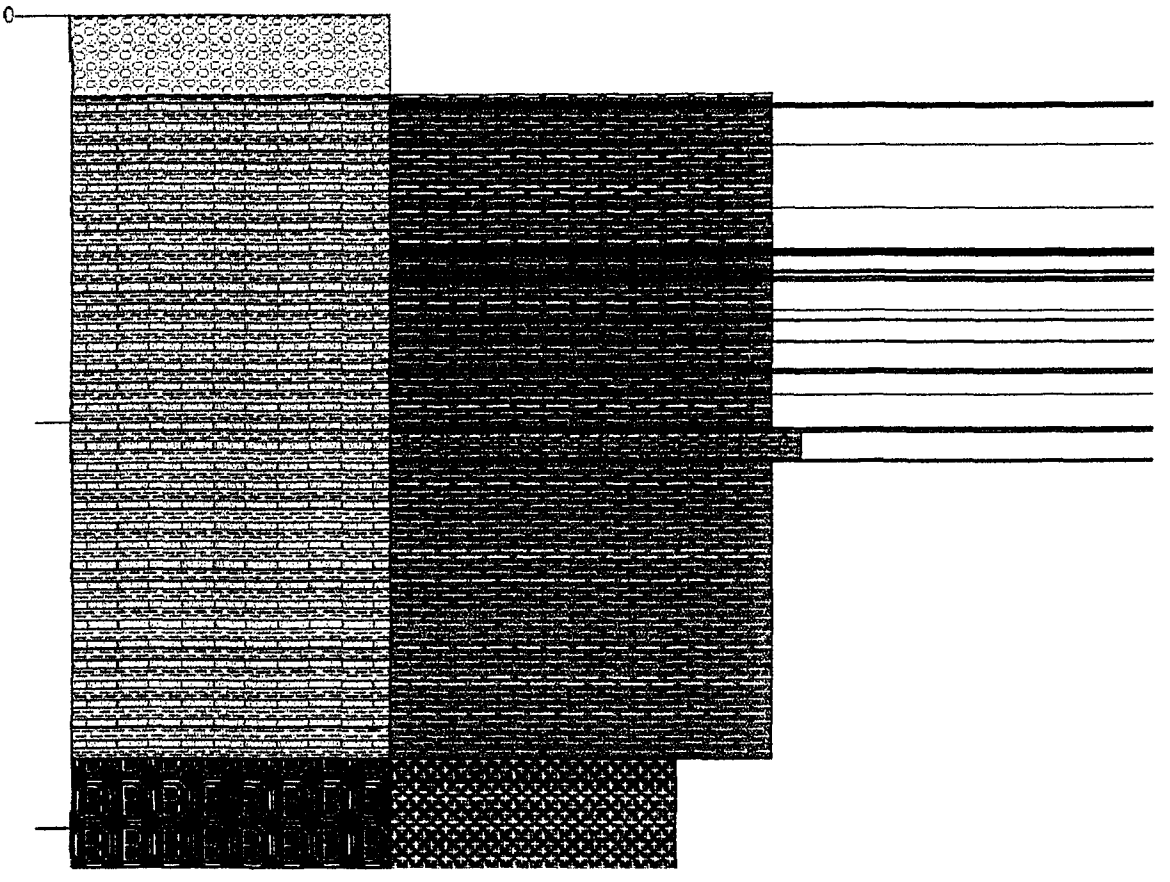

DO-82-4 377300 E, 5410010 N

Channel Island, Rossport Fm			
0.00	0.46	Shale	soil horizon
0.46	0.61	siltstone	
0.61	0.69	Shale	
0.69	0.70	siltstone	
0.70	0.88	Shale	
0.88	0.91	siltstone	
0.91	0.96	Shale	red
0.96	1.00	siltstone	buff
1.00	1.12	Shale	red
1.12	1.22	siltstone	buff
1.22	1.37		missing
1.37	1.38	Sandstone	
1.38	1.42	Shale	
1.42	1.50	Sandstone	
1.50	1.93	Shale	
1.93	1.94	Sandstone	
1.94	1.95	Shale	
1.95	1.97	Sandstone	
1.97	2.38	Shale	
2.38	2.39	Sandstone	
2.39	2.89	Shale	
2.89	2.92	Sandstone	
2.92	2.97	Shale	
2.97	2.99	Sandstone	
2.99	3.15	Shale	
3.15	3.16	Sandstone	
3.16	4.16	Shale	
4.16	4.18	Sandstone	
4.18	4.30	Shale	
4.30	4.32	Sandstone	
4.32	4.34	Shale	
4.34	4.36	Sandstone	
4.36	4.71	Shale	
4.71	4.73	Sandstone	
4.73	5.03	Shale	
5.03	5.15	Sandstone	matrix support
5.15	5.90	Shale	
5.90	5.92	Sandstone	
5.92	5.95	shale	
5.95	5.98	Sandstone	
5.98	6.74	Shale	
6.74	6.76	Sandstone	
6.76	7.19	Shale	
7.19	7.46	Sandstone	
7.46	13.61	Shale	reduction spots
13.61	13.71	Sandstone	
13.71	14.33	Shale	
14.33	14.43	Sandstone	
14.43	14.53	Shale	

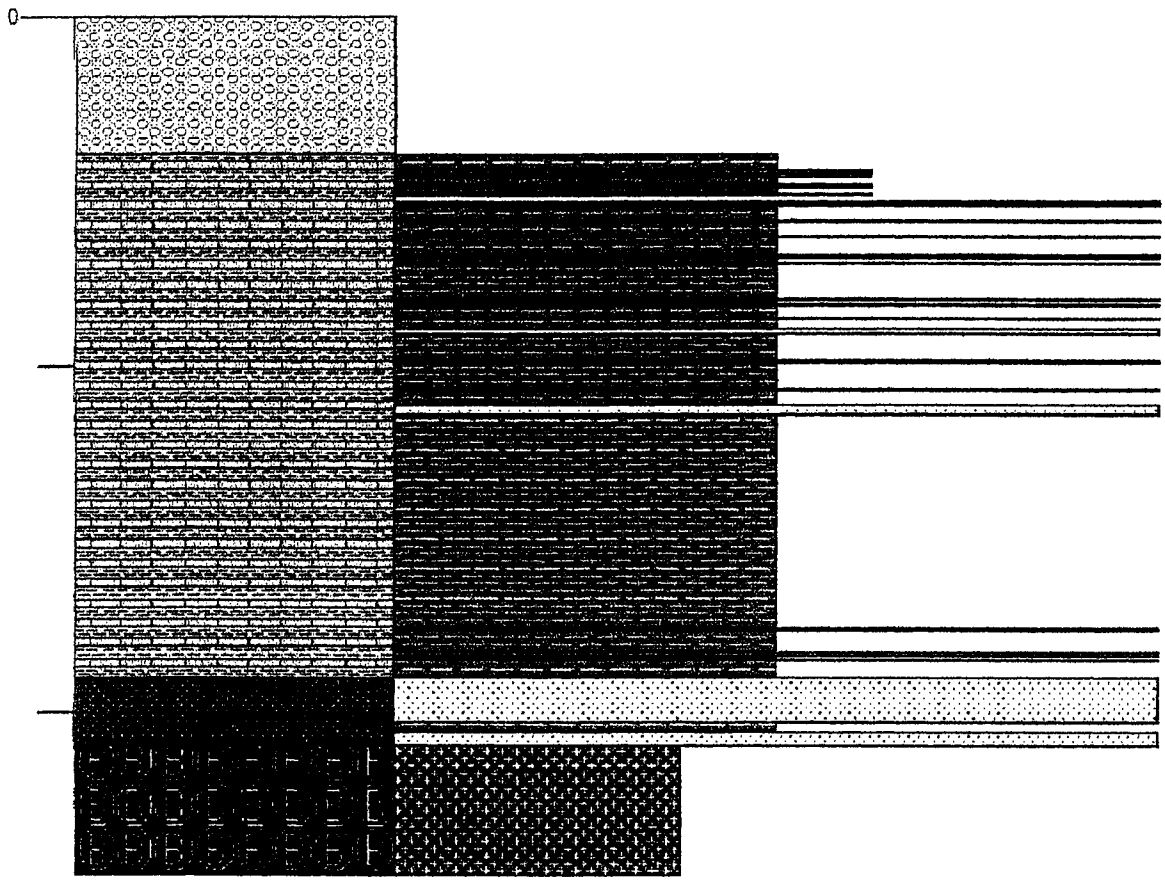

DO-82-5 377410 E, 5409890 N

Channel Island, Rossport Fm			
0.00	0.12	Shale	
0.12	0.14	dolomitic sandstone	msst size
0.14	0.15	Shale	
0.15	0.16	dolomitic sandstone	msst
0.16	1.29	Shale	
1.29	1.30	Sandstone	
1.30	2.51	Shale	
2.51	2.62	Sandstone	
2.62	3.27	Shale	
3.27	3.67	dolomitic sandstone	contains floating sand grains
3.67	4.63	Shale	
4.63	4.64	dolomitic sandstone	msst
4.64	4.65	Shale	
4.65	4.68	dolomitic sandstone	with msst
4.68	4.69	Shale	
4.69	4.70	dolomitic sandstone	with msst
4.70	6.00	Shale	
6.00	6.15	dolomitic sandstone	
Fork Bay Member, Pass Lake Fm			
6.15	6.47	Shale	
6.47	6.49	Sandstone	
6.49	7.79	Shale	reduction spots
7.79	7.94	Sandstone	
7.94	8.64	Shale	
8.64	8.79	Sandstone	
8.79	10.19	Shale	
10.19	11.94	Sandstone	buff
11.94	12.74	graded sandstone	grades to shale at top
12.74	13.02	graded sandstone	grades to silty sand
13.02	13.15	graded sandstone	grades to silty sand
13.15	15.45	graded sandstone	grades to silty sand
15.45	15.78	Conglomerate	grades up to shale
15.78	16.30		missing
16.30	17.80	pebbly sandstone	maroon with abundant clasts
17.80	18.12		missing
18.12	19.22	pebbly sandstone	maroon with clasts
19.22	19.64	Sandstone	buff
19.64	19.96	pebbly sandstone	maroon with clasts
19.96	20.53	Sandstone	buff
Loon Lake Member, Pass Lake Fm			
20.53	21.60	Conglomerate	
21.60	22.26		missing
22.26	22.37	Conglomerate	deep marron matrix, pink sst clasts
22.37	22.67	saprolite	
22.67	23.62		missing
23.62	26.18	saprolite	
26.18	29.25	basement	

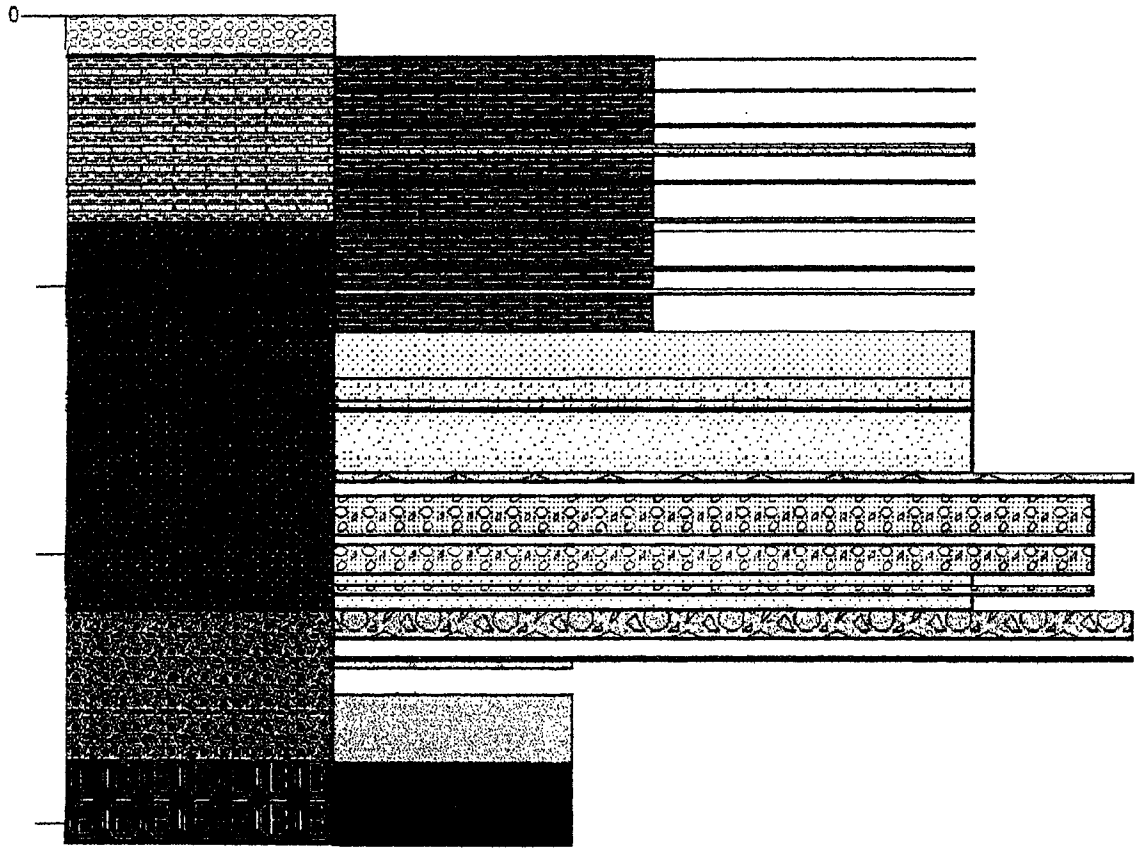

DO-82-6 377660 E, 5410100 N

Fire Hill Member, Rossport Fm			
0.00	0.44	Shale	red
0.44	0.45	Sandstone	
0.45	0.62	Shale	red
0.62	0.66	dolomitic mudstone	msst
0.66	0.81	Shale	
0.81	0.85	Sandstone	
0.85	1.01	Shale	red
1.01	1.02	Sandstone	
1.02	1.04	Shale	red
1.04	1.05	Sandstone	
1.05	1.55	Shale	red
1.55	1.56	Sandstone	
1.56	1.77	Shale	red
1.77	1.82	Sandstone	
1.82	2.03	Shale	red
2.03	2.08	Sandstone	
2.08	2.18	Silty Shale	
2.18	2.20	Sandstone	
2.20	2.98	Shale	massive reduction areas
2.98	3.01	Sandstone	
Channel Island Member, Rossport Fm			
3.01	3.92	Shale	
3.92	3.94	Sandstone	
3.94	4.72	Shale	
4.72	4.74	Sandstone	coarse clasts in matrix
4.74	4.76	Shale	
4.76	4.79	Sandstone	
4.79	6.46	Shale	
6.46	6.49	Sandstone	
6.49	6.68	Shale	
6.68	6.70	Sandstone	
6.70	7.53	Shale	
7.53	7.55	Sandstone	lots of black specks
7.55	9.75	Silty Shale	
9.75	9.76	Sandstone	coarse sand grains in finer matrix
9.76	12.81	Silty Shale	red, bottom 50 cm reduced, calcite veining
12.81	15.21	basement	

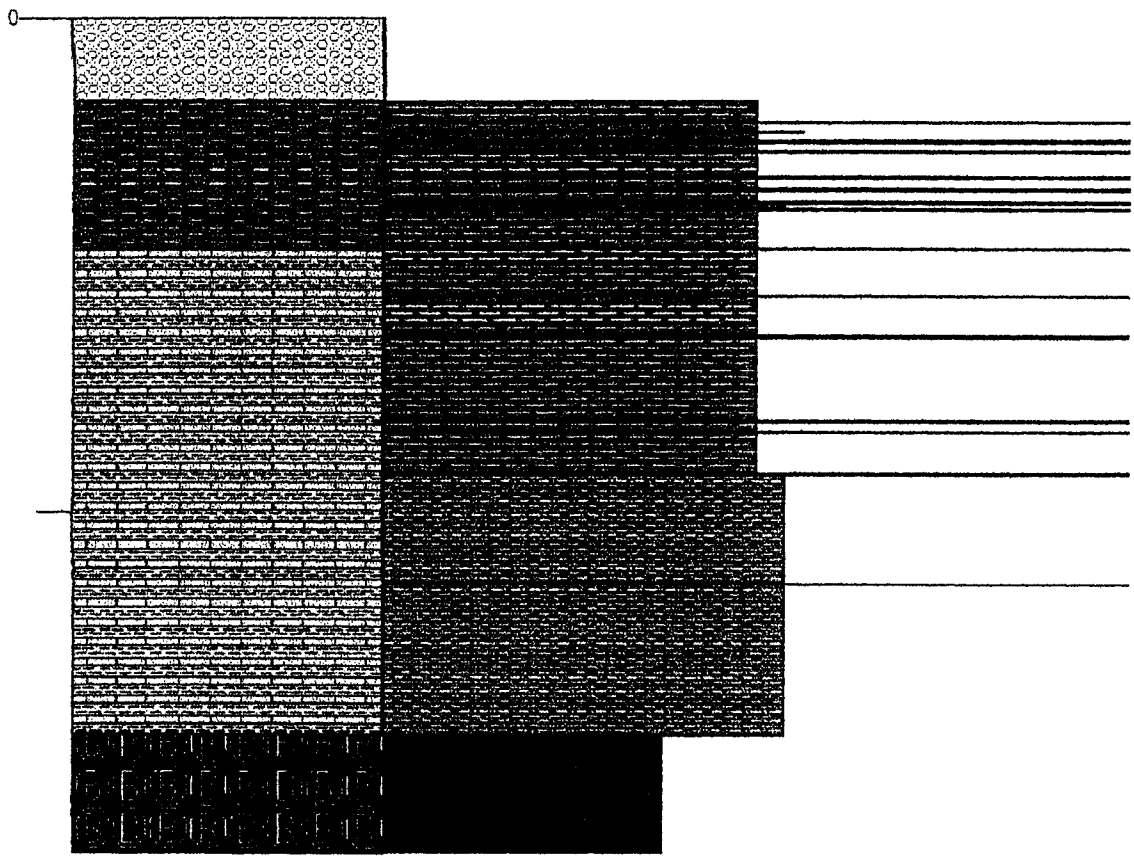

DO-82-7 378850 E, 5410870 N

Kama Hill Fm			
0.00	0.34	Shale	
0.34	0.37	Sandstone	
0.37	0.95	Shale	
0.95	0..97	Sandstone	
0.97	1.07	Shale	
1.07	1.09	Sandstone	
1.09	1.16	Shale	
1.16	1.23	Sandstone	
1.23	1.49	Shale	
1.49	1.50	Sandstone	
1.50	2.00	Shale	
2.00	2.05	Sandstone	
2.05	2.73	Shale	red
2.73	2.74	Sandstone	
2.74	2.78	Shale	red
2.78	2.80	Siltstone	buff
2.80	2.90	Shale	red
2.90	2.93	Sandstone	
2.93	3.68	Shale	red
3.68	3.71	Siltstone	buff
3.71	3.91	Shale	red
3.91	4.14	Siltstone	buff
4.14	4.19	Shale	red
4.19	4.25	Siltstone	buff
4.25	4.64	Shale	
4.64	4.70	Sandstone	
4.70	4.83	Shale	
4.83	4.90	Sandstone	
4.90	5.16	Shale	reduced horizons
5.16	5.21	Sandstone	
5.21	5.25	Shale	
5.25	5.35	Sandstone	
5.35	5.69	Shale	red
5.69	5.70	Sandstone	
5.70	5.71	Shale	
5.71	5.72	Sandstone	
5.72	6.85	Shale	
6.85	6.86	Sandstone	
6.86	7.53	Shale	
7.53	7.59	Sandstone	
7.59	7.71	Shale	
7.71	7.72	Sandstone	
7.72	7.73	Shale	
7.73	7.74	Sandstone	
7.74	7.88	Shale	
7.88	7.90	Sandstone	
7.90	7.97	Shale	
7.97	7.99	Sandstone	
7.99	8.04	Shale	

8.04	8.12	Sandstone	
8.12	8.41	Shale	
8.41	8.44	Sandstone	
8.44	9.66	Shale	
9.66	9.68	Sandstone	
9.68	10.23	Shale	red
10.23	10.24	Sandstone	
10.24	10.90	Shale	red
10.90	10.93	Sandstone	
10.93	10.96	Shale	red
10.96	11.05	Sandstone	
11.05	13.33	Shale	bottom 80 cm reduced, top red
13.33	20.83		missing
Fork Bay Member, Pass Lake Fm			
20.83	35.83	Sandstone	white to pink, some muddy areas
35.83	39.15	Sandstone	peach to white
Loon Lake Member, Pass Lake Fm			
39.15	39.43	conglomerate	maroon
39.43	39.55	Sandstone	buff
39.55	39.65	Conglomerate	maroon
39.65	39.80	Sandstone	red
39.80	40.36		missing
40.36	40.51	Sandstone	buff, medium to coarse with clasts
40.51	41.27		missing
41.27	43.09	Coarse Sandstone	with 1cm diameter clasts
43.09	44.17		missing
44.17	44.77	Conglomerate	
44.77	45.62		missing
45.62	46.27	Conglomerate	deep maroon matrix, mafic-granite-quartz clasts
46.27	46.62		missing
46.62	48.12	Granite	basement

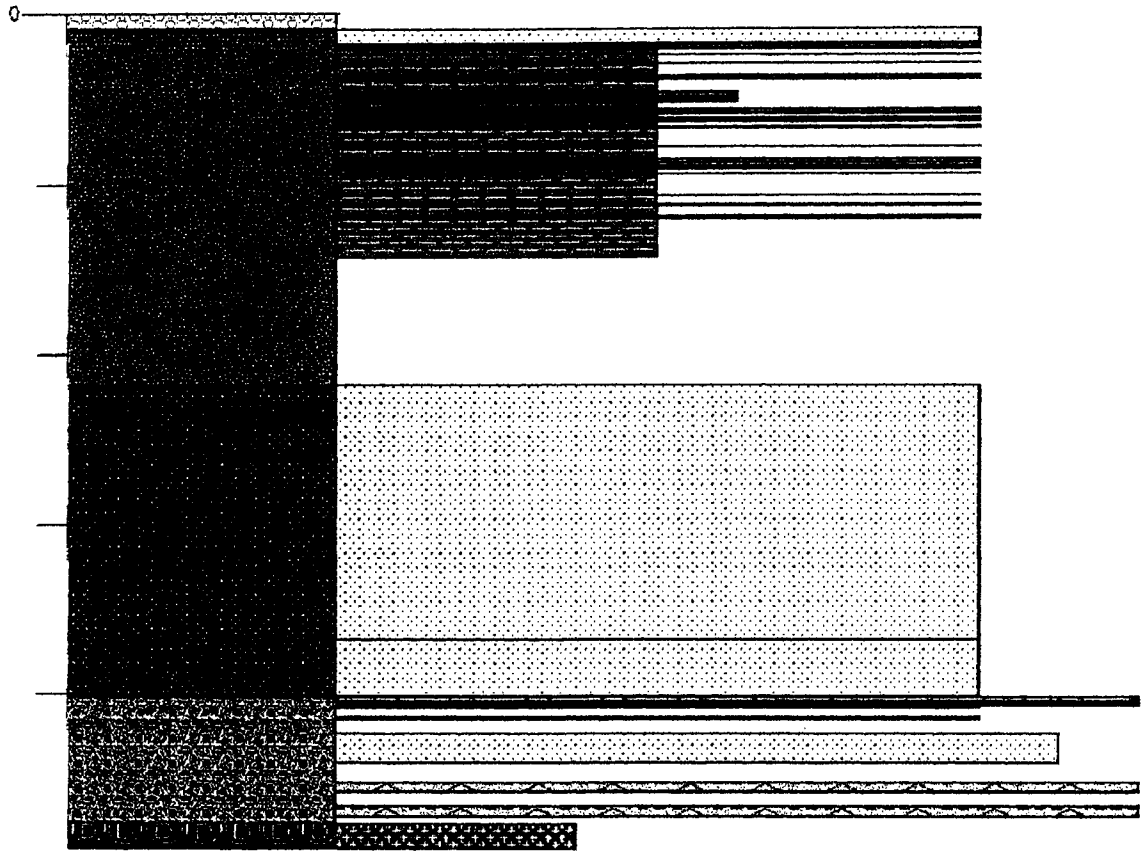

DO-82-8 377670 E, 5410030 N

Fire Hill Member, Rossport Fm			
0.00	0.67	Shale	
0.67	0.75	Sandstone	
0.75	2.80	Shale	
2.80	2.90	Sandstone	
2.90	3.94	Shale	
3.94	4.04	Siltstone	buff
4.04	4.44	Shale	
4.44	4.50	Sandstone	
4.50	4.70	Shale	
4.70	4.71	Sandstone	
4.71	5.18	Shale	
5.18	5.33	Siltstone	buff
5.33	5.60	Shale	
5.60	5.61	Sandstone	
5.61	5.77	Shale	
5.77	5.78	Sandstone	
5.78	7.11	Shale	
7.11	7.12	Sandstone	
7.12	7.14	Shale	
7.14	7.21	Siltstone	buff
7.21	8.09	Shale	
8.09	8.11	Sandstone	
8.11	8.17	Shale	
8.17	8.19	Sandstone	
8.19	8.60	Shale	
8.60	8.61	Sandstone	
8.61	8.94	Shale	
8.94	8.96	Sandstone	
8.96	9.44	Shale	
9.44	9.45	Sandstone	
9.45	9.50	Shale	
9.50	9.51	Sandstone	
9.51	9.75	Shale	
9.75	9.76	Sandstone	
9.76	10.99	Shale	
10.99	11.01	Sandstone	
11.01	11.49	Shale	
11.49	11.74	Sandstone	
11.74	13.86	Shale	
13.86	13.89	Sandstone	
13.89	17.73	Shale	red
Fork Bay Member, Pass Lake Fm			
17.73	17.83	Sandstone	
17.83	17.95	Mudstone	
17.95	18.18	Sandstone	
18.18	18.71	Mudstone	red
18.71	20.47	Sandstone	buff
20.47	20.94	Mudstone	
Loon Lake Member, Pass Lake Fm			

20.94	21.48	Conglomerate	
21.48	22.01	Granite	basement

DO-82-8

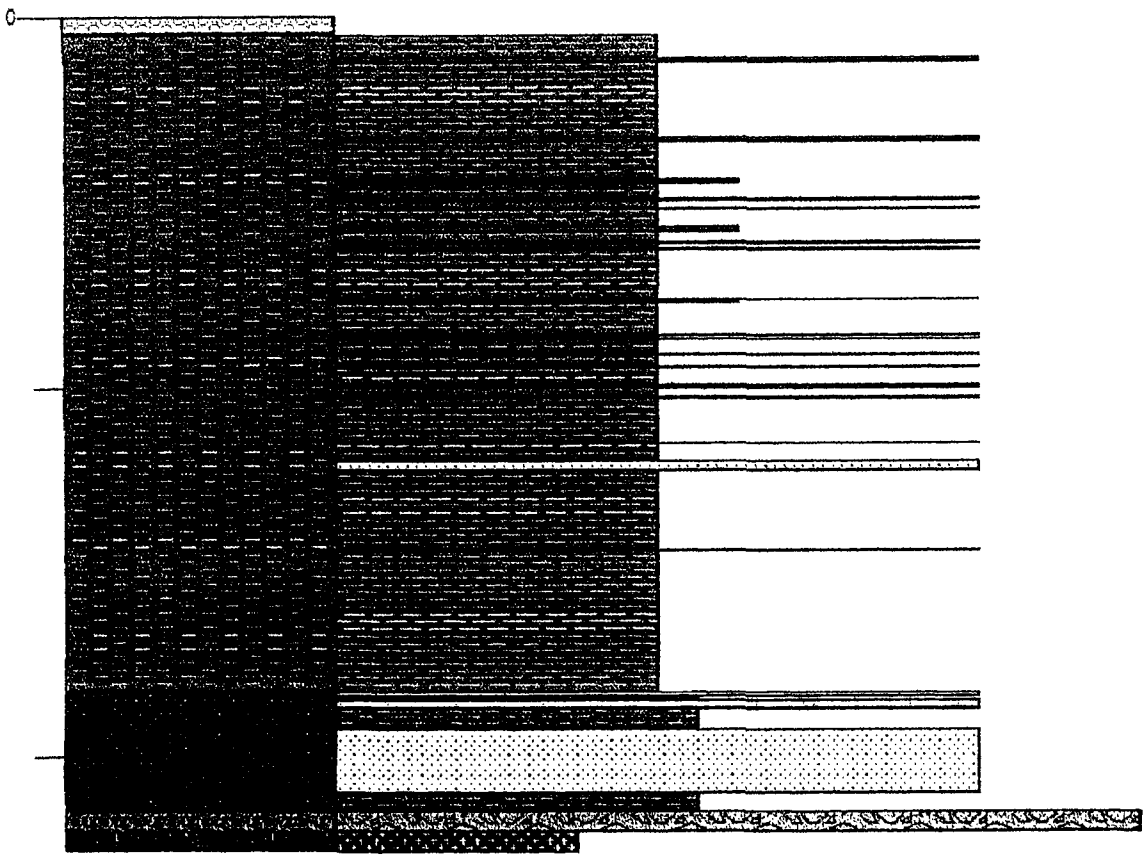

NI-92-5 356750 E, 5468310 N

Kama Hill Fm			
0.00	8.20	siltstone	greenish grey with salt casts
8.20	9.42	siltstone	pink, some clay-rich areas
9.42	9.45	mudstone	
9.45	9.70	siltstone	pink
9.70	9.71	mudstone	
9.71	9.81	siltstone	dark green, spotted
9.81	9.83	shale	
Fire Hill Member, Rossport Fm			
9.83	11.18	siltstone	pink
11.18	11.41	fine sandstone	mauve
11.41	11.58	siltstone	
11.58	11.65	mudstone	crumbly, buff
11.65	11.87	siltstone	coarsens to fsst
11.87	12.21	siltstone	coarsens up to sst
12.21	12.62	sandstone	parallel lam
12.62	13.09	shale	lam with silt
13.09	13.82	shale	mottled with hematite nodules (soil horizon)
13.82	14.22	siltstone	dark green, mudchip congl
14.22	14.75	mudchip conglomerate	fsst matrix
14.75	14.87	sandstone	oxidized at top
14.87	15.12	mudchip conglomerate	
15.12	15.28	siltstone	pink
15.28	15.58	siltstone	soil horizon, crumbles up
15.58	16.13	mudchip conglomerate	congl at base, fine lam up
16.13	16.14	mudstone	with gypsum
16.14	16.44	mudstone	fine lam
16.44	17.54	conglomerate	clast support
17.54	18.13	siltstone	swirly bedding @ top
18.13	18.90	mudstone	dark green mud
18.90	19.02	siltstone	heavily weathered
19.02	19.27	mudchip conglomerate	clast support, silt matrix, evap veins
19.27	19.43	mudchip conglmerate	matrix support, cm/mm-chips
19.43	19.66	mudchip conglomerate	matrix support, mm-chips
19.66	20.10	siltstone	soil horizon
20.10	20.74	conglomerate	blocky, evaporite vein fill
20.74	21.68	mudchip conglomerate	evao veubs, clast support
21.68	21.82	siltstone	contorted bedding
21.82	22.31	mudchip conglomerate	clast support, cm-scale
22.31	22.35	mudchip conglomerate	matrix support
22.35	22.47	mudchip conglomerate	matrix & clast support
22.47	22.70	sandstone	small mudchips, gypsum casts
22.70	22.71	dolomitic mudstone	
22.71	22.75	pebbly sandstone	matrix support, mudchips
22.75	22.80	mudstone	finely lam
22.80	22.87	pebbly sandstone	
22.87	23.07	mudstone	crumbly

23.07	23.30	mudchip conglomerate	mud matrix, cm-scale
23.30	23.52	mudchip conglomerate	sst matrix
23.52	23.80	pebbly sandstone	dolomitic
23.80	23.85	mudstone	red
23.85	24.07	mudchip conglomerate	swirly, mm-scale
24.07	24.18	mudstone	red
24.18	24.82	pebbly sandstone	sst matrix, carb
24.82	25.75	mudstone	red, purple, green
25.75	28.70	sandstone	hor lam
28.70	28.72	mudstone	purple
28.72	29.36	siltstone	
29.36	29.76	silstone	gypsum, soil horizon
29.76	30.09	siltstone	crumbly top
30.09	30.35	sandstone	red with reduc spots
30.35	30.55	mudstone	
30.55	31.10	sandstone	massive
31.10	31.39	sandstone	deeply weathered
31.39	31.41	mudstone	
31.41	31.63	sandstone	hor lam, reduc spots
Channel Island Member, Rossport Fm			
31.63	31.77	dolomitic mudstone	dark purple
31.77	32.27	sandstone	massive
32.27	32.32	siltstone	soil horizon
32.32	33.32	Dolomite	red to pink, sandy at top
Fork Bay Member, Pass Lake Fm			
33.32	34.07	sandstone	hor lam
34.07	34.13	silty sandstone	
34.13	34.14	mudstone	with gypsum
34.14	34.28	fine sandstone	
34.28	34.30	silty sandstone	gypsum layer
34.30	34.35	siltstone	red, hor lam, gypsiferous
34.35	34.40	silty sandstone	gypsiferous
34.40	34.47	sandstone	
34.47	34.55	sandstone	
34.55	34.62	sandstone	
34.62	34.72	sandstone	
34.72	34.82	sandstone	
34.82	34.92	sandstone	
34.92	35.03	sandstone	
35.03	35.11	silty sandstone	messy lam
35.11	35.72	siltstone	hor lam, shale-rich top
35.72	35.73	Gypsum	mush with carb
35.73	35.82	fine sandstone	
35.82	35.88	sandstone	
35.88	35.96	dolomite	
35.96	36.95	sandstone	hor lam
36.95	37.10	sandstone	mud top
37.10	37.17	mudstone	
37.17	38.04	sandstone	some x-strat, some hor lam
38.04	38.29	dolomite	

38.29	38.38	conglomerate	carb
38.38	38.72	sandstone	
38.72	38.74	fine sandstone	fines up to silt
38.74	38.79	siltstone	soil horizon
38.79	39.85	sandstone	
39.85	39.89	mudstone	
39.89	40.24	fine sandstone	mud wisps
40.24	40.28	mudstone	
40.28	40.38	sandstone	white
40.38	40.87	sandstone	red
40.87	40.92	siltstone	soil horizon
40.92	41.25	sandstone	
41.25	41.43	dolomite	
41.43	41.50	mudstone	some dolomite lam
41.50	41.75	sandstone	
41.75	41.76	mudstone	
41.76	41.77	sandstone	
41.77	41.78	mudstone	
41.78	41.79	sandstone	
41.79	41.80	mudstone	
41.80	42.13	sandstone	
42.13	42.15	mudstone	
42.15	42.38	sandstone	

NI-92-5

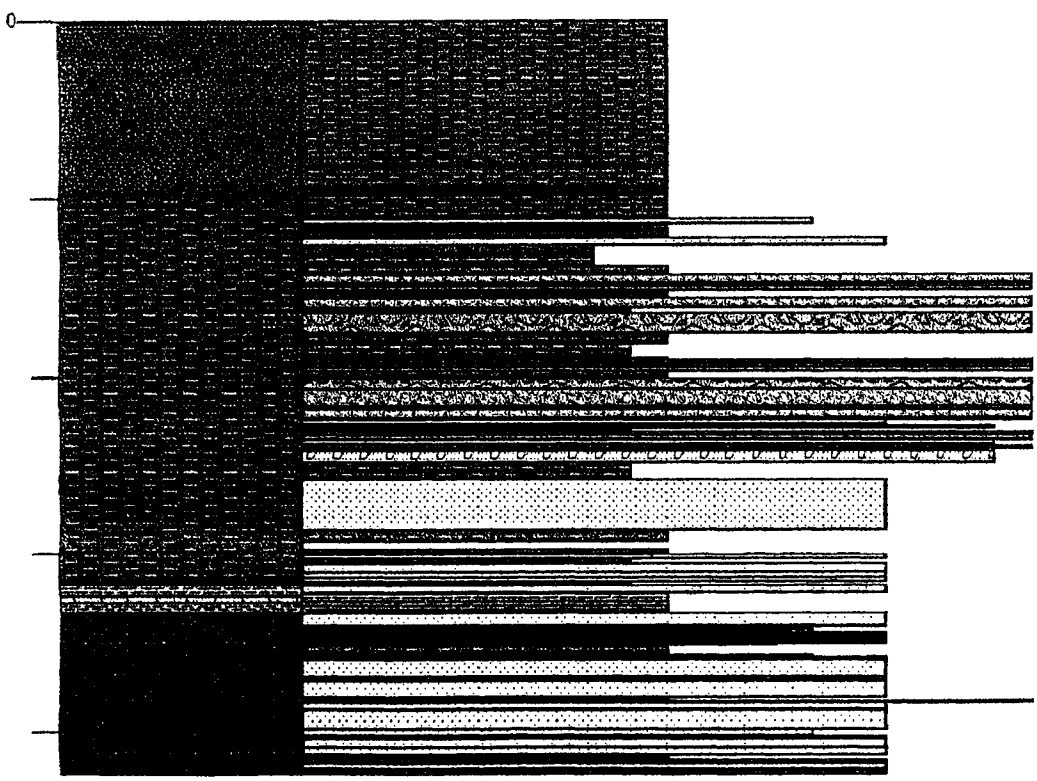

NI-92-7 353850 E, 5443000 N

Kama Hill Fm			
0.00	3.70	cross-stratified siltstone	wave x-strat
3.70	5.90	diabase	
5.90	16.90	cross-stratified siltstone	wave ripples
16.90	17.50	diabase	
Fire Hill Member, Rossport Fm			
17.50	26.00	cross-stratified siltstone	wave ripples
26.00	57.57	shale	some silty, fissile, reduc spots
57.57	61.45	shale	
61.45	62.78	diabase	
62.78	68.08	silty shale	fissile
68.08	68.19	dolomitic sandstone	erosive truncation
68.19	75.69	shale	small reduc spots, evap min
75.69	75.73	fine sandstone	evap min, draped beds
75.73	78.15	silty shale	fine lam
78.15	78.45	dolomitic mudstone	evap min near top
78.45	78.62	shaley siltstone	hor lam
78.62	78.72	dolomitic mudstone	
78.72	78.91	shale	hor lam
78.91	79.45	dolomitic mudstone	fissile at base, gypsum
79.45	79.71	dolomitic mudstone	abund evap min
79.71	79.89	dolomitic mudstone	organic rich
79.89	80.23	shale	fissile
80.23	80.31	dolomitic mudstone	massive
80.31	80.40	siltstone	fissile
Middiebrun Bay Member, Rossport Fm			
80.40	81.27	stromatolite	evap min, dolomitic
Channel Island Member, Rossport Fm			
81.27	81.28	dolomitic mudstone	B
81.28	81.40	shale	A
81.40	81.42	dolomitic mudstone	B
81.42	81.50	shale	A
81.50	81.51	dolomitic mudstone	B
81.51	81.58	shale	A
81.58	81.61	dolomitic mudstone	B
81.61	81.68	shale	A
81.68	81.69	dolomitic mudstone	B
81.69	81.87	shale	A
81.87	81.89	dolomitic mudstone	B
81.89	81.93	shale	A
81.93	82.01	dolomitic mudstone	B
82.01	82.05	shale	A
82.05	82.07	dolomitic mudstone	B
82.07	82.61	shale	A
82.61	82.64	dolomitic mudstone	B
82.64	82.85	shale	A
82.85	82.86	dolomitic mudstone	B
82.86	83.10	Shale	A

83.10	83.12	dolomitic mudstone	B
83.12	83.76	shale	A
83.76	83.79	dolomitic mudstone	B
83.79	84.00	shale	A
84.00	84.02	dolomitic mudstone	B
84.02	84.45	shale	A
84.45	84.49	dolomitic mudstone	B
84.49	84.85	shale	A
84.85	84.86	dolomitic mudstone	B
84.86	84.87	shale	A
84.87	84.88	dolomitic mudstone	B
84.88	85.66	shale	A
85.66	85.69	dolomitic mudstone	B
85.69	85.86	dolomitic mudstone	C
85.86	85.88	dolomitic mudstone	B
85.88	85.97	shale	A
85.97	85.98	dolomitic mudstone	B
85.98	86.74	shale	A
86.74	86.86	dolomitic mudstone	B
86.86	87.26	shale	A
87.26	87.30	dolomitic mudstone	B
87.30	87.44	shale	A
87.44	87.56	shale	A
87.56	87.58	dolomitic mudstone	B
87.58	87.89	shale	A
87.89	87.93	dolomitic mudstone	B
87.93	88.57	shale	A
88.57	88.60	dolomitic mudstone	B
88.60	88.67	shale	A
88.67	88.81	dolomitic mudstone	B
88.81	88.94	shale	A
88.94	89.21	dolomitic mudstone	B
89.21	89.38	shale	A
89.38	89.40	shale	A, surrounded by 2 5mm gyp veins
89.40	89.61	dolomitic mudstone	C
89.61	89.66	shale	A
89.66	89.68	shale	A
89.68	89.76	dolomitic mudstone	B, evap xlls
89.76	89.81	shale	A
89.81	89.84	dolomitic mudstone	B
89.84	89.93	shale	A
89.93	90.05	dolomitic mudstone	C
90.05	90.14	dolomitic mudstone	B, abundant gypsum veins
90.14	90.40	shale	A
90.40	90.66	dolomitic mudstone	B
90.66	90.90	shale	A
90.90	90.93	dolomitic mudstone	B
90.93	91.09	shale	A
91.09	91.10	dolomitic mudstone	B
91.10	91.23	dolomitic mudstone	C

91.23	91.44	dolomitic mudstone	B
91.44	91.57	shale	A
91.57	91.58	dolomitic mudstone	B
91.58	91.69	shale	A
91.69	91.84	dolomitic mudstone	B
91.84	91.91	dolomitic mudstone	C
91.91	92.13	dolomitic mudstone	
92.13	92.37	shale	
92.37	92.42	dolomitic mudstone	
92.42	92.58	shale	
92.58	92.59	dolomitic mudstone	
92.59	92.74	shale	
92.74	92.86	dolomitic mudstone	
92.86	92.96	shale	
92.96	93.07	dolomitic mudstone	
93.07	93.26	shale	
93.26	93.28	dolomitic mudstone	
93.28	93.33	shale	
93.33	93.65	dolomitic mudstone	
93.65	94.39	shale	finely lam
94.39	94.45	dolomitic mudstone	
94.45	94.54	shale	
94.54	94.66	shale	A
94.66	94.82	dolomitic mudstone	B
94.82	95.06	shale	A
95.06	95.20	dolomitic mudstone	B
95.20	95.30	dolomitic mudstone	C
95.30	95.42	dolomitic mudstone	B
95.42	95.60	shale	A
95.60	95.69	dolomitic mudstone	B
95.69	95.88	shale	A
95.88	96.06	dolomitic mudstone	B
96.06	96.29	shale	A
96.29	96.35	dolomitic mudstone	B
96.35	96.64	shale	A
96.64	96.84	dolomitic mudstone	B
96.84	97.10	dolomitic mudstone	C
97.10	97.25	dolomitic mudstone	B
97.25	97.38	shale	A
97.38	97.64	dolomitic mudstone	C
97.64	97.74	dolomitic mudstone	B
97.74	97.83	shale	A
97.83	97.93	dolomitic mudstone	B
97.93	98.00	shale	A
98.00	98.25	dolomitic mudstone	B
98.25	98.50	shale	A
98.50	98.64	dolomitic mudstone	B
98.64	98.84	dolomitic mudstone	C
98.84	99.03	shale	A
99.03	99.07	dolomitic mudstone	B

99.07	99.21	dolomitic mudstone	C
99.21	99.31	dolomitic mudstone	B
99.31	99.54	dolomitic mudstone	C
99.54	99.83	dolomitic mudstone	B
99.83	100.00	shale	A
100.00	100.05	dolomitic mudstone	B
100.05	100.34	shale	A
100.34	100.49	dolomitic mudstone	B
100.49	100.54	dolomitic mudstone	C
100.54	100.66	dolomitic mudstone	B
100.66	100.84	dolomitic mudstone	C
100.84	100.97	dolomitic mudstone	B
100.97	101.14	shale	A
101.14	101.19	dolomitic mudstone	B
101.19	101.27	dolomitic mudstone	C
101.27	101.36	dolomitic mudstone	B
101.36	101.39	shale	A
101.39	101.41	dolomitic mudstone	B
101.41	101.48	shale	A
101.48	101.52	dolomitic mudstone	B
101.52	101.56	shale	A
101.56	101.65	dolomitic mudstone	B
101.65	101.79	shale	A
101.79	101.94	dolomitic mudstone	C
101.94	102.04	shale	A
101.04	102.08	dolomitic mudstone	B
102.08	102.17	shale	A
102.17	102.20	dolomitic mudstone	B
102.20	102.24	Shale	A
102.24	102.27	dolomitic mudstone	B
102.27	102.51	dolomitic mudstone	C
102.51	102.77	shale	A
102.77	102.99	dolomitic mudstone	B
102.99	103.02	shale	A
103.02	103.55	dolomitic mudstone	B
103.55	103.68	shale	A
103.68	103.81	dolomitic mudstone	B
103.81	104.47	shale	A
104.47	104.64	dolomitic mudstone	B
104.64	104.79	shale	A
104.64	104.82	dolomitic mudstone	B
104.82	105.04	shale	A
105.04	105.08	dolomitic mudstone	B
105.04	105.13	shale	A
105.13	105.45	dolomitic mudstone	C
105.45	105.99	siltstone	red, some dolomite-rich bands
106.38	106.59	shale	reduc spots
106.59	106.62	dolomitic mudstone	
106.62	106.64	coarse sandstone	
106.64	107.94	shale	reduc spots

107.94	108.03	dolomitic mudstone	authigenic silica growth
108.03	108.06	dolomitic mudstone	mottled
108.06	108.07	shale	red
108.07	108.13	dolomitic mudstone	
108.13	108.15	coarse sandstone	
108.15	109.97	shaley siltstone	red, coarse dolomitic unit
109.97	110.04	dolomitic sandstone	csst
110.04	111.59	silty shale	well-lam, dolomitic, gypsum xlls
111.59	111.63	dolomitic mudstone	
111.63	111.64	coarse sandstone	
111.64	116.57	dolomitic mudstone	some csst bands
116.70	116.76	dolomitic mudstone	
116.76	117.29	shaley siltstone	red, coarser cycles
Fork Bay Member, Pass Lake Fm			
117.29	123.17	low-angle cross-stratified sandstone	low-angle x-strat, some shale partings
123.17	128.34	shale	some interbedded sst, shale inc up
128.34	133.10	horizontally laminated sandstone	wavy/hor lam, shale partings, oxidized zones
133.10	138.96	low-angle cross-stratified sandstone	hor lam, v. low angle x-strat, mudcracks
138.96	139.44	pebbly sandstone	oxidized up, some pebbles, carb cement
139.44	139.64	sandstone	
139.64	139.87	sandstone	
139.87	140.45	sandstone	
140.45	141.85	sandstone	
141.85	142.99	sandstone	
Loon Lake Member, Pass Lake Fm			
142.99	144.39	pebbly sandstone	mm-scale angular clasts
144.39	144.72	pebbly sandstone	reduced to red
144.72	145.06	siltstone	mm-scale pebbles
145.06	145.16	pebbly sandstone	pebbly, erosive base
145.16	145.31	siltstone	gradational with lower sst
145.31	145.37	pebbly sandstone	mm-scale pebbles
145.37	147.15	basement	mafic, chloritized, crumbling
147.15	151.15	gneiss	basement

CYP-96-01 432500 E, 5419940 N

Fire Hill Member, Rossport Fm			
0.00	1.95	Conglomerate	pebbly, sandy nodules, congl ball
1.95	2.07	sandstone	
2.07	2.18	shale	
2.18	2.36	sandy shale	
2.36	2.60	shale	
2.60	3.10	sandy shale	
3.10	3.40	sandstone	sand dike
3.40	4.77	shale	dolomite clasts near top
4.77	5.13	sandstone	
5.13	5.76	shale	patch fabric@ top
5.76	5.79	sandstone	reduced
5.79	6.61	sandstone	
6.61	6.66	mudstone	reduced
6.66	7.88	shale	
7.88	8.85	graded sandstone	fines to shale
8.85	9.59	shale	
9.59	9.74	sandstone	
9.74	9.90	shale	
9.90	10.28	sandstone	
10.28	10.92	shale	
10.92	12.39	sandstone	qtz-rich
12.39	12.76	shaley sandstone	
12.76	13.50	reverse graded sandstone	massive shale at base
13.50	13.70	cross-stratified sandstone	sm-sc x-trough strat, silty
13.70	13.85	shale	
13.85	14.09	shale	some sst
14.09	14.39	shaley sandstone	
14.39	14.40	mudstone	reduced
14.40	14.80	shale	some sand
14.80	16.13	shaley sandstone	some dolomite clasts
16.13	16.63	shale	A
16.63	16.66	dolomitic mudstone	B
16.66	16.86	shale	A
16.86	16.97	interlaminated shale and dolomite	D
16.97	17.01	shale	A
17.01	17.06	dolomitic mudstone	B
17.06	17.07	shale	A
17.07	17.09	dolomitic mudstone	B
17.09	17.10	shale	A
17.10	17.12	dolomitic mudstone	B
17.12	17.52	shale	A with some B clasts
17.52	17.63	dolomitic mudstone	B
17.63	17.85	shale	A soil horizon
17.85	18.01	shale	A popcorn structure
18.01	18.07	shale	A
18.07	18.16	shale	A popcorn structure
18.16	18.40	shale	A soil horizon
18.40	18.49	dolomitic mudstone	C
18.49	18.58	shale	A

18.58	18.66	dolomitic mudstone	B
18.66	19.00	interlaminated shale and dolomite	D
19.00	19.07	shale	A
19.07	19.34	interlaminated shale and dolomite	D
19.34	19.40	shale	A
19.40	19.63	interlaminated shale and dolomite	D
19.63	19.95	shale	A
19.95	20.07	dolomitic mudstone	B
20.07	20.27	interlaminated shale and dolomite	D
20.27	20.42	dolomitic mudstone	B
20.42	20.77	conglomerate	
20.77	20.91	dolomitic mudstone	B
20.91	21.09	shale	A
21.09	21.79	conglomerate	
21.79	21.83	dolomitic mudstone	B
21.83	22.09	shale	A
22.09	22.18	interlaminated shale and dolomite	D
22.18	22.26	dolomitic mudstone	B
22.26	22.27	shale	A
22.27	22.32	dolomitic mudstone	B
22.32	22.35	shale	A
22.35	22.54	dolomitic mudstone	B
22.54	22.55	shale	A
22.55	22.60	dolomitic mudstone	B
22.60	22.63	shale	A
22.63	22.69	dolomitic mudstone	B
22.69	22.86	dolomitic mudstone	
22.86	22.87	dolomitic mudstone	
22.87	23.05	shale	
23.05	23.08	sandstone	
23.08	23.57	shale	
23.57	24.49	shale	diagenetic min growth
24.49	24.58	sandstone	
24.58	24.92	shale	
24.92	24.99	mudstone	lam, reduced, "pond"
24.99	25.03	sandstone	
25.03	26.83	shale	floating sand granules
26.83	27.00	fine sandstone	calcite veins
27.00	27.76	shale	dolomite inc up, inc friability
27.76	27.77	dolomitic sandstone	pebbly
27.77	28.20	dolomitic mudstone	C
28.20	28.29	shale	A
28.29	28.31	dolomitic sandstone	
28.31	28.50	dolomitic mudstone	C
28.50	28.62	shale	A with some C
28.62	28.66	sandstone	
Channel Island Member, Rossport Fm			
28.66	28.77	shale	A
28.77	28.80	dolomitic mudstone	B
28.80	29.27	shale	
29.27	29.64	shale	friable
29.64	30.64	dolomitic mudstone	

30.64	31.34	sandstone	patch fabric
31.34	31.46	interlaminated shale and dolomite	D
31.46	31.61	dolomitic mudstone	B
31.61	31.70	dolomitic mudstone	C
31.70	31.97	dolomitic sandstone	B sandy
31.97	32.04	shale	A
32.04	32.11	dolomitic mudstone	B
32.11	32.23	shale	A
32.23	32.31	dolomitic mudstone	B
32.31	32.52	shale	A
32.52	32.63	dolomitic mudstone	B
32.63	32.64	shale	A
32.64	32.66	dolomitic mudstone	B
32.66	32.91	shale	A
32.91	33.00	dolomitic mudstone	B
33.00	33.22	interlaminated shale and dolomite	D
33.22	33.25	dolomitic mudstone	B
33.25	33.57	shale	A
33.57	33.59	dolomitic mudstone	B
33.59	33.79	interlaminated shale and dolomite	D
33.79	33.82	sandstone	
33.82	34.16	dolomitic mudstone	
34.16	34.17	sandstone	
34.17	34.65	dolomitic mudstone	C
34.65	34.83	shale	A
34.83	34.89	dolomitic mudstone	B
34.89	34.97	dolomitic mudstone	C
34.97	35.17	dolomitic mudstone	B
35.17	35.35	interlaminated shale and dolomite	D
35.35	35.37	dolomitic mudstone	granular
35.37	35.38	dolomitic mudstone	B
35.38	35.41	pebbly sandstone	pebbly, coarsest at top
35.41	35.61	dolomitic mudstone	B
35.61	35.82	dolomitic mudstone	C
35.82	35.92	shale	A
35.92	35.97	dolomitic mudstone	B
35.97	36.06	interlaminated shale and dolomite	D
36.06	36.14	dolomitic mudstone	B
36.14	36.36	interlaminated shale and dolomite	D
36.36	36.38	dolomitic mudstone	B
36.38	36.45	dolomitic mudstone	C
36.45	36.51	shale	A
36.51	36.75	interlaminated shale and dolomite	D
36.51	36.82	dolomitic mudstone	B
36.82	37.02	interlaminated shale and dolomite	D with more dolomite
37.02	37.19	dolomitic mudstone	B
37.19	37.29	dolomitic mudstone	C
37.29	37.50	dolomitic mudstone	B
37.50	37.65	interlaminated shale and dolomite	D
37.65	38.06	dolomitic mudstone	B
38.06	38.35	interlaminated shale and dolomite	D
38.35	38.45	dolomitic mudstone	C

38.45	38.47	dolomitic mudstone	B
38.47	38.61	dolomitic mudstone	C
38.61	38.70	shale	A
38.70	39.01	interlaminated shale and dolomite	C & D
39.01	39.10	shale	A
39.10	39.20	dolomitic mudstone	B
39.20	39.55	interlaminated shale and dolomite	D
39.55	39.61	pebbly sandstone	
39.61	39.66	dolomitic mudstone	C
39.66	39.77	sandstone	
39.77	40.15	dolomitic mudstone	C
40.15	40.42	interlaminated shale and dolomite	D
40.42	40.51	dolomitic mudstone	B
40.51	40.84	interlaminated shale and dolomite	D
40.84	40.92	dolomitic mudstone	B
40.92	41.04	dolomitic mudstone	C
41.04	41.23	interlaminated shale and dolomite	D
41.23	41.31	dolomitic mudstone	C
41.31	41.44	shale	A really baked
41.44	41.49	dolomitic mudstone	B
41.49	41.51	interlaminated shale and dolomite	D
41.51	41.53	shale	A
41.53	41.71	interlaminated shale and dolomite	D
41.71	41.77	shale	A
41.77	41.84	interlaminated shale and dolomite	D
41.84	41.87	dolomitic mudstone	B
41.87	42.02	dolomitic mudstone	C
42.02	42.17	shale	A
42.17	42.36	interlaminated shale and dolomite	D
42.36	42.52	shale	A
42.52	42.76	dolomitic mudstone	B
42.76	42.82	shale	A
42.76	42.86	dolomitic mudstone	B
42.86	43.01	interlaminated shale and dolomite	D
43.01	43.21	dolomitic mudstone	C
43.21	43.37	shale	A
43.37	43.50	dolomitic mudstone	B
43.50	43.55	shale	A
43.55	43.57	dolomitic mudstone	B
43.57	43.66	shale	A
43.66	43.77	dolomitic mudstone	B
43.77	43.89	interlaminated shale and dolomite	D
43.89	43.97	shale	A
43.97	43.99	dolomitic mudstone	B
43.97	44.04	shale	A
44.04	44.09	dolomitic mudstone	B
44.09	44.21	dolomitic mudstone	C
44.21	44.39	interlaminated shale and dolomite	D
44.39	44.52	dolomitic mudstone	B
44.52	44.58	shale	A
44.58	44.78	dolomitic mudstone	B
44.78	44.87	interlaminated shale and dolomite	D

44.87	44.93	dolomitic mudstone	B
44.93	45.02	shale	A
45.02	45.10	dolomitic mudstone	C
45.10	45.15	shale	A
45.15	45.31	dolomitic mudstone	B
45.31	45.48	shale	A
45.48	45.85	interlaminated shale and dolomite	D
45.85	45.96	shale	A
45.96	45.98	dolomitic mudstone	C
45.98	46.03	dolomitic mudstone	B
46.03	46.10	dolomitic mudstone	C
46.10	46.21	shale	A
46.21	46.31	dolomitic mudstone	C
46.31	46.40	shale	A
46.40	46.46	dolomitic mudstone	B
46.46	46.66	interlaminated shale and dolomite	D
46.66	46.72	shale	A
46.72	46.75	dolomitic mudstone	B
46.75	46.82	shale	A
46.82	47.04	dolomitic mudstone	B
47.04	47.09	shale	A
47.09	47.29	dolomitic mudstone	B
47.29	47.49	interlaminated shale and dolomite	D with popcorn structure
47.49	47.55	dolomitic mudstone	C
47.55	47.58	shale	A
47.58	47.62	dolomitic mudstone	C
47.62	47.65	shale	A
47.65	47.75	dolomitic mudstone	B
47.75	49.07	shale	some sand horizons
Fork Bay Member, Pass Lake Fm			
49.07	49.29	pebbly sandstone	shaley
49.29	49.31	sandstone	
49.31	49.34	shale	
49.34	49.39	sandstone	
49.39	49.51	shale	
49.51	49.71	sandstone	
49.71	51.50	reverse graded sandstone	dolomitic, sandier upwards
51.50	51.60	sandstone	
51.60	52.44	shale	some lam
52.44	52.50	sandstone	
52.50	52.72	shale	
52.72	52.78	sandstone	
52.78	53.48	shale	slight effervescence
53.48	53.57	sandstone	
53.57	54.05	shale	
54.05	54.14	sandstone	
54.14	54.46	shale	few sand lam @ base
54.46	54.50	sandstone	
54.50	54.67	shale	few sand lam @ base
54.67	54.70	sandstone	
54.70	55.28	shale	many sand lam @ base
55.28	55.47	sandstone	

55.47	55.75	shale	
55.75	55.79	sandstone	
55.79	55.99	shale	
55.99	56.03	sandstone	
56.03	56.16	shale	
56.16	56.17	sandstone	
56.17	56.19	shale	
56.19	56.20	sandstone	
56.20	56.22	shale	
56.22	56.23	sandstone	
56.23	56.92	shale	pebbles near base
56.92	57.09	sandstone	
57.09	57.23	shale	
57.23	57.60	pebbly sandstone	mudchips, mafics, granite
57.60	58.02	shale	
58.02	58.37	pebbly sandstone	pebbly horizons
58.37	58.57	shale	fissile, gyp veins
58.57	58.67	pebbly sandstone	
58.67	58.79	shale	crumbly
58.79	58.91	pebbly sandstone	lg pebbles up to 6 cm
58.91	59.04	granite	

CYP-96-01

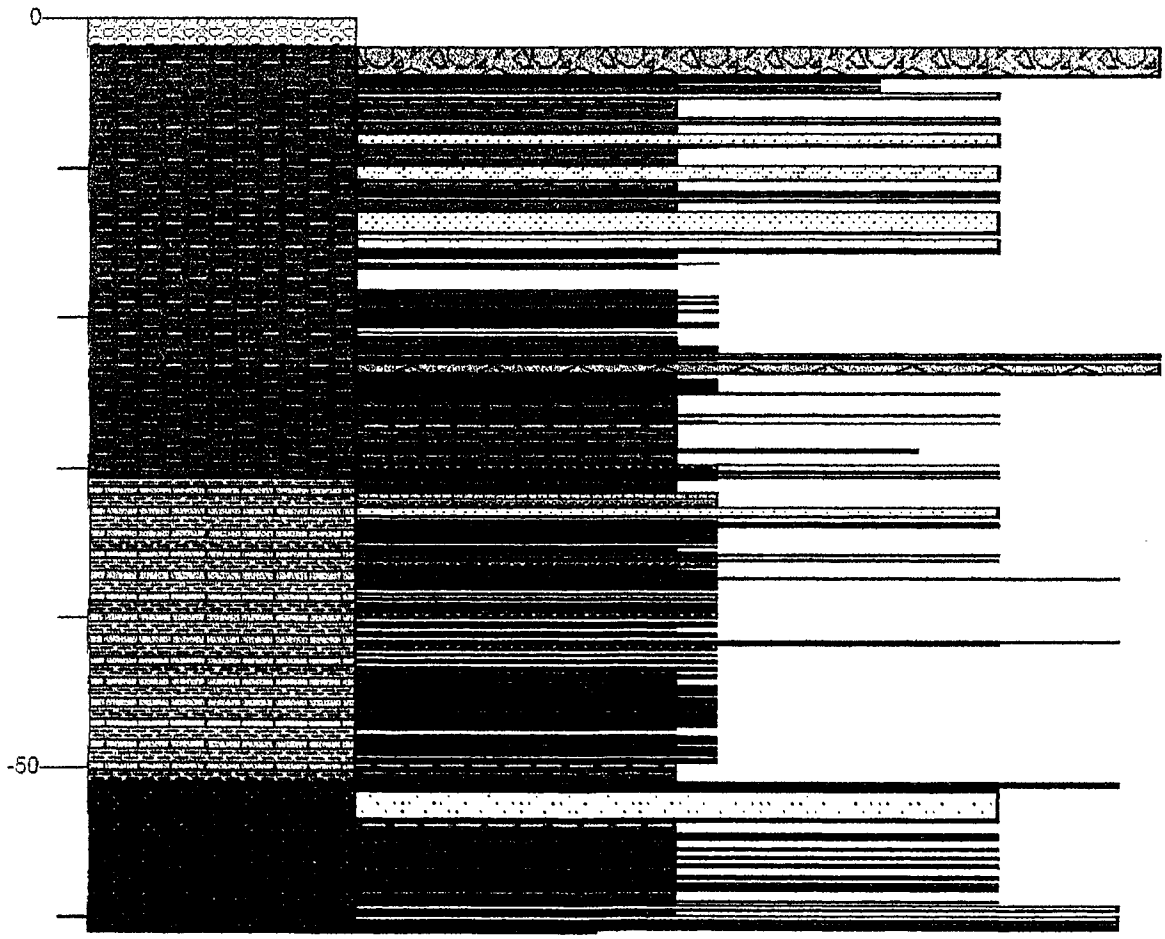

NB-97-2 426990 E, 5416241 N

Hele Member, Outan Island Fm			
0.00	4.50	sandy siltstone	heavily weathered
4.50	18.44	laminated shale	[floodplain pond]
18.44	60.14	mudstone	[floodplain]
60.14	68.14	cross-stratified sandstone	[channel sand]
68.14	68.99	conglomerate	sand matrix, fines up
68.99	75.09	cross-stratified sandstone	[channel sand]
75.09	85.39	laminated shale	[floodplain]
85.39	86.57	sandstone	[crevasse splay]
86.57	93.57	mudstone	[floodplain]
93.57	94.91	sandstone	[crevasse splay]
94.91	95.87	mudstone	[floodplain]
95.87	134.51	cross-stratified sandstone	[channel sand]
134.51	139.43	diabase	
139.43	144.68	laminated siltstone	some sandy ripples, [floodplain pond]
144.68	168.68	cross-stratified sandstone	current rip, [channel sands], fine up (m-fsst)
168.68	173.08	cross-stratified siltstone	shaley up, current rip, rip-up clasts, contorted top
173.08	223.33	mudcracked siltstone	mudchips, patch fabric, red [floodplain]
223.33	224.74	graded sandstone	some clay layers, fine up [ephemeral fluvial]
224.74	227.98	reverse graded sandstone	some mud lam, beds thicken up
227.98	228.84	cross-stratified sandstone	wavy shale, current rip, mudcracks
228.84	229.42	low-angle cross-stratified sandstone	mudchips throughout
229.42	230.42	reverse graded sandstone	fine to med, some shale lam, tiny mudchips
230.42	235.06	silty sandstone	shale interbeds, tiny mudchips, regular shale lam
235.06	235.98	sandstone	fine shale lam @base, mudchip congl @ top
235.98	236.74	mudchip conglomerate	[bank collapse], fist-sized pieces
236.74	239.28	low-angle cross-stratified sandstone	gyp veins
239.28	239.35	Conglomerate	csst matrix
239.35	240.82	sandstone	massive, sparse mudchips
240.82	241.71	mudchip conglomerate	some mudchip conl, wavy & low angle x-strat layers
241.71	241.89	reverse graded sandstone	coarsens upward
241.89	242.13	mudchip conglomerate	vcsst matrix, mostly angular mudchips
242.13	242.55	interbedded mudstone and siltstone	loading, soln collapse, fissile shale @ top
242.55	242.85	cross-stratified sandstone	fine mudchip congl layers x-strat
242.85	243.72	low-angle cross-stratified sandstone	sand patch @ base, low angle x-lam mud @ top
243.72	244.12	low-angle cross-stratified sandstone	
244.12	245.29	low-angle cross-stratified sandstone	patch fabric, mudchips, current rip in fs
245.29	245.55	low-angle cross-stratified sandstone	current ripples, some massive
245.55	245.82	cross-stratified sandstone	sand patch fabric, current x-lam
245.82	246.21	cross-stratified sandstone	m/f-grained, low and x-strat @ base & top, opp dir
246.21	246.26	shale	some sand interbed @base
246.26	246.81	sandstone	f/m-grained
246.81	248.51	shale	area of x-lam sand, sand patches
248.51	249.73	sandstone	poorly sorted, mud wisps&partings
249.73	318.73	shale	interbed w rip silty sand (wave), more rip up
318.73	320.54	cross-stratified sandstone	wave, silty
320.54	321.84	shale	interbedded w rip silty sandst
321.84	322.18	cross-stratified sandstone	wave, silty
322.18	325.01	shale	
325.01	325.21	cross-stratified siltstone	current

325.21	328.65	shale	
328.65	329.65	cross-stratified sandstone	dunes
329.65	330.15	cross-stratified sandstone	vc @ top, x-strat, rip-up clasts
Lyon Member, Outan Island Fm			
330.15	330.91	shale	
330.91	331.39	cross-stratified sandstone	
331.39	338.56	contorted mudstone	
338.56	338.67	sandstone	
338.67	343.71	shale	
343.71	343.81	sandstone	
343.81	351.90	shale	odd evap min
Kama Hill Fm			
351.90	352.10	cross-stratified sandstone	current ripple
352.10	354.40	shale	
354.40	354.43	cross-stratified sandstone	current ripple
354.43	355.24	shale	
355.24	355.36	cross-stratified sandstone	current ripple
355.36	357.06	shale	
357.06	357.28	laminated siltstone	broken up [drying out]
357.28	358.22	silty shale	
358.22	358.82	laminated siltstone	broken up [drying out]
358.82	359.79	shale	
359.79	360.12	sandstone	
Fire Hill Member, Rossport Fm			
360.12	368.91	silty shale	some shale horizons
368.91	369.29	sandstone	some x-strat, shaley hor
369.29	381.11	graded sandstone	silty @ base, fines up
381.11	381.41	sandy siltstone	blotchy
381.41	382.38	silty shale	some contortions near top
382.38	382.68	silty sandstone	load pillows w contorted shale layers
382.68	383.17	silty shale	
383.17	383.85	sandstone	
383.85	384.52	silty shale	
384.52	384.79	sandstone	
384.79	385.59	silty shale	diagenetic min growth
385.59	385.75	shale	gyp veins
385.75	385.76	dolomitic mudstone	
385.76	385.86	shale	purply red
385.86	385.87	dolomitic mudstone	
385.87	385.89	sandstone	
385.89	386.37	silty shale	
386.37	386.61	shale	diagenetic min growth
386.61	390.64	silty shale	
390.64	390.68	sandstone	
390.68	390.73	shale	
390.73	392.07	silty shale	diagenetic min growth
392.07	392.10	shale	
392.10	392.42	silty shale	
392.42	392.43	shale	
392.43	393.69	siltstone	diagenetic min growth
393.69	393.76	shale	
393.76	394.07	siltstone	

394.07	394.13	shale	
394.13	394.51	siltstone	
394.51	394.64	mudchip conglomerate	silty
394.64	394.86	siltstone	
394.86	394.91	shale	
394.91	395.08	siltstone	peachy with shale lam
395.08	395.10	shale	
395.10	395.25	siltstone	
395.25	395.63	mudchip conglomerate	dolomitic
395.63	395.77	dolomite	[solid]
395.77	395.79	shale	
395.79	395.93	mudchip conglomerate	dolomitic
Channel Island Member, Rossport Fm			
395.93	396.26	shale	
396.26	396.31	dolomitic mudstone	
396.31	396.53	shale	
396.53	396.67	dolomitic mudstone	
396.67	396.79	shale	
396.79	397.09	dolomitic mudstone	
397.09	397.17	shale	
397.17	397.22	mudstone	dolomitic, fine lam
397.22	397.41	mudchip conglomerate	
397.41	397.48	shale	
397.48	397.62	mudchip conglomerate	some clasts laminated
397.62	397.70	silty shale	
397.70	399.30	shale	some dolomite layers, evap min, crumbly
399.30	399.53	dolomitic sandstone	some loading
399.53	400.85	siltstone	
400.85	401.30	sandstone	
401.30	401.60	sandstone	loaded into mud
401.60	402.50	siltstone	
402.50	402.74	sandstone	
402.74	403.74	siltstone	
403.74	404.04	sandstone	loaded at base
404.04	408.84	shaley siltstone	
408.84	406.09	sandstone	some silty layers
406.09	407.13	sandy siltstone	some shalier beds
407.13	407.38	sandstone	
407.38	407.94	sandy siltstone	
407.94	408.61	sandstone	
408.61	408.89	sandy siltstone	
408.89	409.01	sandstone	
409.01	409.93	sandy siltstone	loading
409.93	410.38	sandstone	
410.38	411.16	siltstone	some loaded sandstone
411.16	411.56	sandstone	
411.56	412.64	siltstone	floating cs granules
412.64	413.55	sandstone	
413.55	413.56	shale	parting
413.56	413.88	sandstone	massive, some hor layers
413.88	414.96	mudstone	pillows loaded into mudstone
414.96	415.25	sandstone	

415.25	415.29	sandstone	microfault
415.29	415.59	dolomitic sandstone	
415.59	417.47	sandy siltstone	red, brecciation zone
417.47	417.50	dolomitic sandstone	B
417.50	417.61	dolomitic mudstone	C
417.61	417.71	shale	A
417.71	417.91	dolomitic mudstone	C
417.91	417.96	shale	B broken up in A
417.96	418.15	shale	A
418.15	418.19	shale	B broken up in A
418.19	418.35	mudchip conglomerate	some B clasts
418.35	418.58	shale	A
418.58	418.81	mudchip conglomerate	some B clasts
418.81	418.89	dolomitic sandstone	B
418.89	419.01	shale	A
419.01	419.07	dolomitic sandstone	B
419.07	419.19	shale	A
419.19	419.27	dolomitic mudstone	C
419.27	419.35	shale	A
419.35	419.39	erbedded dolomitic sandstone and sha	C
419.39	419.41	dolomitic sandstone	B
419.41	419.47	shale	A
419.47	419.57	dolomitic sandstone	B
419.57	420.02	dolomitic mudstone	C
420.02	420.03	dolomitic sandstone	B
420.03	420.11	shale	A
420.11	420.12	dolomitic sandstone	B
420.12	420.13	shale	A
420.13	420.14	dolomitic sandstone	B
420.14	420.24	shale	A
420.24	420.25	dolomitic sandstone	B
420.25	420.35	dolomitic mudstone	C
420.35	420.65	shale	A
420.65	421.03	dolomitic mudstone	C
421.03	421.11	dolomitic sandstone	B
421.11	421.19	shale	A
421.19	421.20	dolomitic sandstone	B
421.20	421.21	shale	A
421.21	421.23	dolomitic sandstone	B
421.23	421.25	dolomitic mudstone	C
421.25	421.26	dolomitic sandstone	B
421.26	421.43	shale	A
421.43	421.47	dolomitic mudstone	C
421.47	421.52	dolomitic sandstone	B
421.52	421.60	shale	A
421.60	421.64	dolomitic sandstone	B
421.64	421.66	shale	A
421.66	421.81	dolomitic sandstone	B
421.81	422.03	shale	A
422.03	422.16	dolomitic sandstone	B
422.16	422.30	shale	A
422.30	422.31	dolomitic sandstone	B

422.31	422.40	shale	A
422.40	422.41	gypsum	vein
422.41	422.44	dolomitic mudstone	C
422.44	422.46	dolomitic sandstone	B
422.46	422.47	shale	A
422.47	422.48	dolomitic sandstone	B
422.48	422.50	shale	A
422.50	422.52	dolomitic sandstone	B
422.52	422.53	shale	A
422.53	422.54	dolomitic sandstone	B
422.54	422.55	shale	A
422.55	422.57	dolomitic sandstone	B
422.57	422.58	shale	A
422.58	422.60	dolomitic sandstone	B
422.60	422.61	shale	A
422.61	422.62	dolomitic sandstone	B
422.62	422.63	shale	A
422.63	422.64	dolomitic sandstone	B
422.64	422.65	shale	A
422.65	422.68	dolomitic sandstone	B
422.68	422.75	dolomitic mudstone	C
422.75	422.88	dolomitic sandstone	B
422.88	422.94	dolomitic mudstone	C
422.94	422.95	dolomitic sandstone	B
422.95	422.99	dolomitic mudstone	C
422.99	423.01	shale	A
423.01	423.02	dolomitic sandstone	B
423.02	423.05	shale	A
423.05	423.06	dolomitic mudstone	C
423.06	423.12	shale	A
423.12	423.19	dolomitic mudstone	C
423.19	423.26	dolomitic sandstone	B
423.26	423.28	shale	A
423.28	423.29	dolomitic sandstone	B
423.29	423.30	shale	A
423.30	423.33	dolomitic sandstone	B
423.33	423.40	shale	A
423.40	423.41	dolomitic sandstone	B
423.41	423.42	shale	A
423.42	423.44	dolomitic sandstone	B
423.44	423.45	shale	A
423.45	423.47	dolomitic sandstone	B
423.47	423.49	shale	A
423.49	423.50	dolomitic mudstone	C
423.50	423.55	shale	A
423.55	423.73	dolomitic mudstone	C
423.73	423.74	dolomitic sandstone	B
423.74	423.76	dolomitic mudstone	C
423.76	423.78	shale	A
423.78	423.92	dolomitic mudstone	C microfault
423.92	423.95	dolomitic sandstone	B microfault

423.95	424.07	shale	A
424.07	424.13	erbedded dolomitic sandstone and sha	C
424.13	424.16	dolomitic sandstone	B
424.16	424.21	dolomitic sandstone	B
424.21	424.36	shale	A
424.36	424.46	dolomitic sandstone	B microfault
424.46	424.53	shale	A
424.53	424.58	dolomitic sandstone	B
424.58	424.73	shale	A
424.73	424.75	dolomitic sandstone	B
424.75	424.80	shale	A
424.80	424.93	dolomitic sandstone	B
424.93	425.06	shale	A
425.06	425.10	dolomitic mudstone	C
425.10	425.12	dolomitic sandstone	B
425.12	425.13	shale	A
425.13	425.15	dolomitic sandstone	B
425.15	425.16	shale	A
425.16	425.19	dolomitic sandstone	B
425.19	425.25	shale	A
425.25	425.32	dolomitic sandstone	B
425.32	425.38	shale	A
425.38	425.46	dolomitic sandstone	B
425.46	425.53	shale	A
425.53	425.66	dolomitic sandstone	B
425.66	425.72	dolomitic mudstone	C
425.72	425.75	dolomitici sandstone	B
425.75	425.79	shale	A
425.79	426.00	dolomitic sandstone	B brecciated
426.00	426.08	shale	A
426.08	426.15	dolomitic mudstone	C
426.15	426.20	shale	A
426.20	426.21	dolomitic sandstone	B
426.21	426.34	shale	A
426.34	426.38	dolomitic sandstone	B
426.38	426.50	dolomitic mudstone	C
426.50	426.56	shale	A
426.56	426.77	dolomitic mudstone	C
426.77	426.85	shale	A
426.85	426.93	dolomitic mudstone	C
426.93	427.05	shale	A
427.05	427.13	dolomitic sandstone	B
427.13	441.73		in lab
441.73	447.73	siltstone	some shaley & sst layers, high dolo content
447.73	448.13	sandstone	some shale interbedded, coarse pebbly unit @ top
448.13	452.63	siltstone	massive, some wispy clay
452.63	452.75	sandstone	some mud in matrix
452.75	453.19	shaley siltstone	
453.19	453.48	sandstone	some qtz rich hor
453.48	455.58	sandy siltstone	loaded sand blobs
455.58	455.63	dolomitic sandstone	
455.63	456.25	sandy siltstone	sand blobs loaded into sand

456.25	457.84	sandstone	some irregular mud layers
457.84	458.17	sandstone	qtz with mud loaded @ base, detached sand blobs
458.17	459.42	shaley siltstone	reduc spots, high dolomite
Fork Bay Member, Pass Lake Fm			
459.42	459.53	sandstone	
459.53	461.60	shaley siltstone	shalier @ base, some sst layers
461.60	461.95	sandstone	
461.95	462.40	shale	
462.40	462.47	sandstone	loaded base, sharp top
462.47	462.81	shaley siltstone	sm reduc spots
462.81	462.85	sandstone	loaded [into soupy mud]
462.85	463.75	siltstone	floating cs granules, some dolomite layers
463.75	463.87	sandstone	few shaley layers
463.87	463.95	shale	
463.95	463.99	sandstone	
463.99	464.51	shale	many gypsum veins, varied dolomite content
464.51	464.53	sandstone	
464.51	464.66	shale	thin sandy beds
464.66	464.67	sandstone	
464.67	466.19	silty shale	few reduc spots
466.19	469.19	diabase	
469.19	471.65	sandy shale	some cs lam, dolomitic layers, loaded sand blobs
471.65	472.87	pebbly sandstone	coarse granules and pebbles, qtz veins
472.87	476.83	granite	basement

NB-97-2

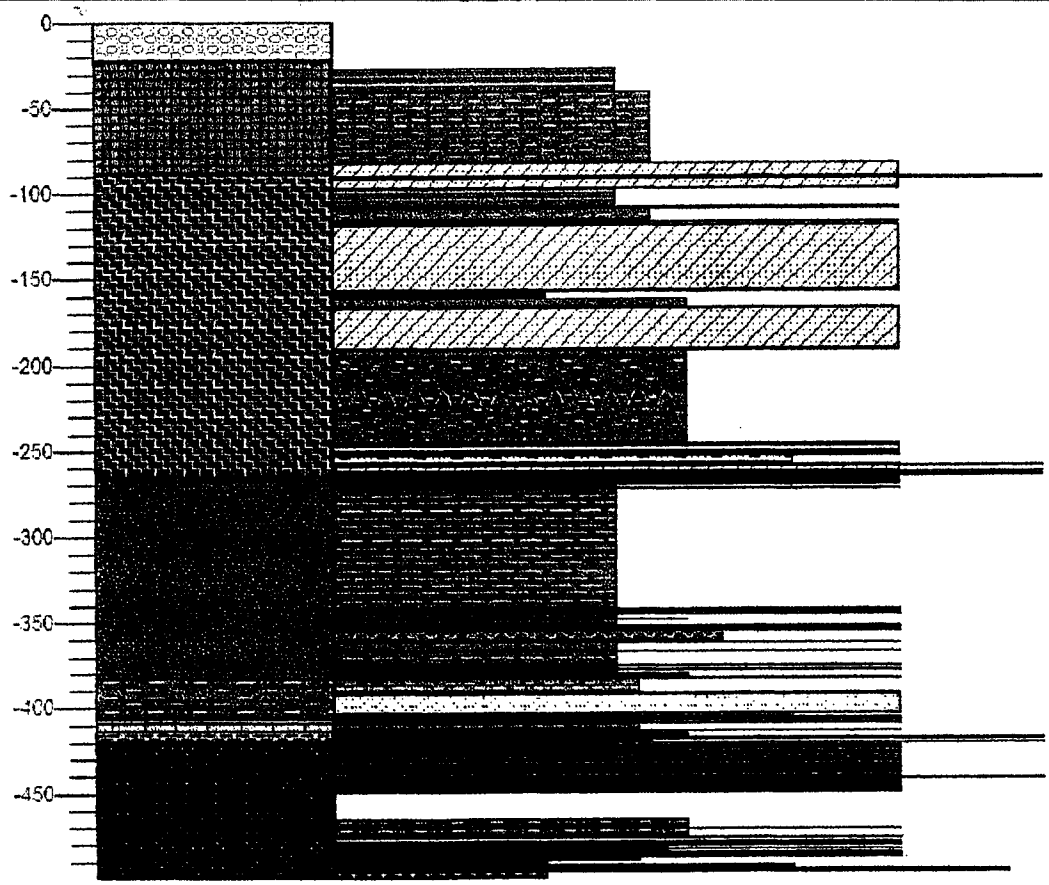

NB-97-4 425430 E, 5410540 N

Nipigon Bay Fm			
0.00	15.30	high-angle cross-stratified sandstone	1m sets
15.30	18.36	horizontally laminated sandstone	30cm set of high angle
18.36	32.69	high-angle cross-stratified sandstone	50cm sets
32.69	41.32	low-angle cross-stratified sandstone	13, 67 cm, w some fissile shale layers
41.32	49.58	high-angle cross-stratified sandstone	60, 215 cm
49.58	61.21	horizontally laminated sandstone	some v. low x-strat
61.21	134.65	low-angle cross-stratified sandstone	high angle @ top & bottom, fissile silty layers
134.65	149.95	horizontally laminated sandstone	some low angle x-strat
149.95	155.61	low-angle cross-stratified sandstone	230 cm set
155.61	165.29	horizontally laminated sandstone	
165.29	219.02	high-angle cross-stratified sandstone	78, 348 cm x-sets
219.02	220.39	horizontally laminated sandstone	
220.39	231.67	high-angle cross-stratified sandstone	90-200cm, v. mottled colour
231.67	232.25	sandstone	some hor. lam, dk red
232.25	295.21	high-angle cross-stratified sandstone	20-300 cm sets, nearly reverse dir
295.21	298.98	sandstone	red, some hor lam
298.98	336.39	high-angle cross-stratified sandstone	cs, fs; some lam coarsen up, 30, 60, 110 cm sets
336.39	341.28	horizontally laminated sandstone	m/cs, some muddy, gradational contact betw. angles
341.28	352.31	high-angle cross-stratified sandstone	gradational from low
352.31	352.36	horizontally laminated sandstone	muddy
352.36	377.60	high-angle cross-stratified sandstone	red & buff, some cs lam, 40 cm sets
377.60	380.11	horizontally laminated sandstone	
380.11	401.77	high-angle cross-stratified sandstone	20cm sets
401.77	427.88	high-angle cross-stratified sandstone	angle varies, 13-30 cm sets, some cs, odd mudchip
Hele Member, Outan Island Fm			
427.88	485.13	sandstone	abund silty shale lam, lots of rip-up horizons
485.13	485.63	very fine sandstone	hor lam w clay
485.63	486.65	horizontally laminated sandstone	overall fines up, rip-up horizons
486.65	487.08	shale	dom, some diagen & fsst
487.08	505.59	horizontally laminated sandstone	some fs/silty lam, carb veins, mudchip lam
505.59	515.47	graded sandstone	fines up, lots of rip-up/mudchip horizons, mudcracks
515.47	515.73	siltstone	clay lam
515.73	516.68	reverse graded sandstone	coarsens from silt, some rip-ups
516.68	516.94	siltstone	red, massive, odd clay lam
516.94	534.64	horizontally laminated sandstone	lots of mud rip-ups
534.64	536.63	reverse graded sandstone	fsst to msst, some internal lam fine up
536.63	538.33	sandstone	clay lam
538.33	538.76	reverse graded sandstone	fsst to msst, muddy, individual lam fine up
538.76	558.54	graded sandstone	csst to msst, some mudchip congl
558.54	572.15	horizontally laminated sandstone	msst, some x-lam, some c-msst grading
Lyon Member, Outan Island Formation			
572.15	581.69	fine sandstone	large mudcracks, mudchips, rare x-lam
581.69	592.00	sandstone	some mud fragments
592.00	593.31	fine sandstone	silty, odd mudchips
593.31	601.18	sandstone	lots of mudchips floating in it
Kama Hill Fm			
601.18	649.43	mudcracked siltstone	get inc fsst up, abund mudchips
649.43	664.34	sandstone	occasional mudchip, rare x-lam
Fire Hill Member, Rossport Fm			

664.34	737.49	reverse graded sandstone	fs, mudcracks, rip-ups, load & slump structures
737.49	744.51	mudcracked siltstone	mudchip hor. assoc with mudcracks
744.51	744.57	laminated siltstone	
744.57	745.17	contorted mudstone	
745.17	745.62	laminated siltstone	slump area
745.62	746.12	contorted mudstone	
746.12	746.92	laminated siltstone	shaley
746.92	755.47	shale	siltier up, evap-rich area
755.47	755.77	mudcracked siltstone	high evap content
755.77	771.29	shale	fissile, slump features
771.29	772.16	graded sandstone	msst to fsst
772.16	772.86	laminated siltstone	sand blobs, post-lithification faults
772.86	773.36	graded sandstone	msst to silt
773.36	784.27	siltstone	shaley at top, high evap
784.27	784.77	mudchip conglomerate	silty top
784.77	789.97	mudstone	
789.97	790.29	sandstone	clay cap
790.29	790.99	graded sandstone	fsst to silt
790.99	792.89	siltstone	somewhat fissile
792.89	793.43	fine sandstone	
793.43	796.18	siltstone	coarsens up from shale
796.18	796.74	reverse graded sandstone	fsst to msst
796.74	797.48	siltstone	lam @ bottome with shale
797.48	798.24	reverse graded sandstone	silt to fsst to msst
798.24	798.96	fine sandstone	some msst grains
798.96	799.95	shale	laminated with silt, siltier up
799.95	800.55	sandstone	shale lam at top
800.55	801.25	graded sandstone	shalier upwards
801.25	801.93	graded sandstone	msst to clay (white to red)
801.93	802.35	graded sandstone	msst to fsst w. red clay lam, oxidized top
802.35	802.55	graded sandstone	msst to fsst w. red clay lam, oxidized top
802.55	803.22	sandstone	lots of coarser grains, lam preserved upward
803.22	804.87	graded sandstone	very gradual from msst to silt/clay lam
804.87	805.89	mudstone	some well-preserved lam
805.89	806.39	sandstone	
806.39	806.85	laminated siltstone	with shale, some diagen at bottom
806.85	808.18	sandstone	
808.18	808.67	mudstone	some preserved lam
808.67	809.80	sandstone	oxidation & clay content inc up
809.80	810.52	shaley siltstone	messy sandy lam @ bottom, irregular mud lam
810.52	811.82	sandstone	well-sorted
811.82	812.17	mudstone	sandy patches at top
812.17	812.69	mudcracked siltstone	
812.69	812.75	contorted mudstone	
812.75	812.76	shale	
812.76	813.75	sandstone	well-sorted
813.75	813.92	graded sandstone	msst to shale, coarse clasts throughout
813.92	814.19	graded sandstone	msst to shale, coarse clasts throughout
814.19	814.23	laminated mudstone	
814.23	814.26	cross-stratified sandstone	ripples in msst
814.26	814.31	mudstone	
814.31	814.48	sandstone	some slump/soft sed defm, x-strat @ top

814.48	814.51	mudstone	
814.51	814.72	sandstone	ripple fsst @ top
814.72	814.86	sandstone	
814.86	815.01	sandstone	coarser grains, mudchips
815.01	815.02	sandstone	
815.02	815.18	cross-stratified sandstone	some climbing ripples
815.18	815.21	sandstone	
815.21	815.25	sandstone	clay partings
815.25	815.39	sandstone	coarse horizons
815.39	815.57	graded sandstone	msst to fsst
815.57	815.61	dolomitic mudstone	x-strat silt, odd climbing ripple
815.61	815.87	graded sandstone	m/csst to silty fsst
815.87	815.93	laminated siltstone	
815.93	816.24	fine sandstone	coarse grains, hint of x-strat
Channel Island Member, Rossport Fm			
816.24	816.37	silty shale	A
816.37	816.46	dolomitic mudstone	C
816.46	816.67	dolomitic mudstone	B
816.67	816.91	silty shale	A
816.91	817.00	dolomitic mudstone	B
817.00	817.10	silty shale	A
817.10	817.16	dolomitic mudstone	C
817.16	817.27	silty shale	A
817.27	817.43	dolomitic mudstone	C
817.43	817.46	silty shale	A
817.46	817.57	dolomitic mudstone	C
817.57	817.79	silty shale	A
817.79	817.87	dolomitic sandstone	
817.87	818.32	silty shale	A, diagenetic areas
818.32	818.44	dolomitic mudstone	C
818.44	818.60	silty shale	A, angled lam
818.60	818.76	dolomitic mudstone	C
818.76	819.28	sandy siltstone	A
819.28	819.33	dolomitic mudstone	C
819.33	819.55	silty shale	A with dolomitic blobs
819.55	819.61	dolomitic mudstone	C
819.61	819.77	silty shale	A
819.77	819.86	dolomitic mudstone	C
819.86	820.24	silty shale	A
820.24	820.26	dolomitic mudstone	B
820.26	820.30	silty shale	A
820.30	821.00	dolomitic mudstone	B, some diagenetic min
821.00	821.05	dolomitic mudstone	C, gypsum @ top
821.05	821.15	silty shale	A
821.15	821.25	dolomitic mudstone	C
821.25	821.45	dolomitic mudstone	B
821.45	821.56	dolomitic mudstone	C
821.56	821.62	silty shale	A, thin lam
821.62	821.84	dolomitic mudstone	C, clay lam @ top
821.84	822.04	silty shale	A, lots of diagen min
822.04	822.21	dolomitic sandstone	very granular/sandy top
822.21	822.49	silty shale	A

822.49	822.69	dolomitic mudstone	C, some sandy lam
822.69	822.76	silty shale	A
822.76	822.93	dolomitic sandstone	B
822.93	824.13	dolomitic mudstone	B, some graded lam
824.13	824.24	silty shale	A
824.24	824.33	dolomitic mudstone	C
824.33	824.51	silty shale	some rip-up shale, diagen min
824.51	824.63	dolomitic sandstone	C
824.63	824.77	dolomitic mudstone	B
824.77	824.85	dolomitic mudstone	C
824.85	824.90	silty shale	A, with pinched dolomite layers
824.90	825.04	dolomitic mudstone	C
825.04	825.12	silty shale	A
825.12	825.20	dolomitic mudstone	B
825.20	825.28	dolomitic mudstone	C
825.38	825.36	silty shale	A
825.36	825.46	dolomitic mudstone	C
825.46	825.53	silty shale	A
825.53	825.61	dolomitic mudstone	C
825.61	825.75	dolomitic mudstone	B, ripped up
825.75	825.84	dolomitic mudstone	C
825.84	826.14	dolomitic mudstone	B, some gypsum veins
826.14	825.18	dolomitic sandstone	fine sst
825.18	826.41	silty shale	reduction spots
826.41	826.58	dolomitic mudstone	C, some sand blobs
826.58	826.80	dolomitic mudstone	B, contorted
826.80	827.00	dolomitic sandstone	C
827.00	827.16	dolomitic mudstone	B
827.16	827.23	dolomitic mudstone	C, some sandy lam
827.23	827.36	silty shale	A
827.36	827.54	dolomitic mudstone	C, grades to A
827.54	827.61	silty shale	A
827.61	827.78	dolomitic mudstone	C, clayey near top
827.78	827.82	silty shale	A
827.82	827.92	dolomitic mudstone	C
827.92	828.14	silty shale	A, dolomitic areas
828.14	828.28	dolomitic mudstone	C, topped with 3 cm sand
828.28	828.59	silty shale	A
828.59	828.75	dolomitic mudstone	C, some sandy patches
828.75	828.96	silty shale	A, some carbonate crusts
828.96	829.05	dolomitic mudstone	C, granular patch
829.05	829.21	silty shale	A
829.21	829.44	dolomitic sandstone	C, layers thin up
829.44	829.50	silty shale	A, with large dolo block in it
829.50	829.56	dolomitic mudstone	C
829.56	829.69	silty shale	A, some diagen min
829.69	829.86	dolomitic mudstone	C
829.86	830.05	silty shale	A
830.05	830.15	dolomitic mudstone	C
830.15	830.30	silty shale	A
830.30	830.54	dolomitic mudstone	C
830.54	830.73	dolomitic mudstone	B, gradational with next C & A

830.73	830.94	dolomitic mudstone	C
830.94	831.07	dolomitic mudstone	B, grades to shale
831.07	831.37	dolomitic mudstone	C, sand & mud lam
831.37	831.53	dolomitic mudstone	B
831.53	831.63	silty shale	A
821.63	831.93	dolomitic mudstone	B, diagenetic horizons
831.93	832.11	dolomitic mudstone	C, mudchip layers
832.11	832.32	dolomitic mudstone	B, some inclined layers
832.32	832.43	dolomitic mudstone	C, dolo layers massive to granular
832.43	832.81	silty shale	A
832.81	833.98	dolomitic mudstone	C
833.98	834.26	shale	A, very fissile
834.26	834.38	dolomitic mudstone	B
834.38	834.61	silty shale	A
834.61	834.76	dolomitic mudstone	C, diagen layers
834.76	834.84	silty shale	A
834.84	834.88	dolomitic mudstone	C
834.88	835.08	dolomitic mudstone	B
835.08	835.33	dolomitic mudstone	C
835.33	835.58	silty shale	reduc spots, diagen crusts (angled)
835.58	835.72	dolomitic mudstone	B
835.72	835.88	dolomitic mudstone	C, diagen min in thicker lam
835.88	835.99	dolomitic mudstone	B, lots of little gypsum lam
835.99	836.10	dolomitic mudstone	C
836.10	836.27	silty shale	A
836.27	836.31	dolomitic mudstone	C
836.31	836.33	dolomitic mudstone	B
836.33	836.41	silty shale	A
836.41	836.89	dolomitic mudstone	C, sandy patches, load structures
836.89	836.99	silty shale	A
836.99	837.14	dolomitic mudstone	C
837.14	837.30	dolomitic mudstone	B, gypsum vein
837.30	837.72	dolomitic mudstone	C, dolo inc up
837.72	837.86	silty shale	A, some dolo mottling
837.86	837.92	dolomitic mudstone	B, clay drape
837.92	838.10	silty shale	A
838.10	838.18	dolomitic mudstone	C
838.18	838.26	silty shale	A, mottled
838.26	838.36	dolomitic mudstone	C, mottled
838.36	838.45	silty shale	A
838.45	838.52	dolomitic mudstone	C
838.52	838.76	silty shale	A, gypsum veining, contorted
838.76	838.86	dolomitic mudstone	C
838.86	838.96	silty shale	A, diagenetic areas
838.96	839.07	dolomitic mudstone	C, layers fine up
839.07	839.22	silty shale	A, grades to dolo
839.22	839.46	dolomitic mudstone	C, granular in mid-layers
839.46	840.10	silty shale	some coarse granules, dolomite content inc up
840.10	840.29	dolomitic mudstone	granular in areas (some too big for aeolian transport)
840.29	840.50	silty shale	A
840.50	840.60	dolomitic mudstone	C, coarse grains on top
840.60	841.19	dolomitic mudstone	C, coarse granules in layers

841.19	841.69	silty shale	A
841.69	841.85	dolomitic sandstone	C, some diagen min
841.85	842.13	silty shale	A
842.13	842.45	dolomitic mudstone	B
842.45	842.99	silty shale	A
Fork Bay Member, Pass Lake Fm			
842.99	844.14	siltstone	some dolo areas, lots of gyp veins, some fsst
844.14	844.45	dolomitic mudstone	carb content inc up
844.45	844.47	graded sandstone	msst to very fsst
844.47	844.66	graded sandstone	vcsst to fsst
844.66	845.53	dolomitic mudstone	barite blob, gypsum veins
845.53	845.67	sandstone	some fsst, coarse grain horizon
845.67	846.21	shaley siltstone	dolomitic spots, some gypsum veins
846.21	846.42	graded sandstone	fsst to shale
846.42	846.68	dolomitic mudstone	silt/fsst block assoc w mud layers & calcite blobs
846.68	846.90	graded sandstone	msst to fsst, some coarse qtz grains
846.90	848.19	graded sandstone	fsst to shale, dolomitic areas
848.19	848.24	dolomitic mudstone	disrupted lam
848.24	848.55	siltstone	dolomite-rich patches
848.55	848.87	dolomitic mudstone	some disrupted layers
848.87	849.14	siltstone	
849.14	849.16	pebbly sandstone	fsst with csst & jasper clasts
849.16	849.79	shaley siltstone	varied carb content, conc in shaley areas
849.79	849.99	siltstone	relatively high carb content
849.99	850.47	fine sandstone	some shale lam, inc up, m/csst blobs
850.47	850.83	graded sandstone	msst to silt, inc carb content up
850.83	850.96	reverse graded sandstone	fsst to msst, jasper clasts inc up
850.96	850.99	sandstone	silt cap
850.99	852.02	reverse graded sandstone	fsst to msst, jasper & other clasts inc size up
852.02	852.55	graded sandstone	csst to msst to shaley silt
852.55	853.44	sandstone	coarse japer & qtz grains
853.44	853.79	fine sandstone	
853.79	853.81	sandstone	mud cap
853.81	853.87	graded sandstone	fsst to mud
853.87	854.29	graded sandstone	msst quickly to mud
853.87	854.68	graded sandstone	msst, mud inc up
854.68	855.49	graded sandstone	msst, muddier up
855.49	855.76	mudstone	
855.76	855.82	laminated mudstone	black
855.82	855.91	saprolite	
855.91	856.08	graded sandstone	csst to msst
856.08	856.17	graded sandstone	fsst to mud, carb areas throughout
856.17	856.28	sandstone	some mud and carb areas
856.28	856.35	graded sandstone	msst to muddy fsst
856.35	856.41	sandstone	
856.41	856.51	mudstone	carb areas
856.51	856.53	graded sandstone	msst to fsst
856.53	856.71	sandstone	calcitic mud near top
856.71	856.77	graded sandstone	scattered coarse grains
856.77	860.57	saprolite	sand content inc up
860.57	875.26	granite	basement, some diabase

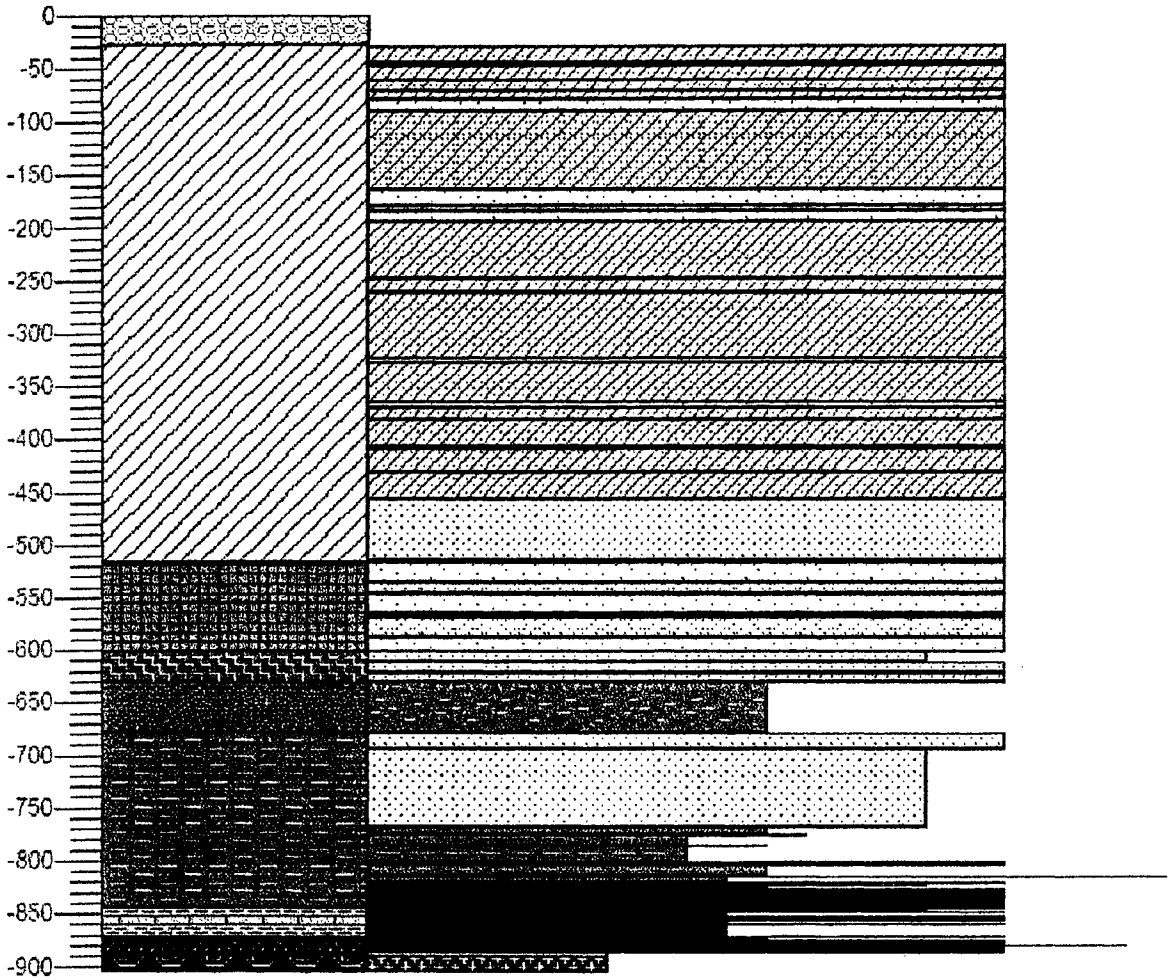

NB-97-5 427140 E, 5411800 N

Nipigon Bay Fm			
0.00	73.20	surface	
73.20	117.84	horizontally laminated sandstone	some sm-sc ripple x-strat, some carb content
117.84	156.84	horizontally laminated sandstone	some low angle x-strat, some graded
156.84	299.34	high-angle cross-stratified sandstone	buff, msst, well-sorted, 150 cm sets
299.34	303.84	low-angle cross-stratified sandstone	some hor lam, mottled
303.84	479.00	horizontally laminated sandstone	some fissile shale areas, some x-lam ~80 cm
479.00	488.00	low-angle cross-stratified sandstone	very low to hor lam
Hele Member, Outan Island Fm			
488.00	510.14	laminated siltstone	sand beds, chert nodules, mudchip lam, patchy fabric
510.14	511.74	horizontally laminated sandstone	
511.74	514.39	silty shale	some sand
514.39	516.64	cross-stratified sandstone	sharp erosive base
516.64	517.84	sandy shale	loading
516.64	519.74	sandstone	some x-strat
519.74	541.21	shaley siltstone	with sand-shale interbeds
541.21	543.59	cross-stratified sandstone	some hor lam
543.59	547.34	laminated mudstone	some sand interbeds, soupy texture
547.34	557.96	cross-stratified sandstone	some gypsum veins, dunes
557.96	579.14	laminated mudstone	silt, sand (with mudchips), shale beds
579.14	595.24	graded sandstone	graded beds with shale partings
595.24	595.79	very fine sandstone	some silt/shale
595.79	611.98	graded sandstone	vcsst @ base
611.98	612.72	contorted mudstone	abundant mudchips @ base
612.72	612.94	sandstone	some silty lam
612.94	613.76	mudstone	irregular "mushy" bedding
613.76	614.09	sandstone	
614.09	614.50	mudstone	overlain by beds of sand/silt
614.50	615.77	sandstone	
615.77	620.27	horizontally laminated sandstone	with shale, loading, partial bed preservation
620.27	631.21	low-angle cross-stratified sandstone	m/fsst, mudchip horizons
631.21	632.51	sandstone	lam with shale, loading
632.51	646.51	sandstone	some fine shale lam, rip-ups, coarse bands
646.51	679.91	silty shale	x-strat & fine lam, coarse based sand beds near top
679.91	697.13	cross-stratified siltstone	mudcracks, current ripple lam, convoluted bedding
697.13	707.76	sandstone	flame structure
707.76	709.02	cross-stratified sandstone	csst, some vcsst lam, some hor lam

NB-97-5

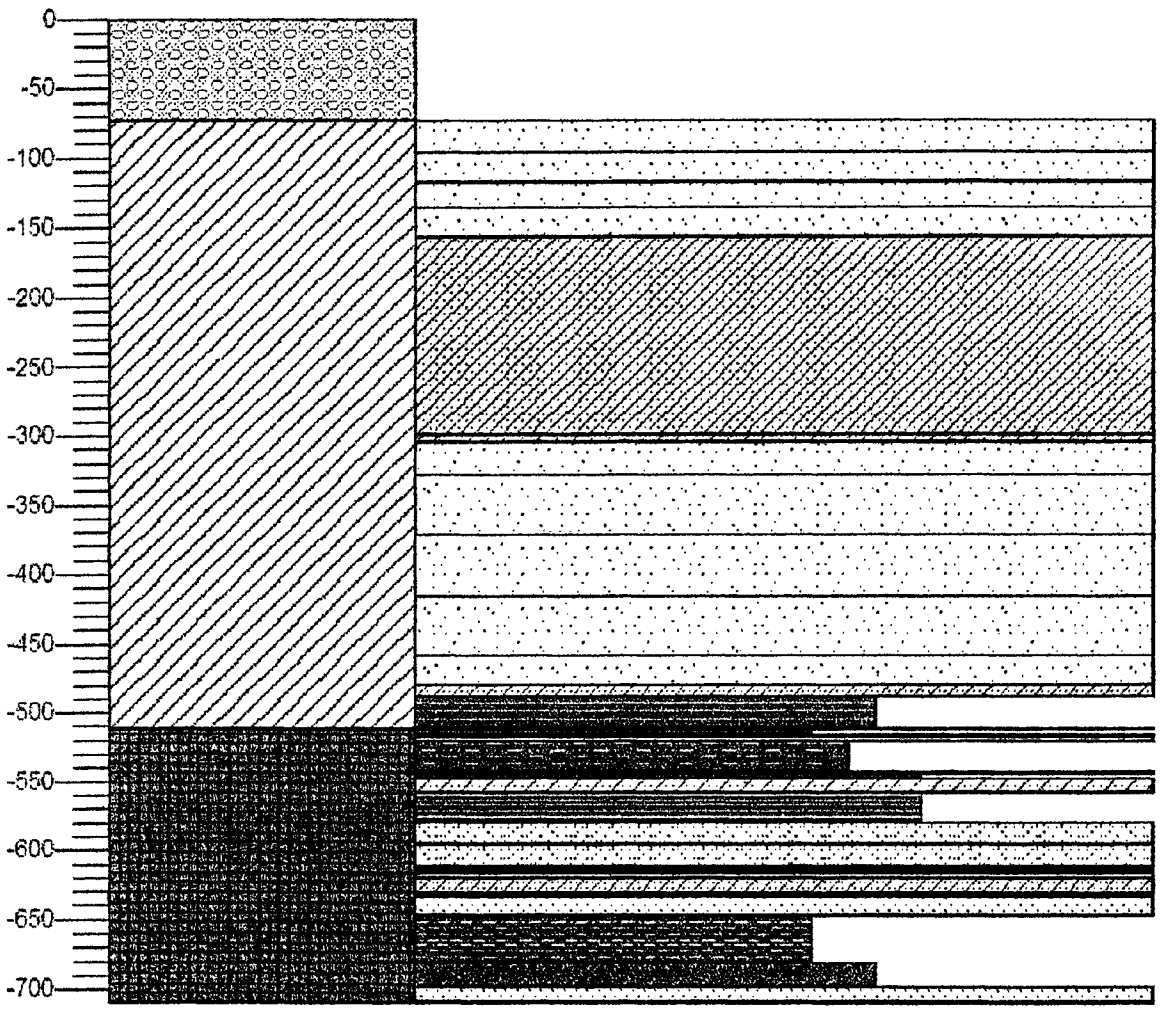

HE-02-01 50 E, 5423148 N

0	135	diabase
Kama Hill Fm		
135	136.04	shale
136.04	136.07	shale
136.07	136.44	shale
136.44	137.92	shale
137.92	138.87	sandy shale
138.87	139.16	shale
139.16	139.2	cross-stratified siltstone
139.2	139.22	shale
139.22	140.57	silty shale
140.57	140.75	shale
140.75	140.91	mudstone
140.75	141.59	shale
141.59	142.38	shale
142.38	142.5	saprolite
142.5	142.78	shale
142.78	142.94	sandstone
142.94	144.13	mudstone
144.13	144.46	siltstone
144.46	144.79	silty shale
144.79	144.99	very fine sandstone
144.99	145.16	laminated mudstone
145.16	145.35	mudstone
145.35	145.51	laminated mudstone
145.51	146.21	laminated mudstone
146.21	146.37	siltstone
146.37	148.06	laminated siltstone
148.06	148.26	laminated siltstone
148.26	149.34	laminated siltstone
149.34	149.96	laminated siltstone
149.96	151.36	fine sandstone
151.36	152.16	siltstone
152.16	152.22	siltstone
152.22	152.51	siltstone
152.51	152.81	sandstone
152.81	153.86	siltstone
153.86	153.98	contorted mudstone
153.98	154.09	siltstone
154.09	154.19	siltstone
154.19	154.24	siltstone
154.24	154.31	siltstone
154.31	154.48	siltstone
154.48	154.71	siltstone
154.71	155.08	siltstone
155.08	155.18	siltstone
155.18	155.26	siltstone
155.26	156.61	siltstone
156.61	157.07	contorted mudstone
157.07	157.42	sandy siltstone
157.42	157.48	laminated siltstone
157.48	158.06	siltstone
158.06	158.98	siltstone
158.98	159.82	siltstone
159.82	160.17	siltstone
160.17	161.16	mudstone
161.16	161.81	dolomitic mudstone
161.81	162.89	sandstone
162.89	164	sandstone
164	164.21	sandstone
164.21	164.27	sandstone
164.27	164.37	sandstone
164.37	165.24	siltstone
165.24	165.5	graded sandstone
165.5	165.56	laminated mudstone
165.56	165.77	sandstone
165.77	167.93	siltstone
167.93	168.93	siltstone
168.93	169.2	mudchip conglomerate
169.2	170	mudchip conglomerate
170	170.52	siltstone
170.52	173.52	mudchip conglomerate
173.52	175.79	siltstone
175.79	177.01	sandstone
177.01	177.11	mudchip conglomerate
177.11	178.12	sandstone
178.12	178.14	siltstone
178.14	178.33	sandstone
178.33	179.07	silty shale
179.07	179.15	sandstone
179.15	179.29	mudchip conglomerate
179.29	179.49	sandstone
179.49	179.78	mudchip conglomerate
179.78	179.88	laminated siltstone
179.88	179.98	mudchip conglomerate
179.98	180.14	laminated mudstone
180.14	180.3	mudchip conglomerate
180.3	180.65	laminated siltstone
180.65	181.07	mudchip conglomerate
181.07	181.49	siltstone
181.49	181.78	siltstone
181.78	182.5	siltstone
182.5	183	mudchip conglomerate
183	183.5	mudstone
183.5	184.43	mudchip conglomerate
184.43	184.73	mudstone
184.73	184.8	mudchip conglomerate
184.8	185.3	mudstone

185.3	185.62	conglomerate
185.62	186.03	siltstone
Fire Hill Member, Rossport Fm		
186.03	186.65	conglomerate
186.65	186.75	laminated mudstone
186.75	186.85	conglomerate
186.85	186.95	siltstone
186.95	187.37	conglomerate
187.37	187.53	siltstone
187.53	188.76	conglomerate
188.76	188.94	siltstone
188.94	189.04	mudchip conglomerate
189.04	189.2	fine sandstone
189.2	190.12	conglomerate
190.12	190.22	mudstone
190.22	190.26	mudchip conglomerate
190.26	190.3	laminated mudstone
190.3	190.35	mudchip conglomerate
190.35	191.15	conglomerate
191.15	192.57	siltstone
192.57	192.7	mudstone
192.7	192.72	siltstone
192.72	193.35	contorted mudstone
193.35	193.57	siltstone
193.57	193.62	sandstone
193.62	194.84	siltstone
194.84	195.58	sandstone
195.58	195.74	sandy siltstone
195.74	195.81	siltstone
195.81	196.61	graded sandstone
196.61	196.81	graded sandstone
196.81	197.18	graded sandstone
197.18	197.55	graded sandstone
197.55	199.05	sandstone
199.05	199.9	sandstone
199.9	201.63	siltstone
201.63	202.38	sandstone
202.38	203.05	fine sandstone
203.05	203.22	siltstone
203.22	203.35	graded sandstone
203.35	204.18	siltstone
204.18	204.44	sandstone
204.44	205.64	contorted mudstone
205.64	207.36	sandstone
207.36	207.7	siltstone
207.7	208.23	sandstone
208.23	209.35	graded sandstone
209.35	210.23	graded sandstone
210.23	211.12	siltstone
211.12	211.73	sandstone

211.73	211.77	mudstone
211.77	213.08	sandstone
213.08	214.83	fine sandstone
214.83	214.94	laminated mudstone
214.94	214.96	sandstone
214.96	215.53	siltstone
215.53	215.8	shale
215.8	217.29	siltstone
217.29	217.4	laminated mudstone
217.4	220.84	siltstone
220.84	221.36	laminated siltstone
221.36	221.61	siltstone
221.61	222.06	laminated siltstone
222.06	222.16	mudchip conglomerate
222.16	222.28	siltstone
222.28	222.4	laminated siltstone
222.4	222.46	cross-stratified siltstone
222.46	223.26	laminated siltstone
223.26	223.28	siltstone
223.28	223.66	shaley siltstone
223.66	223.76	sandstone
223.76	224.31	laminated siltstone
224.31	224.33	sandstone
224.33	225.02	laminated siltstone
225.02	226.16	contorted mudstone
226.16	226.39	laminated siltstone
226.39	226.69	sandstone
226.69	227.17	laminated siltstone
227.17	227.28	breccia
227.28	227.39	siltstone
227.39	227.59	sandstone
227.59	227.77	siltstone
227.77	227.82	siltstone
227.82	227.84	siltstone
227.84	227.89	siltstone
227.89	227.97	dolomitic conglomerate
227.97	228.02	siltstone
228.02	228.07	dolomitic conglomerate
228.07	228.08	siltstone
228.08	228.18	dolomitic conglomerate
228.18	228.19	contorted mudstone
228.19	228.24	dolomitic conglomerate
228.24	228.32	conglomerate
228.32	228.39	dolomitic conglomerate
228.39	228.92	siltstone
228.92	228.93	sandstone
228.93	229.1	siltstone
229.1	229.12	sandstone
229.12	229.46	laminated siltstone
229.46	230.35	contorted mudstone

230.35	230.42	laminated siltstone
230.42	230.59	siltstone
230.59	231.21	siltstone
231.21	231.54	cross-stratified siltstone
231.54	231.95	laminated siltstone
231.95	232.07	contorted mudstone
232.07	232.13	laminated siltstone
232.13	232.2	dolomitic mudstone
232.2	232.34	cross-stratified siltstone
232.34	232.63	dolomitic mudstone
232.63	232.87	siltstone
232.87	232.94	laminated siltstone
232.94	233.14	siltstone
233.14	233.44	contorted mudstone
233.44	233.66	siltstone
233.66	234.55	siltstone
234.55	234.66	siltstone
234.66	234.85	siltstone
234.85	235.89	sandstone
234.89	235.5	conglomerate
235.5	235.6	siltstone
235.6	235.83	siltstone
235.83	235.96	sandstone
235.96	236.16	graded sandstone
236.16	236.21	siltstone
236.21	236.34	sandstone
236.34	236.59	laminated siltstone
236.59	236.61	sandstone
236.59	236.69	laminated siltstone
236.69	236.74	sandstone
236.74	237.53	siltstone
237.53	237.58	sandstone
237.58	237.98	siltstone
237.98	238.08	shaley siltstone
238.08	238.46	siltstone
238.46	238.54	siltstone
238.54	238.64	siltstone
238.64	239.19	siltstone
239.19	239.2	gypsum
239.2	239.38	graded sandstone
239.38	239.58	siltstone
239.58	239.65	sandstone
239.65	239.72	siltstone
239.72	239.85	dolomitic sandstone
239.85	240.17	dolomitic mudstone
240.17	240.57	dolomitic sandstone
240.57	240.92	dolomitic mudstone
240.92	241.09	laminated siltstone
241.09	241.51	siltstone
241.51	241.66	siltstone

241.66	242.22	conglomerate
242.22	242.4	sandstone
242.4	242.51	siltstone
242.51	242.58	dolomitic mudstone
242.58	242.72	dolomitic conglomerate
242.72	242.77	sandstone
242.77	242.84	siltstone
242.84	242.99	dolomitic mudstone
242.99	243.06	mudstone
243.06	243.12	graded sandstone
243.12	243.3	siltstone
243.3	243.6	dolomitic mudstone
243.6	243.75	laminated siltstone
243.75	243.92	dolomitic mudstone
243.92	244.18	siltstone
244.18	244.31	dolomitic mudstone
244.31	244.34	siltstone
244.34	244.5	dolomitic mudstone
244.5	244.61	dolomitic sandstone
244.61	245.12	siltstone
245.12	245.43	dolomitic sandstone
245.43	245.64	dolomitic mudstone
245.64	245.71	dolomite
245.71	245.91	siltstone
245.91	245.98	dolomitc mudstone
245.98	246.05	silty shale
246.05	246.17	dolomtic sandstone
246.17	246.66	siltstone
246.66	246.92	dolomitic mudstone
246.92	247.27	siltstone
247.27	247.41	dolomitic mudstone
247.41	248.25	dolomitic mudstone
248.25	248.54	dolomitic mudstone
248.54	248.65	siltstone
248.65	248.84	silty shale
248.84	249.24	laminated siltstone
249.24	249.37	dolomitic siltstone
249.37	249.58	dolomitic siltstone
249.58	249.81	mudstone
249.81	250.05	siltstone
250.05	250.24	dolomitic conglomerate
250.24	250.56	dolomitic conglomerate
250.56	250.67	laminated siltsotne
250.67	250.77	dolomitic mudstone
250.77	251.01	siltstone
251.01	251.28	dolomitic mudstone
251.28	251.43	laminated siltstone
251.43	251.62	dolomitic mudstone
251.62	252.04	laminated siltstone
252.04	252.52	mudcracked siltstone

252.52	252.97	siltstone
252.97	253.62	graded sandstone

HE-02-01

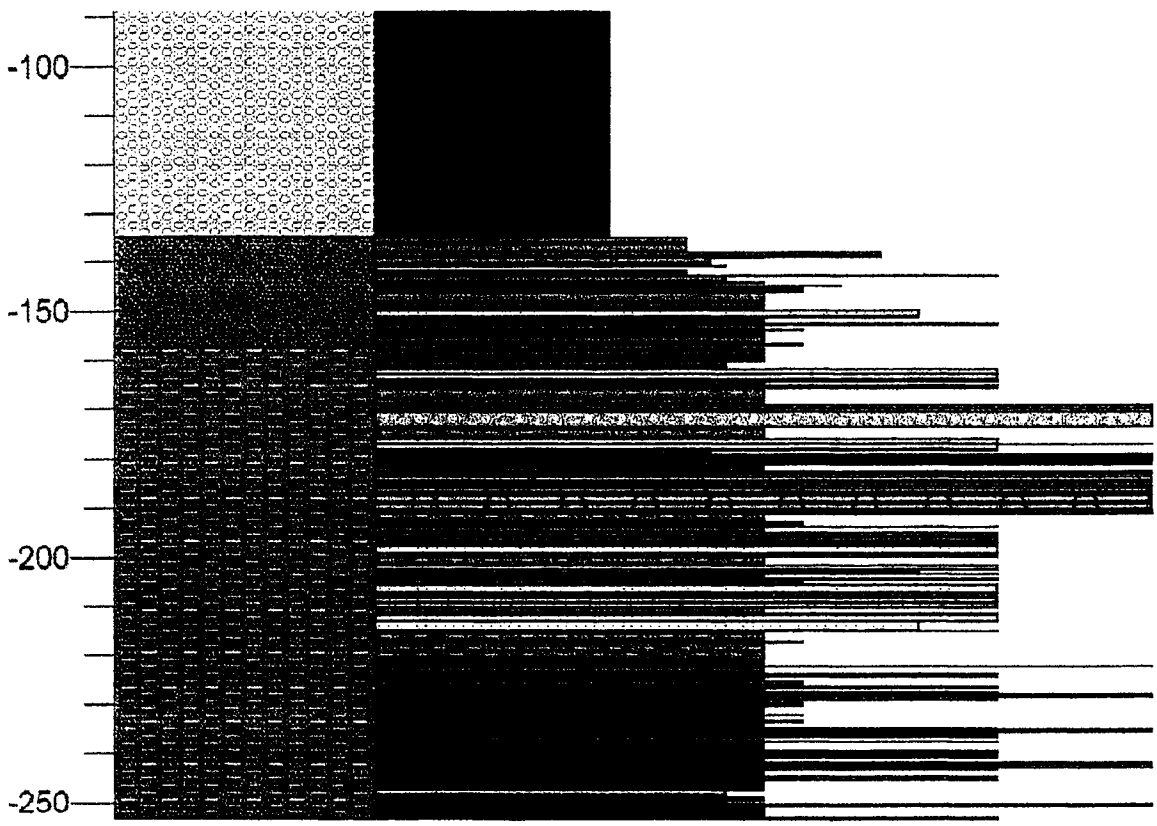

HE-02-02 393007 E, 5449701 N

Hele Member, Outan Island Fm			
0	0.34	diabase	
0.34	1.01	fine sandstone	hor lam
1.01	1.18	diabase	
1.18	1.29	laminated siltstone	with fsst
1.29	1.67	diabase	
1.67	2.31	laminated siltstone	with shale
2.31	3.94	diabase	
3.94	4.68	laminated siltstone	
4.68	4.76	cross-stratified siltstone	ripple
4.76	5.31	laminated siltstone	
5.31	5.37	cross-stratified siltstone	ripple
5.37	5.47	laminated siltstone	
5.47	5.48	cross-stratified siltstone	ripple
5.48	5.53	fine sandstone	mud rip-ups
5.53	5.71	horizontally laminated sandstone	fsst/silt, thick
5.71	5.9	horizontally laminated sandstone	fsst/silt, thin
5.9	6.41	silty shale	salt cast
6.41	6.53	sandstone	
6.53	7.37	laminated siltstone	
7.37	7.4	cross-stratified siltstone	
7.4	7.47	laminated siltstone	
7.47	7.52	laminated siltstone	
7.52	7.64	siltstone	with fsst
7.64	7.72	fine sandstone	laminated
7.72	8.84	siltstone	rare ripple lam
8.84	8.95	siltstone	messy lam
8.95	9	cross-stratified siltstone	
9	9.12	shale	purple
9.12	9.14	sandy siltstone	some fsst
9.14	9.27	shale	some silt @ base
9.27	9.34	coarse sandstone	
9.34	9.98	reverse graded sandstone	overall fine up
9.98	10.36	fine sandstone	mudcracked top
10.36	10.46	fine sandstone	some ripple lam
10.46	10.77	graded sandstone	fsst to silt
10.77	11.37	siltstone	rip-up clasts at base
11.37	12.17	graded sandstone	fsst to shale, rippled 25 cm @ base
12.17	12.35	laminated mudstone	mud rip-ups
12.35	12.52	cross-stratified sandstone	fsst
12.52	12.62	laminated mudstone	
12.62	13.35	horizontally laminated sandstone	with silt, some ripples
13.35	13.52	laminated fine sandstone	
13.52	13.67	siltstone	with fsst
13.67	13.81	laminated fine sandstone	
13.81	14.51	graded sandstone	fsst to silt, salt casts
14.51	15.04	graded sandstone	fsst to silt
15.04	15.29	fine sandstone	hor lam & ripple lam

15.29	16.04	silty shale	fine up, rip-ups @ bottom
16.04	17.11	fine sandstone	lam with silt/shale areas
17.11	17.15	siltstone	
17.15	17.52	siltstone	some fsst layers
17.52	17.58	laminated fine sandstone	with shale
17.58	17.7	siltstone	
17.7	17.9	laminated fine sandstone	shale area in middle
17.9	17.96	siltstone	mud rip-ups
17.96	18.5	fine sandstone	ripples @ top, mudcracks
18.5	18.84	siltstone	red
18.84	19.09	cross-stratified sandstone	ripple, fsst
19.09	19.51	siltstone	mud rip-up lam near top
19.51	19.59	fine sandstone	contain mud rip-ups
19.59	20.19	mudcracked siltstone	some fsst layers
20.19	20.37	cross-stratified sandstone	ripple fsst to hor lam fsst
20.37	21.17	mudcracked siltstone	some fsst
21.17	21.65	graded sandstone	csst to fsst, 1 ripple lam
21.65	21.78	siltstone	some sand
21.78	21.82	fine sandstone	some contorted mud
21.82	22.55	mudcracked siltstone	some fsst
22.55	22.7	laminated fine sandstone	rip-ups, mudcracks
22.7	22.88	mudcracked siltstone	
22.88	23.26	laminated fine sandstone	some contorted silt
23.26	23.31	graded sandstone	fsst to shale
23.31	23.53	siltstone	
23.53	23.65	laminated siltstone	some ripples, fsst
23.65	23.9	siltstone	
23.9	23.98	fine sandstone	contorted, rip-ups, shale
23.98	24.34	graded sandstone	fsst to silt, wavy to ripple lam
24.34	24.57	conglomerate	mud clasts in fsst
24.57	25.16	laminated fine sandstone	siltier upwards
25.16	25.47	fine sandstone	rip-ups, some hor lam
25.47	25.6	diabase	
25.6	25.7	fine sandstone	
25.7	25.87	cross-stratified siltstone	wavy
25.87	25.96	sandstone	
25.96	26.24	graded sandstone	fsst to shaly silt
26.24	26.47	mudstone	some fsst blobs
26.47	27.62	mudcracked siltstone	rip-ups, rare ripples, some fsst
27.62	27.82	graded sandstone	msst to fsst lam
27.82	27.86	silty shale	
27.86	27.95	fine sandstone	some low angle x-lam
27.95	29.44	siltstone	some fsst, thick mud rafts, wavy base
29.44	29.54	fine sandstone	ripple lam to hor lam
29.54	29.57	laminated mudstone	
29.57	29.66	cross-stratified sandstone	dune to ripple x-lam
29.66	30.07	laminated mudstone	contorted shale, fsst balls
30.07	30.72	laminated fine sandstone	minor low angle x-lam
30.72	30.74	shale	
30.74	31.11	graded sandstone	msst to fsst to silt lam, rip-up horizons, soft sed

31.11	31.16	silty shale	
31.16	31.21	fine sandstone	contorted to hor. lam.
31.21	31.38	graded sandstone	msst to fsst, clay cap
31.38	31.42	graded sandstone	black csst to msst, clay cap
31.42	31.81	fine sandstone	csst horizons, msst blobs, calcitic
31.81	31.88	graded sandstone	m/csst to shale, erosive base
31.88	31.96	fine sandstone	silty contorted top, hor lam below
31.96	31.98	shale	
31.98	35.32	siltstone	calcitic, evap, rare contorted/ripple lam
35.32	35.66	graded sandstone	shalier upwards, some individual layers graded
35.66	36.3	reverse graded sandstone	mudstone, sandier upwards, mudcracks
36.3	36.53	cross-stratified sandstone	fsst, ripple & dune lam
36.53	36.94	mudcracked siltstone	rare x-lam
36.94	37.17	sandstone	calcitic
37.17	38.48	mudcracked siltstone	, sandy layers, 1 ripple lam
38.48	39.44	fine sandstone	calcitic, rare ripple lam
39.44	40.18	graded sandstone	msst to fsst to silt
40.18	40.45	graded sandstone	fsst to silt
40.45	40.61	siltstone	
40.61	40.78	laminated siltstone	with fsst
40.78	41.06	laminated fine sandstone	many mudcracks, contorted lam
41.06	41.12	reverse graded sandstone	shaley silt to sand
Kama Hill Fm			
41.12	41.21	sandstone	clay caps
41.21	41.55	mudstone	wavy lam, rip-ups
41.55	42.86	siltstone	
42.86	42.97	laminated fine sandstone	calcitic
42.97	44.78	siltstone	
44.78	44.81	laminated fine sandstone	some ripple lam
44.81	45.13	siltstone	
45.13	45.16	fine sandstone	
45.16	45.62	mudcracked siltstone	
45.62	45.72	fine sandstone	irregular, sharp base
45.72	48.09	siltstone	sandy aread, rip-ups, shale inc up
48.09	48.22	fine sandstone	wide mudcracks, rip-ups, broken lam
48.22	48.69	graded sandstone	fsst to mud
48.69	48.88	siltstone	mud rafts
48.88	49.27	fine sandstone	minor ripple lam
49.27	50.23	graded sandstone	hor lam fsst to contorted silt with rip-ups
50.23	50.47	fine sandstone	rip-ups @ base
50.47	51.12	siltstone	rip-ups
51.12	51.78	graded sandstone	cycles of fsst to silt, mudcracked tops
51.78	52.77	siltstone	
52.77	53.07	fine sandstone	silty areas
53.07	53.27	mudcracked siltstone	
53.27	54.26	graded sandstone	fsst to silt dom, mudcracks, contorted
54.26	56.01	siltstone	sandy
56.01	57.23	mudcracked siltstone	shale up
57.23	58.95	graded sandstone	fsst to silt, contorted & mudcracks @ base
58.95	59.67	mudcracked siltstone	calcitic, rip-ups

59.67	60.11	laminated shale	
60.11	64.27	siltstone	several small fst layers
64.27	64.72	laminated siltstone	some shale/fsst layers, rip-ups
64.72	64.97	siltstone	
64.97	65.24	graded sandstone	fsst to silt, contorted top
65.24	67.26	siltstone	some hor. lam, ripple lam
67.26	67.52	laminated siltstone	
67.52	71.24	siltstone	minor laminated mud, calcitic
71.24	71.57	laminated siltstone	minor lam mud
71.57	72.02	siltstone	
72.02	72.24	siltstone	with thick mud lam
72.24	76.45	cross-stratified siltstone	ripple lam, some sandy areas, cracks
76.45	76.87	mudchip conglomerate	clast support, calcitic
76.87	76.93	stromatolite	crinkly/wavy carb layers
Fire Hill Member, Rossport Fm			
76.93	77.03	silty shale	layers thin up, graded calcitic top
77.03	77.08	dolomitic mudstone	silty top
77.08	77.19	contorted mudstone	dolomitic
77.19	77.81	stromatolite	silicified
77.81	78.55	siltstone	carb-rich top
78.55	79.29	siltstone	
79.29	79.34	siltstone	carbonate lam
79.34	79.37	siltstone	
79.37	79.38	shale	
79.38	79.4	siltstone	
79.4	79.42	graded sandstone	sst to silt, mud cap
79.42	79.46	shaley siltstone	
79.46	79.48	fine sandstone	
79.48	79.6	mudstone	
79.69	79.76	dolomitic sandstone	
79.76	80.53	dolomitic mudstone	
80.53	82.94	siltstone	mudchips
82.94	83.04	fine sandstone	
83.04	83.13	shaley siltstone	
83.13	83.19	siltstone	
83.19	83.21	siltstone	diagenetic min
83.21	83.54	siltstone	shaley top
83.54	83.92	silty shale	
83.92	84.02	fine sandstone	silty, mud cap
84.02	84.12	mudchip conglomerate	1 sand clast, elongate mud clasts
84.12	84.56	laminated fine sandstone	mud drapes, ripple lam at base
84.56	84.69	shaley siltstone	
84.69	84.72	fine sandstone	
84.72	84.88	laminated siltstone	
84.88	84.96	fine sandstone	
84.96	84.98	laminated siltstone	
84.98	85.04	fine sandstone	
85.04	85.08	mudstone	
85.08	85.17	fine sandstone	
85.17	85.82	laminated mudstone	

85.82	86.13	laminated mudstone	diagenetic min
86.13	86.56	laminated mudstone	silt block
86.56	86.59	sandstone	contorted
86.59	86.65	laminated mudstone	
86.65	86.95	mudstone	diagen min.
86.95	87.04	mudstone	
87.04	87.24	mudstone	heavy diagen min
87.24	90.36	cross-stratified sandstone	fsst, silty, minor diagen. nodules
90.36	90.7	shale	fissile, 3 cm gypsum area
90.7	92.11	laminated mudstone	silty, some diagenetic min
92.11	92.18	laminated siltstone	
92.18	92.51	shaley siltstone	
92.51	92.52	fine sandstone	mudcracked
92.52	92.57	mudstone	
92.57	92.69	dolomitic mudstone	mudcracks
92.69	93.66	siltstone	
93.66	94.56	graded sandstone	fsst with some ripple lam, silt inc up
94.56	94.84	cross-stratified sandstone	fsst, wavy to current to hor lam
94.84	95.62	siltstone	some f/msst
95.62	96.81	laminated siltstone	shale inc up, large mudcrack
96.81	97.48	siltstone	friable @ top
97.48	97.72	shale	laminated, large mudcrack
97.72	97.98	fine sandstone	
97.98	100.72	laminated mudstone	sandy @ top
100.72	101.12	sandstone	
101.12	105.3	siltstone	fissile, some ripple to hor lam fsst, diagen min
105.3	105.7	fine sandstone	grey, lots of gypsum veins
105.7	110.64	mudstone	few fsst lam & rip-ups
110.64	110.83	siltstone	
110.83	111.48	mudstone	
111.48	111.91	siltstone	muddier upwards
111.91	112.08	laminated mudstone	
112.08	112.27	siltstone	some gypsum
112.27	113.24	siltstone	some diagenetic min, dec. up
113.24	114.44	siltstone	
114.44	114.84	mudchip conglomerate	
114.84	114.96	mudstone	
114.96	115.04	mudchip conglomerate	
115.04	115.17	siltstone	
115.17	115.37	mudchip conglomerate	
115.37	116.35	siltstone	
116.35	116.75	mudstone	evap, rip-ups
116.75	117.57	mudstone	lots of rip-ups assoc with silty area
117.57	117.65	mudstone	high evap conc
117.65	118.84	mudstone	
118.84	119.11	mudstone	high evap conc
119.11	119.36	mudstone	low evap conc
119.36	119.39	calcite	silicified
119.39	121.32	siltstone	shalier up, few evap (esp @ top)
121.32	122.62	siltstone	sandy

122.62	122.8	sandstone	shale cap
122.8	123.58	sandstone	silt cap
123.58	123.91	siltstone	
123.91	124.75	graded sandstone	msst to silt
124.75	125.48	siltstone	evap, rip-ups, mud cap
125.48	125.68	shale	laminated
125.68	131.24	siltstone	few evap nodules, shaley areas
131.24	131.3	shale	mud balls loaded @ base, wavy lam top
131.3	131.84	siltstone	
131.84	131.94	fine sandstone	some clay lam
131.94	134.04	siltstone	contorted lam, some mud blobs
134.04	134.51	laminated siltstone	shalier at top, evap near base
134.51	134.76	siltstone	carbonate rich
134.76	134.97	siltstone	mottled
134.97	135.32	conglomerate	clasts (silt, fs, clay) fine up
135.32	135.47	contorted mudstone	
135.47	135.67	siltstone	
135.67	135.74	dolomitic mudstone	laminated
135.74	135.8	brecciated	dolomitic mud in clay
135.8	135.88	mudstone	
135.88	136.26	fine sandstone	x-lam area, "rolled" mud balls, microfaulted
Channel Island Member, Rossport Fm			
136.26	137.81	mudstone	heavy diagen.
137.81	138.11	siltstone	
138.11	138.54	siltstone	heavy diagen.
138.54	138.64	siltstone	
138.64	138.88	graded sandstone	msst to clay, heavy diagen
138.88	139.29	graded sandstone	msst to clay
139.29	139.51	graded sandstone	csst to msst
139.51	141.04	siltstone	
141.04	141.83	graded sandstone	msst, shaley/silty top
141.83	142.32	sandstone	
142.32	142.88	graded sandstone	msst to silt
142.88	144.8	laminated siltstone	some shale areas
144.8	145.19	sandstone	a bit silty @ top
145.19	145.63	graded sandstone	msst to silty sand
145.63	148.08	siltstone	
148.08	148.27	sandstone	
148.27	149.66	siltstone	
149.66	150.75	sandstone	
150.75	151.06	mudstone	
Fork Bay Member, Pass Lake Fm			
151.06	151.66	cross-stratified sandstone	climbing ripple lam/ripple lam
151.66	151.98	laminated mudstone	with fsst
151.98	152.55	sandstone	
152.55	152.89	laminated siltstone	with sst
152.89	153.38	sandstone	
153.38	153.97	siltstone	
153.97	156.29	sandstone	
156.29	156.99	siltstone	

156.99	157.67	sandstone	
157.67	158.06	Conglomerate	sand clasts @ top
158.06	158.29	mudstone	
158.29	158.8	dolomitic mudstone	
158.8	159.87	siltstone	
159.87	245	diabase	

HE-02-02

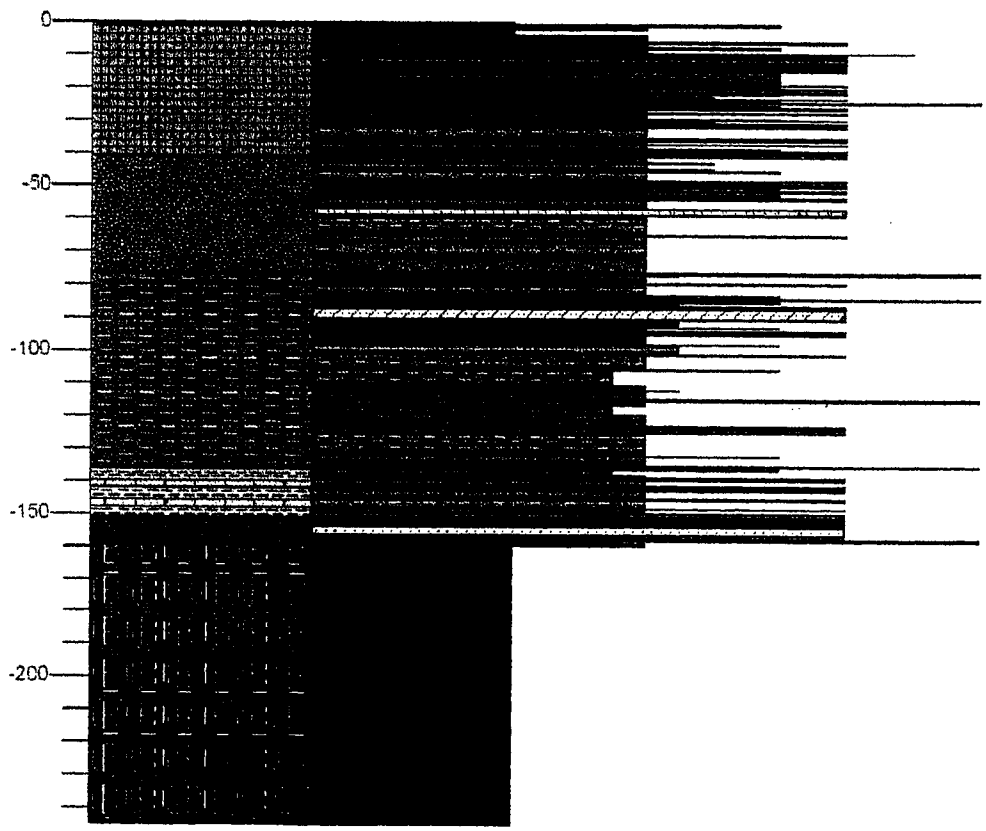

SR-02-01 363501 E, 5439302 N

0	72	diabase	
Fire Hill Member, Rossport Fm			
72	72.07	saprolite	
72.07	72.12	sandstone	
72.12	72.5	saprolite	
72.5	72.66	dolomitic mudstone	
72.66	73.14	sandstone	muddy
73.14	73.35	siltstone	
73.35	73.49	dolomtic mudstone	laminated, silt dom
73.49	73.61	laminated siltstone	with msst lam
73.61	73.76	dolomitic mudstone	
73.76	73.85	mudstone	
73.85	74.03	dolomitic mudstone	carb content inc up
74.03	74.23	sandstone	muddy
74.23	74.63	dolomitic mudstone	salt casts, mud balls
74.63	75.05	siltstone	
75.05	75.41	graded sandstone	mudddy top
75.41	75.5	saprolite	
75.5	75.75	saprolite	
75.75	76.03	graded sandstone	msst to fsst, inc carb up
76.03	77.39	graded sandstone	csst to msst, salt casts
77.39	77.8	saprolite	
77.8	78.39	graded sandstone	msst to fsst
78.39	78.45	saprolite	
78.45	79.36	graded sandstone	msst to silt
79.36	79.59	saprolite	
79.59	79.71	graded sandstone	msst to fsst
79.71	79.93	saprolite	
79.93	80.03	sandstone	
80.03	80.15	saprolite	
80.15	80.23	sandstone	
80.23	80.3	saprolite	
80.3	81.62	graded sandstone	3 cycles msst to fsst, some coarser
81.62	82.47	siltstone	
82.47	83.35	dolomitic mudstone	mudballs
83.35	83.66	laminated siltstone	calcitic mud wisps
83.66	83.86	graded sandstone	fsst to silt
83.86	84.12	mudstone	mud balls
84.12	84.49	mudstone	sandy areas
84.49	89.2	graded sandstone	cycles of msst to mud
89.2	89.56	graded sandstone	fsst to mud/carb nodules, friable
89.56	89.74	graded sandstone	fsst to mud/carb nodules, friable
89.74	89.85	graded sandstone	fsst to mud/carb nodules, friable
89.85	90.02	graded sandstone	fsst to mud/carb nodules, friable
90.02	90.25	graded sandstone	fsst to mud/carb nodules, friable
90.25	90.33	graded sandstone	fsst to mud/carb nodules, friable
90.33	90.4	graded sandstone	fsst to mud/carb nodules, friable

90.4	90.45	graded sandstone	fsst to mud/carb nodules, friable
90.45	90.5	graded sandstone	fsst to mud/carb nodules, friable
90.5	90.62	graded sandstone	fsst to mud/carb nodules, friable
90.62	90.68	graded sandstone	fsst to mud/carb nodules, friable
90.68	90.92	graded sandstone	fsst to mud/carb nodules, friable
90.92	91.49	graded sandstone	fsst to mud/carb nodules, friable
91.49	91.55	graded sandstone	fsst to mud/carb nodules, friable
91.55	91.91	graded sandstone	fsst dom to mud/carb areas
91.91	92.42	graded sandstone	fsst dom to mud/carb areas
92.42	92.62	graded sandstone	fsst dom to mud/carb areas
92.62	92.8	graded sandstone	fsst dom to mud/carb areas
92.8	92.89	graded sandstone	fsst dom to mud/carb areas
92.89	93.57	sandstone	
93.57	94.6	graded sandstone	fsst to mud
94.6	94.72	siltstone	mud balls
94.72	95.55	fine sandstone	some mud lam
95.55	95.73	mudchip conglomerate	mud blocks
95.73	97.57	siltstone	caliche horizones
97.57	99.46	fine sandstone	some friable shaley areas
Channel Island Member, Rossport Fm			
99.46	99.82	contorted mudstone	mud balls
99.82	99.92	dolomitic mudstone	
99.92	100.96	contorted mudstone	
100.96	110.42	dolomitic mudstone	poorly consolidated, dissolved
110.42	125.62	saprolite	fsst to silty, calcitic, partly dissolved
125.62	132.97	saprolite	dissolved cap
132.97	359	diabase	

SR-02-01

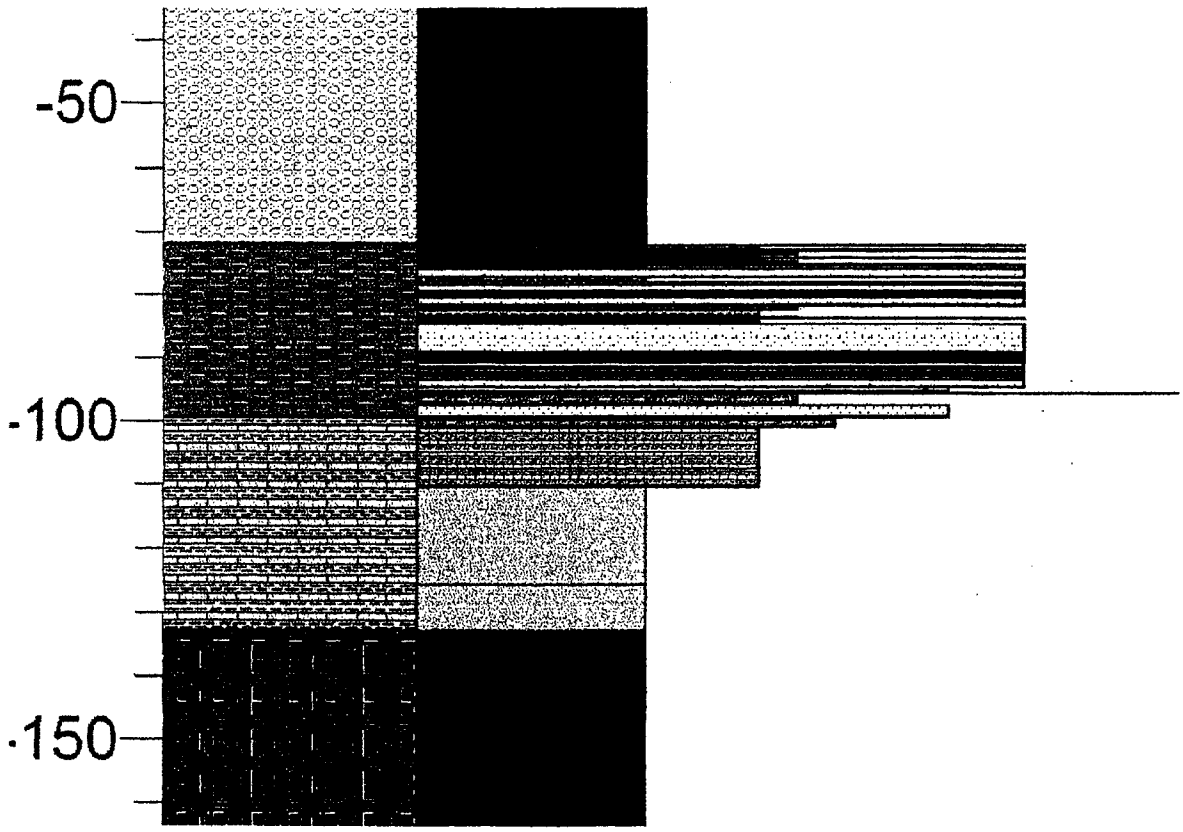

DDH-1 376290 E, 5437493 N DDH-1

Channel Island Member, Rossport Fm			
0.00	9.64	mudstone	diagen min, some calcified gypsum layers
9.64	39.07	saprolite	fine sed, yellow alteration at base
39.07	40.36	diabase	
40.36	49.13	saprolite	brecciated, calcite veins at top, mottled, fine sed
49.13	51.85	diabase	brecciated, chloritic
51.85	53.31	mudstone	a bit brecciated, purple & green
Fork Bay Member, Pass Lake Fm			
53.31	60.06	sandstone	silicified, some diabase
60.06	62.95	diabase	
62.95	103.45	sandstone	some clay separation, congl layer (clasts fine up)
103.45	120.81	horizontally laminated sandstone	thick lam, no red clay, some carb

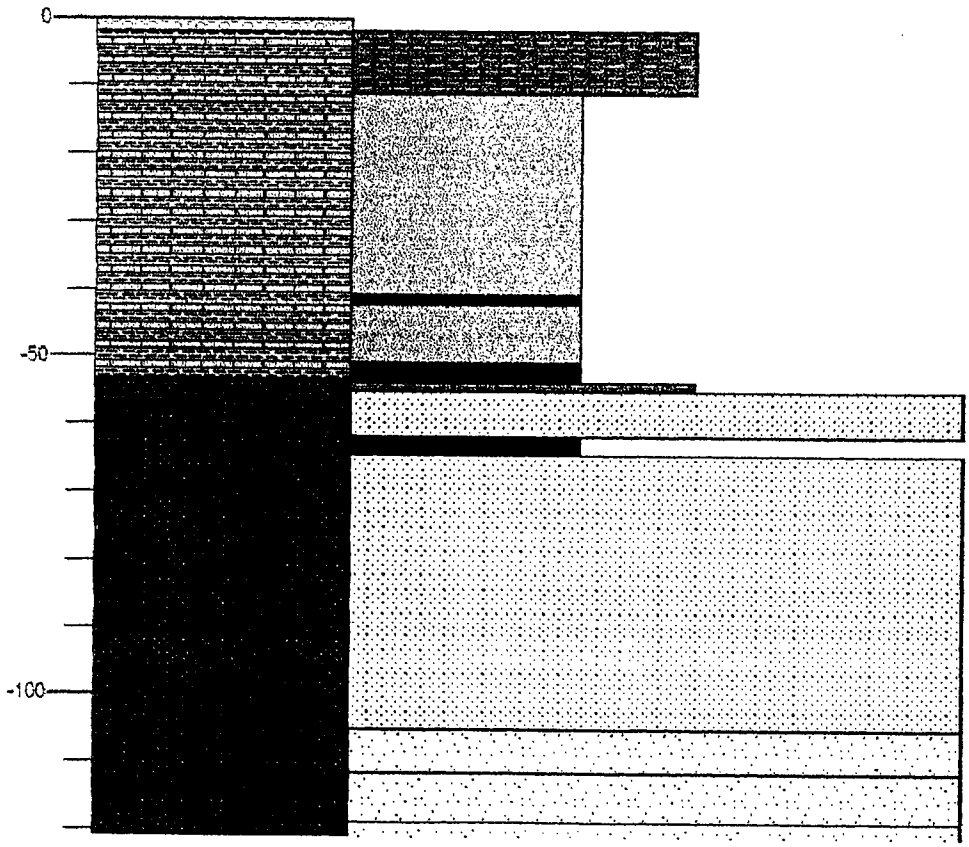

DDH-2 376371 E, 5446449 N DDH-2

Fire Hill Member, Rossport Fm			
0.00	15.44	silty shale	some msst areas with carb (some 2ndary)
15.44	17.00	mudstone	some msst lam with mud drapes
17.00	23.19	siltstone	some muddy & fsst areas (non-carb)
23.19	26.98	shaley siltstone	common m/fsst, angled x-lam
26.98	49.83	graded sandstone	silty upwards, some contorted lam, silicified bottom
49.83	60.64	diabase	alteration grades into fine sed
60.64	61.22	breccia	silt/shale and diabase clasts
61.22	67.60	fine sandstone	massive, high qtz, well-sorted, come calc cement
67.60	84.63	diabase	

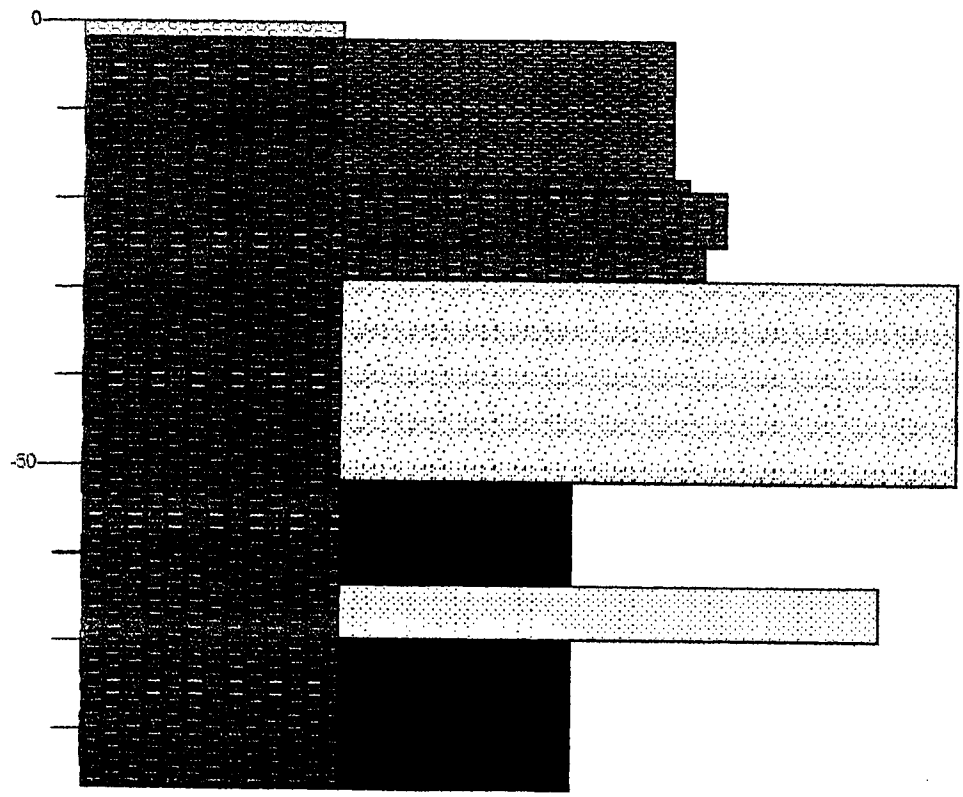

DDH-3 376299 E, 5446449 N DDH-3

Fire Hill Member, Rossport Fm			
0.00	29.56	laminated mudstone	rare diagen, some carb, some fsst near top
29.56	30.06	fine sandstone	silicified
30.06	30.84	siltstone	brecciated
30.84	31.23	fine sandstone	soupy bottom contact, sharp upper
31.23	38.33	mudstone	some gypsum replacement
38.33	45.30	conglomerate	silty clasts, brecciated upwards, mud matrix
45.30	45.97	conglomerate	diabase block, mud clasts
45.97	51.61	diabase	
51.61	51.75	breccia	sibley and diabase clasts

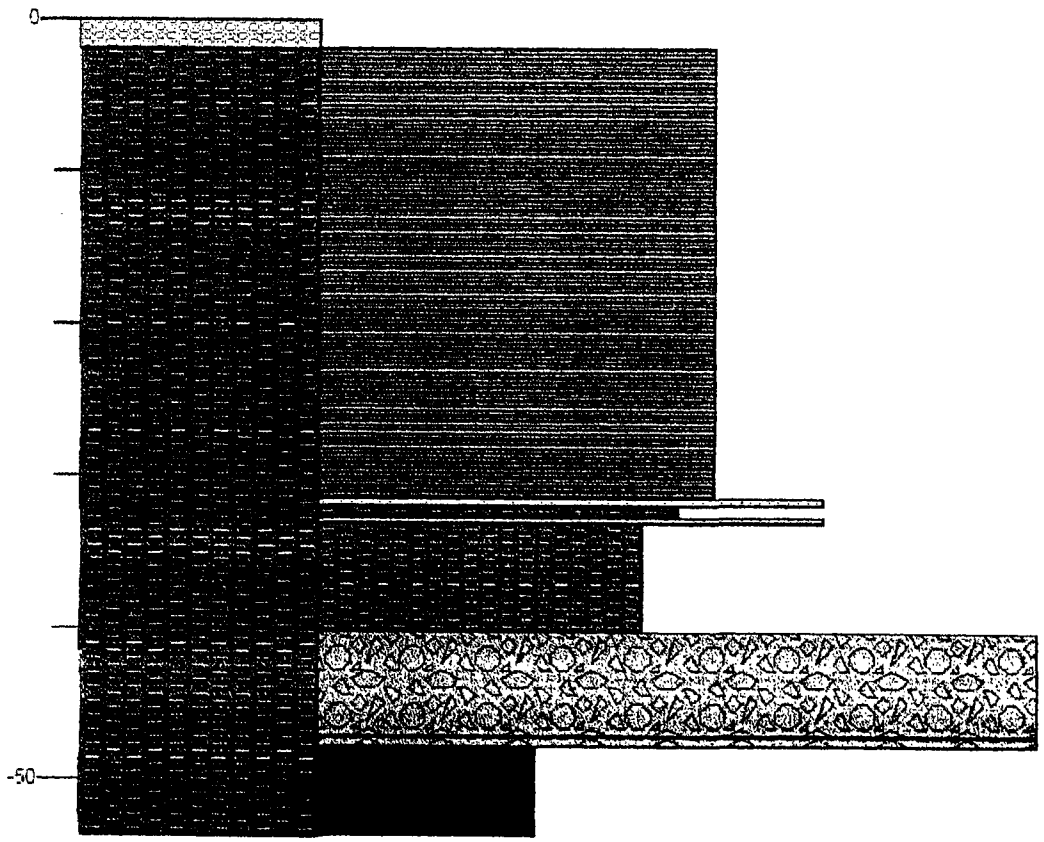

Fire Hill Member, Rossport Fm			
0.00	11.84	siltstone	red and peach, mottled, dissolved diagenetic min
11.84	12.23	conglomerate	mud and sand clasts in silt
12.23	34.41	diabase	messy contact - diabase clasts in fsst
Fork Bay Member, Rossport Fm			
34.41	35.66	fine sandstone	
35.66	37.30	fine sandstone	very qtz-rich

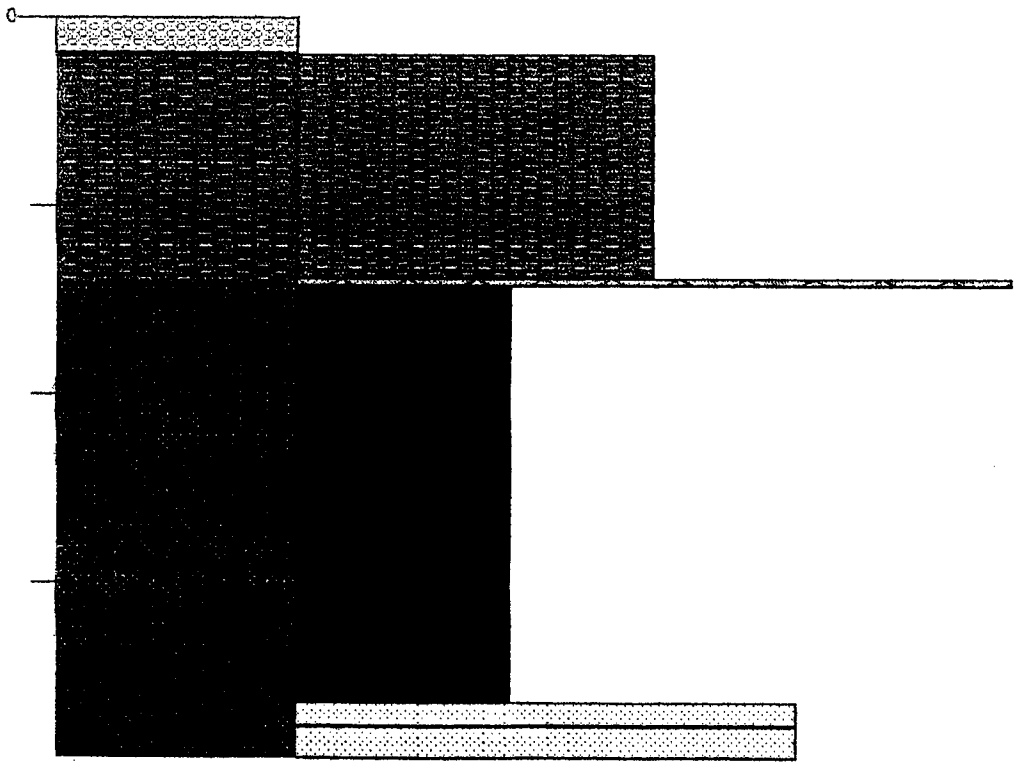

Appendix B:

GEOCHEMICAL DATA

Tables for the major and minor elements are provided for the stratigraphic comparisons used in chapter 3.

Table B-1. Major Elements for the Sibley Group													
Sample	SiO2	TiO2	Al2O3	Fe2O3T	MnO	MgO	CaO	Na2O	K2O	P2O5	H2Op	CO2	Total
01-1	83.56	0.11	7.38	0.84	0.05	1.08	1.15	0.24	3.80	0.05	0.72	1.03	100
01-2	89.29	0.05	5.18	0.51	0.02	0.64	0.47	0.09	2.56	0.04	0.63	0.51	100
01-3	91.06	0.04	4.65	0.37	0.02	0.51	0.34	0.07	1.80	0.05	0.72	0.37	100
01-4	89.16	0.13	5.01	1.78	0.01	0.45	0.13	0.07	2.39	0.05	0.63	0.18	100
01-5	87.83	0.04	3.86	1.47	0.04	1.08	1.43	0.08	1.82	0.04	0.63	1.98	100.3
01-6	90.05	0.03	3.93	0.63	0.02	0.68	0.74	0.05	2.49	0.04	0.36	0.99	100
01-7	88.78	0.10	4.82	1.51	0.03	0.53	0.35	0.07	2.77	0.06	0.54	0.44	100
01-8	88.15	0.18	5.37	1.26	0.02	0.57	0.24	0.08	3.09	0.06	0.72	0.26	100
01-9	91.68	0.03	3.80	0.27	0.01	0.44	0.41	0.06	2.36	0.04	0.36	0.55	100
01-10	94.03	0.03	3.66	0.30	0.00	0.26	0.10	0.02	1.14	0.03	0.36	0.18	100
01-11	89.46	0.07	3.89	1.40	0.02	0.75	0.78	0.06	2.25	0.04	0.36	0.92	100
01-12	90.03	0.06	4.19	1.53	0.01	0.42	0.32	0.09	2.26	0.04	0.72	0.33	100
01-13	83.16	0.16	5.60	2.66	0.04	1.56	1.11	0.09	3.14	0.04	0.90	1.54	100
01-14	75.43	0.11	5.24	1.85	0.06	2.86	3.91	1.22	3.64	0.04	0.72	6.01	101.1
01-15	80.25	0.15	6.95	2.75	0.04	2.49	0.74	0.12	4.73	0.06	0.99	0.73	100
01-16	85.47	0.23	5.83	2.36	0.04	0.39	0.35	0.11	4.47	0.07	0.27	0.40	100
01-17	78.29	0.26	4.60	4.45	0.04	2.12	2.67	0.09	2.99	0.07	0.54	3.89	100
01-18	85.49	0.19	5.54	2.93	0.03	0.67	0.58	0.06	3.35	0.06	0.36	0.73	100
01-19	84.17	0.16	6.06	2.34	0.04	0.79	0.75	0.09	3.93	0.07	0.54	1.06	100
01-20	85.97	0.13	4.59	2.95	0.03	0.67	0.60	0.07	3.23	0.06	0.45	1.06	100
01-21	65.94	0.28	7.33	0.94	0.15	5.71	5.94	0.18	5.35	0.14	0.09	7.96	100
01-22	80.13	0.54	6.40	3.07	0.02	5.26	0.17	0.13	2.96	0.09	1.08	0.15	100
01-23	89.51	0.49	3.95	2.26	0.02	0.58	0.53	0.04	1.92	0.03	0.63	0.44	100.4
01-24	92.01	0.08	3.83	0.41	0.01	0.53	0.38	0.05	1.79	0.03	0.45	0.44	100
01-25	91.49	0.05	4.32	0.75	0.01	0.36	0.28	0.04	1.86	0.02	0.45	0.37	100
01-26	88.98	0.03	3.98	0.32	0.03	0.89	1.08	0.07	2.58	0.03	0.54	1.47	100
01-27	87.21	0.09	4.29	1.66	0.05	1.00	1.15	0.07	2.62	0.03	0.36	1.47	100
01-29	91.41	0.08	4.09	0.35	0.00	0.39	0.17	0.06	2.22	0.04	0.81	0.37	100

01-30	92.26	0.06	3.44	0.26	0.01	0.60	0.55	0.05	1.82	0.03	0.18	0.73	100
01-31	81.75	0.13	3.61	1.39	0.04	2.35	3.19	0.07	2.42	0.04	0.54	4.47	100
01-32	83.15	0.30	4.95	2.22	0.03	1.38	1.73	0.07	3.33	0.06	0.54	2.24	100
01-33	71.31	0.31	5.57	2.41	0.06	3.84	4.78	0.13	4.07	0.08	0.81	6.64	100
01-35	59.81	0.35	8.72	3.15	0.09	5.52	6.46	0.23	6.06	0.12	0.99	8.51	100
01-36	53.90	0.34	9.19	2.25	0.08	6.43	8.75	0.34	5.87	0.10	1.35	11.40	100
01-37	79.44	0.03	1.44	0.65	0.00	0.56	15.81	0.05	1.00	0.14	0.18	0.70	100
01-38	77.24	0.05	1.27	0.47	0.03	4.85	6.07	0.07	0.63	0.01	0.36	8.95	100
01-39	75.85	0.05	1.45	0.52	0.03	4.94	6.94	0.08	0.73	0.02	0.45	8.95	100
01-40	70.78	0.07	1.81	0.58	0.03	5.69	8.15	0.11	0.94	0.02	0.45	11.37	100
01-41	75.46	0.13	3.86	1.72	0.02	6.90	9.40	0.18	1.83	0.04	0.09	0.37	100
01-42	78.19	0.09	2.77	0.72	0.07	8.09	4.70	0.28	0.73	0.02	1.89	2.46	100
01-43	66.99	0.14	4.51	1.47	0.04	6.67	10.29	0.31	2.29	0.03	1.62	5.65	100

Table B-2. Minor Elements for the Sibley Group									
Sample	**Ba**	**Sr**	**Y**	**Zr**	**Nb**	**Zn**	**V**	**Co**	**Ni**
01-1	387	46.1	14.9	65.8	5.8	11.3	10.1	32.6	6.4
01-2	476	28.3	6.6	35.0	2.7	3.6	5.0	21.7	4.0
01-3	281	17.8	6.0	33.1	3.6	11.1	4.6	25.1	5.5
01-4	233	26.8	12.1	69.8	4.7	10.5	14.1	26.9	5.9
01-5	351	22.8	7.1	27.7	4.6	0.6	4.0	30.4	2.9
01-6	268	24.7	5.2	27.7	1.9	1.9	2.9	11.6	3.3
01-7	377	28.7	10.7	55.8	3.8	8.0	13.2	16.1	5.6
01-8	325	26.6	14.0	95.4	5.7	10.4	14.0	21.9	6.6
01-9	297	25.1	4.5	26.4	3.9	1.0	3.2	26.2	3.5
01-10	31	5.6	5.4	26.4	3.5	1.7	7.4	25.6	3.5
01-11	209	21.6	5.3	68.0	5.0	3.4	7.3	26.7	3.8
01-12	272	40.7	5.7	51.2	5.5	1.4	9.1	39.6	3.6
01-13	274	22.3	11.2	79.6	8.1	17.9	18.9	49.0	6.8
01-14	318	23.4	11.6	58.6	11.1	8.5	13.7	58.8	3.3
01-15	1277	27.6	11.9	67.6	6.8	28.8	37.8	29.8	14.7
01-16	539	23.0	9.9	89.4	9.4	4.1	28.5	46.2	2.7
01-17	240	27.7	14.1	96.0	11.4	7.9	32.6	38.4	6.1
01-18	225	18.7	15.6	101.3	9.4	7.6	27.6	35.4	6.5
01-19	323	23.0	14.0	84.3	8.9	8.9	22.7	40.1	8.1
01-20	189	26.0	9.2	75.0	8.6	4.7	29.3	45.9	5.5
01-21	965	46.5	21.1	129.4	8.5	38.6	63.8	20.4	8.5
01-22	284	22.8	13.0	132.0	8.2	121.0	60.0	28.2	8.5
01-23	311	17.8	6.1	66.2	3.3	3.2	12.3	13.7	21.4
01-24	283	17.0	6.4	65.9	4.0	0.4	20.5	25.2	3.5
01-25	168	11.8	5.3	32.7	5.3	0.9	4.8	45.3	2.3
01-26	263	26.5	5.3	30.3	3.8	0.5	5.2	23.0	1.9
01-27	236	23.8	7.5	69.1	4.6	5.9	9.2	23.6	2.0
01-29	239	31.9	6.4	63.2	3.7	4.7	6.1	14.4	4.7

01-30	365	18.0	5.7	59.2	4.4	188.9	7.3	25.4	2.7
01-31	450	23.8	10.7	66.5	6.7	12.3	12.8	27.2	6.6
01-32	218	24.0	14.6	112.6	8.2	17.2	25.8	20.7	7.4
01-33	2821	88.9	16.3	142.1	8.8	22.6	29.0	22.1	7.4
01-35	956	99.9	30.7	141.7	11.7	31.0	60.2	16.8	12.8
01-36	3028	188.0	24.1	117.7	10.9	25.9	37.7	13.6	9.7
01-37	234	925.8	3.4	19.4	8.8	0.0	7.1	4.2	0.2
01-38	7422	538.5	6.9	53.4	7.1	0.9	18.4	21.8	2.3
01-39	5605	380.5	5.2	34.8	6.6	15.7	23.6	16.0	9.2
01-40	2807	149.9	7.4	103.2	6.9	0.9	69.1	11.8	3.0
01-41	1855	150.5	8.1	78.5	7.9	5.2	19.8	10.7	2.6
01-42	367	52.0	6.3	44.6	19.3	17.0	12.1	8.6	4.6
01-43	836	83.3	7.6	45.2	8.8	21.1	18.2	11.3	4.7